

BOOK OF ABSTRACTS

19th International Conference on Cohesive Sediment Transport Processes

Inha University
Incheon, Republic of Korea
September 18-22, 2023



BOOK OF ABSTRACTS

19th International Conference on Cohesive Sediment Transport Processes

Inha University
Incheon, Republic of Korea
September 18-22, 2023



INHA UNIVERSITY

Inha University



CENTER FOR
ANTHROPOCENE
STUDIES

KAIST Center for Anthropocene Studies



Korea Institute of Ocean Science and Technology



Underwater Survey Technology 21, Inc

17th International Conference on

On behalf of Inha University, it is my distinct pleasure to extend my warmest congratulations on the publication of the abstract book for the International Conference on Cohesive Transport Processes (INTERCOH). As the president of Inha University, I commend your dedication and contributions to this esteemed gathering of minds.

The abstract book serves as a testament to the collective brilliance and groundbreaking research showcased during the conference. It encapsulates the spirit of inquiry, collaboration, and intellectual curiosity that drives our scientific community forward. The abstracts contained within its pages represent the culmination of countless hours of research, analysis, and innovative thinking.

Cohesive transport processes, with their inherent complexities and profound impact on various natural systems, have been at the forefront of scientific exploration. By delving into the intricacies of sediment transport, erosion, deposition, and related phenomena, you have contributed to our understanding of these critical processes that shape our environment.

The diversity of perspectives and interdisciplinary approaches represented in the abstract book is a testament to the transformative power of collaborative research. It is through the convergence of ideas, expertise, and shared experiences that we can unravel the mysteries of cohesive transport processes and pave the way for sustainable and resilient coastal and riverine systems.

I would like to express my deep appreciation to the organizing committee for their exceptional efforts in bringing together researchers from around the world to exchange knowledge, challenge conventional wisdom, and chart new frontiers in the field. Your dedication and commitment to advancing cohesive transport research are truly commendable.

To the authors whose abstracts grace the pages of this book, I extend my heartfelt congratulations. Your contributions have added immeasurable value to the conference, fostering dialogue and inspiring new avenues of investigation. Your commitment to excellence and your pursuit of scientific discovery will undoubtedly leave a lasting impact on the field of cohesive transport processes.

I am confident that the abstract book will serve as an invaluable resource for researchers, scholars, and practitioners alike. May it inspire further investigations, spark fruitful collaborations, and guide future endeavors in the pursuit of sustainable and resilient coastal and riverine systems.

Once again, congratulations to all those involved in the publication of the INTERCOH abstract book. I wish you continued success in your research and endeavors, and I hope that the knowledge shared within these pages will contribute to the betterment of our global community.

Keeyoung Choi
Provost
Inha University



17th International Conference on
Cohesive Sediment Transport Processes
September 18-22, 2023
Inha University, Incheon, Republic of Korea



Steering Committee

Carl Friedrichs, VIMS, USA
Qing He, East China Normal University, China
Guan-hong Lee, Inha University, Korea
Yasuyuki Nakagawa, PARI, Japan
Francisco Pedocchi, Universidad de la República - Uruguay
Larry Sanford, University of Maryland Center for Environmental Science, USA
Jarrell Smith, ERDC, US Army Corps of Engineers, USA
Mohsen Soltanpour, K. N. Toosi University of Technology, Iran
Jez Spearman, HR Wallingford, UK
Erik Toorman, KU Leuven, Belgium
Bram van Prooijen, TU Delft, The Netherlands
Susana Vinzon, Federal University of Rio de Janeiro, Brazil (Chair)
Romaric Verney, IFREMER, France

Local Organizing Committee

Ho Kyung Ha, Inha University, Korea
Kyu-Nam Hwang, Jeonbuk National University, Korea
Jae-Il Kwon, Korea Institute of Ocean Science and Technology, Korea
Guan-hong Lee, Inha University, Korea
Byung Joon Lee, Kyungbook National University, Korea
Hee Jun Lee, Korea Institute of Ocean Science and Technology, Korea (emeritus)
Seungbuhm Woo, Inha University, Korea

Editors for Research Topic of Frontiers in Marine Science

Guan-hong Lee, Inha University, Korea
Jez Spearman, HR Wallingford, UK
Ho Kyung Ha, Inha University, Korea
Bram van Prooijen, TU Delft, The Netherlands
Francisco Pedocchi, Universidad de la República, Uruguay
Byung Joon Lee, Kyungpook National University, Korea

INTERCOH 2023 is organized by the local organizing committee with support from Inha University, KIOST (Korea Institute of Ocean and Science Technology), Center for Anthropocene Research of KAIST (Korea Advanced Institute of Science and Technology), and UST21 (Underwater Survey Technology 21).



17th International Conference on
Cohesive Sediment Transport Processes
September 18-22, 2023
Inha University, Incheon, Republic of Korea



Scientific Program at a Glance

	September 18 Monday	September 19 Tuesday	September 20 Wednesday	September 21 Thursday	September 22 Friday
9:00	Registration	Session 3 Sediment Transport I	Session 7 Sediment Transport II	Session 9 Sediment Transport III	Session 13 Sediment Transport V
9:20					
9:40	Opening				
10:00					
10:20-10:40	BREAK	BREAK	BREAK	BREAK	BREAK
10:40	Session 1 Model I	Session 4 Bed Erosion	Session 8 Fluid Mud	Session 10 Flocs II	Session 14 Bed Rheology
11:00					
11:20					
11:40					
12:00	Lunch (12:20-14:00)				
14:00	Session 2 Flocs I	Session 5 Model II	Excursion	Session 11 Model III	Krone Award & Closing
14:20					
14:40					
15:00					
15:20	BREAK		BREAK		
15:40-16:00	BREAK		BREAK		
16:00	Poster Pitch	Session 6 Seabed Processes		Session 12 Sediment Transport IV	
16:20					
16:40					
17:00					
18:00-20:00		Steering Committee Meeting		Conference Dinner	

Schedule For Scientific Program

Date/Time	Title	Authors
September 18 Monday	Model I (Chair: Carl Friedrich)	
10:40-11:00	Modelling the thixotropic behavior of fluid mud: revised	Erik.A.Toorman and D.S.Ch.Praveen
11:00-11:20	Application of an 1-DV TCPBE model with Bayesian calibration to diagnose the flocculation potential in the laboratory experiments and field measurement	T. T. Huynh, Michael Fettweis, Byung Joon Lee
11:20-11:40	On numerical modeling of flocculation and cohesive sediment transport in the bottom boundary layer	J. A. Penaloza-Giraldo, L. Yue, T.J Hsu, B. Vowinkel, E. Meiburg, A.J. Manning
11:40-12:00	Modeling the transport and Abrasion of dense mud aggregates in the James River estuary	Earl J. Hayter, Jonathan C. Hollingsworth, S. Jarrell Smith, and Danielle R. Tarpley
12:00-12:40	Development of a three-phase CFD model for cohesive sediment transport	D.S.Ch.Praveen and Erik.A.Toorman
September 18 Monday	Flocs I (Chair: Ho Kyung Ha)	
14:00-14:20	Reconstructing 3-dimentional morphological structure of fine sediment floc and settling process using a multi-camera system	L. Ye, Z. Chen, J. Wu and R. Liao
14:20-14:40	The potential of cohesive sediment and diverse microalgae to flocculate in demanding growth conditions	Que Nguyen Ho, Michael Fettweis, Jin Hur, Sang Deuk Lee, and Byung Joon Lee
14:40-15:00	The role of microalgae in cohesive sediment flocculation: Insights from stochastic modeling and laboratory experiments	Mingze Lin, Xiaoteng Shen
15:00-15:20	Changes in suspended particle composition in the water column affect floc dynamics	M. Fettweis, L. Delhaye, B.J. Lee, R. Riethmüller, M. Schartau, S. Silori and X. Desmit

15:20-15:40	Depositional characteristics of oil-mineral flocs in estuarial and coastal waters	A.J. Manning, L. Ye, T-J, Hsu, J. Holyoke, J.A. Penaloza-Giraldo
September 18 Monday	Posters (Chair: Jae-II Kwon)	
16:00-17:30	Effects of reduced erosion of fine sediments from the shoreline and seabed on estuarine water clarity: Results from a Chesapeake Bay modeling study	J.S. Turner, P. St-Laurent, M.A.M. Friedrichs, and C.T. Friedrichs
	Application of GEMS Experiment Parameters in the Sediment Model for Intertidal Slope Within a Semi-closed Harbor	J. Y. Choi, J. W. Kim, H. M. Lee, S.-B. Woo, J. Y. Seo, H. K. Ha
	Idealized model of sediment transportation and nitrogen cycling in Nakdong River Estuary	Dongyoung Back, Courtney K. Harris and Bongkeun Song
	Measurement and comparison of settling velocities of cohesive sediments from the German estuaries Weser, Ems and Elbe	Patzke, J., Witt, M., Hesse, R. F., Nehlsen, E. and Fröhle, P.
	A Study on Distribution and Behavior of In-Situ Suspended Particulate Matter in Taehan Coastal, West Sea, Korea	Byoung Kwan Lee
	Isolation and Characterization of the Molecular Composition of Algal Dissolved Organic Matter	Thi Thuy Trang Pham, Que Nguyen Ho, Sang Deuk Lee, Michael Fettweis, and B.J. Lee
	Application of sediment-carrying capacity over a spring-neap tide in the Yangtze Estuary	Simin Zhou, Chunyan Zhu, Jiamin Chen and Qing He
	Sediment transport imbalance in the meso-tidal bay controlled by tidal pumping and residual circulation	S.I. Kim, J.Y. Seo, J.H. Park, P.J. Kim, and H.K. Ha
	Dynamics on sediment resuspension by wind-induced estuarine circulation in a semi-enclosed bay: Preliminary results	C.Y. Eun, J.Y. Seo, S.M. Choi, W.J. Lee and H.K. Ha
Annual changes of the surface sediment characteristics near the port of Incheon	J.W. Kim, M.H. Kim, Y.J. Song and S.B. Woo	

	Physicochemical Effects of Pyrolyzed OS on the Stabilization of Coastal Sediment	I. Jeong, H.E. Woo and K. Kim
	Comparison of different techniques for the determination of detailed vertical density profiles in cohesive sediment layers in the area of the Port of Hamburg	M. Witt, J. Patzke, E. Nehlsen and P. Fröhle
	Rheological Properties of Sediment-Water Mixtures: Experimental and empirical investigation	Mingze Lin, Xiaoteng Shen, Fang Pan
September 19 Tuesday	Sediment Transport I (Chair: Byung Joon Lee)	
09:00-09:20	Sediment fluxes at the interface between estuary and coastal sea: unravelling the role of tides, waves and river discharge from long term (2015-2022) high frequency monitoring at the SCENES Station	R. Verney, D. Le Berre, M. Repecaud, A Bocher, C. Poppeschi, F. Grasso
09:20-09:40	Tidal creeks affect the hydromorphology of bare tidal flats	J.L.J. Hanssen, Romaric Verney, Florent Grasso, D.C. van Maren, P.M.J. Herman, B.C. van Prooijen
09:40-10:00	Quantitative evaluation of the contribution of flocs to sediment flux in a Cohesive Sediment Environment	Wenjian Li, Guan hong Lee, Jongwi Chang, Ojudoo Darius Ajama, and Jae-il Kwon
10:20-10:40	Unveiling the role of marsh creeks in delivering sediment: Insights from Paulina saltmarsh	J. Sun, B. C. van Prooijen, X. Wang and Q. He
September 19 Tuesday	Bed Erosion (Chair: Guan-hong Lee)	
10:40-11:00	Effect of air exposure time on erodibility of intertidal mud flats	T. van Kessel, J. Hanssen, F. van Rees, S. Gamberoni and A. Talmon
11:00-11:20	Hydrodynamic characteristics of a field instrument of mud bed erosion response (FIMER)	Yuyang Shao, Yulin Tang, Jerome P.-Y. Maa
11:20-11:40	A novel, automatic rotating annular flume for cohesive sediment erosion experiments: Calibration and preliminary results	S.M. Figueroa and M. Son

11:40-12:00	In situ resuspension and sedimentation characteristics of tropical peat sediments in Bengkalis Island	K. Yamamoto, S. Sutikno, N. Basir, Y. Nakagawa, K. Murakami and H. Shirozu
12:00-12:40	Assessing the relationship between in-situ bed erodibility and suspended sediment concentration in intertidal flat	S.M. Choi, J.Y. Seo and H.K. Ha
September 19 Tuesday	Model II (Chair: Yasuyuki Nakagawa)	
14:00-14:20	Comprehensive analysis of siltation dynamics of approach channel: A case study of Deendayal Port, India	Balaji Ramakrishnan
14:20-14:40	Intertidal density-driven sediment flux into a port in a macro-tidal environment	S.-B. Woo, J.-S. Jeong, J. I. Song, H. S. Lee, Morhaf Aljber
14:40-15:00	The influence of lateral dynamics on the sediment dynamics in tidally dominated estuaries	M.P. Rozendaal, Y.M. Dijkstra, H.M. Schuttelaars
15:00-15:20	Upstream sediment transport in the Elbe Estuary	H. Weilbeer and S. Fuerst
15:20-15:40	Controls of the sediment composition in tidal systems	A. Colina Alonso , D.S. van Maren and Z.B. Wang
September 19 Tuesday	Seabed Processes (Chair: Francisco Fedocchi)	
16:00-16:20	A fuel cell type sensor for continuous monitoring of seabed deposition and erosion	K. Kim, Y. Nakagawa, T. Hibino, T. Nishimoto and K. Ajiki
16:20-16:40	Enhancing the quality and accuracy of mud settling and consolidation experiments	B. Brouwers, D. Meire and J. Vanlede
16:40-17:00	Estimation of sediment pickup rate in bare and vegetated channels	Yuan Xu, Qing He, Danxun Li, and Heidi Nepf

17:00-17:20	Nearbed concentration of cohesive sediments in the Río de la Plata estuary	F. Pedocchi and R. L. Mosquera
September 20 Wednesday	Sediment Transport II (Chair: Jarrell Smith)	
09:00-09:20	Storm-induced sediment transport and recovery in a tidal flat	Haisheng Yu, Zhong Peng, Weiming Xie, Xianye Wang, Qing He
09:20-09:40	Seasonal influences on land-sea fine-grained particle dynamics	T.N Markussen, R. Verney
09:40-10:00	Morphodynamic time lag effects in response to reduced fluvial sediment supply from the watershed to the estuary	Chunyan Zhu, Leicheng Guo, Bas van Maren, Zheng Bing Wang, and Qing He
10:20-10:40	Sediment exchange in mudflat-creek-marsh continuum: The evolution mechanism of intertidal environments	Weiming Xie, Leicheng Guo, Yi Meng, Xianye Wang, Zhong Peng, Qing He
September 20 Wednesday	Fludi Mud (Chair: Mohsen Soltanpour)	
10:40-11:00	Shear instabilities and stratified turbulence in an estuarine fluid mud	Junbiao Tu, Daidu Fan, Alexis Kaminski, William Smyth
11:00-11:20	Practical prediction method of nautical depths in muddy areas	Kenji Sakata, Yasuyuki Nakagawa, Mitsuyasu Iwanami
11:20-11:40	Nautical depth and rheological analysis of fine sediments in Iranian Ports	F. Shokri Alikhanlou, M. Soltanpour, F. Samsami, and S.A. Haghshenas
11:40-12:00	Using ultrasound shear waves to measure mud rheological properties a 10-year revisit	Maa, Jerome Peng-Yea, XioTeng Shan, Yuyang Shao, and Jae-Il Kwon
12:00-12:40	Numerical simulations of towing test cases for validation of a three-phase flow solver for nautical bottom problems	D.S.Ch.Praveen, Marco S. Sotelo, Djahida Boucetta, Wim Van Hoydonck, Marc Vantorre, Guillaume Delefortrie and Erik A. Toorman

September 21 Thursday	Sediment Transport III (Chair: Jez Spearman)	
09:00-09:20	Dredging impacts on concentration and settling velocity of suspended particles in Gyeonggi Bay, Korea	H.J. Ha, S.M. Choi and H.K. Ha
09:20-09:40	How subsidence and cyclone driven sediment flux within Galveston Bay has caused elevated siltation within the Bayport Channel and Flare	Timothy M. Dellapenna, Nathalie Jung, Richard Schenk, Scott Sudduth, Peng Lin, and Jens Figlus
09:40-10:00	Impacts of consecutive typhoons on the resuspension of sediment and microphytobenthos in the macro-tidal flat	S.W. Jeong, H.J. Ha and H.K. Ha
10:20-10:40	Different effects of cold front and tropical cyclone on short-term sediment dynamics in the delta front of the Changjiang Estuary	Xuefeng Wu, Chunyan Zhu, Jianliang Lin, Jian Shen and Qing He
September 21 Thursday	Flocs II (Chair: Erik Toorman)	
10:40-11:00	Estuarine light attenuation, scattering, and absorption as a function of suspended floc properties and other water column constituents	K.A. Fall, C.T. Friedrichs, and G.M. Massey
11:00-11:20	Quantitative evaluation of the influence of floc composites on floc dynamics	O.D. Ajama, G. Lee, J. Chang, and W. Li, and J.I. Kwon
11:20-11:40	Field experiments on settling velocity and flocculation ability of muddy sediments in estuaries	S. Defontaine, I. Jalon-Rojas and A. Sottolichio
11:40-12:00	Experimental study on the effects of sediment size gradation on the settling velocity of cohesive sediment	Yige Jing, Jinfeng Zhang, Qinghe Zhang, Jerome P.-Y. Maa
12:00-12:40	Do cohesive sediment flocs contain sand particles and does it matter?	J.Spearman and A.Manning
September 21 Thursday	Model III (Chair: Bram van Prooijen)	

14:00-14:20	Mud mass transport around the access channel of Bushehr Port – the Persian Gulf	S. Movahedinejad, M. Soyuf Jahromi, S. M. Siadatmousavi, A. Farhangmehr and S. A. Haghshenas
14:20-14:40	Assessing the environmental impacts of the bypass navigation channel in Mekong delta, Southern Vietnam	H.S. Nguyen, L.T.D. Tran, V.N. Dau, T.T. Huynh, and T.V. Bui
14:40-15:00	Evolution of suspended sediment fluxes following seagrass loss in a mesotidal lagoon	Arnaud Le Pevedic, Florian Ganthy, Aldo Sottolichio
15:00-15:20	Seasonal and interannual sediment dynamics in the Bay of Biscay: exploring 20y hindcast model results	Y. Fossi Fotsi, R. Verney, S. Le Gac, and A. Gangloff
15:20-15:40	Suspended sediment dispersal offshore of the Ayeyarwady delta, Myanmar	C.K. Harris, M.J. Fair, E. Whitehead-Zimmers, and D. Yin
September 21 Thursday	Sediment Transport IV (Chair: Romaric Verney)	
16:00-16:20	Application of sediment composition index to predict suspended particulate matter concentration in the North Sea	D. Tran, X. Desmit, R. Verney and M. Fettweis
16:20-16:40	Estimating bed shear stress with inertial dissipation methods using suspended sediment concentration on the Songdo tidal flat	J. Chang, W. Li, G. Lee, and O.D. Ajama
16:40-17:00	Extracting suspended sediment concentration periodicity from diverse datasets	Y. Wang, H. Lin, Q. Yu and S. Gao
September 22 Friday	Sediment Transport V (Chair: Seungbuhm Woo)	
09:00-09:20	Gravity-driven sediment transport processes on muddy coasts	Q. Yu, Y. Peng and S. Gao
09:20-09:40	Foraminifera response to changes in mud sedimentation and marine environmental health, case of Bushehr port, Iran	Shadan Nasserri Doust, Mehrnoosh Abbasian, Majid Shah-hosseini, S. Abbas Haghshenas

09:40-10:00	Mud particle velocity in the near wall region and entrainment into suspension	Kyle Strom, Thomas Ashley, and Juergen Schieber
10:20-10:40	Erosion, transport, and abrasion of dense mud aggregates	S. Jarrell Smith, Kelsey A. Fall, David W. Perkey, Richard Styles, and Danielle R. Tarpley
September 22 Friday	Mud Rheology/Consolidation (Chair: Carl Friedrichs)	
10:40-11:00	Application of artificial neural network for determining rheological properties of mixed sediment in the Persian Gulf	M. Hajibaba, F. Samsami and S. A. Haghshenas
11:00-11:20	Simulation of fluid mud flow through FVCOM model with considering three-dimensional rheological properties	Gaochuang Shi, Qinghe Zhang, Jinfeng Zhang
11:20-11:40	Turbulence measurements in a hyperturbid estuary	M. Becker, R. Kopte, M. Naulin, C. Maushake and C. Winter
11:40-12:00	A new unified consolidation concept based on Terzaghi and Gibson theories	A. Malcherek, K. Kaveh

Session: Model 1
10:40 – 12:40
Monday, September 18, 2023



17th International Conference on
Cohesive Sediment Transport Processes
September 18-22, 2023
Inha University, Incheon, Republic of Korea



Modelling the thixotropic behavior of fluid mud: revised

Erik.A.Toorman¹ and D.S.Ch.Praveen¹

¹Hydraulics & Geotechnics Section, Department of Civil Engineering, KU Leuven,
Leuven, Belgium, erik.toorman@kuleuven.be

1. Introduction

Fluid mud can be defined as a mixture of cohesive sediments (clay, silt, sand and organic matter) in water at concentrations just above the gel point, the solids volume fraction where the particles form a 3D continuous matrix. The corresponding bulk density typically lies in the range 1100-1200 kg/m³. The study of the flow behaviour of fluid mud (and other similar slurries) is of practical engineering importance for dredging, the study of ship-mud interaction (nautical bottom research), submarine and terrestrial gravity flows (density currents) and wave-mud interactions. Numerical simulation of such flows requires a rheological closure for the effective viscosity of such mixtures.

Fluid mud is typically characterized as a yield stress fluid, but its effective viscosity is found to depend on the instantaneous microstructure of the particle matrix, as a result of break-up and/or aggregation of the cohesive clay particles and polymeric organic matter. Therefore, the stress-strain rate relationship is not only a function of the shear rate, but also depends on the local structure. This time-dependent behaviour is known as thixotropy.

A lot of viscosity measurements on mud do not consider thixotropy, which leads to unsuitable protocols, wrong interpretations and subsequently erroneous viscosity closures in numerical modelling. Existing models still show various flaws. We propose a new dual-structure thixotropic viscosity closure for mud, validated with new dedicated rheometric experiments in a wide-gap Couette viscometer.

2. Methodology

The most practical and successful approach to include thixotropy into a rheological closure, suitable for implementation in a CFD code, is with structural kinetics, similar as for flocculation. Toorman (1997) developed such a model, which was validated with a wide range of experimental data from the literature. Nevertheless, Dullaert (2005) noticed that the model shows a flaw, i.e. that its asymptotic behaviour for high shear rates is not entirely correct. This (small) error, resulting from a wrong assumption by lack of the necessary experimental data, has immediately been corrected. The corrected model has subsequently been revised again to result in a more elegant form, which eventually has been described in (Toorman *et al.*, 2014). Over these years, many measurements on mud were carried out in the sediments laboratory of Flanders Hydraulic Research, but the data showed various deviations from the ideal behaviour predicted by the model. The discrepancies were attributed to additional effects that could not be taken into account, i.e. slip and gravitational effects. Moreover, the data also provided hints that the thixotropy involves multiple time scales and/or non-linear kinetics. Therefore, as the work was unfinished, the report with the updated model has not been made publically available. The “Nautical Bottom” FWO project G0D5319N (2019-2023) provided the means to investigate the problem in further depth. The combination of new dedicated experiments and

numerical modelling of the behavior of fluid mud in the rheometer resulted in the replacement of the usual spindle types by a serrated spindle, which greatly reduces the slip problems with a smooth cylindrical spindle at low rotation speeds and the secondary flow problems with a vane spindle at high rotation speeds (Praveen & Toorman, 2023a). The processed data, using the iterative method of Toorman (1994), confirm that the Worrall-Tuliani rheological model gives the best representation of the equilibrium flow curve of fluid mud.

The resulting transient data for a change in rotation speed (from very high to break-up the structure) to any given RPM shows that, even in the long run, no true equilibrium is achieved. It is suspected that gravitational effects start to play a role over the longer time. The initial stress growth with time shows not a single but a double exponential behavior. The latter suggests that the thixotropic behavior involves two time scales, to be associated to different structural changes.

After consideration of different ways of incorporating this observation into a thixotropy closure, an elegant solution was found by introducing two structural parameters, each with their own structural kinetic equation, incorporated in an extended version of the available single-structure model. A procedure has been developed to process transient data from the shear-rate step change experiments in a wide-gap Couette viscometer to determine all the parameters of the new dual-structure model. A full description of the model and its validation is found in (Toorman & Praveen, 2023).

A further improvement of the data processing of mud rheometry in a wide-gape Couette viscometer which additionally assesses the effect of gravity is under investigation by incorporating the relevant physical processes in a two-phase mixture CFD model (Praveen & Toorman, 2023b).

Acknowledgments

This work is partially funded by the Science Foundation - Flanders through the FWO project G0D5319N. Flanders Hydraulics Research is thanked for allowing the use of their rheometer (Anton Paar Physica MCR301).

References

- Dullaert, K. (2005). Constitutive equations for thixotropic dispersions. PhD dissertation, Dept. of Chemical Engineering, K. U. Leuven, 197 pp.
- Praveen, D.S.Ch., Toorman E.A. (2023a). The determination of the true equilibrium flow curve for fluid mud in a wide gap Couette rheometer. (submitted to) *J. Non-Newtonian Fluid Mechanics*.
- Praveen, D.S.Ch., Toorman E.A. (2023b). Development of a three-phase CFD model for cohesive sediment transport. Book Of Abstracts, INTERCOH 2023.
- Toorman, E.A. (1994). An analytical solution for the velocity and shear rate distribution of non-ideal Bingham fluids in concentric cylinder viscometers, *Rheologica Acta*, 33(3), 193–202. doi: 10.1007/BF00437304.
- Toorman, E.A. (1997). Modelling the thixotropic behaviour of dense cohesive sediment suspensions, *Rheologica Acta*, 36(1), 56–65. doi: 10.1007/BF00366724.
- Toorman, E.A., Liste, M., Heredia, M., Rocabado, I., Vanlede, J., Delefortrie, G., Verwaest, T., Mostaert, F. (2014). CFD Nautical Bottom: Subreport 1: Rheology of Fluid Mud and its Modeling. Version 3_0. WL Reports, 00_048. Flanders Hydraulics Research, KU Leuven Hydraulics Laboratory & Antea Group: Antwerp, Belgium.

Toorman E.A., Praveen, D.S.Ch. (2023). A dual-structure thixotropy model for cohesive slurries, validated with wide-gap Couette viscometry for fluid mud. (in preparation for) J. Rheology.



17th International Conference on
Cohesive Sediment Transport Processes
September 18-22, 2023
Inha University, Incheon, Republic of Korea



Application of an 1-DV TCPBE model with Bayesian calibration to diagnose the flocculation potential in the laboratory experiments and field measurement

T. T. Huynh¹, Michael Fettweis², Byung Joon Lee¹

¹ Department of Advanced Sciences and Technology Convergence, KNU, Sangju 37224, Korea

² Royal Belgian Institute of Natural Sciences, Rue Vautier 29, 1000 Brussels, Belgium

Abstract

In the aquatic environment, flocculation plays an important role in determining the size, settling velocity and deposition rate of the cohesive sediment. The aggregation and breakage of the particles under turbulent flow field regulates the deposition process. This paper describes a Two-Class Population Balance Equation (TCPBE) in couple with the Reynold-averaged Navier Stokes based 1-Dimension Vertical (1-DV) model to diagnose the flocculation potential in both laboratory experiments and in-situ measurement. The Bayesian analysis is utilized as the calibration tool which examines the unknown posterior parameters, model uncertainties compared with the experimental and field observation data. Results show that, the 1-DV TCPBE with the effect of k - ϵ turbulent closure and mass balance equation is capable to simulate the bimodal flocculation of the marine and estuarine sediment. In addition, the simplified model also showed its capability on the implementing of the large-scale multimodal flocculation in the flow field of estuary and marine area.

Keywords: *Cohesive sediment, Flocculation, Population Balance Equation, Reynolds-averaged Navier-Stokes.*

The govern equations

The Reynold-averaged Navier Stokes based 1-Dimension Vertical (1-DV) and Two-Class Population Balance (TCPBE) equation.

$$\frac{\partial N_i}{\partial t} = \frac{\partial}{\partial z} \left(C'_\mu \frac{k^2}{\epsilon} \frac{\partial N_i}{\partial z} \right) - w_{s,i} \frac{\partial N_i}{\partial z} + (A_i + B_i) \quad (1)$$

$$(A_P + B_P) = \frac{dN_P}{dt} = -\frac{1}{2} \alpha \beta_{PP} N_P N_P \left(\frac{N_C}{N_C - 1} \right) - \alpha \beta_{PF} N_P N_F + f N_C a_F N_F$$

$$(A_F + B_F) = \frac{dN_F}{dt} = +\frac{1}{2} \alpha \beta_{PP} N_P N_P \left(\frac{1}{N_C - 1} \right) - \frac{1}{2} \alpha \beta_{FF} N_F N_F + a_F N_F \quad (2)$$

$$(A_T + B_T) = \frac{dN_T}{dt} = +\frac{1}{2} \alpha \beta_{PP} N_P N_P \left(\frac{N_C}{N_C - 1} \right) + \alpha \beta_{PF} N_P N_F - f N_C a_F N_F$$

Preliminary results

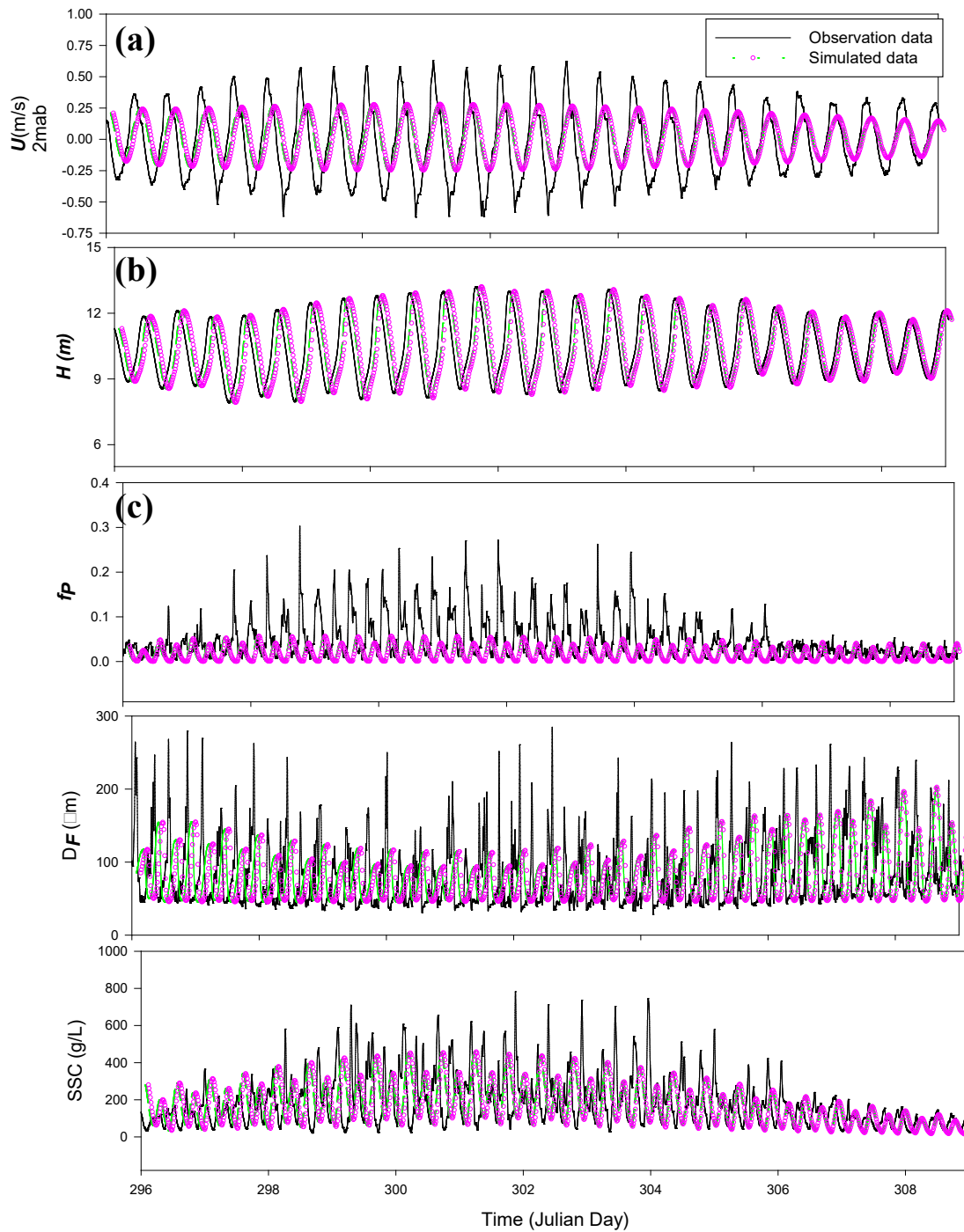


Figure 1. Time series of the measured and simulated results (a) bottom shear velocity U_{2mab} ; (b) water depth H ; (c) flocculi mass fraction f_p ; (d) volume mean floc diameter D_F ; (e) Suspended solid concentration SSC .

Acknowledgement

This work was supported by the National Research Foundation of Korea (Grant No. NRF-2020R1I1A3A04036895).



17th International Conference on
Cohesive Sediment Transport Processes
September 18-22, 2023
Inha University, Incheon, Republic of Korea



On numerical modeling of flocculation and cohesive sediment transport in the bottom boundary layer

J. A. Penaloza-Giraldo¹, L. Yue^{2,3}, T.J Hsu², B. Vowinckel⁴, E. Meiburg⁵, A.J. Manning^{3,6}

¹ Department of Civil and Environmental Engineering, Center for Applied Coastal Research, University of Delaware, Newark-Delaware, Unit States of America, japg@udel.edu

² Department of Civil and Environmental Engineering, The Bob and Norma Street Environmental Fluid Mechanics Laboratory, Stanford University, Stanford, CA 94305, USA

³ Department of Civil and Environmental Engineering, Center for Applied Coastal Research, University of Delaware, Newark-Delaware, Unit States of America

⁴ Leichtweiß-Institute for Hydraulic Engineering and Water Resources, Technische Universität Braunschweig, Braunschweig, Lower Saxony 38106, Germany

⁵ Department of Mechanical Engineering, UC Santa Barbara, Santa Barbara, CA 93106, United States

⁶ HR Wallingford Ltd, Coasts and Oceans Group, Wallingford OX10 8BA, United Kingdom

1. Introduction

Cohesive sediment transport is crucial in aquatic systems since many processes (e.g., dissolved oxygen transfer, light extinction, fate of spilt oil, morphodynamics) can be altered via the flocculation, causing deterioration in ecosystems (Ye et al., 2020). Hence, many cohesive sediment transport models with flocculation capabilities have been developed using turbulence closures such as Reynolds-averaged models (Sherwood et al., 2018) or Large Eddy Simulation (LES) (Liu et al., 2019) to represent the physics of the aggregation/breakup process. These models use the computed turbulent shear rate $S = \sqrt{\varepsilon/\nu}$ in the entire computation domain by calculating the turbulent dissipation rate ε and the kinematic viscosity ν . However, our general understanding on flocculation effect of cohesive sediment transport in bottom boundary layer is limited. This study focuses on developing a modelling framework for a statistically averaged turbulent flow in dilute conditions, which incorporates the Population Balance Equation (PBE) and predict the weight-averaged floc property profiles such as floc density, floc diameter and settling velocity. To obtain high-fidelity turbulence statistics in bottom boundary layer, we use Direct Numerical Simulation (DNS) data (Yue et al., 2020) to establish the initial conditions (i.e., turbulent shear rate and fine sediment profiles). The DNS model uses a constant particle settling velocity w_s and a flocculation effect on w_s is not included.

2. Methodology

The modelling framework requires a statistically averaged flow and sediment concentration profile as input to drive the population balance equation flocculation model FLOCMOD (Verney et al., 2011) and a fractal relationship for calculating floc settling velocity at each vertical location. The newly obtained variable settling velocity profile is computed considering the distributed mass concentration over the floc size distribution via a weighted-average operation. This settling velocity profile is then used to calculate a new sediment concentration

profile using the statistically averaged mass balance equation under the dilute assumption (turbulent flow statistics remain unchanged) expressed as

$$K_s \frac{dC}{dx_3} + W_f C - \langle u'_3 c' \rangle = 0, \quad (1)$$

where, x_3 is the vertical direction, C is the statistically averaged sediment concentration, K_s is the sediment diffusivity, $\langle u'_3 c' \rangle$ is the turbulent flux of sediment, and W_f is the settling velocity. Here, the estimated sediment concentration profile C is forced to conserve the total mass concentration in the domain identical to that of the initial input. From the DNS data, eddy viscosity ν_t can be calculated and turbulent Schmidt number $Sc_t = \nu_t/K_t = 1$ is specified, consistent with DNS data for dilute condition. This emphasizes that any initial profile from another source (e.g., measurements or models) can be used in this modeling framework. The newly integrated concentration profile becomes the input to run the PBE model for the next iteration step. This iterative process is repeated until the settling velocity profile W_f reaches a convergence.

The first case to test the modelling framework is a statistically steady boundary layer flow at Reynolds number $Re_\tau = 180$ based on the friction velocity $u_\tau = 0.009$ m/s and channel depth. For fine sediment transport, a constant settling velocity of 0.5 mm/s (no flocculation) is specified, and the bottom critical shear stress is set to be $\tau_c = 1 \times 10^{-1}$ Pa. The resulting suspended sediment is dilute (the maximum concentration is about 0.1 kg m^{-3} , see Figure 2b) and the turbulent shear rate profile S remains unchanged with the presence of sediment (see Figure 1a). These two profiles are used as input to run the flocculation model. 75 floc size classes is chosen to discretize the floc size distribution, which has been shown to have a good representation in coarse fraction (Penaloza-Giraldo et al., 2023). The maximum floc size class is specified to be 2500 μm and the simulation time is 5000 min. This computational time is more than enough for an equilibrium state to be reached at each vertical value of the profile. For flocs located closer to the bed where turbulence and sediment concentration are both large, it only requires about 120 min to reach the equilibrium state. The iterative process is completed when a convergence for the settling velocity profile is obtained for a tolerance value of 1×10^{-6} m/s.

3. Results

Profiles for floc properties due to aggregation/breakup effects are presented in Figure 1 in a given simulation. The results show that a convergence is reached in four iterations for $r = 5$ (see magenta line in Figure 1), and a strong vertical variability in the floc properties is observed (see Figure 1 c, d and e). Moreover, a more well-mixed sediment concentration profile in the water column (see blue line Figure 2b) and a bimodal distribution in floc size distribution (see blue line Figure 2c) are obtained when the breakup dominates ($r = 2.5$). In contrast, when the aggregation dominates ($r = 10$), the concentration at bottom increases due increases of settling velocity (see red line Figure 2b), and the floc size distribution becomes unimodal (see red line Figure 2c). More results will be presented at the conference.

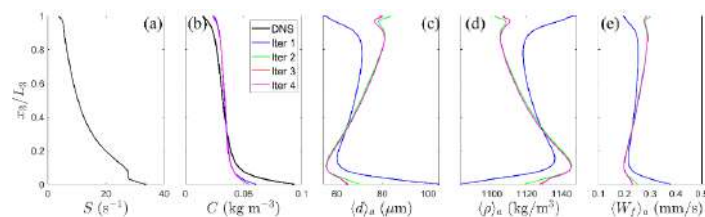


Figure 1. Vertical profiles of (a) Turbulent shear rate, (b) sediment mass concentration, (c) averaged floc diameter, (d) floc density and (e) settling velocity at different iterations

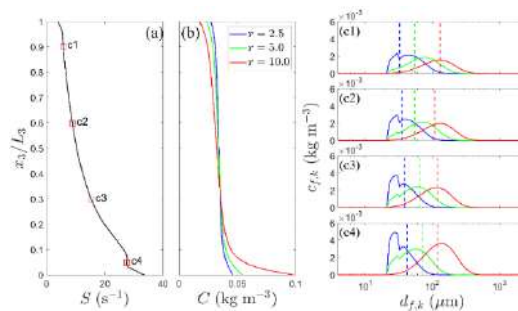


Figure 2. The effect of aggregation dominance (increasing $r = \alpha/\beta$). (a) Turbulent shear rate profile, (b) mass concentration profile, and (c) mass concentration distributions over floc size classes at four different locations (c1) $x_3/L_3 = 0.9$, (c2) $x_3/L_3 = 0.6$, (c3) $x_3/L_3 = 0.3$, and (c4) $x_3/L_3 = 0.05$. The dashed lines correspond to the d_{50} .

4. Conclusions

A new cohesive sediment transport model framework for a statistically steady turbulent flow in dilute conditions is reported. This framework allows the study of floc properties and the resulting settling velocity and concentration distribution in the bottom boundary layer. Results reveal the relative importance of aggregation versus breakup on cohesive sediment transport. The results show that vertical variability of settling velocity is significant (at least by a factor of 2) even in dilute conditions.

References

- Liu, J., Liang, J.-H., Xu, K., Chen, Q., and Ozdemir, C. E.: Modeling Sediment Flocculation in Langmuir Turbulence, *J. Geophys. Res. Ocean.*, 124, 7883–7907, <https://doi.org/10.1029/2019JC015197>, 2019.
- Penaloza-Giraldo, J. A., Hsu, T.-J., Manning, A. J., Ye, L., Vowinckel, B., and Meiburg, E.: On the importance of temporal floc size statistics and yield strength for population balance equation flocculation model, *Water Res.*, 233, 119780, <https://doi.org/https://doi.org/10.1016/j.watres.2023.119780>, 2023.
- Sherwood, C. R., Aretxabaleta, A. L., Harris, C. K., Rinehimer, J. P., Verney, R., and Ferré, B.: Cohesive and mixed sediment in the Regional Ocean Modeling System (ROMS v3.6) implemented in the Coupled Ocean–Atmosphere–Wave–Sediment Transport Modeling System (COAWST r1234), *Geosci. Model Dev.*, 11, 1849–1871, <https://doi.org/10.5194/gmd-11-1849-2018>, 2018.
- Verney, R., Lafite, R., Claude Brun-Cottan, J., and Le Hir, P.: Behaviour of a floc population during a tidal cycle: Laboratory experiments and numerical modelling, *Cont. Shelf Res.*, 31, S64–S83, <https://doi.org/10.1016/j.csr.2010.02.005>, 2011.
- Ye, L., Manning, A. J., and Hsu, T.-J.: Oil-mineral flocculation and settling velocity in saline water, *Water Res.*, 173, 115569, <https://doi.org/https://doi.org/10.1016/j.watres.2020.115569>, 2020.
- Yue, L., Cheng, Z., and Hsu, T.-J.: A Turbulence-Resolving Numerical Investigation of Wave-Supported Gravity Flows, *J. Geophys. Res. Ocean.*, 125, e2019JC015220, <https://doi.org/10.1029/2019JC015220>, 2020.



17th International Conference on
Cohesive Sediment Transport Processes
September 18-22, 2023
Inha University, Incheon, Republic of Korea



Modeling the Transport and Abrasion of Dense Mud Aggregates in the James River Estuary

Earl J. Hayter¹, Jonathan C. Hollingsworth², S. Jarrell Smith¹, and Danielle R. Tarpley¹

¹ U.S. Army Engineer Research and Development Center, Vicksburg, Mississippi, USA

Earl.Hayter@usace.army.mil

² Aquanuity, LLC. Greenwood, CO, USA

1. Introduction

Dredged sediment erodes as aggregates and is a primary transport mechanism for cohesive dredged sediment. Aggregate transport is significantly different than primary particles or floc transport and typically reduces dispersion of clay/silt. However, aggregate transport is not commonly available in sediment transport models used to evaluate, e.g., beneficial use (BU) of dredged material. Therefore, a primary process in estuarine sediment transport is missing, leading to increased model uncertainty. Testing of mud aggregates collected in the James River, a tributary of the Chesapeake Bay, US in an aggregate tumbler and a flume found that the aggregates undergo abrasion when being transported as bedload (Perkey et al., 2020). Without simulating the transport and abrasion of aggregates, fine-grained sediment transport models would generally over predict dispersion and under predict stability, and would not be able to appropriately quantify strategically placed sediment benefits to targeted resources (such as marshes), amount returning to the nearby navigation channel, or risks associated with BU applications. This study describes a preliminary evaluation of aggregate transport and abrasion modeling, with application in the James River.

2. Study Description

Using the results presented by Perkey et al. (2020), an aggregate abrasion routine was developed and added to a simplified one-dimensional (1D) sediment transport model and to an existing three-dimensional (3D) hydrodynamic and sediment transport model that simulated four size classes of mud aggregates (3,500 μm , 300 μm , 80 μm and 20 μm). The abrasion routine was developed using a theory by Parker (1991) to simulate the abrasion of mud aggregates that were being transported at bedload. Instead of changing the diameter of the aggregate as it is transported and undergoes abrasion, abrasion was simulated by transferring mass from aggregates moving as bedload to the next smaller size aggregate size class as well as to a 20 μm aggregate size class that represents the by-product of abrasion. As the smaller mud aggregates were less likely to deposit, this resulted in less mass of mud aggregates in the sediment bed when abrasion was being simulated. As the 1D and 3D sediment transport models use an Eulerian grid and time frame, transferring mass between aggregate size classes allows the abrasion routine to be used as opposed to a Lagrangian particle tracking model where the diameter of each individual aggregate would decrease while being transported as bedload.

The 1D model application provided an appropriate platform to test the ability of the abrasion routine to simulate the process of abrasion in a closed system, including the transfer from larger to smaller size classes of aggregates. These tests showed that abrasion resulted in a decrease in

the mass of model aggregates transported as bedload and an increase in the mass of mud aggregates transported in suspension.

The aggregate abrasion routine was added to the 3D Geophysical Scale Multi-Block (GSMB) modeling system developed by Chapman et al. (2020) and applied to a hydrodynamic, salinity and sediment transport model of the Chesapeake Bay. The SEDZLJ mixed sediment bed model developed by Jones and Lick (2001) is used in GSMB. A month long simulation with abrasion resulted in the bedload concentrations of the two largest aggregate size classes, analysed at 1.2 km and 2.2 km away from a dredged material placement site in the James River to be less than five percent of the bedload concentrations given by the model simulation without abrasion. This indicated that the mud aggregates transport as bedload were losing over 95 percent of the mass of the 3,500 μm and 300 μm aggregate size class within the first few kilometres of transport due to abrasion. This finding was expected based on the research by Perkey et al. (2020). In the portions of the navigation channel that were analysed, all within 11 km of the placement site in the James River, the simulation of abrasion resulted in a 55 to 75 percent decrease in the total mass of mud aggregates in the sediment bed compared to the simulation without abrasion. This was due to the abrasion routine transferring mass from larger mud aggregates being transported as bedload to smaller mud aggregates, primarily in suspension that were less likely to deposit.

3. Conclusions

This modeling study of the transport and abrasion of dense mud aggregates in addition to the transport of mixed cohesive and noncohesive sediment as was performed in the modeling of the James River estuary found that the simulation of aggregate transport and abrasion could be important for certain applications, particularly for disturbances of densely consolidated sediments as produced by dredging, slope or bank failure, or extreme events.

References

- Chapman, Ray S, Phu Luong, Sung-Chan Kim, and Earl Hayter. 2022. "Development of Three Dimensional Wetting and Drying Algorithm for the Geophysical Scale Transport Multi-Block Hydrodynamic, Sediment and Water Quality Transport Modeling System ," ERDC/TN DOER-L2, Dredging Operations and Environmental Research Program, U.S. Army Engineer Research and Development Center, Vicksburg, MS.
- Hollingsworth, Jonathan C. 2021. "Modeling the Abrasion and Transport of Mud Aggregates in the James River, VA." MS Thesis, Department of Civil Engineering, Clemson University, Clemson, SC.
- Jones, Craig A., and Willy Lick. 2001. SEDZLJ: A Sediment Transport Model. *Final Report*. University of California, Santa Barbara, California.
- Parker, Gary. 1991. "Selective sorting and abrasion of river gravel. I: Theory." *Journal of Hydraulic Engineering* 117 (2): 131-147.
- Perkey, David W, S Jarrell Smith, Kelsey A Fall, Grace M Massey, Carl T Friedrichs, and Emmalynn M Hicks. 2020. "Impacts of Muddy Bed Aggregates on Sediment Transport and Management in the Tidal James River, VA." *Journal of Waterway, Port, Coastal, and Ocean Engineering* 146 (5): 04020028. [https://doi.org/10.1061/\(ASCE\)WW.1943-5460.0000578](https://doi.org/10.1061/(ASCE)WW.1943-5460.0000578)



17th International Conference on
Cohesive Sediment Transport Processes
September 18-22, 2023
Inha University, Incheon, Republic of Korea



Development of a three-phase CFD model for cohesive sediment transport

D.S.Ch.Praveen¹ and Erik.A.Toorman¹

¹Hydraulics & Geotechnics Section, Department of Civil Engineering, KU Leuven,
Leuven, Belgium, praveen.suryachalapraveen@kuleuven.be

1. Introduction

Most engineering applications involving cohesive sediment laden free-surface flows require a numerical three-phase solver, where water and sediment mix together, while the air phase and water-sediment suspension phase remain immiscible. However, many existing models simplify the problem by presuming the water-sediment mixture as a single phase and solving the Reynolds-Averaged Navier-Stokes equations with an additional sediment transport equation. These models fail to capture the two- and four-way coupling between the phases, leading to the omission of velocity lag and momentum transfer between phases. Experimental evidence suggests that sediment particles do not follow the fluid velocity but lag behind it, emphasizing the need for a more reliable approach, such as using a rheological closure with physics-based methods. Recently, Ouda and Toorman, (2019) developed a physics-based three-phase model for non-cohesive sediments that includes slip velocity, momentum transfer, and granular rheology. The present study aims to this model to a three-phase solver for cohesive sediments by modifying the non-cohesive sediment closures to cohesive sediment closures.

1.1 Governing equations

Equations 1-3 depict the sediment volume conservation, the volume of fluids (VOF) equation for tracking the free surface, and the three-phase moment conservation equation as a function of mixture velocity, slip velocity, and source terms of momentum transfer between phases. A detailed derivation for these equations is found in (Ouda & Toorman, 2019).

$$\frac{\partial \alpha_s}{\partial t} + \nabla \cdot (\alpha_s \mathbf{v}) + \nabla \cdot \left[\alpha_s \left(\frac{\alpha_w}{\gamma} - \frac{\alpha_w \alpha_s (\rho_s - \rho_w)}{\rho} + \frac{\alpha_s \alpha_w \alpha_a (1-S)}{\rho} \right) \mathbf{w} \right] = 0 \quad (1)$$

$$\frac{\partial \alpha_w}{\partial t} + \nabla \cdot (\alpha_w \mathbf{v}) + \nabla \cdot \left[\alpha_w \left(-\frac{\alpha_s}{\gamma} - \frac{\alpha_w \alpha_s (\rho_s - \rho_w)}{\rho} + \frac{\alpha_s \alpha_w \alpha_a (1-S)}{\gamma(\alpha_w + \alpha_s S)} \right) \mathbf{w} \right] + \nabla \cdot (\alpha_w \alpha_a \mathbf{U}_c) = 0 \quad (2)$$

$$\frac{\partial \rho \mathbf{v}}{\partial t} + \nabla \cdot (\rho \mathbf{v} \mathbf{v}) = -\nabla (p_{rgh} + p_s) + \nabla \cdot [\bar{\tau} + \tau^T + \tau_{s-w}^D + \tau_{m-a}^D] \quad (3)$$

where, $\alpha_s, \alpha_w, \alpha_a$ = air, water and sand volume fraction, \mathbf{v} = mixture velocity (vector), \mathbf{w} = slip velocity (vector), ρ = mixture density, ρ_w, ρ_s = water and sand density, and $\tau_{s-w}^D, \tau_{m-a}^D$ = momentum diffusion between the phases due to the slip velocity.

These equations apply to both non-cohesive and cohesive sediments. However, equation 3 requires modification in its closures to replace the non-cohesive terms by cohesive sediment

closures. The terms $\bar{\tau}$ = viscous stress and p_s = solid pressure differ for non-cohesive sediments and cohesive sediments (mud). The first term requires a mixture viscosity and eddy viscosity, and the latter requires consolidation closures. To obtain the mixture viscosity, an improved rheology experiment protocol and new thixotropic constitutive equations have been developed. Whereas the additional pressure due to consolidation will be updated with permeability and pore pressure data obtained from mud consolidation experiments. In addition to rheology, thixotropy and consolidation closures, a wall-distance free low-Reynolds turbulence model is developed to capture the flow in all the regimes.

2. Mud Rheology

2.1. Fluid mud rheometry

The procedure to obtain the mixture viscosity is improved by three major changes. Firstly, the vane spindle is replaced with a 3D printed serrated spindle, shown in Figure 1a. The four bladed vane configuration is presumed to have the advantage of avoiding the slip effect and therefore used to study the rheology of fluid mud. However, recent studies show that the fluid between the vane blades yields and thus underestimates the equilibrium flow curve. Therefore, a new serrated spindle, which consists of sharp vertical grooves on the cylinder surface to avoid slip effect, was designed, which improved the determination of the equilibrium flow curve.

Secondly, changes have been made to the rheological protocol of Flanders Hydraulics Research (Claeys et al., 2015). In his protocol, a shear-rate-step change method is used with pre-shear before each RPM. However, in the present work, the time for each RPM has been increased. It has been observed, as shown in Figure 1b, that the equilibrium is not reached at 100 s but much later, depending on the density. Equilibrium values are reached earlier for higher densities compared to lower densities. Therefore, the protocol time must be monitored for each density and RPM until equilibrium is reached.

Finally, the non-Newtonian end correction, obtained with the help of CFD, is applied. A 2D wedge type mesh is developed as the flow is axisymmetric around the vertical axis (Figure 1c). It is observed that this correction factor slightly increases with RPM, but the change with the fluid density is nominal. In the end, the torque values obtained from the rheometer with the end correction can be converted to shear stress values and the RPM is converted to shear rate data by using the iterative procedure proposed by Toorman (1994) with the Worrall-Tuliani model.

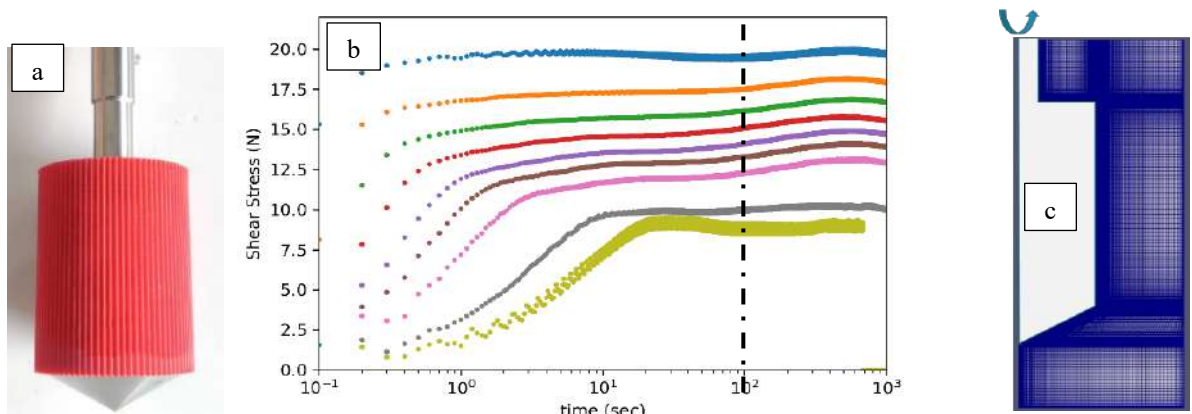


Figure 1 (a) serrated spindle, (b) stress evolution for each constant RPM and (c) vertical section of the 2D mesh to obtain end corrections in CFD

2.2. Thixotropic constitutive equation for fluid mud rheology

The thixotropic constitutive equation for cohesive mud is a corrected version of (Toorman, 1997). However, this model is based on a structural kinetic equation which considers a single

exponential behaviour of the stress evolution. But in rheological experiments it is observed that the stress evolution has a double exponential behaviour (Figure 1b). The first exponential curve is to deform the soil skeleton, while the second exponential curve represents the floc evolution. Therefore, a new thixotropic model, using structural kinetic theory, is developed considering the double exponential behaviour and included in the mixture viscosity model to capture the stress evaluation over time (Toorman & Praveen, 2023).

3. Consolidation closure

Consolidation experiments are carried out to determine the gel point and the excess pore pressure profiles over the column. The excess pore pressure and density profile data are used to estimate the permeability coefficient and the change in effective stress over time, which will be used with Darcy's law to obtain the pressure difference due to consolidation. This pressure difference is used as a closure in equation 3.

4. Turbulence closure

A new wall-distance free low-Re turbulence model is developed to estimate the flow profiles from the laminar viscous sub-region, the transition region and the fully-developed turbulence region. In this model, the mixture viscosity is coupled with the eddy viscosity to dampen the turbulence in high viscous regions.

5. Conclusions

In the present work, a new three-phase solver is developed for free-surface flows of cohesive sediment suspensions. The model consists of different closures including the mixture viscosity with an improved rheology protocol, a new thixotropic constitutive equation which captures the double exponential behaviour, a consolidation closure and an improved wall-distance free low-Reynolds turbulence model.

Acknowledgments

This work is funded by the Science Foundation - Flanders through the FWO project G0D5319N,.

References

- Claeys, S., Staelens, P., Vanlede, J., Heredia, M., Van Hoestenbergh, T., Van Oyen, T. and Toorman, E. (2015). A rheological lab measurement protocol for cohesive sediment, Book of Abstracts 13th Int. Conf. on Cohesive Sediment Transport Processes (Oostende: VLIZ), 20-21.
- Ouda, M. and Toorman, E. A. (2019). Development of a new multiphase sediment transport model for free surface flows, *International Journal of Multiphase Flow*, 117, 81–102. doi: 10.1016/j.ijmultiphaseflow.2019.04.023.
- Toorman, E.A. (1994). An analytical solution for the velocity and shear rate distribution of non-ideal Bingham fluids in concentric cylinder viscometers, *Rheologica Acta*, 33(3), 193–202. doi: 10.1007/BF00437304.
- Toorman, E.A. (1997). Modelling the thixotropic behaviour of dense cohesive sediment suspensions, *Rheologica Acta*, 36(1), 56–65. doi: 10.1007/BF00366724.
- Toorman E.A., Praveen, D.S.Ch. (2023). Modelling the thixotropic behavior of fluid mud: revised. Book of Abstracts, INTERCOH 2023.

Session: Flocs 1
14:00 – 15:40
Monday, September 18, 2023



17th International Conference on
Cohesive Sediment Transport Processes
September 18-22, 2023
Inha University, Incheon, Republic of Korea



Reconstructing 3-dimensional morphological structure of fine sediment floc and settling process using a multi-camera system

L. Ye^{1,2}, Z. Chen¹, J. Wu^{1,2} and R. Liao³

¹ School of Marine Sciences, Sun Yat-sen University, Zhuhai, Guangdong, China,
yeleiping@mail.sysu.edu.cn

² Southern Marine Science and Engineering Guangdong Laboratory (Zhuhai), Zhuhai, Guangdong, China

³ Institute for Ocean Engineering, Shenzhen International Graduate School, Tsinghua University, Shenzhen, China

1. Introduction

Fine particles (such as clay minerals, biological organic matter and other pollutants) are widely distributed in estuarine and coastal waters, which are prone to flocculation, thus forming flocs with irregular shapes and structures. The floc properties such as geometry and settling may directly affect the water quality in lakes, estuaries and coastal seas. The geometry of floc is essential for predicting the distribution of fine particulate matters in natural environments. The suspended sediment flocs in natural water tend to be fragile, highly irregular and loosely structured. In many field observations and laboratory simulations of flocculation process, it is found that the three-dimensional (3D) structures of natural floc show highly irregularity and changeable morphologies during the continuous aggregation and fragmentation processes when they transport. The geometric shape/size of an individual floc observed from different angles can show large differences. However, most previous studies generally measured and analyzed the flocs by means of single angle two-dimensional (2D) floc observation and average size estimation, such as optical instrument and single mirror camera devices, which were used to record and describe the 2D image characteristics of flocs in laboratory experiments or field observations. These may not reflect the actual morphology of floc in nature with irregular 3D geometry. Recently, high standard 3D scanning approach has been successfully applied on individual floc analysis (Huang et al., 2018; Spencer et al., 2022 etc.). However, the 3D observations of large numbers of floc especially during their settlings are still very limited both in field and laboratory studies.

2. Methodology

In this study, we designed a multiple cameras observation system (Figure 1) to monitor and analyse floc geometry and settling from different angles simultaneously. It is combined by a bottom guide rail controlling the cameras positions, observation devices (CCD camera with high-resolution lens) and a transparent settling column in the middle location.

In additional, a multi-view segmentation algorithm is developed, which uses the multi-view of floc to reconstruct the rough 3D model and obtain the upper limit of its volume. Then the smooth surface of floc can be reconstructed by B-spline fitting method.

Using the method of template matching, all the captured individual settling floc can be tracked by a single target, so as to obtain its settling velocity for every captured floc by camera recording.

In order to further evaluate the inner structure and density of floc, we also used a polarized light device designed by Tsinghua University in China. More details will be presented.

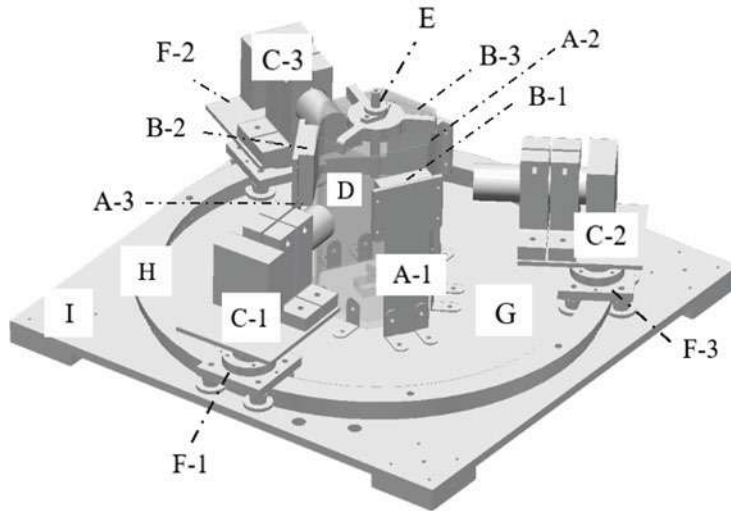


Figure 1. Self-designed multiple cameras observation system. A-1~A-3: Light-controlling; B-1~B-3: LED lights; C-1~C-3: Sliding rail with camera stands; D: Transparent settling column; E: Central digital-controlled settling column; F-1~F-3: High precision lifting platforms; G: Glass film plate; H: Circular slide rail; I: Base support.

3. Results and conclusions

From the images analysis, we reconstructed 3D flocs (such as Figure 2) and calculated the maximum volume of each capture floc.

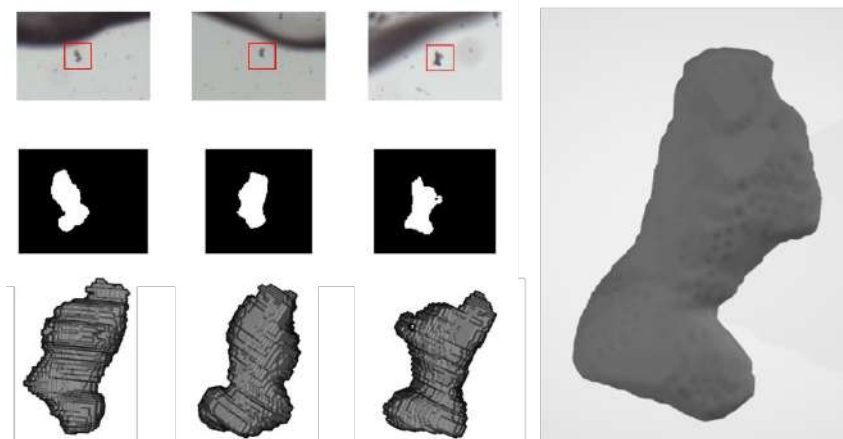


Figure 2: Reconstruction of a 3D floc during its settling.

From the multiple videos analysis, we tracked all the captured flocs settling process (such as Figure 3) and calculated their settling velocities for further studies.

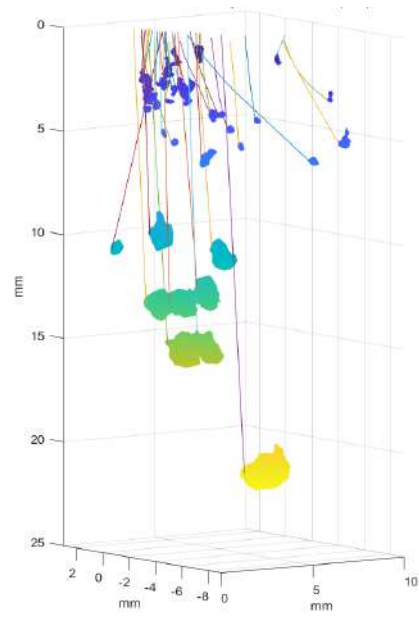


Figure 3. Settling tracking of captured flocs by the multi-camera system. The coloured symbols are the captured flocs with their actual shapes and sizes; the coloured lines are their settling tracks.

It is also found that the 3D volume of floc presents a logarithmic relationship with the settling velocity, and the shape of floc also greatly affects the settling velocity.
(More statistical data analysis is still in processing and more detailed results will be presented.)



17th International Conference on
Cohesive Sediment Transport Processes
September 18-22, 2023
Inha University, Incheon, Republic of Korea



The potential of cohesive sediment and diverse microalgae to flocculate in demanding growth conditions.

Que Nguyen Ho^{1,2}, Michael Fettweis³, Jin Hur⁴, Sang Deuk Lee⁵, and Byung Joon Lee^{1,6*}

¹ Energy Environment Institute, Kyungpook National University, 2559 Gyeongsang-daero, Sangju, Gyeongbuk 37224, Korea

² Faculty of Environment and Labour Safety, Ton Duc Thang University, Ho Chi Minh City, Vietnam

³ Operational Directorate Natural Environment, Royal Belgian Institute of Natural Sciences, Rue Vautier 29, B-1000 Bruxelles, Belgium

⁴ Department of Environment & Energy, Sejong University, Seoul 05006, South Korea.

⁵ Nakdonggang National Institute of Biological Resources (NNIBR), Sangju, Gyeongsangbuk-do 37242, South Korea

⁶ Department of Advanced Science and Technology Convergence, Kyungpook National University, 2559 Gyeongsang-daero, Sangju, Gyeongbuk 37224, Korea, bjlee@knu.ac.kr

This study investigates the flocculation potential of *Microcystic* and *Chlorella vulgaris* microalgae in low nutrient concentrations, using a standard jar test experiment. Biopolymer and humic substance (HS) concentrations were found to control flocculation potential, with different kinetic patterns observed for each microalgae in the presence of clay suspension particles. The findings suggest that appropriate concentrations of biopolymers can enhance floc-to-floc collision and attachment, but excessive amounts can lead to stabilization due to steric effects. Overall, this study offers insights into the fate of suspended particulate matter in aquatic environments. The flocculation kinetics of *Microcystic* and *Chlorella vulgaris* microalgae with clay suspension can be explained in Figure 1. The flocculation potential of both *Microcystic* and *Chlorella vulgaris* microalgae was observed to begin during the exponential phase due to an increase in cell numbers and secretion of biopolymers, such as extracellular polymeric substances/transparent exopolymer particles (Naveed S et al., 2019). The production of biopolymers by microalgae was found to increase with time as nitrogen content became depleted (Babiak W et al., 2021). This led to an increase in the flocculation potential of *Chlorella vulgaris* with incubation time, whereas for *Microcystic*, an adequate concentration of biopolymers during the exponential, stationary, and early death phases was necessary for the development of large flocs (Avnimelech Y et al., 1982; Ho QN et al., 2022). However, excessive amounts of biopolymers and humic substances in the final death phase did not significantly change the volumetric fraction of flocculi and flocs, as it may simultaneously encourage flocculation and stability. The accumulation of biopolymer and humic substances may enhance stabilization due to steric effects, which can decrease attachment between flocs. At the equilibrium stage, an excess of organic matter concentration may enhance flocculation up to a particular size, after which the build-up of biopolymers and humic substances may cover flocs, leading to enhanced steric stability and decreased attachment between flocs (Ho QN et al., 2022).

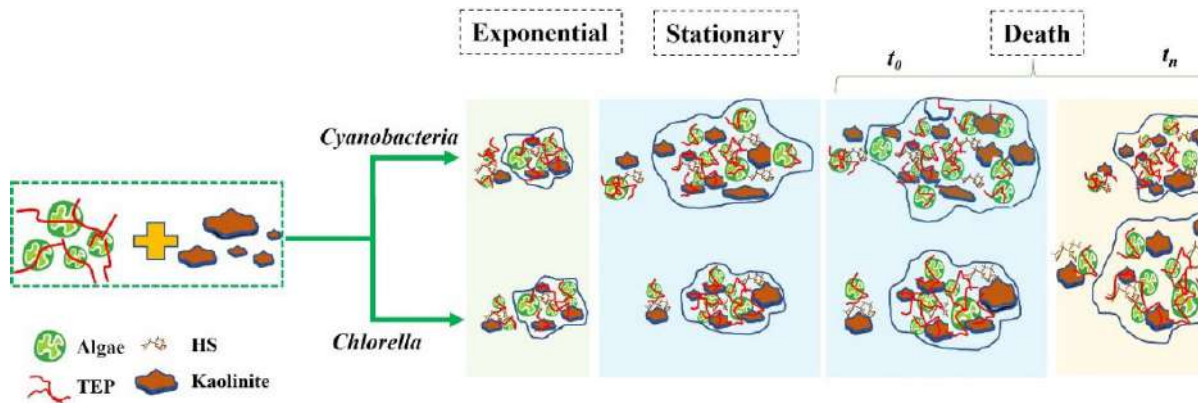


Figure 1. The general model conception of the varying flocculation kinetics of *Microcystic* and *Chlorella vulgaris* with clay-suspended particles is presented in a schematic diagram.

Acknowledgment

This work was supported by the National Research Foundation of Korea (Grant No. NRF-2020R111A3A04036895) and the Nakdonggang National Institute of Biological Resources (Grant No. NNIBR-202302104).

References

- Naveed S, Li C, Lu X, Chen S, Yin B, Zhang C, Ge Y: Microalgal extracellular polymeric substances and their interactions with metal (loid) s: A review. *Critical Reviews in Environmental Science and Technology* 2019, 49(19):1769-1802.
- Babiarz W, Krzemińska I: Extracellular polymeric substances (EPS) as microalgal bioproducts: A review of factors affecting EPS synthesis and application in flocculation processes. *Energies* 2021, 14(13):4007.
- Avnimelech Y, Troeger BW, Reed LW: Mutual flocculation of algae and clay: evidence and implications. *Science* 1982, 216(4541):63-65.
- Ho QN, Fettweis M, Hur J, Desmit X, Kim JI, Jung DW, Lee SD, Lee S, Choi YY, Lee BJ: Flocculation kinetics and mechanisms of microalgae-and clay-containing suspensions in different microalgal growth phases. *Water Research* 2022:119300.



17th International Conference on
Cohesive Sediment Transport Processes
September 18-22, 2023
Inha University, Incheon, Republic of Korea



The Role of Microalgae in Cohesive Sediment Flocculation: Insights from Stochastic Modeling and Laboratory Experiments

Mingze Lin¹, Xiaoteng Shen¹,

¹ State Key Laboratory of Hydrology-Water Resources and Hydraulic Engineering, Hohai University, Nanjing, China, xiaoteng.shen@hhu.edu.cn

The transport of cohesive sediments in natural waters is an important aspect of environmental and engineering problems, as it plays a significant role in understanding coastal evolution, contaminant dispersion, and offshore engineering. In aquatic environments, the presence of microalgae and the secreted extracellular polymeric substances (EPS) tend to aggregate with the suspended sediments, potentially modifying the physical characteristics and transport of pure mineral flocs. Despite the significant influence of biomineral flocculation between microalgae and cohesive sediment, the mechanisms remain insufficiently investigated. Precise evaluation of floc size distributions (FSDs) for biomineral aggregates is a crucial factor in comprehending the dynamics of cohesive sediments (Maggi, 2009; Ho et al., 2022). The objective of this study is to investigate the influence of two typical microalgae, namely *Skeletonema costatum* and *Cyclotella meneghiniana*, on the flocculation of suspended fine-grained sediments under diverse turbulent shear and environmental conditions by laboratory experiments and stochastic modeling. The results indicate that turbulent shear exerts a substantial impact on biomineral flocculation mechanisms, and the addition of microalgae generally enhances the aggregation of mineral particles. Moreover, this study demonstrates that the mean sizes and FSDs are also affected by different algal species and concentrations, particularly in strong turbulent conditions.

Additionally, the bivariate population balance equation is solved using the quasi-Monte Carlo (QMC) method to predict the FSDs of biomineral flocs, which accounts for the influence of bioactivities on collision frequency, collision efficiency, and breakup frequency (Singh et al., 2018). The analytical solutions and laboratory observations provide reasonably validated results for the proposed model, indicating that the bivariate model has the potential extension to track the heterogeneous properties of microalgae-associated sediment flocs due to the discrete nature of the QMC method.

In conclusion, this study provides important insights into the biomineral flocculation between microalgae and cohesive sediments, which can help improve our understanding of suspended sediment dynamics. Future research can build upon the findings of this study to better understand the complex processes of biomineral flocculation and the heterogeneity of environmental flocs.

Table 1. Experimental conditions. Note that *S. C* represents *Skeletonema costatum* and *C. M* represents *Cyclotella meneghiniana*.

Experimental material	Shear rate G (s^{-1})	Sediment concentration (g/L)	Algal concentration c_a (cells/L)
Kaolinite	20, 40, 60, 80	0.1	6×10^5 , 3×10^6

Kaolinite+S. C	20, 40, 60, 80	0.1	$6 \times 10^5, 3 \times 10^6$
Kaolinite+C. M	20, 40, 60, 80	0.1	$6 \times 10^5, 3 \times 10^6$

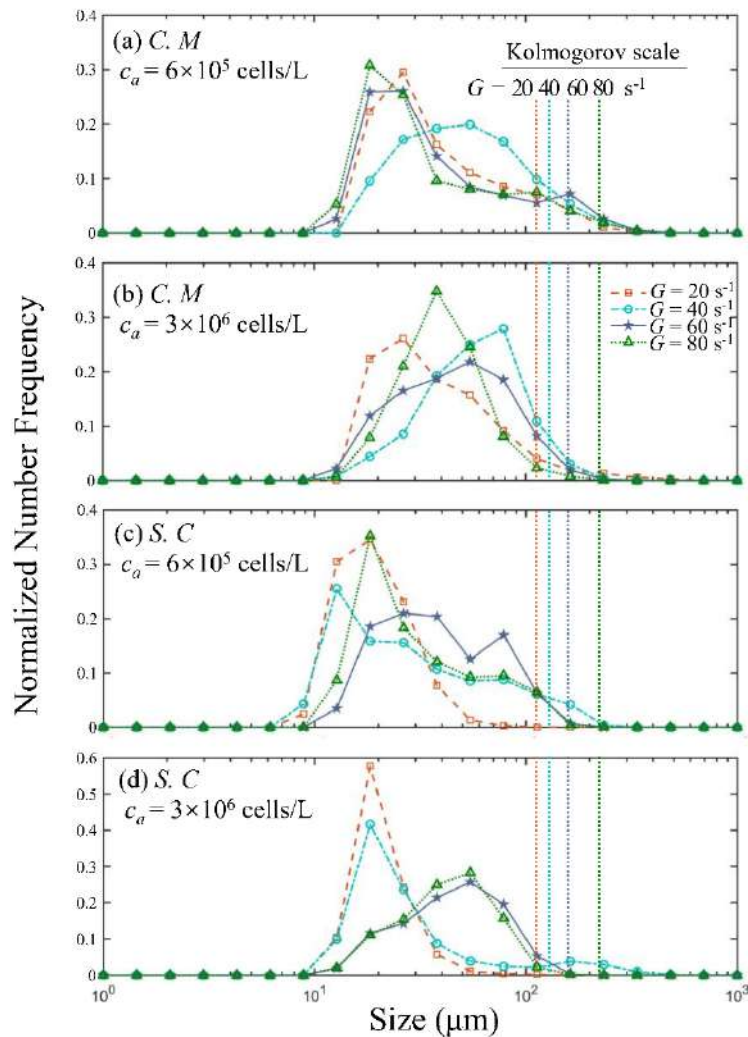


Figure 1. The experimental FSDs for kaolinite incubated with microalgae of different shear rates G . ($C. M$ represents *Cyclotella meneghiniana*, and $S. C$ represents *Skeletonema costatum*.)

References

- Maggi, F. (2009). Biological flocculation of suspended particles in nutrient-rich aqueous ecosystems. *J. Hydrol.* 376(1-2), 116-125. <https://doi.org/10.1016/j.jhydrol.2009.07.040>
- Ho, Q. N., Fettweis, M., Spencer, K. L., and Lee, B. J. (2022). Flocculation with heterogeneous composition in water environments: A review. *Water Res.* 118147. <https://doi.org/10.1016/j.watres.2022.118147>
- Singh, M., Kaur, G., De Beer, T., and Nopens, I. (2018). Solution of bivariate aggregation population balance equation: a comparative study. *React. Kinet. Mech. Cat.* 123, 385-401. <https://doi.org/10.1007/s11144-018-1345-9>



17th International Conference on
Cohesive Sediment Transport Processes
September 18-22, 2023
Inha University, Incheon, Republic of Korea



Changes in suspended particle composition in the water column affect floc dynamics

M. Fettweis¹, L. Delhaye¹, B.J. Lee², R. Riethmüller³, M. Schartau⁴, S. Silori¹ and X. Desmit¹

¹ Royal Belgian Institute of Natural Sciences, Rue Vautier 29, Brussels, Belgium,
mfettweis@naturalsciences.be

² Department of Environmental and Safety Engineering, Kyungpook National University,
Sangju, Korea

³ Institute of Carbon Cycles, Helmholtz Centre hereon, Geesthacht, Germany

⁴ GEOMAR Helmholtz Centre for Ocean Research, Kiel, Germany

1. Introduction

Suspended particulate matter (SPM) consist of solid particles (from clay to sand size), loose particles (biomineral flocs) and particulate organic matter (POM). The structure, composition and size of biomineral flocs varies along time scales from seconds to seasons, and along the cross-shore. Physical processes dominate particle dynamics at short time scales, while biological processes dominate at the seasonal scale. With distance from the coast the portion of terrestrial waters diminishes and the water depth generally increases. These changes generate and form coastal ocean specific hydrodynamic processes that influence the availability of mineral and organic matter of terrestrial origin and primary production and thus the size, composition and texture of biomineral flocs.

Mass concentration of flocs in suspension depends strongly on their density and size, controlled by the rate of inelastic collisions, which in turn depends on the turbulence, the SPM concentration and the particle stickiness (Winterwerp & van Kesteren, 2004). Flocs in the turbid nearshore are smaller, denser and consist mainly of settleable biomineral aggregates, while in the offshore flocs are larger, biomass-enriched and have lower densities (Fettweis et al., 2022). The increase of the POM content with decreasing SPM concentration is a characteristic feature and well described along the nearshore to offshore transect (Riebesell, 1991; Lai et al., 2018; Schartau et al., 2019).

2. Scope of the study

In this study we show that in the high turbid nearshore similar gradients also occur in the vertical, i.e. an organic enrichment of the SPM towards the surface layer, which is most prominent during slack waters. This means that size, composition and density of suspended particles vary with water depth. Although studies (e.g., Ho et al, 2022; Zhu et al., 2022) have revealed that minerals and microorganisms together can change the size and settling velocities of biomineral flocs through the occurrence of Transparent Exopolymer Particles (TEP), our data indicate that during slack water, when the flocs are largest and the settling highest, the organic enriched particles have a lower probability to settle than the biomineral flocs. In addition, also fine mineral particles ($\sim 2\mu\text{m}$) during slack water escape the incorporation into flocs (see also Alber, 2000).

Our hypotheses are: 1) Two types of phytoplankton coexist: a floc-associated and a free one. The occurrence of free-phytoplankton is controlled by the primary production and thus the age

of a phytoplankton cell. A young phytoplankton cell would thus have a lower probability to be incorporated into a floc than an older one. 2) The fine mineral particles are non-cohesive and occur as wash load.

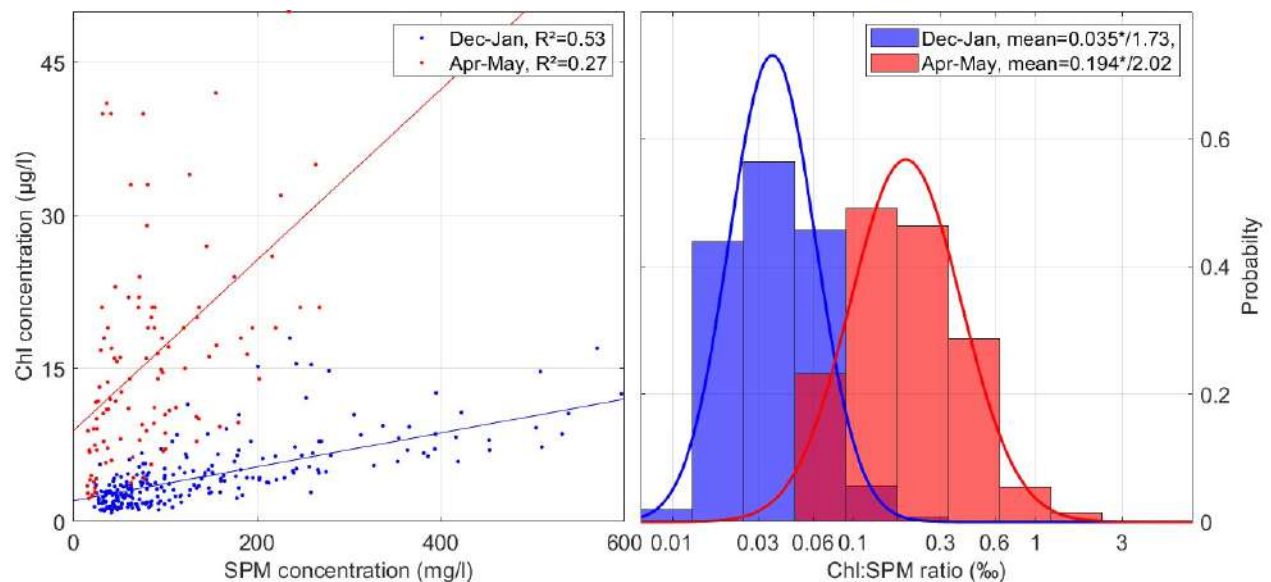
3. Results

We have used in situ data of SPM, Chlorophyll (Chl) and POM concentration together with particle size data measured by a LISST from 2012 till 2021 in a turbid station in the southern North Sea. The Chl data have been used as proxy measure for the occurrence of phytoplankton, while particulate organic carbon and nitrogen were used as indicator of POM. The data from the turbid nearshore reveal that:

1) In winter SPM and Chl concentration are well correlated (see Figure). We postulate that the phytoplankton is floc-incorporated and behaves similar as biomineral flocs, i.e. tide controlled resuspension and deposition. It occurs in a dormant stage, free phytoplankton is absent.

2) During the biological active period the correlation between SPM and Chl is less good and the probability density distribution of the Chl:SPM ratio is larger than in winter (see Figure). We postulate that only part of the phytoplankton is floc-associated, while the other part is free phytoplankton. The free phytoplankton has a higher probability to be in the euphotic layer than the floc-associated. The TEP produced during photosynthesis will increase the floc sizes. As larger flocs sink faster, they are removed from the water column on the long run. This results in a decrease of the mean SPM concentration to a minimum in summer. In the meantime, the probability of all phytoplankton to be in the photic layer will increase.

3) During slack water, when turbulence is small and the larger flocs have settled, the remaining SPM consist of very large ($>250\mu\text{m}$) and very small ($<20\mu\text{m}$) particles. Both do not or only very slowly settle and are interpreted as the free phytoplankton and fine-grained minerals (quartz, amorphous silica, carbonates) that have not collided with flocs or that have a low adhesiveness. These findings have also been found in low turbid offshore locations.



Correlation between winter and spring SPM and Chl concentration (left) and the probability density of the Chl:SPM ratio (right). Data are from 2012-2021.

4. Conclusions

The results underline that the composition of the SPM controls, together with concentration and turbulence, the flocculation of particles. The composition of the SPM changes with concentration, it is getting more organic when the concentration decreases, this occurs along a nearshore to offshore gradient but also along the vertical in the water column. Changes in composition are more pronounced in spring and summer than in winter. The results indicate the presence of mineral and organic particles that are incorporated in flocs and others that are not (free-phytoplankton and wash load). Flocculation models should take into account these heterogenous characteristics, by including non-settleable minerals and phytoplankton cells and by incorporating changes in composition of the SPM. The latter can be estimated with an empirical model that relates the POM content to the SPM concentration as proposed by Schartau et al. (2019) and Fettweis et al. (2022).

Acknowledgments

This research was supported by the Belgian Science Policy (BELSPO) within the BRAIN-be program (BG-PART and PiNS projects), the Maritime Access Division of the Flemish Ministry of Mobility and Public Works (MOMO project), and the RBINS BGCMonit program.

References

- Alber, M. 2000. Settleable and Non-Settleable Suspended Sediments in the Ogeechee River Estuary, Georgia, U.S.A. *Estuarine, Coastal and Shelf Science* (2000) 50, 805–816
- Fettweis, M., Schartau, M., Desmit, X., Lee, B.J., Terseleer, N., Van der Zande, D., Parmentier, K., Riethmüller, R. 2022. Organic matter composition of biomineral flocs and its influence on suspended particulate matter dynamics along a nearshore to offshore transect. *Journal of Geophysical Research Biogeosciences*, 126, e2021JG006332.
- Ho, N.Q., Fettweis, M., Hur, J., Desmit, X., Kim, J.I., Jung, D.W., Lee, S.D., Lee, S., Choi, Y.Y., Lee, B.J. 2022. Flocculation kinetics and mechanisms of microalgae- and clay-containing suspension in different microalgae growth phases. *Water Research* 226, 119300.
- Lai, H., Fang, H., Huang, L., He, G., Reible, D. 2018. A review on sediment bioflocculation: Dynamics, influencing factors and modeling. *The Science of the Total Environment*, 642, 1184–1200.
- Riebesell, U., 1991. Particle aggregation during a diatom bloom. II. Biological aspects. *Marine Ecology Progress Series* 69, 281–291.
- Schartau, M., Riethmüller, R., Flöser, G., van Beusekom, J.E E., Krasemann, H., Hofmeister, R., Wirtz, K. 2019. On the separation between inorganic and organic fractions of suspended matter in a marine coastal environment. *Progress in Oceanography*, 171, 231–250.
- Winterwerp, J.C., van Kesteren, W.G.M. 2004. *Introduction to the Physics of Cohesive Sediment in the Marine Environment*. Elsevier.
- Zhu, Y., Lin, M., Shen, X., Fettweis, M., Zhang, Y., Zhang, J., Bi, Q., Lee, B.J., Maa, J.P.-Y., Chen, Q. 2022. Biomineral flocculation of kaolinite and microalgae: Laboratory experiments and stochastic modeling. *Journal of Geophysical Research: Oceans*, 127, e2022JC018591.



17th International Conference on
Cohesive Sediment Transport Processes
September 18-22, 2023
Inha University, Incheon, Republic of Korea



Depositional characteristics of oil-mineral flocs in estuarial and coastal waters

A.J. Manning^{1,2,4}, L. Ye³, T-J, Hsu⁴, J. Holyoke^{4,5}, J.A. Penaloza-Giraldo⁴,

¹ School of Biological and Marine Sciences, University of Plymouth, Drake Circus,
Plymouth, U.K. PL4 8AA.

² Coasts and Oceans Group, HR Wallingford Ltd, Wallingford, United Kingdom, OX10 8BA.
a.manning@plymouth.ac.uk, a.manning@hrwallingford.com

³ School of Marine Sciences, Sun Yat-sen University, and Southern Marine Science and
Engineering Guangdong Laboratory (Zhuhai), Zhuhai, China, China
yeleiping@mail.sysu.edu.cn

⁴ Center for Applied Coastal Research, University of Delaware, Newark, DE 19716, USA
thsu@udel.edu, japg@udel.edu

⁵ Department of Civil, Architectural and Environmental Engineering, University of
Texas at Austin, Austin, TX USA
jameshol@udel.edu, jameshol@utexas.edu

1. Introduction

In recent decades, oil spill contamination has tended to occur more commonly in coastal and estuarial systems around the world, including the waters around the U.K (Manning *et al.*, 2022). The management of such oil spillages, such as the 2010 Deepwater Horizon (DWH) disaster in the Gulf of Mexico, has been a major challenge in coastal and estuarial regions due to the highly sensitive nature of deltaic ecosystems and related public health. Many coastal and estuarial regions tend to have an abundance of clay minerals, and these cohesive particles - which can readily flocculate (e.g. Mehta *et al.*, 2014; Zhang *et al.*, 2018; Spencer *et al.*, 2021; Krahl *et al.*, 2022; Vowinckel *et al.*, 2022) - play an important role in determining the transport of spilled oil contamination and its eventual fate, particularly given that suspended sediment and microbial activities are often prevalent and diverse in natural environments.

2. Methodology

As part of the Consortium for Simulation of Oil-Microbial Interactions in the Ocean (CSOMIO; <https://csomio.org/>), the primary work presented here mainly focuses on the laboratory experimental studies in order to help for developing improved parameterizations of flocculation processes for the oil-sediment-biogeochemical modeling system. Oil-mineral flocs have been successfully created from a series of laboratory flocculation experiments with seawater, crude oil and clay minerals (Bentonite and Kaolin clay) and Xanthan gum (a proxy of Extracellular polymeric substance) using a Magnetic Stirrer and reciprocal shaker (Ye *et al.*, 2020, 2021). In order to obtain high quality floc population data (including floc size, settling velocity, density, mass, etc), a novel floc video instrument LabSFLOC-2 (Laboratory Spectral Flocculation Characteristics; see Manning, 2006; Manning *et al.*, 2017) has been adopted for the first time to study oil mineral aggregates (OMAs; Ye *et al.*, 2018; 2019). Meanwhile, a Vectrino-II profiling velocimeter is adopted to measure flow turbulence statistics and identify homogeneous turbulence.

3. Results

The experimental results reveal that the OMAs can easily form in any oil, cohesive sediment and seawater mixtures. However, the kaolin and bentonite clays form dramatically different structures of oil-mineral aggregate which leads to their variable characteristics. In bentonite clay cases, the oil flocs tend to be much larger and with higher densities than those in kaolin clay cases, which could result in the significant variability of the flocs' settling velocities (e.g.

Manning and Dyer, 2007; Soulsby *et al.*, 2013). This is because the Kaolin particles/flocs directly attach to oil droplets to form OMAs, while the Bentonite mineral flocs interact with the oil component more by absorbing each other to form more structurally complex oil flakes and strings (Fig. 1).

4. Conclusions

Eventually, this part of the work aims to improve the parameterization of fine sediment transport and oil transport/degradation module in regional-scale ocean modeling system (e.g. Dukhovskoy *et al.*, 2021). Macrofloc fractions (> 160 μm) of OMAs can be focused on to improve the OMA models, because the addition of oil has been proven more sensitive to macroflocs (< 160 μm) than the microfloc group.

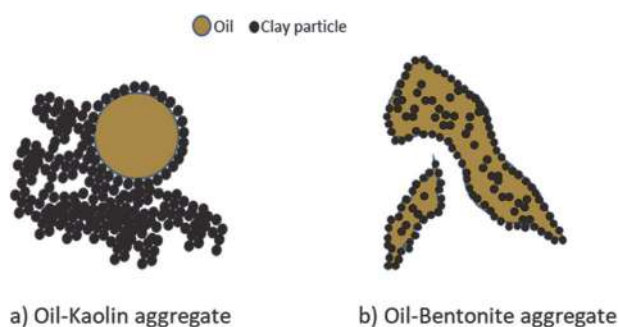


Figure 1. Illustration showing the conceptual structure of kaolin clay formed oil aggregates and bentonite clay formed oil aggregates with difference.

References

- Dukhovskoy, D.S., Morey, S.L., Chassignet, E.P., Chen, X., Coles, V.J., Cui, L., Harris, C.K., Hetland, R., Hsu, T-J., Manning, A.J., Stukel, M., Thyng, K. and Wang, J. (2021). Development of the CSOMIO Coupled Ocean-Oil-Sediment-Biology Model. *Frontiers in Marine Science*, 8:629299. doi: 10.3389/fmars.2021.629299.
- Krahl, E., Vowinckel, B., Ye, L., Hsu, T-J. and Manning, A.J. (2022). Impact of the Salt Concentration and Biophysical Cohesion on the Settling Behavior of Bentonites. *Frontiers in Earth Science (Marine Geoscience)*, <https://doi.org/10.3389/feart.2022.886006>
- Manning, A.J. (2006). LabSFLOC – A laboratory system to determine the spectral characteristics of flocculating cohesive sediments. *HR Wallingford Technical Report*, TR 156.
- Manning, A.J. and Dyer, K.R. (2007). Mass settling flux of fine sediments in Northern European estuaries: measurements and predictions. *Marine Geology*, 245, 107-122, doi:10.1016/j.margeo.2007.07.005.
- Manning, A.J., Whitehouse, R.J.S. and Uncles, R.J. (2017). Suspended particulate matter: the measurements of flocs. In: R.J. Uncles and S. Mitchell (Eds), *ECSA practical handbooks on survey and analysis methods: Estuarine and coastal hydrography and sedimentology*, Chapter 8, pp. 211-260, Pub. Cambridge University Press, DOI: 10.1017/9781139644426, ISBN 978-1-107-04098-4.
- Manning, A.J., Ye, L., Hsu, T-J., Holyoke, J., and Penaloza-Giraldo, J.A. (2022). Oil-Mineral Flocculation and Settling Dynamics. In: Andrew J. Manning (Editor), *River Deltas*

Research – Recent Advances, Publisher: IntechOpen (London, UK), DOI: 10.5772/intechopen.103805

- Mehta, A.J., Manning, A.J. and Khare, Y.P. (2014). A Note on the Krone deposition equation and significance of floc aggregation. *Marine Geology*, 354, 34-39, doi.org/10.1016/j.margeo.2014.04.002.
- Soulsby, R.L., Manning, A.J., Spearman, J. and Whitehouse, R.J.S. (2013). Settling velocity and mass settling flux of flocculated estuarine sediments. *Marine Geology*, doi.org/10.1016/j.margeo.2013.04.006.
- Spencer, K.L., Wheatland, J.A.T., Bushby, A.J., Carr, S.J., Droppo, I.G. and Manning, A.J. (2021). A structure–function based approach to floc hierarchy and evidence for the non-fractal nature of natural sediment flocs. *Nature - Scientific Reports*, 11:14012, doi.org/10.1038/s41598-021-93302-9.
- Vowinckel, B., Zhao, K., Ye, L., Manning, A.J., Hsu, T-J., Meiburg, E. and Bai, B. (2022). Physics of Cohesive Sediment Flocculation and Transport: State-of-the-Art Experimental and Numerical Techniques. In: Andrew J. Manning (Editor), *Sediment Transport Research – Recent Advances*, Publisher: IntechOpen (London, UK), DOI: 10.5772/intechopen.104094
- Ye, L., Manning, A.J., Holyoke, J., Penaloza-Giraldo, J.A. and Hsu, T-J. (2021). The Role of Biophysical Stickiness on Oil-Mineral Flocculation and Settling in Seawater. *Frontiers in Marine Science (Marine Pollution section)*, 8:628827. doi: 10.3389/fmars.2021.628827
- Ye, L., Manning, A.J., Hsu, T-J. (2020). Oil-mineral flocculation and settling velocity in saline water. *Water Research*, 173, 115569, <https://doi.org/10.1016/j.watres.2020.115569>
- Ye, L., Manning, A.J., Hsu, T-J., Morey, S., Chassignet, E.P. and Ippolito, T.A. (2018). Novel Application of Laboratory Instrumentation Characterizes Mass Settling Dynamics of Oil-Mineral Aggregates (OMAs) and Oil-Mineral-Microbial Interactions. *Marine Technology Society Journal*, Technology Center Overview, Vol. 52, No. 6., doi.org/10.4031/MTSJ.52.6.14
- Ye, L., Manning, A.J., Hsu, T-J. and Holyoke, J.G. (2019). Oil-mineral flocculation and settling dynamics. Center for Applied Coastal Research, University of Delaware, *Research Report* No. CACR-19-05, May 2019.
- Zhang, N., Thompson, C.E.L., Townend, I.H., Rankin, K.E., Paterson, D.M. and Manning, A.J. (2018). Nondestructive 3D Imaging and Quantification of Hydrated Biofilm-Sediment Aggregates Using X-ray Microcomputed Tomography. *Environmental Science & Technology*, 52, 13306-13313.

Session: Posters
16:00 – 17:30
Monday, September 18, 2023



17th International Conference on
Cohesive Sediment Transport Processes
September 18-22, 2023
Inha University, Incheon, Republic of Korea



Effects of reduced erosion of fine sediments from the shoreline and seabed on estuarine water clarity: Results from a Chesapeake Bay modeling study

J.S. Turner¹, P. St-Laurent², M.A.M. Friedrichs*², and C.T. Friedrichs²

¹ Department of Marine Sciences, University of Connecticut, Groton, CT, USA

² Virginia Institute of Marine Science, Gloucester Point, VA, USA.

*marjy@vims.edu, presenting & corresponding author

Abstract

Shoreline erosion often supplies fine sediments to estuaries and coastal waters, influencing water clarity and primary production. Globally, shoreline erosion sediment inputs are changing with anthropogenic alteration of coastlines in populated regions. Chesapeake Bay, a prime example of such a system where shoreline erosion accounts for a large proportion of fine sediments entering the estuary, serves here as a case study for investigating the effects of changing sediment inputs on water clarity. Long-term increases in shoreline armoring have contributed to decreased erosional sediment inputs to the estuary, reducing the supply of easily erodible bed sediment, and changing the composition of suspended particles in surface waters. This study examined the impact of shoreline erosion and related changes in bed erodibility on water clarity using a coupled hydrodynamic-biogeochemical model. Experiments were conducted to simulate realistic shoreline conditions representative of (i) a reference case from the early 2000s, (ii) more shoreline erosion, and (iii) highly armored shorelines (Table 1). Together, reduced shoreline erosion and a corresponding reduction in seabed erodibility resulted in a decreased concentration of inorganic particles in suspension. The lower concentration of suspended inorganic sediment decreased light attenuation, particularly in the lower Bay and in dry years where and when riverine sediment influence is low. This improvement in light penetration relaxed light limitation, which then increased the production of organic particles.

In going from the “more erosion” to the “highly armored” case, the experiments revealed that in the mid-estuary in late winter and early spring, surface inorganic suspended sediment concentrations decreased by ~50%, while organic suspended solids increased by ~50%. The resulting increase in the organic-to-inorganic ratio often had opposite effects on clarity according to different metrics, improving clarity in mid-Bay central channel waters in terms of light attenuation depth (K_d^{-1}), but simultaneously degrading clarity in terms of Secchi depth (Z_{SD}), because the resulting increase in organic suspended solids decreased the water's transparency (Figure 1). This incongruous water clarity effect, the spatial extent of which is defined here as an Organic Fog Zone (Figure 2), was present in February to April in all years studied, but occurred farther south in wet years.

Table 1. Modeling experiments conducted 2000-2005 (2000 spin-up, 2001-2005 analysis).

Model Run	Shoreline Erosion?	Seabed Erodibility, i.e., Mud Critical Shear Stress (Erosion, Deposition)
Reference Run	Yes, realistic	Representative, 0.09 Pa
More Shoreline Erosion 	Yes, x2	More Erodible, 0.03 Pa
Highly Armored Shorelines 	No	More stable, 0.12 Pa

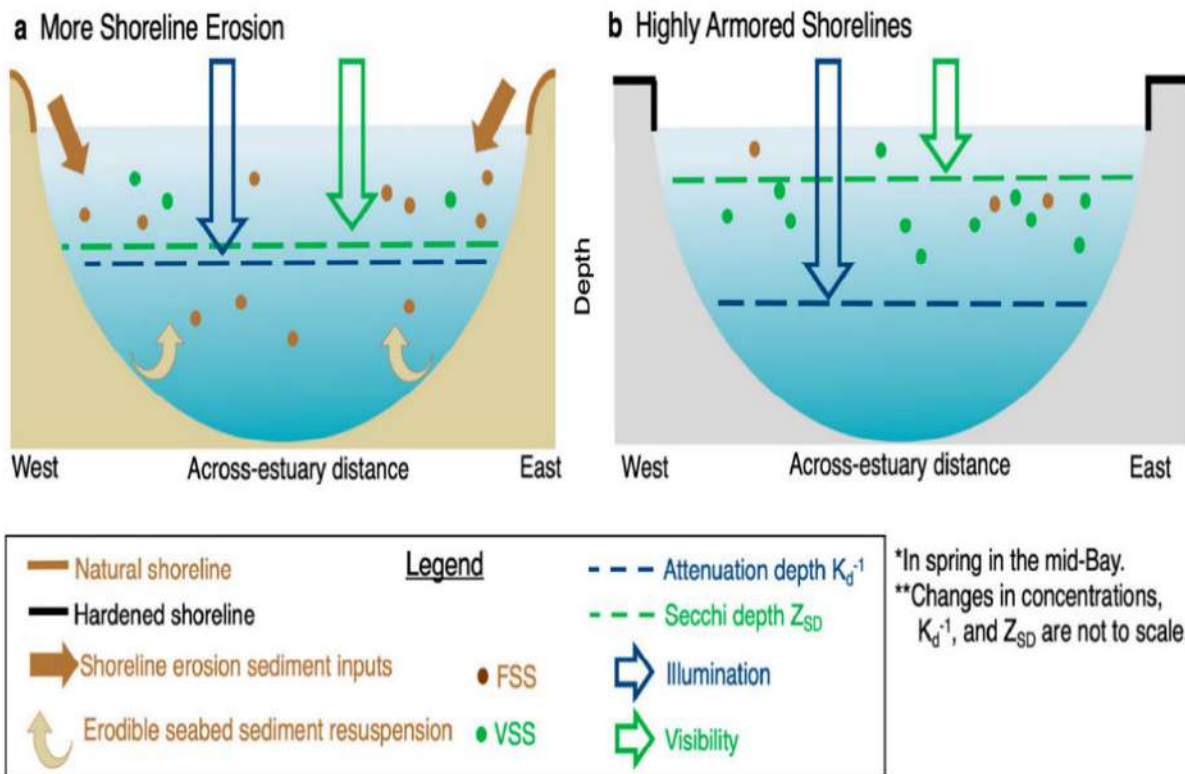


Figure 1. Conceptual diagram of water clarity changes in an idealized across-estuary transect through the mid-Bay during times of high organic solids concentrations (February–April), in model runs (a) More Shoreline Erosion and (b) Highly Armored Shorelines. Changes shown are particular to the Organic Fog Zone region in deep waters. Relative concentrations and clarity depths are not drawn to scale.

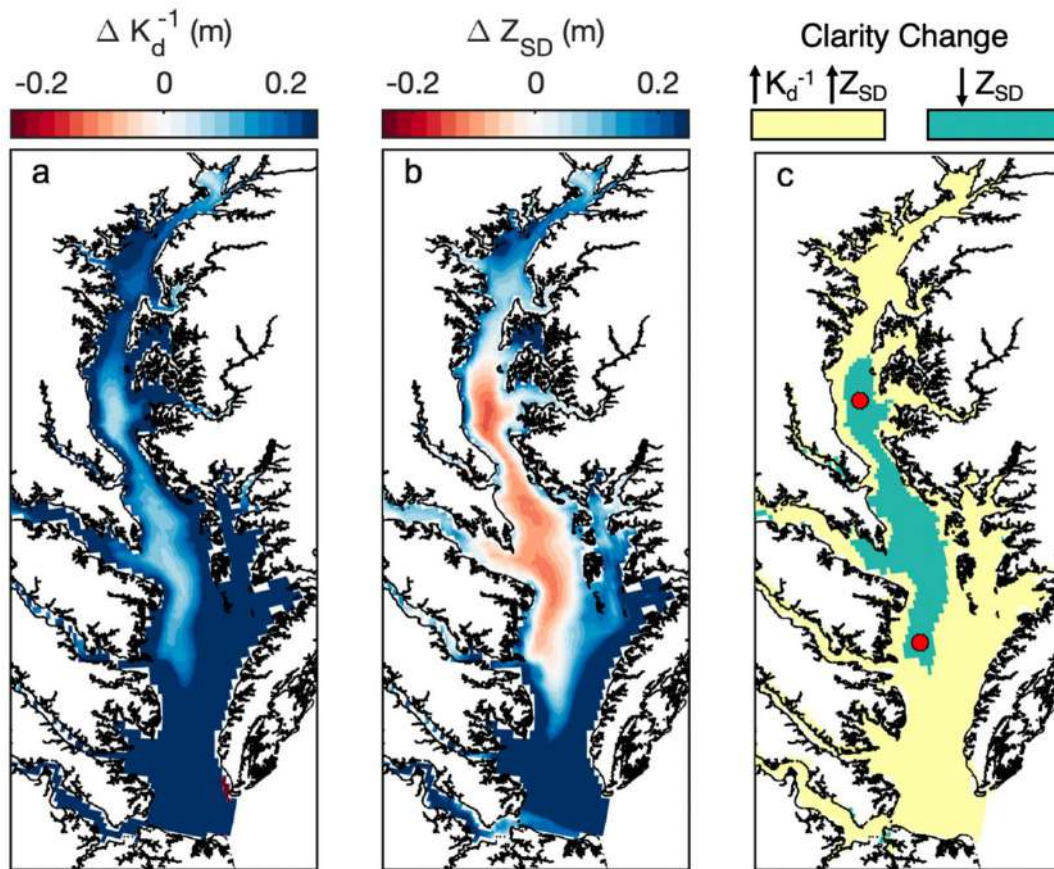


Figure 2. Changes due to reduced shoreline erosion February to April 2001, including (a) K_d^{-1} effects and (b) Z_{SD} effects in surface waters, in terms of the difference (Δ) between Highly Armored Shorelines minus More Shoreline Erosion. Blue colour in difference plots represents clearer water in terms of each metric. Zones (c) of clarity change are defined by the respective ΔK_d^{-1} and ΔZ_{SD} shown in (a) and (b). Zones in (c) are defined as: Enhanced Visibility Zone (yellow) with $\Delta K_d^{-1} > 0$ m (deeper) and $\Delta Z_{SD} > 0$ m (deeper); Organic Fog Zone (green) with $\Delta Z_{SD} < 0$ m (shallower). Red circles in (c) indicate stations US EPA Chesapeake Bay Program monitoring stations CB4.2C and CB5.5, highlighting the northern and southern extents of the Organic Fog Zone.



17th International Conference on
Cohesive Sediment Transport Processes
September 18-22, 2023
Inha University, Incheon, Republic of Korea



Application of GEMS Experiment Parameters in the Sediment Model for Intertidal Slope Within a Semi-closed Harbor

J. Y. Choi^{1,2}, J. W. Kim¹, H. M. Lee¹, S.-B. Woo^{1*}, J. Y. Seo¹, H. K. Ha¹

¹Department of Ocean Science, Inha University, Incheon, Korea, sbwoo@inha.ac.kr
²GeoSystem Research Corporation, Gunpo, Korea

1. Introduction

There are various types of sedimentary parameters in sediment transport models. In understanding sediment behaviours, the most important parameters in these models are settling velocity, critical shear stress for erosion, and erosion rate (Ge et al., 2015). Since the sedimentary parameters has high spatial and temporal variability, however, applying them to numerical models for large-scale coastal areas with different particle size distributions is challenges (Chen et al., 1999). Moreover, it requires significant efforts in sensitivity analysis to select calibration parameters for cohesive sediments depending on site-specific condition. In this study, therefore, proposes an approach that sediment parameters in sediment transport model are based on *in-situ* measurements from the Gust Erosion Microcosm System (GEMS). And improve the representation of sediment calibration parameters in numerical models by simulate the sediment transport in intertidal slope in the semi-closed harbor.

2. Results

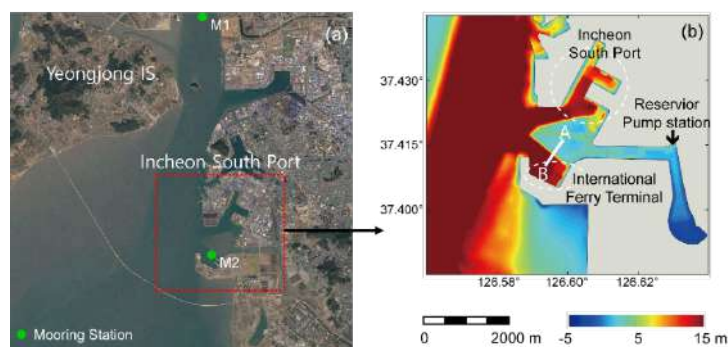


Figure 1. Two acoustic Doppler current profilers with turbidity (green circles) were moored at M1 and M2 (a). The sediment cores for GEMS experiments were collected at M2 (a). enlarged view of is shown in (b) which is the bathymetry of IFT.

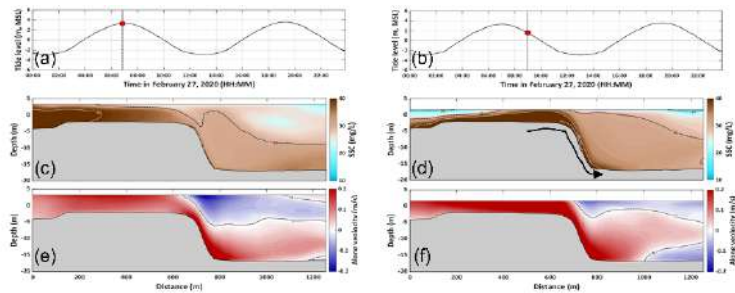


Figure 2. The tide level time series variation at Incheon tide station (a, b). Distribution of sediment concentration (c, d) and current velocity (e, f) in the cross-section A-B (Figure 1, (b)) at high tide and 2 hours after high tide.

In this study a coupled model consisting of Finite Volume Community Ocean Model (FVCOM), Simulating WAVE Nearshore, SWAVE (SWAN), and Community Sediment Transport Modeling System (CSTMS) were used for International Ferry Terminal (IFT) that includes a semi closed harbor and intertidal zone. The model was simulated during 2020 winter (from 1 Feb to 17 Mar) and Spring (23 May to 10 June).

In the IFT erosion and deposition processes occurred with the tidal cycle. During high tide, the intertidal zone is submerged, leading to the erosion and suspension of sediment in the water column. During ebb tide, sediment transported from the offshore area combines with the eroded sediment from the intertidal zone, resulting in the transport of sediments towards the direction of the IFT (Figure 2). This process contributes to sediment dynamics within the study area and plays a significant role in shaping the sediment distribution patterns and morphological changes in the vicinity of the IFT. Since the semi-enclosed harbors are usually less affected by external forcings, stable sediment beds are developed by the repetitive erosion-deposition.

Given the presence of these recurring processes and the relatively stable nature of the environment without significant temporal fluctuations, it can be inferred that this environment is suitable for applying experimentally derived parameters. This suggests that the parameters obtained through experimentation can be appropriately applied in this environment, enhancing the accuracy and reliability of the numerical model in simulating sediment transport processes. The M1 exhibited a wide range of variations in suspended sediment concentrations (SSCs), ranging from 50 to 300 mg/L, compared to M2. It served as a suitable dataset for comparing and validating the changes in SSCs resulting from parameter adjustments. Specifically, calibrated the sediment model parameters for cohesive sediments with a silt grain size. As the inner harbor, including Yeongjong Island and the IFT, mainly consisted of silts (> 50% in total), the silt parameter significantly influences the simulation of sediment transport processes in the Incheon Harbor region. The erosion rate and critical shear stress for erosion parameters applied in this study were derived from GEMS experiments conducted on June 14, 2021. Samples collected from the southern intertidal zone of IFT yielded values of erosion threshold shear stress ranging from 0.071 to 0.088 Pa and an erosion rate of 3.0×10^{-5} kg/m²/s (Figure 3). Among the cases presented in Table 1, the highest SSC reproducibility was achieved when utilizing critical shear stress for the erosion of 0.07 Pa and erosion rate of 3.0×10^{-5} kg/m²/s for C10. These parameters closely resemble the parameters obtained from GEMS *in-situ* data, and the sensitivity test results indicate that the parameters acquired from GEMS experiment data are the most suitable for application in the numerical model.

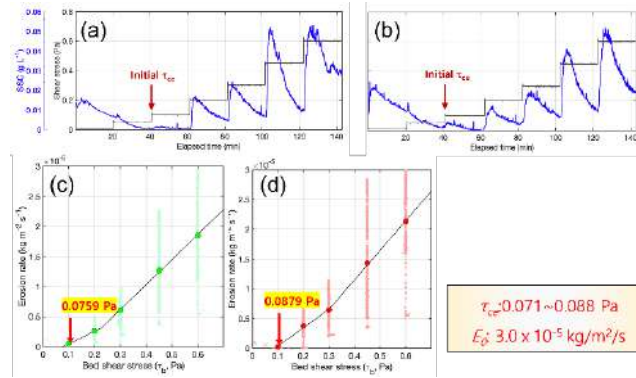


Figure 3. (a and b) Time series of SSC and (c and d) relationships between critical shear stresses for erosion and erosion rates derived from GEMS experiments for M2.

Table 1. Sensitivity test of Suspended Sediment Concentration of M1 according to the Parameters of Erosion Rate and Critical shear stress. Model reproducibility was evaluated by skill score (defined by Willmott (1981)).

Case	C1	C2	C3	C4	C5	C6	C7	C8	C9	C10
E_0 (10^{-5} kg/m ² /s)	5.0	4.0	5.0	5.0	2.0	1.0	3.0	3.0	3.0	3.0
τ_{cr} (Pa)	0.15	0.15	0.05	0.1	0.15	0.1	0.09	0.06	0.08	0.07
Skill score	0.35	0.27	0.22	0.45	0.34	0.31	0.39	0.51	0.61	0.77

3. Conclusions

The conclusions of this study can be summarized as follows:

1. Sediment transport in the study area is the submergence of the intertidal zone during high tide and sediment transport towards the IFT during low tide.
2. When conducting sensitivity tests on the sediment transport model, using GEMS *in-situ* parameters in semi-closed harbor with repetitive sediment transport processes was yielded the highest representation of suspended sediment concentration. Based on this result, it can be suggested that GEMS *in-situ* parameters can be applied to the model can lead to improved accuracy in simulating sediment transport processes and enhance the overall reliability of the model
3. It is proposed to apply numerical model parameters of erosion rate and critical shear stress for erosion with values of E_0 : 3.0×10^{-5} kg/m²/s and 0.07 Pa, respectively, for silt, which amounts ratio for the largest sediment grain size in the harbor and coastal area in Gyeonggi bay.

References

- Chen, J., Li, D., Chen, B., Hu, F., Zhu, H., & Liu, C. (1999). The processes of dynamic sedimentation in the Changjiang Estuary. *Journal of Sea Research*, 41(1-2), 129-140.
- Ge, J., Shen, F., Guo, W., Chen, C., & Ding, P. (2015). Estimation of critical shear stress for erosion in the C hangjiang E stuary: A synergy research of observation, GOCI sensing and modeling. *Journal of Geophysical Research: Oceans*, 120(12), 8439-8465.
- Willmott, C. J. (1981). On the validation of models. *Physical geography*, 2(2), 184-194.



17th International Conference on
Cohesive Sediment Transport Processes
September 18-22, 2023
Inha University, Incheon, Republic of Korea



Idealized model of sediment transportation and nitrogen cycling in Nakdong River Estuary

Dongyoung Back¹, Courtney K. Harris¹ and Bongkeun Song¹

¹ Virginia Institute of Marine Science, William & Mary, Gloucester Point, VA, USA
dback@vims.edu

1. Introduction

The Nakdong River, the longest river in South Korea, is an important source of drinking water for more than ten million Korean citizens (Lee et al., 2018; Ji and Lee, 2016). In the 1980s, the Nakdong River Estuary Dam (NRED) was constructed at the river mouth in the southeast part of Korea (35°06'26"N, 128°57'09"E). Since then, intensive harmful algal blooms have frequently occurred due to blocking water flow and accumulating nutrients. The Korean government has proposed a restoration project for the Nakdong River by dismantling the NRED and has conducted a field manipulation experiment with a controlled opening of the dam gates. There is some concern, however, that experiments with the long-term opening of dam gates may cascade unexpected negative consequences such as increases in sediment resuspension and benthic nitrogen fluxes. With the dam gate opening, tidal mixing of seawater and freshwater may promote sediment resuspension and transport and may alter benthic nitrogen cycling processes. Thus, it is important to develop a numerical model to forecast how sediment transport and nitrogen cycling respond to the dam gate opening.

2. Approach

We have been developing a numerical model that couples hydrodynamics, sediment transport, and biogeochemistry (HydroBioSed) within an idealized implementation of the Regional Ocean Modeling System (ROMS). ROMS is a split-explicit, free-surface, terrain-following numerical model (Shchepetkin and McWilliams, 2005). ROMS includes modules for sediment transport (Warner et al. 2008), water column biogeochemistry (Fennel et al. 2008), and a new sediment bed geochemistry module called HydroBioSed (Moriarty et al. 2017). Our idealized model domain was based on Figueroa et al. (2022). The horizontal resolution was chosen to represent along-channel gradients, and the model was implemented with 20 vertical layers. The model was configured to represent the evolution of conditions and the tidal exchanges of estuarine water and sediments when the dam is opened. Furthermore, nutrient concentrations in water columns have been monitored monthly by K-Water Institute, and the rates of N cycling processes were measured during the experimental dam gate opening in 2020. These data will be used for biogeochemical model development.

3. Anticipated Results

Depending on the model settings for tides, river discharge, and time, the degree of seawater intrusion and sediment transport up the river changes (Figure 1). The faster flows with seawater intrusion and sediment transport expect to change the nitrogen cycling and nutrient distribution in the sediment bed. First, since the nutrient concentrations and dissolved oxygen (DO) outside

the dam are relatively low, opening the dam gates can dilute the relatively high nutrient concentrations upstream of the dam. Our model simulates the lowering of nutrient concentrations in the sediment and in the water column as sediment and water move upstream of the dam. Second, the seawater intrusion in the bottom layer has a great influence on the nitrogen cycling processes. For example, seawater intrusion into the bottom layer can result in increasing ammonium (NH_4^+) availability for nitrification and coupled denitrification in the sediments (Rysgaard et al., 1999). The prediction of the impacts on nitrogen cycling will be performed through tracking changes in the modeled NH_4^+ , nitrate (NO_3^-), DO, and salinity.

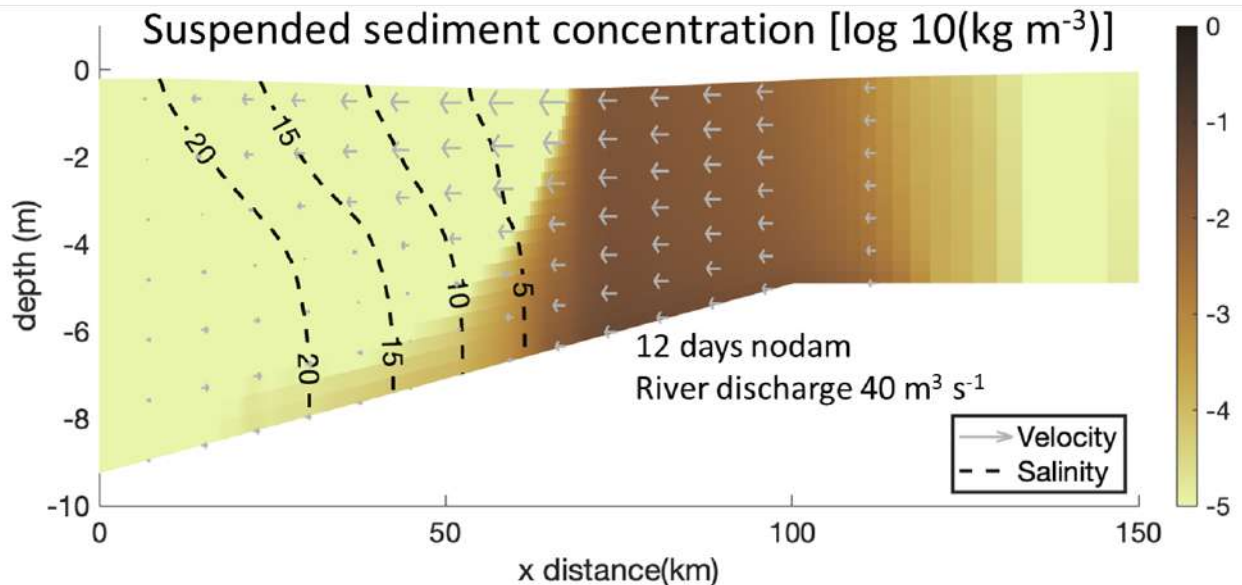


Figure 1. Sediment transport model representing an idealized-domain model of the Nakdong Estuary showing modeled sediment concentrations and isopycnals during slack tide following ebb tide.

4. Conclusions and Future Research

This model predicts the decrease in nutrient concentrations in the bottom water with the dam opening since seawater will be transported and mixed with the upstream river water. In addition, the model predicts the increase of the microbial nitrogen removal processes associated with the transported sediments. As a result, the model predicts a decrease in nutrient concentration in the river upstream when the dam gates are opened, predicting the mitigation of intensive harmful algal blooms in the Nakdong River Estuary.

Metagenomes data have been obtained for 4 years at one location inside the dam before and after the dam gates opened. This will be used to identify nitrogen cycle pathways in sediments. A long overarching goal for this project will compare HydrobioSed model's nitrogen fluxes to this data.

References

- Figuroa, S.M., Lee, G., Chang, J., and Jung, N.W., 2022. Impact of estuarine dams on the estuarine parameter space and sediment flux decomposition: idealized numerical modeling study. *J. Geophys. Res.: Oceans*, 127 (2022), Article e2021JC017829.
- Ji, H.W. and Lee, S.I., 2016. Assessment of risk due to chemicals transferred in a watershed: A case of an aquifer storage transfer and recovery site. *Water*, 242.

Lee, S.H., Jung, S.G., Park, S.M., and Lee, B.D., 2018. Evaluation of the tributaries by influence index on the mid-lower portion of the Nakdong River basin. *Environ Eng Res.* 23(2)150–158

Rysgaard, S., P. Thastum, T. Dalsgaard, P.B. Christensen, and N.P. Sloth. 1999. Effects of salinity on NH_4^+ adsorption capacity, nitrification, and denitrification in Danish estuarine sediments. *Estuaries* 22: 21–30. <https://doi.org/10.2307/1352923>.

Shchepetkin, A.F. and McWilliams, J.C., 2005. The Regional Ocean Modeling System: a split-explicit, free-surface, topography-following coordinates ocean model *Ocean Modelling*, 9, pp. 347-404.



17th International Conference on
Cohesive Sediment Transport Processes
September 18-22, 2023
Inha University, Incheon, Republic of Korea



Measurement and comparison of settling velocities of cohesive sediments from the German estuaries Weser, Ems and Elbe

Patzke, J.¹, Witt, M.¹, Hesse, R. F.², Nehlsen, E.¹ and Fröhle, P.¹

¹ Department of River and Coastal Engineering, Hamburg University of Technology,
Justus.Patzke@tuhh.de

² Federal Waterways and Engineering Institute (BAW), Hamburg, Germany,
Roland.Hesse@baw.de

1. Introduction

Settling and sedimentation of fine-grained sediments is a physical phenomenon influenced by bio-geochemical processes that occurs in natural water bodies such as rivers, channels and estuaries. Of particular concern are estuaries maintained for navigation. The deepening of waterways to improve the navigability for ever larger container ships has the potential to intensify sedimentation and the accumulation of cohesive sediments, particularly within the estuarine turbidity maximum (ETM). For example, significant net sedimentation and accumulation are observed in the ETM of the Weser estuary even in the centre of the navigational channel, where high flow velocities favour sediment transport and erosion. Dredging is the main method of maintaining a channel, which requires large financial investment and also has potential negative environmental impacts. In engineering practice, numerical modelling of the ETM and accumulation zones is an important tool to improve channel maintenance. Knowledge of site-specific information on settling velocities is therefore essential, as underlying processes cannot be simulated universally valid yet and require sufficient local parametrisation.

The research project FAUST (For An improved Understanding of estuarine Sediment Transport) addressed the challenge of net sedimentation and accumulation in the navigational channel by investigating the transport properties of cohesive sediments (mainly from the Weser estuary) in field and in laboratory studies. The conceptual design of the project FAUST has been presented in Patzke et al. (2019). Research on sediment erodibility, sediment fractions and density profiles has been published recently (Patzke et al. 2021; Patzke et al. 2022). The follow-up project ELMOD (Simulation and analysis of the hydrological and morphological development of the Tidal Elbe for the period from 2013 to 2018) focuses on sediment transport processes in the Elbe estuary. The findings and derived model parameterisations of the projects contribute to the development of large-scale 3D morphodynamical-numerical models. In this submission, laboratory-derived effective settling velocities of natural cohesive sediments from three German estuaries are examined.

2. Investigations

Mainly due to flocculation, the effective settling velocity w_s of a cohesive sand-mud-mixture is more complex than that of sand. Many factors that affect flocculation also affect the settling velocity, such as sediment concentration, salinity and temperature. At low concentrations, individual particles or flocs settle freely. In this regime, the settling velocity increases with

concentration due to the increased probability of floc growth by collision. As the suspended sediment concentration increases, the sinking of the flocs is increasingly hindered and the effective settling velocity decreases. At structural density (gelling point), aggregates form an interconnected network, causing settling velocities to decrease further by up to several orders of magnitude. The further settling process is now referred to as consolidation (Winterwerp et al. 2021).

The methodology used to measure settling velocities has been developed within the FAUST-project. By using ultrasonic sensors in a settling column, see fig. 1, containing a cohesive suspension the effective settling velocity of particles and flocs is estimated. Phase and transit time of the ultrasonic pulses reflected from solid particles are measured. As the particle moves, the reflected ultrasonic pulse undergoes a phase shift from which the velocity of motion can be estimated (called the doppler-effect). The sensors from company Signal-Processing operate at a frequency of 1, 4 or 8 MHz and are capable of measuring velocities for every beam throughout the depth of a 50 cm settling column in gates approximately 1 mm in size. The transmission, reflection and reception (one measurement) of a beam takes about 1 second. The effective settling velocity is estimated by averaging over a set of 100 beams and the measurement depth.

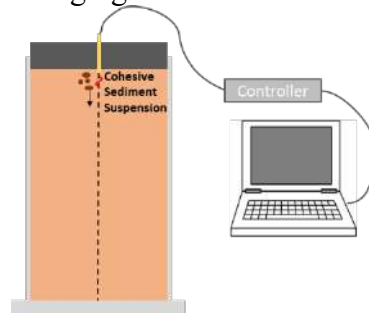


Figure 1. Measurement set-up to measure settling velocities

The experiments carried out cover sediments from three German estuaries, namely the Weser, Ems and Elbe. Direct laboratory or field measurements of settling velocities for these estuaries don't exist or are rare. For each sediment, a concentration range of 0.5 to 100 g/L is analysed, covering both, the flocculation and the hindered settling phase of sedimentation, while allowing the detection of the critical concentration c_h for the phase shift. By additionally varying the salinity and temperature of the suspension, the variability in settling velocities caused by important influencing factors can be quantified.

3. Conclusions

Using the new approach, it is possible to measure settling velocities over a wide range of concentrations covering the flocculation and hindered settling phases. The results of the experiments indicate settling velocities in the range of $w_s = 0.3 - 1.7$ mm/s, depending on the experimental set-up. In the flocculation phase, an increase in settling velocity with suspended sediment concentration and salinity was observed. In the hindered settling phase, no significant changes are observed with varying salinity, but the settling velocity generally decreases with increasing concentration. On the other hand, the concentration, at which the phase change between flocculation settling and hindered settling is observed, is positively correlated with salinity. The significant data obtained allows to carry out model fits, such as Raudkivi (1998) for the flocculation settling regime or Winterwerp (2007) for the hindered settling regime and thus to derive the gelling point.

Acknowledgments

The authors would like to express their sincere thanks to all those involved in the field trips and laboratory experiments. We'd also like to thank the BAW for funding the research in the FAUST project. We'd like to thank the waterways and shipping administration in Bremerhaven and Emden and the Hamburg Port Authority (HPA) for their help in carrying out the field trips by providing ship capacity and staff.

References

- Patzke, J.; Nehlsen, E.; Fröhle, P.; Hesse, R. F. (2022): Spatial and Temporal Variability of Bed Exchange Characteristics of Fine Sediments From the Weser Estuary. In: *Front. Earth Sci.* 10, Article 916056. DOI: 10.3389/feart.2022.916056.
- Patzke, Justus; Hesse, Roland; Zorndt, Anna; Nehlsen, Edgar; Fröhle, Peter (2019): Conceptual design for investigations on natural cohesive sediments from the Weser estuary, INTERCOH 2019, Istanbul, Institut für Wasserbau, TU Hamburg, <https://doi.org/10.15480/882.3599>.
- Patzke, Justus; Nehlsen, Edgar; Fröhle, Peter (2021): Lab prepared sediment samples from the weser estuary - density profiles, settling & grain size curve. Unter Mitarbeit von TUHH Universitätsbibliothek.
- Raudkivi, Arved J. (1998): *Loose Boundary Hydraulics*. Boca Raton: CRC Press.
- Winterwerp, Johan Christian (2007): On the sedimentation rate of cohesive sediment, *Intercoh 2003, Estuarine and coastal fine sediments dynamics*, Bd. 8, Amsterdam, London: Elsevier (*Proceedings in Marine Science*, 8), S. 209–226. Online at <http://www.sciencedirect.com/science/article/pii/S1568269207800143>.
- Winterwerp, Johan Christian; van Kessel, Thijs; van Maren, Dirk S.; van Prooijen, Bram C. (2021): *Fine Sediment in Open Water*: World Scientific Pub. Co (55)



17th International Conference on
Cohesive Sediment Transport Processes
September 18-22, 2023
Inha University, Incheon, Republic of Korea



A study on distribution and behavior of in-situ suspended particulate matter in Taehan Coast, West Sea, Korea

Byoung Kwan Lee

Marine Research Center, National Park Research Institute, Korea National Park Service,
Yeosu, Jellanamdo, Korea

In-situ suspended particulate matter (SPM) concentration of the water column and particle size distribution above the middle layer and bottom layer were measure in the Taehan-Haeon National Park, west coast of Korea.

The short-term series of in-site suspended particulate matter concentration, total volume concentration, beam attenuation coefficient, mean grain size, floc size and distribution have been ensemble-averaged according to tidal variation. Time variation of in-situ particle size and concentration shows bottom layer supplies relatively fine-grained particles with compared with middle layer. This explains a good correlation between sediment concentration and beam attenuation coefficient due to well defined, monotonous size distribution. Abundance of small microfloc and large macroflocs with time and water column size distribution indicated the difference between organic matter in marine snow of turbidity maximum near-bottom layer and fine grain primary particles of water column. The particles supplied toward lower water column from upper water column during low tide showed a multi-modal distribution with two-three peak at coarse fraction, possibly due to the resuspension and the flocculation associated with marine biological activity and the increased shear velocity at near bottom, break-up of large particles.

This study can be used to qualitative and quantitative analysis of in-situ fine suspended sediment distribution, resuspension and flocculation, land (freshwater) and marine (seawater) based source of suspended particulate matters, according to marine environmental relationship and global climate change.

Keywords: National park, LISST-100x, suspended particulate matter, beam attenuation coefficient, flocculation



17th International Conference on
Cohesive Sediment Transport Processes
September 18-22, 2023
Inha University, Incheon, Republic of Korea



ISOLATION AND CHARACTERIZATION OF THE MOLECULAR COMPOSITION OF ALGAL DISSOLVED ORGANIC MATTER

Thi Thuy Trang Pham¹, Que Nguyen Ho¹, Sang Deuk Lee², Michael Fettweis³, and B.J. Lee¹

¹Department of Advanced Sciences and Technology Convergence, KNU, Sangju 37224, Korea

²Nakdonggang National Institute of Biological Resources (NNIBR), Sangju 37242, Korea

³Royal Belgian Institute of Natural Sciences, Rue Vautier 29, 1000 Brussels, Belgium

Abstract

In the aquatic environment, dissolved organic matter (OM) can increase either flocculation or stabilization of suspended particulate matter (SPM) (Lee BJ, 2019; Lee Byung Joon, 2017). Colloidal stabilization and flocculation of SPM in a water environment depend on the chemical/molecular composition of DOM. Cell exudates of microalgae are one of the primary sources of DOM. Extracellularly released DOM from microalgae consists of various chemical/molecular components (Findlay Stuart, 2003; Huangfu Xiaoliu, 2013; Qualls, 2013). DOM has been known as critical in controlling the global carbon cycle and the fate and transport of chemical pollutants (Huangfu Xiaoliu, 2013; Wilkinson Kevin J, 1997; Xu Huacheng, 2016). Despite its importance, the chemical/molecular composition of DOM and its roles in SPM flocculation and stabilization are still largely unknown. This study focuses on identification and characterization of the key DOM components, including polysaccharides and Humic substances, which mainly affect the flocculation and stabilization of SPM. The chemical/molecular composition of algal DOM was isolated and quantified by using Nuclear Magnetic Resonance (NMR), Fluorescence Excitation Emission Matrices (FE-EM), and Liquid Chromatography – Organic Carbon Detection (LC-OCD) techniques. In association with laboratory and field studies on SPM behaviours (i.e., flocculation and stabilization), these analytical techniques on the DOM composition will help us to understand the fundamental mechanisms of the biological and physicochemical processes in the aquatic environment containing various DOM and SPM.

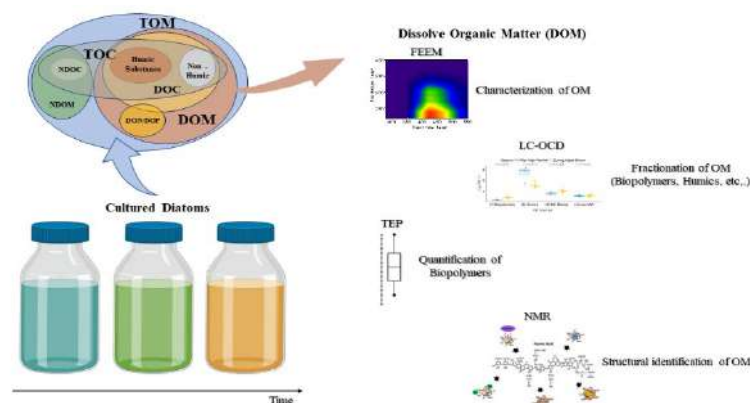


Figure 1. Schematic diagram of the analytical techniques for measuring the chemical/molecular composition of algal dissolved organic matter: Nuclear Magnetic Resonance (NMR),

Fluorescence Excitation Emission Matrices (FE-EM), and Liquid Chromatography – Organic Carbon Detection (LC-OCD) techniques.

Acknowledgement

This work was supported by the National Research Foundation of Korea (Grant No. NRF-2020R1I1A3A04036895) and Nakdonggang National Institute of Biological Resources (Grant No. NNIBR-202302104).

References

- Findlay Stuart, Sinsabaugh Robert L. (2003). Aquatic ecosystems: interactivity of dissolved organic matter: Academic press.
- Huangfu Xiaoliu, Jiang Jin, Ma Jun, Liu Yongze, Yang Jing. (2013). Aggregation kinetics of manganese dioxide colloids in aqueous solution: influence of humic substances and biomacromolecules. *Environmental science & technology*, 47(18), 10285-10292.
- Lee BJ, Kim J, Hur J, Choi IH, Toorman EA, Fettweis M, Choi JW. (2019). Seasonal dynamics of organic matter composition and its effects on suspended sediment flocculation in river water. *Water Resources Research*, 55(8), 6968-6985.
- Lee Byung Joon, Hur Jin, Toorman Erik A. (2017). Seasonal variation in flocculation potential of river water: Roles of the organic matter pool. *Water*, 9(5), 335.
- Qualls, Robert G. (2013). Dissolved organic matter. *Methods in biogeochemistry of wetlands*, 10, 317-329.
- Wilkinson Kevin J, Negre J-C, Buffle Jacques. (1997). Coagulation of colloidal material in surface waters: the role of natural organic matter. *Journal of Contaminant Hydrology*, 26(1-4), 229-243.
- Xu Huacheng, Yang Changming, Jiang Helong. (2016). Aggregation kinetics of inorganic colloids in eutrophic shallow lakes: influence of cyanobacterial extracellular polymeric substances and electrolyte cations. *Water Research*, 106, 344-351.



17th International Conference on
Cohesive Sediment Transport Processes
September 18-22, 2023
Inha University, Incheon, Republic of Korea



Application of sediment-carrying capacity over a sping-neap tide in the Yangtze Estuary

Simin Zhou ¹, Chunyan Zhu ¹, Jiamin Chen ¹ and Qing He ¹

¹ State Key Laboratory of Estuarine and Coastal Research, East China Normal University, P.R. China, 52183904009@stu.ecnu.edu.cn

1. Introduction

The response of suspended sediment concentrations (SSC) to sediment decline primarily due to reservoir construction and other factors is a research focus in estuaries (Besset et al., 2019). During the last decades, SSC in the Yangtze Estuary has decreased by 75% at the tidal limit Datong station, whereas the SSC remains stable for a long time in the estuarine turbidity maximum (ETM) (Yang et al., 2017). Although many studies have explored the reasons, the underlying mechanisms still need more research. Sediment-carrying capacity is often used to detect sediment transport in the river but rarely used in estuaries where the equilibrium state is difficult to attain. This study aims to quantify the sediment transport capacity to understand the sediment dynamics in the ETM under insufficient sediment supply.

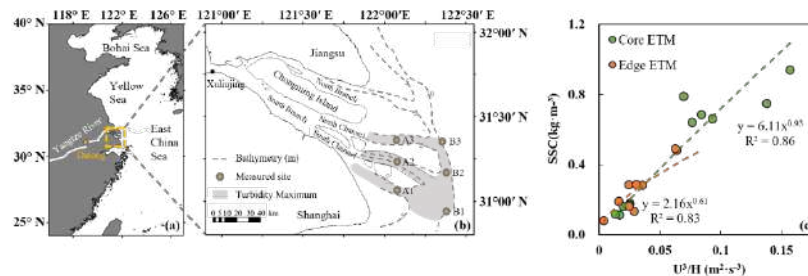


Fig 1. Map showing the study area, with (a) the location of Yangtze Estuary in China and the location of Datong station; (b) locations of measured sites (yellow dots) in the ETM; the area where station A1, A2, and A3 located is the core ETM, whereas the area where stations B1, B2, B3 located is the edge ETM; (c) correlation between tidally depth-averaged SSC and hydrodynamics parameter (u^3/h).

2. Methods

2.1 Field observation

We collected data at six stations (A1, A2, A3, B1, B2, B3) during spring and neap tide in the ETM of the Yangtze Estuary in September 2019. During the spring and neap tide, discharges at Datong were 24,700 m³/s and 20,100 m³/s, respectively. Water samples in six layers (0.0h, 0.2h, 0.4h, 0.6h, 0.8h, and 1.0h, where h is the water depth) were used to measure the velocity, salinity, and SSC. An onboard acoustic Doppler current profiler (ADCP) was employed to measure the current velocity profile during the survey, and the vertical turbidity profiles of the water column were measured using an optical backscatter sensor (OBS-3A).

2.2 Sediment-carrying capacity

The sediment-carrying capacity was used to calculate the amount of sediment transported for the given flow and boundary

conditions. The sediment transport capacity formula suggested by Zhang and Xie (1993) has been widely used as:

$$S_* = k \left(\frac{u^3}{h} \right)^m \quad (1)$$

where S_* is the sediment transport capacity in mass per unit volume; u is the depth-averaged velocity; h is the water depth; and k , m are calibrated coefficients. In this study, we performed curve fitting by tidally average parameters to obtain the parameters in the ETM (Fig. 1c).

In order to evaluate the sediment transport in different areas deviating from the sediment transport capacity under the equilibrium condition, we introduced a dimensionless parameter C_d :

$$C_d = \frac{S - S_*}{S + S_*} \quad (2)$$

Where S is the instantaneous depth-averaged suspended sediment concentration. The $C_d < 0$ suggests the suspended sediment is less than the flow can be transported (under-saturated condition) and therefore erosion is likely to occur. The larger C_d deviating from 0, the under-saturated state is more significant.

3. Results

The sediment-carrying capacity is larger in the core ETM than that in the edge of the ETM due to higher velocity and SSC in the core ETM than edge ETM (Fig 1c), indicating that the variation of hydrodynamics could drive noticeable SSC variation in the core ETM. Moreover, in the core ETM, the tidally averaged vertical gradients of SSC decreased from 0.16 kg/m² to 0.06 kg/m² from spring tide to neap tide, whereas the tidally averaged vertical gradients of SSC in the edge ETM decreased from 0.06 kg/m² to 0.05 kg/m². This indicated larger variations of SSC-induced stratification over the spring-neap tidal cycle in the core ETM than the edge ETM. The results of potential energy anomaly (PEA) suggested that the stratification in the edge ETM was dominant by salinity-induced density gradients, and the spring-neap variation of stratification was slight, meaning the relatively similar vertical mixing of sediment. With the large variations of sediment-induced density gradients, sediments' vertical mixing significantly changed in the core ETM. Therefore, high sediment-carrying capacity and effects of sediment-induced stratification cause the pronounced variation of the vertical SSC gradients over the spring-neap tide in the core ETM, whereas stratification dominated by salinity-induced gradients and smaller variation in SSC under low sediment-carrying capacity determine a relatively stable SSC vertical structure in the edge ETM.

The instantaneous sediment transport suggested different spring-neap responses in the core and edge ETM. In the core ETM, C_d had a mean value of -0.11, whereas C_d was -0.03 in the edge ETM (Fig. 2). In the core ETM, the C_d at the peak ebb was greater than that at the peak flood during the spring tide, indicating the stronger erosion at the ebb tide, while the C_d at the peak ebb was closed to that at the peak flood during the neap tide. In the edge ETM, the C_d at the peak ebb was smaller than that at the peak flood during the spring tide, whereas the C_d at the peak ebb was greater than that at the peak flood during the neap tide, suggesting that the main erosion period changes from flood tide to ebb tide.

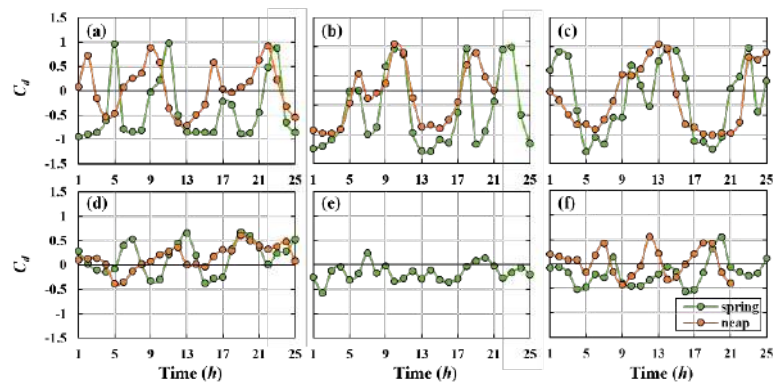


Fig 2. Time series of C_d at (a) A1, (b) A2, (c) A3, (d) B1, (e) B2, and (f) B3 during the wet season in 2019.

4. Conclusions

Our investigations indicated that sediment-carrying capacity is higher in the core ETM than that in the edge ETM, corresponding to stronger changes in sediment dynamics over a spring-neap tidal period in the core ETM than that in the edge ETM. The deviation from sediment-carrying capacity (C_d) indicates different spring-neap responses in the core and edge ETM. In the core ETM, C_d at the peak ebb was greater than that at the peak flood, indicating stronger erosion at the ebb tide, whereas in the edge ETM, the larger values of C_d occurred at the flood tide during the spring tide and at ebb tide during the neap tide, suggesting that the main erosion period changes from flood tide to ebb tide. Our study indicates that sediment-carrying capacity could suggest changes in sediment transport over a spring-neap tidal cycle and is valuable in future research on sediment dynamics.

Acknowledgments

This work is financially supported by the National Natural Science Foundation of China (Nos. U2040216 ,42206169), Shanghai Committee of Science and Technology (Nos. 21230750600, 20DZ1204701) and Shanghai Pujiang program (No. 22PJD020).

References

- Yang, Y.P., Deng, J.Y., Zhang, M.J., Li, Y.T., Liu, W.L. (2015). The synchronicity and difference in the change of suspended sediment concentration in the Yangtze River Estuary. *Journal of Geographical Sciences*, 25(04): 399-416. doi: 10.1007/s11442-015-1176-9
- Besset, M., Anthony, E.J., Sabatier, F. (2017). River delta shoreline reworking and erosion in the Mediterranean and Black Seas: the potential roles of fluvial sediment starvation and other factors. *Elementa: Science of the Anthropocene*, 5: 54-67. doi: 10.1525/elementa.139
- Zhang, R.J., and Xie J.H. (1993). *Sedimentation Research in China: Systematic Selections*, China Water and Power Press, Beijing, China, pp. 57–60. (in Chinese)



17th International Conference on
Cohesive Sediment Transport Processes
September 18-22, 2023
Inha University, Incheon, Republic of Korea



Sediment transport imbalance in the meso-tidal bay controlled by tidal pumping and residual circulation

S.I. Kim¹, J.Y. Seo¹, J.H. Park¹, P.J. Kim² and H.K. Ha^{1,*}

¹Department of Ocean Sciences, Inha University, Incheon, Republic of Korea,
[*hahk@inha.ac.kr](mailto:hahk@inha.ac.kr)

²Underwater Survey Technology 21, Incheon, Republic of Korea

1. Introduction

Bay, as a main connection between ocean and continent, is a transition zone where various physical, chemical, and biological processes are complicatedly combined. Imbalanced transport of sediment in the bay causes the dredging issues related to deposition in port navigation waterways. It can also determine the distribution of pollutants and nutrients in water bodies, which can affect water quality and benthic-pelagic ecosystem. Sediment transport is influenced by hydrodynamic factors such as residual circulation, tidal currents and asymmetries, river discharges, and wind-induced waves. The combination of these factors, each with different characteristics, creates heterogeneity in sediment distribution in bay. In estuarine sediment dynamics, the predominant mechanisms of sediment transport reveal different site-specific configurations (e.g., shape, slope, and bathymetry), thus they remain a challenging research topic. More comprehensive investigation is necessary to better comprehend the impact of these factors on sediment transport in various environments. This study aims (1) to understand the imbalance in sediment transport by tidal pumping and residual circulation and (2) to reveal the sediment resuspension mechanism in the meso-tidal bay.

2. Study area

Yeosu Bay is a semi-enclosed embayment surrounded by Namhae Island and Yeosu Peninsula, south coast of Korea. The mouth is open to the south, allowing free exchange with open ocean. The annual freshwater discharge from the Seomjin River is 2.58 billion tons yr⁻¹. The maximum tidal range is 2.9 m for spring tide and 1.1 m for neap tide. The maximum current velocities are 0.60 m s⁻¹ and 0.65 m s⁻¹ during the flood and ebb, respectively. Surface sediments were predominantly composed of mud in M1 (mean grain size of 2.96 mm) and sand in M2 (mean grain size of 8.96 mm).

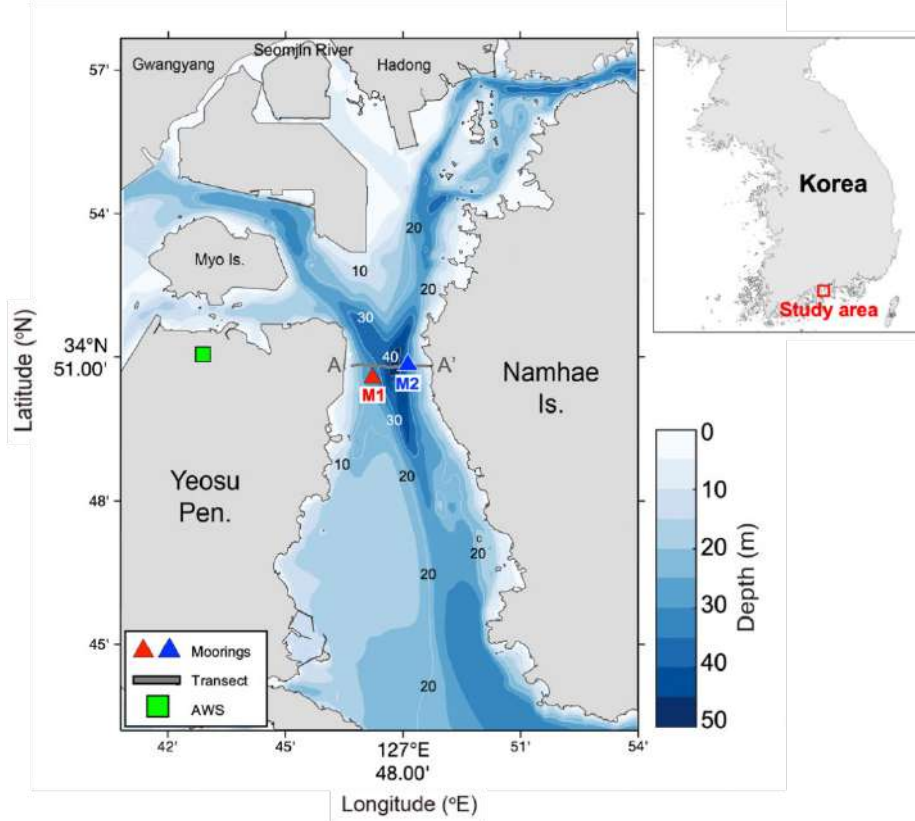


Figure 1. Map of the study area. Two acoustic Doppler current profilers (ADCPs) were concurrently deployed at M1 (red triangle, $34^{\circ} 50' 34.6''\text{N}$, $127^{\circ} 47' 12.6''\text{E}$) and M2 (blue triangle, $34^{\circ} 50' 52.1''\text{N}$, $127^{\circ} 48' 06.4''\text{E}$). The dark gray line indicates the ship-borne ADCP transect (A-A').

3. Materials and methods

In-situ mooring systems with ADCPs were installed in western (M1) and eastern (M2) parts of Yeosu Bay from September 3 to October 2, 2021 to investigate the transport mechanism of suspended sediments (Figure 1). Ship-borne surveys were performed along the transect (A-A') using research vessel on September 7, 2021. Echo intensity derived from ADCP was converted to the suspended sediment concentration (SSC) by the calibration with water samples. Suspended sediment flux (F , $\text{kg m}^{-2} \text{s}^{-1}$) at mooring stations were calculated, and tidal-averaged F (\bar{F}) was decomposed into tidal ($\overline{U' \cdot SSC'}$) and residual ($\overline{\bar{U} \cdot \bar{SSC}}$) mechanisms as follows:

$$F = U(z) \cdot SSC(z); \quad \bar{F} = \overline{\bar{U} \cdot \bar{SSC}} + \overline{U' \cdot SSC'}$$

where U is along-channel current velocity (m s^{-1}), and z is vertical coordinate (m). The overbar and prime notations indicate timescales longer and shorter than the tidal cycles determined by 36-h low- and high-pass filters, respectively. The depth-integrated \bar{F} was represented as total along-channel sediment flux (Q_{s_total} , $\text{kg m}^{-1} \text{s}^{-1}$).

4. Results and discussion

Over the entire mooring periods, the U was in the range of -1.08 - 0.79 m s^{-1} with an ebb-dominance. The \bar{U} at both M1 and M2 usually exhibited that the surface and bottom currents flowed toward the seaward and landward, respectively. It was also characterized by secondary

circulation, which induces a helical flow along the channel in a clockwise orientation without a clear difference depending on the tidal cycle (viewed from seaward). The zero-crossing depths of \bar{U} were frequently changed with relative importance among tide, wind, and freshwater discharge. Two-layered residual currents developed by the freshwater discharge at M2 ($< 0.24 \text{ m s}^{-1}$) was higher than that at M1 ($< 0.16 \text{ m s}^{-1}$). Even if the same current-induced shear stress as M2 (sand) was applied to bed, muddy sediment at M1 could be resuspended with higher SSC (maximum of 233 mg l^{-1}) to reach the water surface compared to that at M2. These differences in current and sediment resuspension created an imbalance in sediment transport. At M1, residual current was slightly positive (in the land direction) over the entire period, but the seaward sediment flux was dominant owing to ebb-dominant tidal pumping (92%). At M2, meanwhile, residual currents (74%) dominated landward sediment flux, followed by tidal pumping. Although they tended to be mutually compensated and balanced by the circulation over the entire period, the suspended sediment flux in M2 ($\sim 2.8 \text{ ton m}^{-1} \text{ day}^{-1}$) were about twice higher than that in M1 ($\sim 1.5 \text{ ton m}^{-1} \text{ day}^{-1}$).

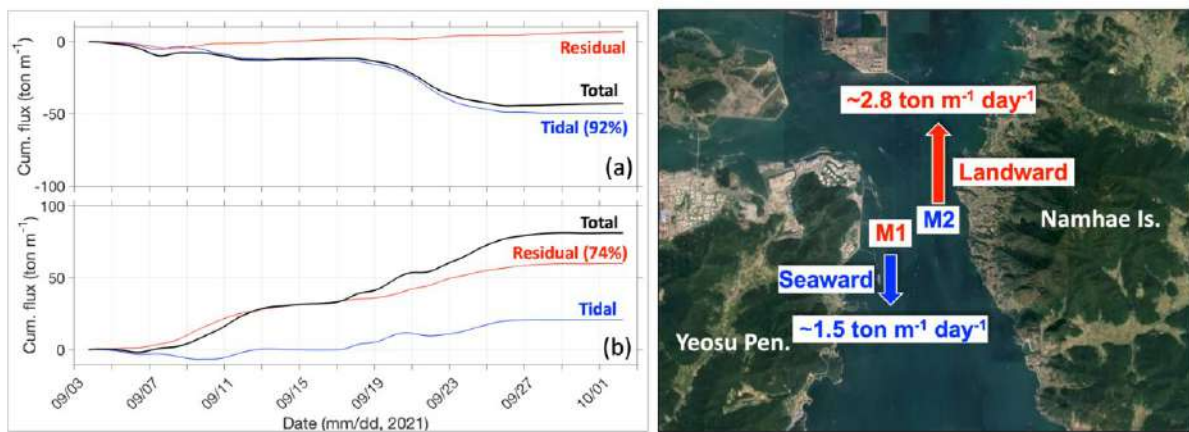


Figure 2. Time series of cumulative sediment flux (ton m^{-1}) over 4 weeks at (a) M1 and (b) M2.

5. Conclusions

Ship-borne surveys and in-situ mooring were conducted to investigate the sediment dynamics along the channel within the meso-tidal bay. Despite similar regional conditions, the difference in mechanisms driving sediment transport at the two stations resulted in imbalance of sediment transport. The seaward sediment flux at M1 was mainly driven by tidal pumping (92%), whereas the landward flux at M2 was mainly driven by residual currents (74%). This highlights the important roles of tidal pumping and residual currents in controlling the sediment transport.

References

- Figuroa, S. M., Lee, G. H., and Shin, H. J. (2020). Effects of an estuarine dam on sediment flux mechanisms in a shallow, macrotidal estuary. *Estuarine, Coastal and Shelf Science*, 238, 106718. doi: 10.1016/j.ecss.2020.106718
- Seo, J. Y., Choi, B. J., Ryu, J., and Ha, H. K. (2022). Dynamic evolution of a secondary turbidity maximum under various forcing conditions in a microtidal estuary. *Marine Geology*, 446, 106760. doi: 10.1016/j.margeo.2022.106760
- Hyun, S. M., Lee, T. H., Choi, J. S., Choi, D. L., and Woo, H. J. (2003). Geochemical characteristics and heavy metal pollutions in the surface sediment of Gwangyang and Yeosu Bay, south coast of Korea. *Sea*, 8(4), 380-391.



17th International Conference on
Cohesive Sediment Transport Processes
September 18-22, 2023
Inha University, Incheon, Republic of Korea



Dynamics on sediment resuspension by wind-induced estuarine circulation in a semi-enclosed bay: Preliminary results

C.Y. Eun¹, J.Y. Seo¹, S.M. Choi¹, W.J. Lee¹ and H.K. Ha^{1,*}

¹ Department of Ocean Sciences, Inha University, Incheon, Republic of Korea,
*hahk@inha.ac.kr

Understanding sediment dynamics is essential to evaluate environmental issues, especially in a semi-enclosed bay. Pollutants within bed sediments can be released into the water column by sediment resuspension, which is closely related to the hydrodynamic variabilities controlled by external forcing such as wind. To reveal characteristics of sediment dynamics by wind-induced estuarine circulation, *in-situ* observations were conducted from October 19 to November 16, 2022 in Ulsan New Port, which is a heavily-polluted area (Sun et al., 2015). Study area is a micro-tidal (tidal range: 0.4 m) bay where the water system can be characterized by seawater inflows and freshwater discharges from the Oehwang River (Ha et al., 2018). Two acoustic Doppler current profilers (ADCPs) were deployed along the channel (M1 and M2) to identify the estuarine circulation structure (Figure 1). Echo intensity, recorded from the ADCPs, was converted into suspended sediment concentration (SSC) using water samples obtained by a Niskin sampler (Kim et al., 2004). During the mooring period, the mean wind speed was about 3.5 m s^{-1} , prevailed by the northerly wind. The along channel current velocity ranged from -0.2 to 0.15 m s^{-1} at M1 and -0.25 to 0.35 m s^{-1} at M2. Residual current in both stations, which was calculated by a 36-h filter, was dominant showing classical estuarine circulation. In detail, it had a baroclinic structure with the seaward and landward flows at surface and bottom layer, respectively (Figure 2). Especially, the bottom current increased up to 0.08 m s^{-1} with the enhancement of northerly wind (up to 6 m s^{-1}). However, the seaward barotropic structure was developed when the wind direction was switched from northerly to southerly. This suggests that the classical estuarine circulation can be strengthened (weakened) by northerly (southerly) wind. Furthermore, by calculating suspended sediment fluxes, it can be identified whether the resuspended sediments within the bay can be imported or exported. During the presentation, the patterns and controlling mechanisms of sediment transport determined by wind-induced estuarine circulation will be discussed in more details.

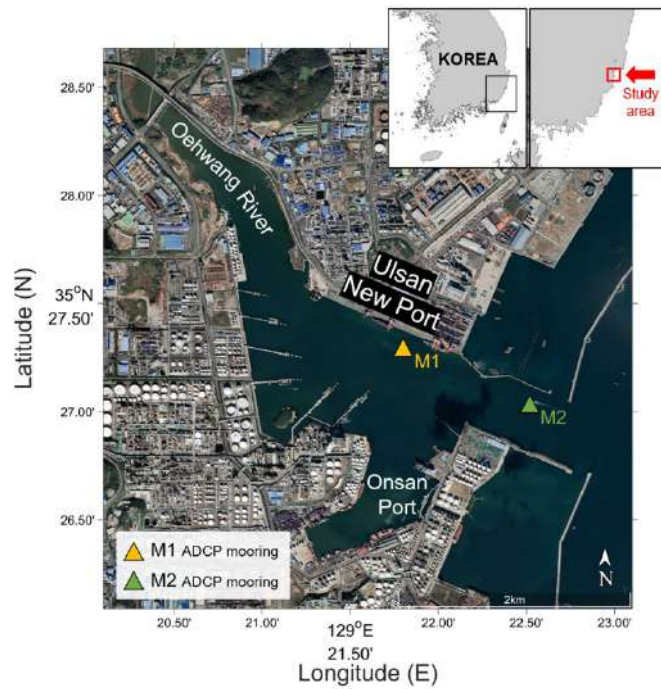


Figure 1. Map of the study area in Ulsan New Port. Triangles indicate two ADCP mooring stations (M1: 35.4544 °N, 129.3627 °E, M2: 35.4503 °N, 129.3747 °E).

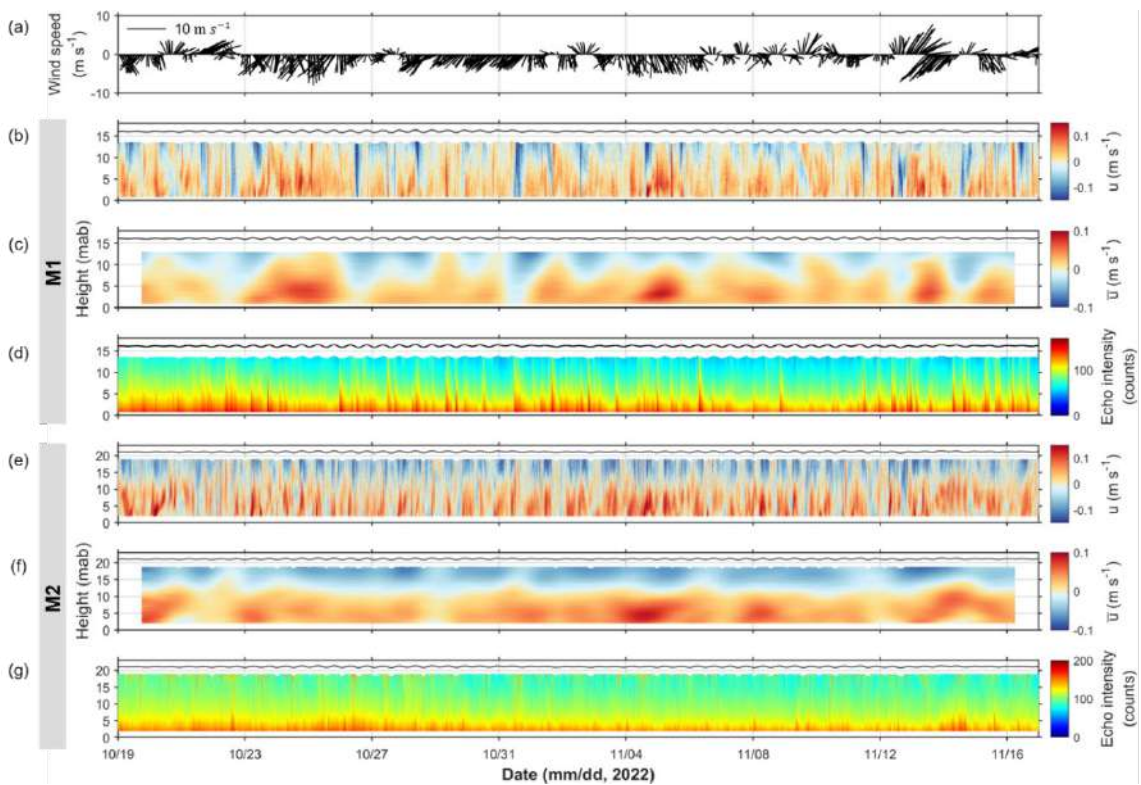


Figure 2. Time series of mooring data at M1 and M2 (October 19 to November 16, 2022): (a) wind speed, (b, e) along current velocity (u), (c, f) residual current velocity (\bar{u}), and (d, g) echo intensity.

References

Ha, H. K., Seo, J. Y., Jung, Y. H., Ha, H. J., Kim, S. B., Kang, J. W., Kim, Y. H., and Ryu, J. (2018). Dynamics of sediment resuspension in the inner harbor under different forcing conditions: A case study of Ulsan, Korea. *Journal of Coastal Research*, 85(10085), 451–455. doi: 10.2112/SI85-091.1

Kim, H. Y., Gutierrez, B., Nelson, T., Dumars, A., Maza, M., Perales, H., and Voulgaris, G. (2004). Using the acoustic Doppler current profiler (ADCP) to estimate suspended sediment concentration. University of South Carolina, 04–01. doi: 10.5281/zenodo.1419625

Sun, C. I., Kim, D. J., Lee, Y. W., and Kim, S. S. (2015). Pollution and ecological risk assessment of trace metals in surface sediments of the Ulsan-Onsan coast. *Journal of the Korean Society for Marine Environment and Energy*, 18(4), 245–253. doi: 10.7846/JKOSMEE.2015.18.4.24



17th International Conference on
Cohesive Sediment Transport Processes
September 18-22, 2023
Inha University, Incheon, Republic of Korea



Annual changes of the surface sediment characteristics near the port of Incheon

J.W. Kim¹, M.H. Kim², Y.J. Song² and S.B. Woo²

¹Artificial Intelligence Convergence Research Center, Inha University, Incheon, Korea,
kaonesis@gmail.com

²Department of Oceanography, Inha University, Incheon, Korea

Abstract

The changes in sediment characteristics at ports are deeply related to the water depth of the navigation channel along with the safety of ships, so continuous attention and monitoring are required. In estuaries with little anthropogenic influence, the sediment distribution patterns are closely related to storm and wave climate, coastal geometry, coastal erosion, the amount, and composition of sediment supplied by freshwater input, the along-channel sediment transport, and local remobilization of sediment by the interaction of the wave and tidal currents (Flemming and Ziegler, 1995). However, human activities such as harbor development and dredging can alter the short- and long-term natural tidal dynamics and thereby cause sediment changes.

The port of Incheon is located at the Han River estuary, which is a semi-enclosed geographical feature of the west coast of South Korea, and over the past 10 years, extensive port development and irregular dredging have been carried out. This region is a hyper-tidal estuary with a tidal range of more than 8 m with semi-diurnal variations, and various changes in the surface sediments occur due to the continuous influx of freshwater and suspended sediment from the Han River, about 50 km away. The overall sedimentation rate of the port ranges from 10 to 100 cm/year, indicating a spatially varied sedimentation distribution relative to the port length scale (Lee et al., 2019). In particular, the sedimentation rate at the inlet is high, so dredging work is steadily progressing to maintain the water depth for the safe navigation of ships. Dredging is cost-intensive, so understanding the underlying factors behind deposition is urgent.

In this study, to investigate the sediment distribution and their transport, the surface sediments were collected between 2011 and 2019 using a van Veen grab sampler (Figure 1). The mud and sand fractions of the samples were separated by wet sieving after removing organic matter and calcium carbonate by treatment with 10% H₂O₂ and 0.1N HCl, respectively. The dried sand fractions and wet mud fractions were analyzed by RO-TAP sieve shaker and Mastersizer 2000, respectively. Textural parameters were calculated by moment statistics. In addition, based on the analyzed grain size, sorting and skewness, the sediment trend analysis of the Gisedtrend program was applied to suggest the movement trend of surface sediments (Poizot and Mear, 2010).

The surface sediment distribution patterns and grain-size compositions reveal remarkable differences between the 2011 and 2019, which is also evident in their annual variation. The mean grain size ranges from sand to mud with a pronounced zonal distribution that differs substantially in navigation channel and inner part of the port (Figure 2). The sediment mainly consists of very coarse sand and silt, mean grain sizes ranging from 3 to 8 phi. Finer sands reach some distance into the upstream at the bed of the navigation channel. Sandy sediments

also line some shores of the northern part bay, whereas the remainder of the bay is covered by a mud blanket that shows a fining trend from the flanks of the main channel toward both opposite coastline, mean grain sizes ranging from 4–7 phi. Overall, the mud fraction increased from 2011 to 2014, and then the sand fraction increased again after 2014. The percentage distributions for 2011 and 2019 are almost similar (Figure 3). In the STA analysis results, the surface sediment transport towards the inner part of the port was evident. This was the same for the North and South ports. A trend of sediment transport converging towards the navigation channel was found around the passage, which may be related to the continuously reported sedimentation phenomena along the passage.

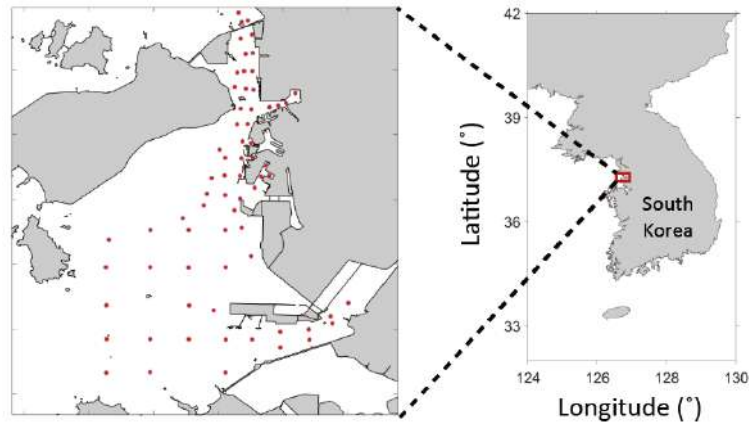


Figure 1. Maps showing the study area and surface sediment observation points.

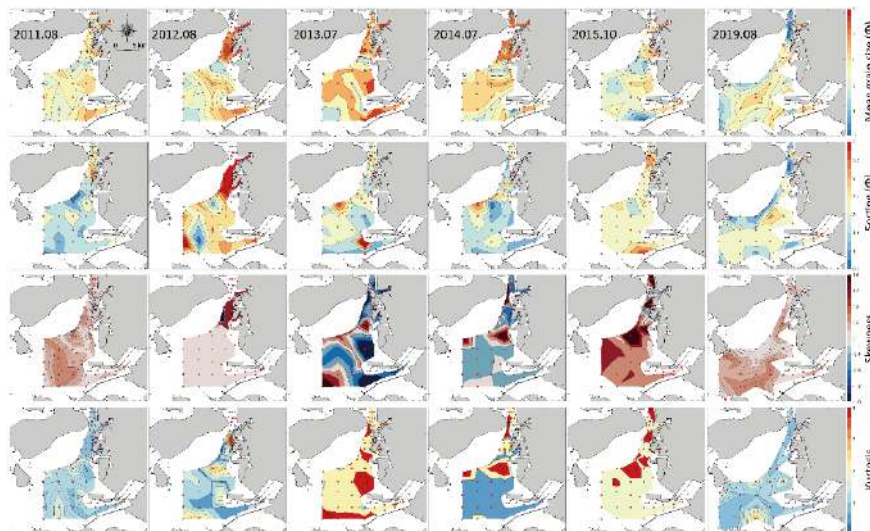


Figure 2. Annual changes of the textural parameters in the surficial sediment between 2011 and 2019.

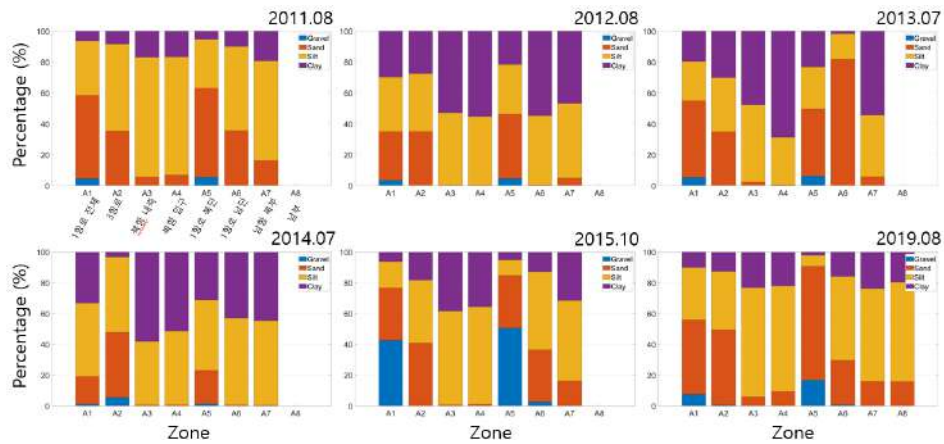


Figure 3. Annual change in percentage of gravel, sand, silt, and clay between 2011 and 2019.

References

- Flemming, B.W., Ziegler, K. (1995). High-resolution grain size distribution patterns and textural trends in the backbarrier tidal flats of Spiekeroog Island (southern North Sea). *Senckenberg Marit* 26, 1–24.
- Lee, G.H., Shin, H.J., Kim, Y.T., Dellapenna, T.M., Kim, K.J., Williams, J., Kim, S.Y., Figueroa, S.M. (2019). Field investigation of siltation at a tidal harbor: North Port of Incheon, Korea. *Ocean Dynamics*. 69, 1101–1120. <http://doi.org/10.1007/s10236-019-01292-0>
- Poizot, E., Mear, Y. (2010). Using a GIS to enhance grain size trend analysis. *Environmental Modelling and Software* 25, 513-525. <http://doi.org/10.1016/j.envsoft.2009.10.002>



17th International Conference on
Cohesive Sediment Transport Processes
September 18-22, 2023
Inha University, Incheon, Republic of Korea



Physicochemical Effects of Pyrolyzed OS on the Stabilization of Coastal Sediment

I. Jeong¹, H.E. Woo¹ and K. Kim²

¹ Research Center for Ocean Industrial Development, Busan, Korea, jeongi@pknu.ac.kr

² Department of Ocean Engineering, Busan, Korea

1. Introduction

Coastal sediments provide suppress the release of contaminants and provide habitats for vegetation and benthic macrofauna. However, due to low strength, highly cohesive coastal sediment is quite vulnerable to playing those roles. Oyster shells pyrolyzed at high temperatures have a high amount of calcium, which can aggregate sediment particles through Van der Waals forces (Kim et al., 2019). In this study, we aimed to investigate the physicochemical effects of pyrolyzed oyster shells on the shear strength of coastal sediments.

2. Materials and methods

Coastal sediment and seawater were taken from Samcheonpo harbour. Oyster shell (OS) was collected from Tongyeong. OS was pyrolyzed for 4 hours at 300 °C (PO-300) to remove water, at 600 °C (PO-600) to remove organic matter, and at 800 °C (PO-800) to increase CaO contents in OS. After then, OS was ground to a particle size of less than 5 mm. Coastal sediments (9 L) were mixed with 0.8 L, 1.6 L, and 2.4 L of pyrolyzed OS at different pyrolysis temperatures and filled in HDPE buckets. And coastal sediment without pyrolyzed OS was also prepared for control. All control and experimental cases were duplicated twice. After two weeks, the shear strength of all control and experimental cases was measured using a vane (50.8×101.6 mm) tester. The structural property was investigated using a scanning electron microscope (SEM) analysis.

3. Results and discussion

The shear strength was 0.07 kPa in control, 0.06–0.07 kPa in PO-300, 0.07–0.09 kPa in PO-600, 0.14–0.18 kPa (Figure 1). The shear strengths in PO-600 and PO-800 were 130% and 200–250% higher than that in control, respectively. The pyrolysis temperature of OS is the main factor in increasing the shear strength of coastal sediment, while the mixing ratio of OS showed less relationship to increase shear strength. CaCO₃ in OS is converted to CaO in high pyrolysis temperatures (700–800 °C). CaO would have formed calcium-silicate-hydrate (CSH) through a pozzolanic reaction, leading to high shear strength in PO-800. The SEM analysis shows that a platy type of sediment particle was observed in the control (Zhang et al., 2020). The formation of CSH was observed in all experimental cases. However, the size of CSH aggregates was higher in PO-800. In addition, the formations of ettringite and effective bridge were observed in PO-800.

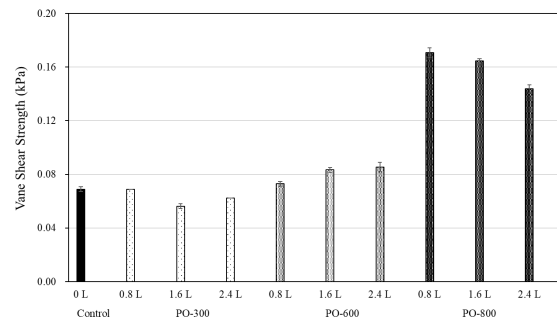


Figure 1. Shear strength of control and experimental cases.

4. Conclusions

Calcium eluted from pyrolyzed OS improved the bonding force of sediment particles, increasing the shear strength of sediments. The increased strength of the coastal sediment can supply stabilized habitat for coastal vegetation and benthic macrofauna. Therefore, utilizing pyrolyzed OS in the coastal sediment will be a promising approach to improve the coastal benthic environment.

References

- Kim, K., Suh, Y.-C., Lee, I.-c., Choi, C.-G., Kim, K., 2019. Changes in Permeability and Benthic Environment of Coastal Sediment based on Calcium Salt Supplier. *Journal of Coastal Research* 91, 311.
- Zhang, W.-L., Zhao, L., McCabe, B., Chen, Y.-H., Morrison, L., 2020. Dredged marine sediments stabilized/solidified with cement and GGBS: Factors affecting mechanical behaviour and leachability. *Science of The Total Environment* 726.



17th International Conference on
Cohesive Sediment Transport Processes
September 18-22, 2023
Inha University, Incheon, Republic of Korea



Comparison of different techniques for the determination of detailed vertical density profiles in cohesive sediment layers in the area of the Port of Hamburg

M. Witt¹, J. Patzke¹, E. Nehlsen¹ and P. Fröhle¹

¹ Institute for River and Coastal Engineering (IWB), Hamburg University of Technology (TUHH), Hamburg, Germany, markus.witt@tuhh.de

1. Introduction

The lower and outer Elbe River is one of the largest estuaries in Europe and provides access to the Port of Hamburg, which is the third-largest European container port. Between 2013 and 2018 several hydrological and morphological changes have been observed in the tidal Elbe, particularly an unusually high increase in tidal range, turbidity and sedimentation rates. The latter has been countered by increased maintenance dredging, which is an economic and ecological burden. Reasons for the described changes are seen in morphological changes in the river mouth, persistently low headwaters and an insufficiently adapted sediment management (Weilbeer et al. 2021).

The numerical models currently in use cannot adequately represent these developments. In particular, the complex behavior of the cohesive sediments in the heavily anthropogenically influenced river section is a major challenge. To tackle this situation and deepen the understanding of estuarine sediment transport in general, the joint project ELMOD is conducted. Involved partners are the Federal Waterways Engineering and Research Institute (BAW, model application), the University of the Bundeswehr Munich (UniBW, development of model approaches) and the Hamburg University of Technology (TUHH, field measurements and laboratory investigations).

2. Investigations

This contribution outlines the conception of the first ship-based measurement campaign in the port of Hamburg and puts a focus on the in-situ measurements of vertical density profiles with different methods. Additionally, the agreement of the in-situ measured density profiles with the vertical density distribution of sediment cores collected during the same campaign is checked.

2.1 Conception of the measurement campaign

The concept involves two ships equipped with several measuring devices e.g., sediment echosounder, density meters, ADCP, multi-parameter probe and a sediment corer, operating at a known sedimentation hotspot in the port area. Measurements are conducted in the vicinity and directly at the positions of sediment sampling around slack water. The overall objectives are i) to characterize the spatial distribution of the sediments in-situ, ii) to describe the hydrological conditions at the time of extraction and iii) to collect sediment samples for further laboratory studies on consolidation and erosion behaviour.

2.2 Density profiles

In-situ density profiles are recorded by different density probes and are supplemented by measurements with a suspended matter probe. The results provide detailed site-specific data of the vertical structure and layering of the bed.

2.3 Sediment sampling

During the field campaign, sediment samples are taken with a coring device described in Patzke et al. 2022. After sampling, density profiles of the cores are measured with an Anton Paar DMA 35. The results are used to assign the extracted cores to the associated sediment layer and are compared to pressure-based extraction-depth measurements.

3. Conclusions

The presented concept of the measurement campaign and especially the in-situ density profiles help to put the collected sediment samples into a three-dimensional context. Moreover, the findings will also assist in the interpretation of results of further laboratory studies.

Acknowledgements

The IWB would like to thank the Federal Ministry of Education and Research (BMBF) and the German Coastal Engineering Research Council (KFKI) for funding and supporting the project and the Hamburg Port Authority (HPA) for providing ship capacities and measurement equipment.

References

Patzke, J.; Nehlsen, E.; Fröhle, P.; Hesse, R. F. (2022): Spatial and Temporal Variability of Bed Exchange Characteristics of Fine Sediments From the Weser Estuary. In: *Front. Earth Sci.* 10, Article 916056. DOI: 10.3389/feart.2022.916056.

Weilbeer, Holger; Winterscheid, Axel; Strotmann, Thomas; Entelmann, Ingo; Shaikh, Suleman; Vaessen, Bernd (2021): Analyse der hydrologischen und morphologischen Entwicklung in der Tideelbe für den Zeitraum von 2013 bis 2018. 73. DOI: 10.18171/1.089104.



17th International Conference on
Cohesive Sediment Transport Processes
September 18-22, 2023
Inha University, Incheon, Republic of Korea



Rheological Properties of Sediment-Water Mixtures: Experimental and empirical investigation

Mingze Lin¹, Xiaoteng Shen^{1,*}, Fang Pan¹

¹ State Key Laboratory of Hydrology-Water Resources and Hydraulic Engineering, Hohai University, Nanjing, China, xiaoteng.shen@hhu.edu.cn

Suspended sediments are present in many natural and engineered systems, including rivers, estuaries, and wastewater treatment facilities. Understanding the rheological behavior of these sediments is crucial for investigating the near-bed particle dynamics, in which the viscosity of highly concentrated suspension is primarily focused on to quantify its resistance to deformation. In this study, the relationship between relative viscosities (η_r) and volumetric concentrations (ϕ) for different sediment types (Table 1) was investigated using a rotational viscometer.

The results show that the conventional Einstein formula for diluted sand severely underestimates the η_r for highly concentrated suspensions. This finding highlights the importance of developing more accurate models for predicting the rheology of sediment-water mixtures. For pure silts and non-cohesive quartz, η_r increased linearly and slowly with ϕ . However, the η_r of clays increased exponentially at first and then reached a plateau, with kaolinite, montmorillonite, and bentonite rising more rapidly than chlorite and illite.

To simulate the $\eta_r \sim \phi$ relationship, a modified viscosity model based on Costa (2005) was proposed, which agreed reasonably well with observations and produced similar results to the measurements. In addition, field mud from Dafeng coastal area was also collected to conduct the viscosity experiments and the proposed model fit the results with good accuracy. Besides, the developed model was coupled with TELEMAC-2D, a hydrodynamic open-source model, to simulate the deposition of a thickened tailings slurry. The simulation results demonstrated the applicability of the developed model for predicting the sediment transport and deposition processes in practical engineering applications.

Future models may need to pay attention to the effects of flow properties, especially for non-Newtonian fluids, and their applications in large-scale modelling. Overall, this study provides important insights into the rheological behavior of suspended sediments, which are critical for understanding sediment transport and deposition in natural and engineered systems. The findings of this study may have implications for environmental and engineering applications, such as sediment dredging and sedimentation control in water treatment facilities.

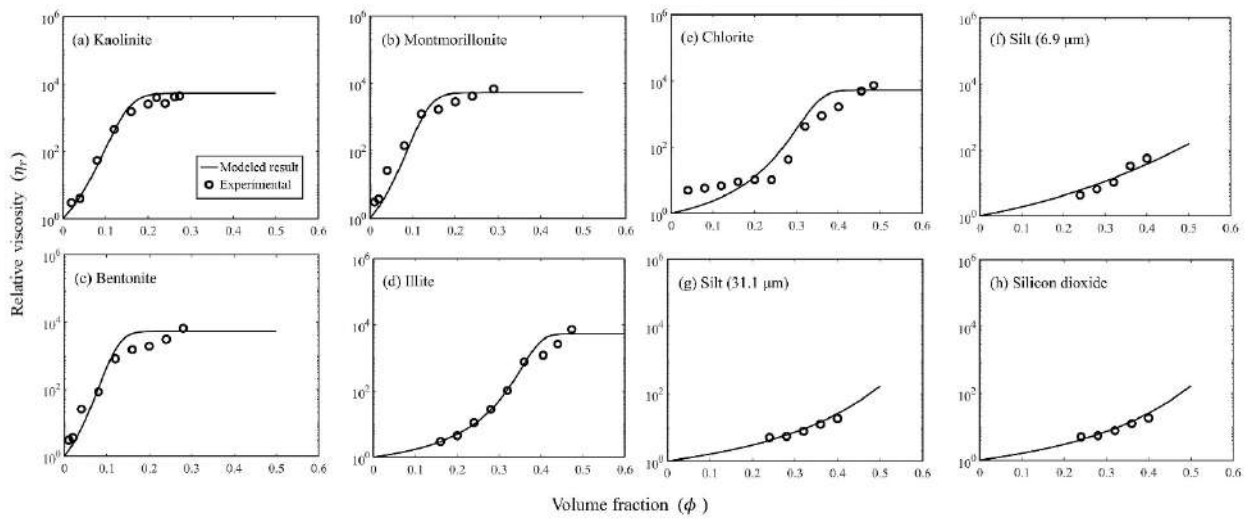


Figure 1. The experimental and modelled results of different type of sediments.

Table 1. Experimental material

size	Kaolinite	Montmorillonite	Bentonite	Chlorite	Illite	Silt (6.9 μm)	Silt (31.1 μm)	Silicon dioxide
D_{50} (μm)	4.0	6.3	9.2	61.5	25.0	6.9	31.1	27.3

References

Costa, A. (2005). Viscosity of high crystal content melts: dependence on solid fraction. *Geophys. Res. Lett.* 32(22). <https://doi.org/10.1029/2005GL024303>

Session: Sediment Transport I
09:00 – 10:40
Tuesday, September 19, 2023



17th International Conference on
Cohesive Sediment Transport Processes
September 18-22, 2023
Inha University, Incheon, Republic of Korea



Sediment fluxes at the interface between estuary and coastal sea: unravelling the role of tides, waves and river discharge from long term (2015-2022) high frequency monitoring at the SCENES Station

R. Verney¹, D. Le Berre¹, M. Repecaud², A Bocher², C. Poppeschi³, F. Grasso¹

¹ Ifremer, DHYSED, Plouzané, France

² Ifremer, RDT, Plouzané, France

³ Ifremer, LOPS, IUEM, CNRS, IRD, Univ. Brest, Plouzané, France

1. Introduction

Along the land-sea continuum, mouths are critical areas as connecting estuaries to their adjacent coastal seas. Investigating the main mechanisms controlling sediment dynamics and sediment fluxes is essential as it contributes to understanding and quantifying sediment import/export to the estuary, and its consequences in terms of morphological changes and environmental management.

Generally, fluxes are examined from model results. In this study, we analyse 7 years of high-frequency observations (coupled optical and acoustic measurements) at the mouth of the Seine Estuary, both in terms of suspended sediment concentration and sediment fluxes. We also discuss the calibration methodology and related uncertainties.

2. Methods

The SCENES station is located at the mouth of the Seine Estuary, by 15m depth (mean water level). This station is part of the SNO COAST-HF and PHRESQUES monitoring networks. It consists in a surface buoy, equipped with a fluorescence/turbidity optical sensor (WetLabs FLNTU), a CTD and an O₂ sensor (all measurements ~1.5m below surface), and a bottom station, including an AWAC (wave, current, acoustic backscatter) and a fluorescence/turbidity optical sensor. This station was deployed in October 2017, until now. Before this, a similar test station (D4) was deployed, with a major difference: the turbidity sensor on the bottom station was measuring 1.4m above the bed, instead of 0.5m for the SCENES configuration. An empirical correction function was applied to standardise all measurements at 1.4m above the bed.

More than 40 field campaigns were conducted at this station to calibrate optical turbidity sensors, and conduct reference CTD-OBS vertical profiles along tidal cycles.

The acoustic backscatter signal was processed using the sonar equation, corrected for spherical spreading, geometric terms and water attenuation. A new calibration procedure combining station-based optical measurements and field survey observations was applied to calculate vertical SSC profiles.

2. Results

2.1 – SSC dynamics at surface and bottom

Analysing surface and bottom time series, we show the strong influence of tidal currents and waves on sediment concentrations, and a weaker influence of the river discharge. At the bottom,

tidal-median SSC increases with tidal ranges, from 5mg/l during neap tides to more than 20mg/l during spring tides. Increasing the river discharge imply a shift of the estuarine turbidity maximum toward the mouth and an increase of the tidal-median SSC ($\sim x2$ from low to high river discharge). Wave conditions are the most impacting forcing, with tidal-median SSC close to 100mg/l when tidal-P90 Hs (Percentile 90 significant wave height) is over 1.5m. At the surface, patterns are similar but tidal-median SSC is much lower. Also, the effect of wave, while visible, is less important compared to bottom SSC, and comparable to the influence of the river discharge at the surface.

2.2 – Sediment fluxes at the mouth

Similarly to SSC, burst-integrated (1800s), depth integrated sediment fluxes (East-West direction) are the largest during storm events, and show high values during high river discharge and spring tides (Figure 1). During spring tides in absence of waves, burst integrated fluxes reach 500kg/m during flood, and less than 100kg/m during ebb, while they only reach 50kg/m during neap tides – flood phase. During storm events, burst-integrated fluxes can reach 2000kg/m, both during ebb and flood.

In order to unravel the influence of forcings on sediment fluxes, tidal-residual fluxes are calculated and averaged per wave, tidal range and river discharge conditions (Figure 2). We can observe that during calm wave conditions (P90 Hs<1m), sediments are imported to the estuary, while above this threshold, sediment is exported toward the bay. In absence of wave, sediment fluxes are positive (i.e. importing) and the strongest for low to moderate tidal ranges, but negative (i.e; exporting) during high tidal ranges. Moreover, we can observe that the sediment flux toward the estuary is stronger during high river discharge, due to the combination of the tidal pumping and the exacerbated density circulation, confirming model simulation results by Schulz et al. (2018). These patterns finally can be used to evaluate long-term fluxes at the mouth, filling gaps in observations.

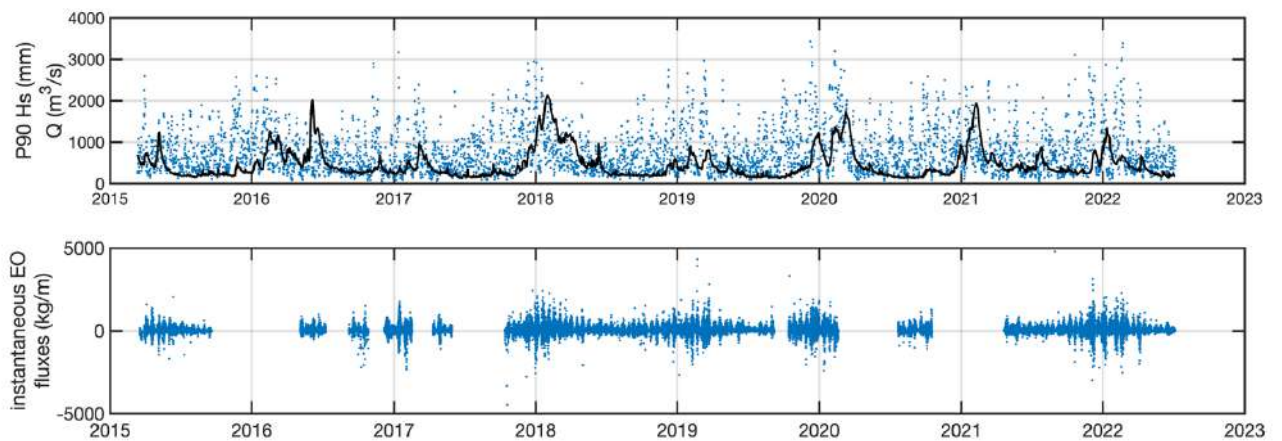


Figure 1: River discharge and Wave condition (percentile 90 Hs per tidal cycle) (top) and instantaneous East-West depth-integrated sediment fluxes from 2015 to 2022 at the mouth of the Seine estuary (bottom).

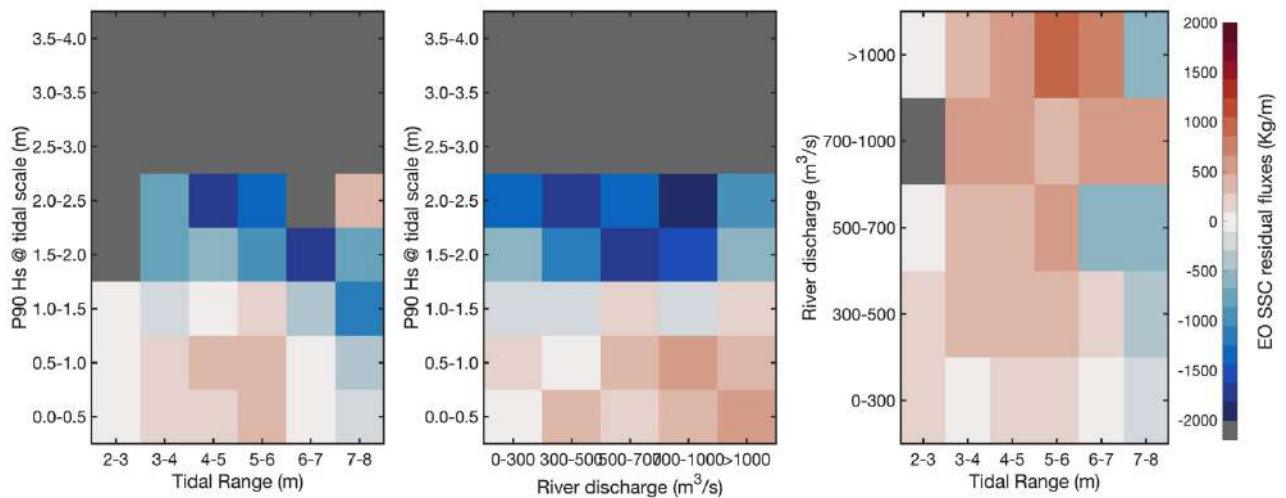


Figure 2: Mean East-West depth-integrated tidal average sediment fluxes map as functions of wave and tidal range (left), river discharge and wave (middle) and tidal range and river discharge (for $H_s < 1\text{m}$). At least observations over 10 tides were necessary to evaluate mean fluxes per forcing conditions (gray color mask otherwise).

2.3 – ...and what about suspended sediment composition?

As demonstrated by Pearson et al. (2021), optical and acoustic measurements can be combined to (at least) qualitatively evaluate the characteristics of suspended sediments, i.e. the presence of sand and mud. We applied this method to measurements obtained at the first cell of the AWAC. This Sediment Composition Index can also be related to the optimal d_{50} evaluated from the sonar equation calibration method. We observe that sand presence probability increases with the tidal range, and is very high during storms, which is in agreement with the energy requested to resuspend sand grains.

3. Conclusions

We investigated the dynamics of sediment fluxes at the interface between an estuary and its adjacent coastal sea, analysing 7 years of *in-situ* measurements from a coastal observatory. The main estuarine mechanisms (tidal pumping, density circulation) and their relation with forcings are clearly identified, together with the importance of wave on residual fluxes direction. From these observations, we can validate model results, and evaluate long term trends on sediment import to/export from the estuary.

4. References

Schulz, E., Grasso, F., Le Hir, P., Verney, R. and Thouvenin, B. (2018). "Suspended sediment dynamics in the macrotidal Seine estuary (France) - Part 2: Numerical modelling of sediment fluxes and budgets under typical hydrological and meteorological conditions." *Journal of Geophysical Research: Oceans*. 123 :578–600

Pearson S. G., Verney R., Prooijen Bram C., Tran D., Hendriks E.C.M., Jacquet M., Wang Z. B. (2021). Characterizing the Composition of Sand and Mud Suspensions in Coastal & Estuarine Environments using Combined Optical and Acoustic Measurements. *Journal of Geophysical Research-oceans*, 126(7), e2021JC017354



17th International Conference on
Cohesive Sediment Transport Processes
September 18-22, 2023
Inha University, Incheon, Republic of Korea



Tidal creeks affect the hydromorphology of bare tidal flats

J.L.J. Hanssen^{1,2}, Romaric Verney³, Florent Grasso³, D.C. van Maren^{1,2}, P.M.J. Herman^{1,2},
B.C. van Prooijen¹

¹ Delft University of Technology, Delft, The Netherlands, j.l.j.hanssen@tudelft.nl

² Deltares, Delft, The Netherlands

³ Ifremer, Brest, France

1. Introduction

Tidal flats are key elements of estuaries and muddy coasts. They are home and feeding grounds for numerous species of birds and fishes. These flats are (however) not entirely flat, as they are often covered with bed forms that affect the biomorphology of the tidal flat (e.g. Weerman et al. 2011). A typical bed form are creeks, which are a type of bed form that cut through the flat in cross-shore direction and can connect to the marsh on the landward side of the flat. Research towards creeks has shown that these can have a large influence on the local hydromorphology and consequently the longevity and effectiveness of the tidal flat as an ecological hub. However, previous research focussed primarily on creeks with a salt marsh connection (e.g. D'Alpaos 2007; 'Lanzoni & D'Alpaos 2014). For bare flat creeks (i.e. not connected to the marsh), the effect on the biomorphology of the flat is scarcely understood, even though many bare tidal flats exist worldwide. Here, we investigate how the creek influences the flow pattern, the bed composition and bathymetry of the surrounding tidal flat.

2. Method

We executed a field campaign on a convex-up flat, to measure the influence of a creek on the upper and lower part of a bare tidal flat. We selected a tidal flat along the Loire (France) because this flat had a creek with sufficient length and depth to accommodate multiple instruments. We installed 10 frames with pressure sensors, acoustic and optical instruments to measure water level, flow velocities, sediment transport and bed level changes in the creek, on the flat close to the creek, and at distance from the creek (Figure 1, left).

We also took bed samples to determine the particle size distribution, water content and density to test the influence of the creek on the upper and lower flat. These samples were taken near the frames and in a grid surrounding the creek at 55 locations in total. For this grid, we pre-defined isolines of inundation time based on the bed level and water level. For each line of inundation time, we took samples; in the creek, at the creek banks and at different distances from the creek (Figure 1, left).

3. Results

Analysis of the measurement data shows that the creek has affected the local hydromorphology of the bare tidal flat in several ways. For example, we found a difference in bed material between the creek and the flat, as well as a gradient in bed characteristics towards the creek (Figure 1, right). This difference was clear for both the upper flat and the lower flat. On the upper flat, the dry density was lower on the flat compared to the creek if the creek depth was

more than 30 cm. On the lower flat the bed material of the flat and the creek differed as well, with dry density higher on the flat compared to the creek. The pattern of the mud content was inverse related to the dry density pattern. This indicates that the hydromorphology is affected by the creek, even when the flat slope becomes steeper on the lower flat.

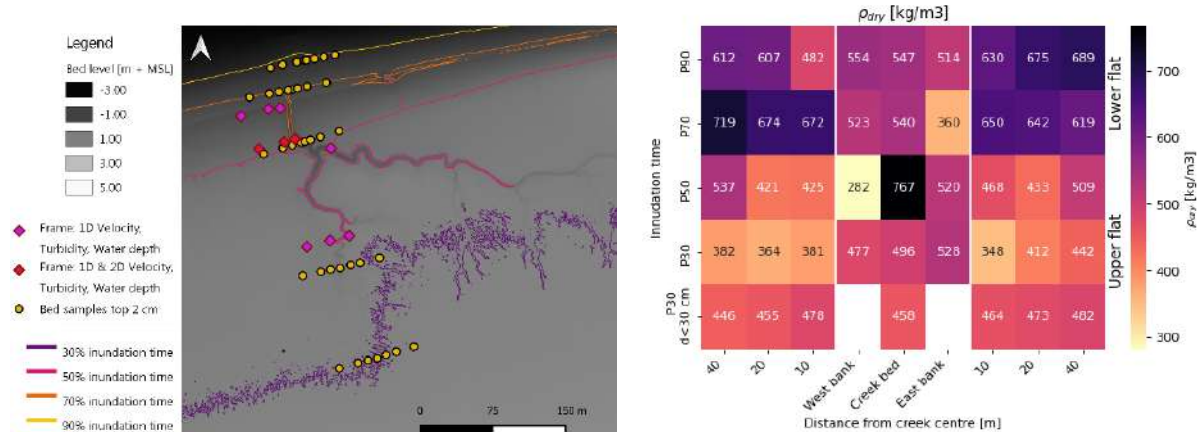


Figure 1. Left, lay-out of fieldwork including frame and sample locations and isolines for the different inundation times at the tidal flat in the Loire. Right, Dry density measured in the creek, on both creek banks and at 10 m, 20 m and 40 m distance from the creek for different lines of inundation time.

Based on the first results of the flow field on the tidal flat, we can explain a part of the bed composition and how this is influenced by the creek. On the lower flat, the flow is predominantly in alongshore direction during a tidal cycle. Here, the flow velocities are too high for fine particles to settle and accumulate. On the upper flat, the flow velocities are dominant in cross-shore direction and the magnitude is smaller compared to the lower flat. Hence, the milder hydrodynamic conditions facilitate a higher mud content on the upper flat. Measurements in the creek showed that the cross-shore flow (i.e. parallel to the creek) was dominant on the upper as well as on the lower flat and almost continuous during a tidal cycle. The continuous flow will wash out the fine material in the creek. Therefore, the creek mud content is lower compared to the flat, on the upper flat. Due to the continuous flow the creek bed is submerged during a large part of the tidal cycle, especially on the lower part of the flat. This results in a larger water content and smaller dry density in the creek compared to the flat. The next step is to investigate if and how the direction and magnitude of the flow are affected by the creek.

With this research, we unravel a new part on how bed forms affect the hydromorphology of the tidal flats. Based on these abiotic insights, we can better understand how creeks influence the stability of the tidal flat and also the biology present. As such, the measurements and insights can assist in improving management of existing tidal flats or the restoration of tidal flats.

References

- D'Alpaos, A., Lanzoni, S., Marani, M., Rinaldo, A. (2007), Landscape evolution in tidal embayments: Modeling the interplay of erosion, sedimentation, and vegetation dynamics, *J. Geophys. Res.*, 112, F01008, doi: 10.1029/2006JF000537
- Lanzoni, S., and A. D'Alpaos (2015), On the funnelling of tidal channels, *J. Geophys. Res. Earth Surf.*, 120, 433-452, doi:10.1002/2014JF003203

Weerman, E., Herman, P., Koppel, J. (2011) Macrobenthos abundance and distribution on a spatially patterned intertidal flat, *Marine Ecology Progress Series*, Vol. 440: 995-103, doi: 10.3354/meps09332



17th International Conference on
Cohesive Sediment Transport Processes
September 18-22, 2023
Inha University, Incheon, Republic of Korea



Quantitative evaluation of the contribution of flocs to sediment flux in a Cohesive Sediment Environment

Wenjian Li^{1,2*}, Guanhong Lee², Jongwi Chang², Ojudoo Darius Ajama², and Jae-il Kwon³

¹ CAS Key Laboratory of Marine Geology and Environment, Institute of Oceanology, Chinese Academy of Sciences, Qingdao 266071, China

² Department of Oceanography, Inha University, Incheon 22212, Korea

³ Coastal Disaster and Safety Research Department, Korea Institute of Ocean Science and Technology, Busan 49111, Korea

* Corresponding author (E-mail: liwenjian@qdio.ac.cn)

1. Introduction

Fine-grained particles in the aquatic environment tend to aggregate into flocs characterized by their fragile structure and higher settling velocity, which significantly influences the sediment transport process. However, there is still a deficiency of quantitative evaluation of the contribution of flocs to sediment flux due to the technical limitations in distinguishing flocs from primary particles in field observations. Over the past few years, Fall et al. (2021) have developed a method for distinguishing them using a floc camera and LISST. Thus, in this study, we followed this method and conducted comprehensive observations in the Songdo tidal flats. By distinguishing the mass contribution of flocs and their variation, we quantitatively evaluate their contribution to transport fluxes. The time series of current observations help us to elucidate the relationship between the mass contribution of flocs and turbulent conditions. The aim of this research will enhance the understanding of the flocculation process of fine-grained sediments and provide a reference for the evolution of coastal geomorphology.

2. Instruments Deployment and Methodology

2.1 Instruments Deployment

The observation site is located at the Songdo tidal flat, Korea (Figure 1a-d). The casting observation involving Floc Camera, CTD and LISST are conducted at a System Support Platform (Figure 1a) during spring and neap tide period (April 4th to May 21st). At the same time, the water samples are also collected during every cast to get the mass concentration of suspended sediment (TSS). A mooring observation system is located near the System Support (Figure d).

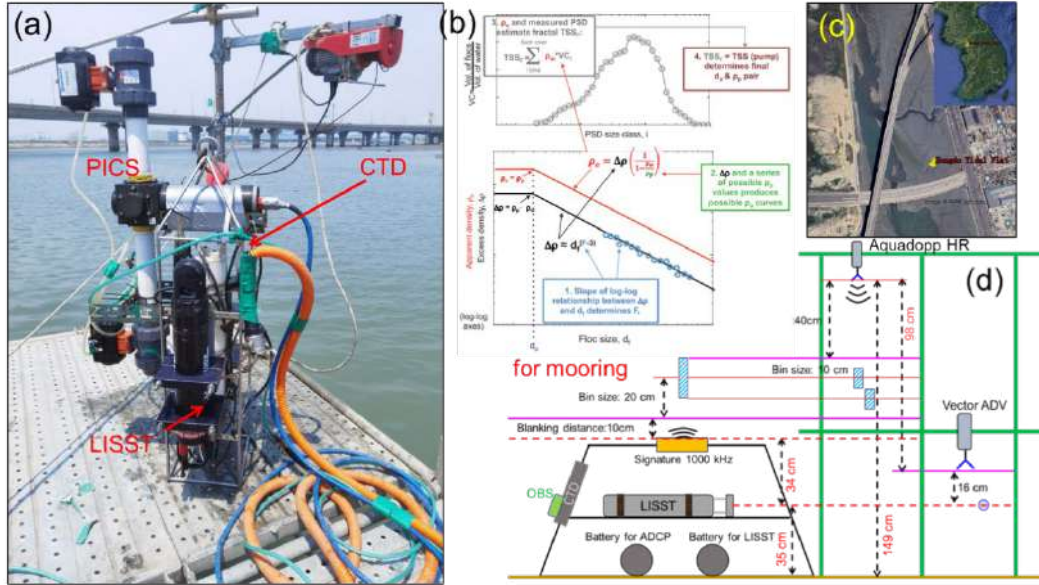


Figure 1. Location map of Songdo site and the instruments deployment. The conceptual model that depicts how the theoretical relationship between $\Delta\rho$ and ρ_a is derived from Fall et al. (2021).

2.2 Methodology

Flocs can be described as the combination of water and constitute particles, and a floc's wet density (ρ_f) can be described as the wet mass of the floc (M_f) divided by the volume of the floc (V_f), then:

$$\Delta\rho = \rho_f - \rho_w = \frac{M_p + M_w}{V_p + V_w} - \frac{M_w}{V_w} = \frac{V_w M_p - V_p M_w}{(V_p + V_w) V_m} \quad (1)$$

where ρ_w , M_w , V_w , are the density, mass and volume of the water, and M_p , V_p are the mass and volume of the constitute particles, respectively. Then a floc's apparent density (ρ_a) is defined as M_p/V_f :

$$\rho_a = \frac{M_p}{V_p + V_w} \quad (2)$$

then

$$\frac{\Delta\rho}{\rho_a} = \frac{V_w M_p - V_p M_w}{V_w M_p} = 1 - \frac{\rho_w}{\rho_p} \quad (3)$$

where $\rho_p = \frac{M_p}{V_p}$ is the primary particle density. According to the self-similar fractal theory (Kranenburg, 1994),

$$\Delta\rho = \rho_f - \rho_w = (\rho_p - \rho_w) \left[\frac{d_p}{d_f} \right]^{3-F} \quad (4)$$

where d_p and d_f are the primary particle and floc diameters, and F is the floc fractal dimension. Combining equations (3) and (4) gives:

$$\rho_a = \rho_p \left[\frac{d_p}{d_f} \right]^{3-F} \quad (5)$$

The equations (4) and (5) can be rewritten as:

$$\log(\Delta\rho) = \log[(\rho_p - \rho_w) d_p^{3-F}] - (3-F) \log(d_f) \quad (6)$$

$$\log(\rho_a) = \log[\rho_p d_p^{3-F}] - (3-F) \log(d_f) \quad (7)$$

Equation (6) indicates the liner relationship between $\log(\Delta\rho)$ and $\log(d_f)$. In addition, similar relationship can be derived from equation (7) and they share same slope of $(3-F)$. Based on

the relationship of density and diameter of flocs, the floc's mass contribution can be obtained as follows (Figure 1b).

Firstly, the $\Delta\rho$ can be derived from the measurement of setting velocity (w_s) and diameter (d_f) of flocs based on the equation (8) (Soulsby, 1997):

$$\Delta\rho = \rho_f - \rho_w = \frac{\rho_w v^2}{g K_2 d_f^3} \left[\left(\frac{w_s c}{v} + K_1 \right)^2 - K_1^2 \right] \quad (8)$$

Where g is the gravitational acceleration, v is the kinematic viscosity, and K_1 and K_2 are the empirical constants ($K_1 = 10.36$, $K_2 = 1.049$). Secondly, slope of log-log relationship between $\Delta\rho$ and d_f can be used to calculate floc fractal dimension (F). Next, a range of possible ρ_p from 1,000:3,000 kg/m³ was assumed to determine ρ_a as a function of d_f over the range of bins contained based on equation (3). The resulting values of ρ_{ai} were matched to each PSD bin, multiplied by the observed volume concentration (VC_i) in each size class, and summed to predict a range of fractal estimates of total suspended sediment concentration (TSS_F). Finally, the ρ_p and d_p can be determined until the TSS_F matched TSS determined from pump sampling.

$$TSS_F = \frac{M_p}{V_s} = \sum_{d_{min}}^{d_{max}} \left\{ \frac{M_p}{V_p + V_w} \right\}_i \left\{ \frac{V_p + V_w}{V_s} \right\}_i = \sum_{d_{min}}^{d_{max}} \{ \rho_a \}_i \{ VC \}_i \quad (9)$$

Once the ρ_p and d_p are determined, the mass contribution of flocs is obtained based on the ρ_p at different bin size d_f . Combining with the hydrodynamic observations, time series of bed turbulence structure and its influence on flocculation and sedimentation process are also analysed.

3. Results and Conclusions

The expected results will give us a quantitatively evaluation of the contribution of flocs to sediment flux in a cohesive sediment environment. Moreover, it provides us with an opportunity to evaluate the effect of flocculation on the geomorphological changes in the study area.

References

- Fall, K. A., Friedrichs, C. T., Massey, G. M., Bowers, D. G., & Smith, S. J. (2021). The importance of organic content to fractal floc properties in estuarine surface waters: Insights from video, LISST, and pump sampling. *Journal of Geophysical Research: Oceans*, 126, e2020JC016787. <https://doi.org/10.1029/2020JC016787>.
- Kranenburg, C. (1994). The fractal structure of cohesive sediment aggregates. *Estuarine, Coastal and Shelf Science*, 29, 451–460. [https://doi.org/10.1016/S0272-7714\(06\)80002-8](https://doi.org/10.1016/S0272-7714(06)80002-8).
- Soulsby, R. L. (1997). *Dynamics of marine sands*. Thomas Telford <http://www.worldcat.org/isbn/072772584X>.



17th International Conference on
Cohesive Sediment Transport Processes
September 18-22, 2023
Inha University, Incheon, Republic of Korea



Unveiling the Role of Marsh Creeks in Delivering Sediment: Insights from Paulina Saltmarsh

J. Sun^{1,2}, B. C. van Prooijen¹, X. Wang² and Q. He²

¹ Department of Hydraulic Engineering, Delft University of Technology, Delft, Netherlands

² State Key Laboratory of Estuarine and Coastal Research, East China Normal University, Shanghai, China

1. Introduction

Salt marshes are valuable ecosystems in coastal wetlands, but they are increasingly threatened by sea-level rise caused by climate change. The survival of salt marshes depends on the availability of sediment for marsh accretion. Marsh creeks play an important role in facilitating the exchange of sediment between mud flats and salt marshes (Reed et al, 1999; Xie et al., 2018). However, the role of marsh creeks in delivering sediment to the marsh is not always straightforward, as they can function both as conduits for importing and exporting sediment. To better understand the factors that determine the role of marsh creeks in sediment delivery, we analysed the dynamic data collected during both calm weather and storm events. Our study sheds light on the different sediment transport regimes that occur varying conditions and highlights the crucial role of creeks in the expansion of marshes during storm events.

2. Methods

To unveiling the role of marsh creeks in sediment delivery, two field campaigns were conducted in Paulina Saltmarsh (the Netherlands) in summer and in winter, respectively. The summer campaign lasted for two weeks while the winter campaign spanned two months, as storm events occur frequently in winter in the Netherlands. Water depth, velocity, sediment concentration, and bed level change were measured simultaneously at three locations, namely the mud flat, the marsh creek, and the marsh edge (Fig. 1). These measurements allowed us to investigate how marsh creeks function as conduits for sediment delivery under varying conditions and their implications for the long-term survival of salt marshes.



Figure 1. Measuring sites in Paulina Saltmarsh, the Netherlands.

3. Results

During the summer field campaign, we observed that sediment concentrations were low both on the mud flat and in the creek due to the limited sediment availability. In addition, the tidal elevation exceeded the bank elevation throughout our measurements, indicating that the lower marsh can be inundated for each tidal cycle. Therefore, more water from the marsh can converge into the creek during ebb tides, leading to the net export of water and sediment via the marsh creek. In contrast, during the winter measurement, there is a clear correlation between wave shear stress (fig 2c) and sediment concentration (fig 2d). This holds for both the concentration on the mud flat as well as in the creek. See e.g., the period of 24/2 - 4/3. This reveals that strong waves in winter could trigger erosion on the mud flat, resulting in more sediment being provided to the marsh creek during flood tides. Consequently, the role of marsh creeks in delivering sediment can shift to importing sediment in this case (Fig. 2f). It's also worth noting that the timing of waves can also have an impact on the function of marsh creeks in sediment delivery. For example, creeks can export sediment during wave events because of the large ebb velocities that occur during high water levels (as seen on March 11th). Both measurements show that the SSC in the marsh creek is not solely related to local erosion but also responds to the erosion on the mud flat. However, erosion can only be triggered by a window of opportunity: large enough shear stress and erodible sediment layers must exist simultaneously.

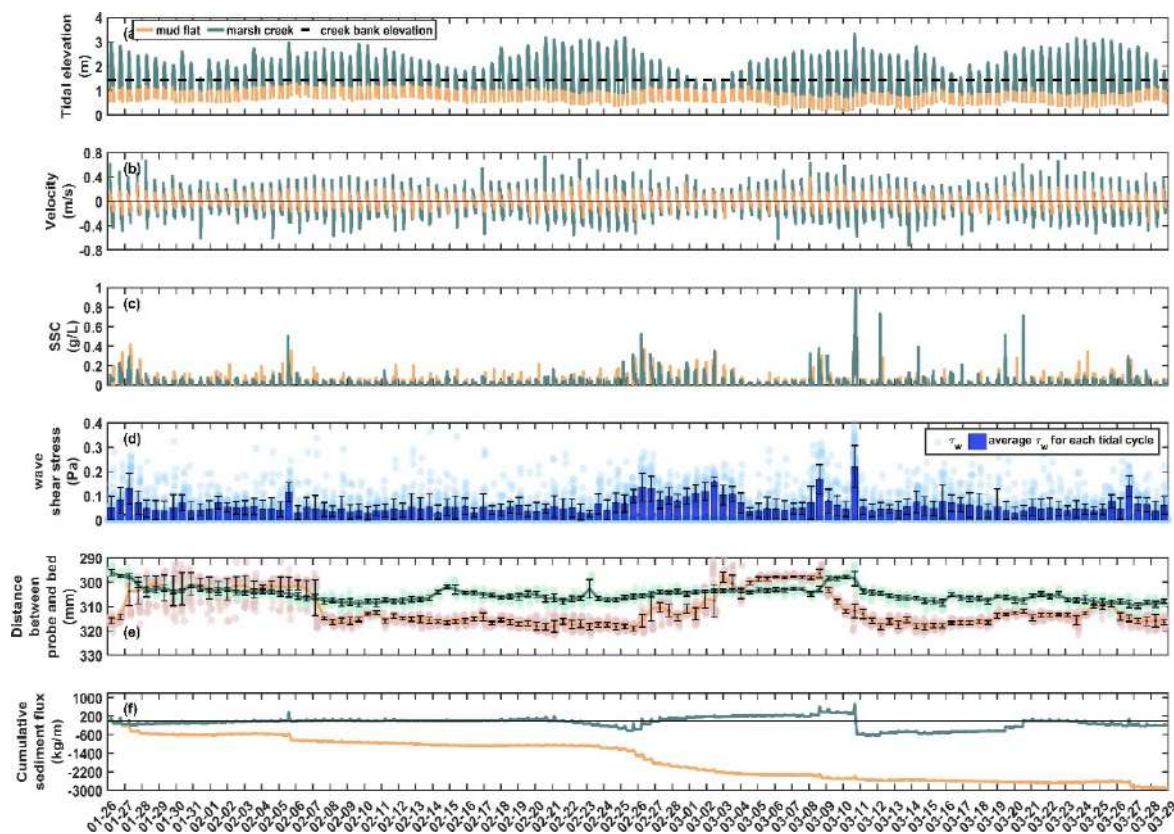


Figure 2. Time series of (a) tidal elevation (the dashed line represents the elevation of the creek bank at the measuring location); (b) velocity (flood velocity is positive); (c) the suspended sediment concentration; (d) wave shear stress; (e) bed level change; (f) cumulative sediment flux on the mud flat (yellow) and in the marsh creek (green) in winter in Paulina Saltmarsh.

4. Conclusions

Our measurements in Paulina Saltmarsh provide insights into the varying conditions under which the marsh creek plays different role in delivering sediment. The marsh creek serves as a conduit for exporting sediment in summer, but imports sediment during storm events in winter. These observations highlight how differences in sediment availability from mud flats can affect the transport regimes in marsh creeks, which can in turn determine the role of marsh creeks in sediment delivery.

Acknowledgments

This study is conducted in the framework of the project ‘Coping with deltas in transition’ within the Programme of Strategic Scientific Alliances between China and the Netherlands (PSA), financed by the Chinese Ministry of Science and Technology (MOST) and the Royal Netherlands Academy of Arts and Sciences (KNAW).

References

- Reed, D. J., Spencer, T., Murray, A. L., French, J. R., and Leonard, L. (1999). Marsh surface sediment deposition and the role of tidal creeks: implications for created and managed coastal marshes. *Journal of Coastal conservation*, 5, 81-90. doi: 10.1007/BF02802742
- Xie, W., He, Q., Wang, X., Guo, L., & Zhang, K. (2018). Role of mudflat-creek sediment exchanges in intertidal sedimentary processes. *Journal of Hydrology*, 567, 351-360. doi: 10.1016/j.jhydrol.2018.10.027

Session: Bed Erosion
10:40 – 12:40
Tuesday, September 19, 2023



17th International Conference on
Cohesive Sediment Transport Processes
September 18-22, 2023
Inha University, Incheon, Republic of Korea



Effect of air exposure time on erodibility of intertidal mud flats

T. van Kessel¹, J. Hanssen^{1,2}, F. van Rees^{1,3}, S. Gamberoni¹ and A. Talmon^{1,2}

¹ Deltares, thijs.vankessel@deltares.nl

² Delft University of Technology

³ Utrecht University

1. Introduction

Erodibility is one of the key parameters in cohesive sediment transport models. A long and rich research history exists on this topic, with prominent attention to the influence of bed composition, sand-mud ratio, density, consolidation, and biota. These influences have been included, either schematically or in substantial detail, in many cohesive sediment transport models. However, in most models, erodibility of intertidal mud flats and salt marshes does not depend on the duration of inundation and exposure to the atmosphere, which influence the consolidation of the bed. The aim of this contribution is to investigate the importance of this omission. Is this a minor effect which may be safely neglected, or does it have a major effect on the stability of mud flats and should evaporation be added to our models?

2. Approach

This study consisted of a combination of lab work, field work and analysis of erosion models for under- and overconsolidated beds.

2.1 Lab work

In the lab the erodibility of bed samples was determined as a function of drying time using a Gust erosion chamber (Figure 1). Of these bed samples, also water content and undrained shear strength were determined.

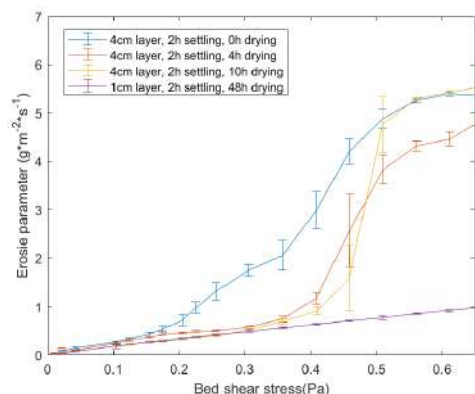


Figure 1. Left: Erosion parameter as function of drying time. Right: Gust lab setup

2.2 Field work

A small-scale field campaign was initiated for sample collection and to determine in-situ water content and undrained shear strength of the top layer (using a field torque vane) as a function

of exposure time. The field work was carried out on Zuidgors tidal flat in the Western Scheldt, the Netherlands. A strong strength increase with time after HW was observed (Figure 2).

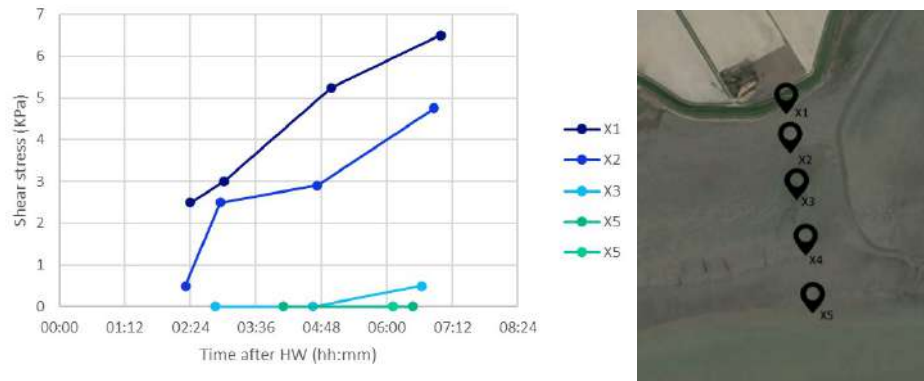


Figure 2. Left: Strength as function of time after HW. Right: Location of sample points X1 (near dike) – X5 (near channel)

2.3 Theory

To put the lab and field results into context and translate these into recommended settings for erodibility in numerical models, erosion formulations were studied. We made a distinction between undrained erosion of fresh, underconsolidated deposits and the drained erosion of mature, overconsolidated deposits, following the approach proposed by Jacobs et al. (2011). Transition between both states is determined by the critical state line (CSL). Pore pressure is used as a proxy for this transition, with positive excess pore pressure representing underconsolidation and negative excess pore pressure (i.e. suction) overconsolidation.

4. Results

Both in the lab (Figure 1) and in the field (Figure 2) a strong increase in strength and so a decrease in erodibility was observed with drying time. Effective drying time depends on local bed slope and microtopography, thickness of the mud deposit, permeability of the subsoil and seasonal variability. Therefore, local depressions on the mud flat may keep the mud permanently covered with a thin layer of water, suppressing any effects of evaporation and drying. If there is sufficient drainage, suction pressure develops in the top layer, resulting in strong pressure gradients, high effective stresses and strong overconsolidation. In such 'dry' state critical shear stress for erosion exceeds the upper limit of the Gust chamber (0.65 Pa). This is a major increase compared to the critical shear stress for fresh deposits (0.1 – 0.2 Pa).

In future research, we translate our findings into a numerical model. These results are first implemented and tested in a simple 1DV column model for erosion and deposition. This model includes adapted expressions for erosion and two bed layers, i.e. an upper underconsolidated layer and a lower overconsolidated layer. Both layers may dewater under influence of pore pressure gradients, either induced by gravity (self-weight consolidation) or evaporation/suction at the top (drying). Examples of bed level development of sub-, inter- and supratidal will be shown, for original and modified expressions for erosion. It is expected that seasonal trends in evaporation may influence mudflat and saltmarsh stability, notably towards and beyond High Water Spring level. After completion of the 1DV tests, we will implement the expressions also into 3D models.

4. Conclusions

The main conclusion is that drying results in a very strong reduction in erodibility. In practice, effective drying time may be much shorter than exposure time depending on local conditions. A model to include these effects will be made available as open source for further scrutiny and application.

Acknowledgments

Deltares is acknowledged for providing the internal funding for this study and NIOZ is acknowledged for support during field work.

References

Jacobs W, Pierre Le Hir, Walther Van Kesteren, Philippe Cann (2011). Erosion threshold of sand–mud mixtures, *Continental Shelf Research*, Volume 31, Issue 10, Supplement, 15 July 2011, Pages S14-S25.



17th International Conference on
Cohesive Sediment Transport Processes
September 18-22, 2023
Inha University, Incheon, Republic of Korea



Hydrodynamic Characteristics of a Field Instrument of Mud bed Erosion Response (FIMER)

Yuyang Shao¹, Yulin Tang¹, Jerome P.-Y. Maa²

¹ *College of Harbour, Coastal and Offshore Engineering, Hohai University, Nanjing 210098, China*

² *Virginia Institute of Marine Science, College of William & Mary, Gloucester Point, VA 23062, USA*

Abstract

To optimize the design of a proposed benthic chamber for measuring erosion rate, numerical simulations of the flow fields of a proposed Field Instrument of Mud bed Erosion Response (FIMER) has been conducted. A computational fluid dynamics code (FLUENT) was used and verified with other available data. The results insured the basic design of FIMER and the selected operational parameters, e.g. the selected disk rotating speeds and the matched pumping rates are acceptable. Furthermore, it also explains the reason of having a tornado-alike sediment plume generated at the center and the proposed revision to eliminate it. Comparison of the FIMER measured critical shear stresses and that from the Shields diagram show very reasonable agreement

Key words: numerical simulation, bed shear stress, benthic chamber, CFD

The objective of this study is to optimize the design of a benthic erosion chamber which has a relative large erosion area when compared with that of the Microcosmic (Gust and Muller, 1997) and a relative small size for field deployment and auto-operation. To achieve these goals, a geometry of the benthic erosion chamber (Fig. 1) is suggested. This chamber is built from an aluminum tube with an inside diameter of 25.45 centimeter, which gives an erosion surface area of around 500 cm². This chamber will penetrate into sea floor by its own weight and stopped by a bearing disk to form an erosion chamber. A disk that can rotate at selected speeds, Ω , is installed at 10 cm from seafloor. With a combination of selected pumping out rates, Q , at top center, reasonable uniform bed shear stresses can be developed for most of the chamber area. By starting with a small bed shear stress for a selected duration, and then increases stepwise for a preselected numbers of bed shear stresses, a complete erosion experiment can be finished within a few hours

Model setup for simulating the flow in FIMER

Quantify the hydrodynamic characteristic of FIMER is carried out by using a commercially available software FLUENT (Fluent Inc., 2020). The model performance are first checked by comparing with available data, and then, study to reveal the flow pattern of FIMER and bed shear stress distributions are presented.

Results and conclusions

The computation of bed shear stress distribution (Fig. 2) shows that the FIMER has a reasonable uniform bed shear stress distribution. The maximum bed shear stress of FIMER was less than 25% higher than the average. If exclude the close-to-zero locations next to the FIMER center and the wall, this difference would be much smaller. This demonstrates the average values can be used to represent the nominal bed shear stress reasonably well for the selected erosion area which is about 81% of the FIMER geometric flume area.

To ascertain the validity of the mathematical model, we conducted physical model experiments by using a lab version of FIMER to investigate the behavior of fine-grain sand. The results obtained were subsequently confirmed by compared with the Shields curve. This study reveals that a reasonable uniform bed shear stresses distribution in FIMER can be achieved within 85% of the FIMER area and the rest can be considered as a dead zone.

References

Fluent, Inc. FLUENT documentation; 2020; Available at www.fluent.com

Gust, G., & Muller, V., 1997. Interfacial hydrodynamics and entrainment functions of currently used erosion devices. In: Burt, N., Parker, R., Watts, J. (Eds.), *Cohesive Sediments*. Wiley, Chichester, UK pp. 149-174.

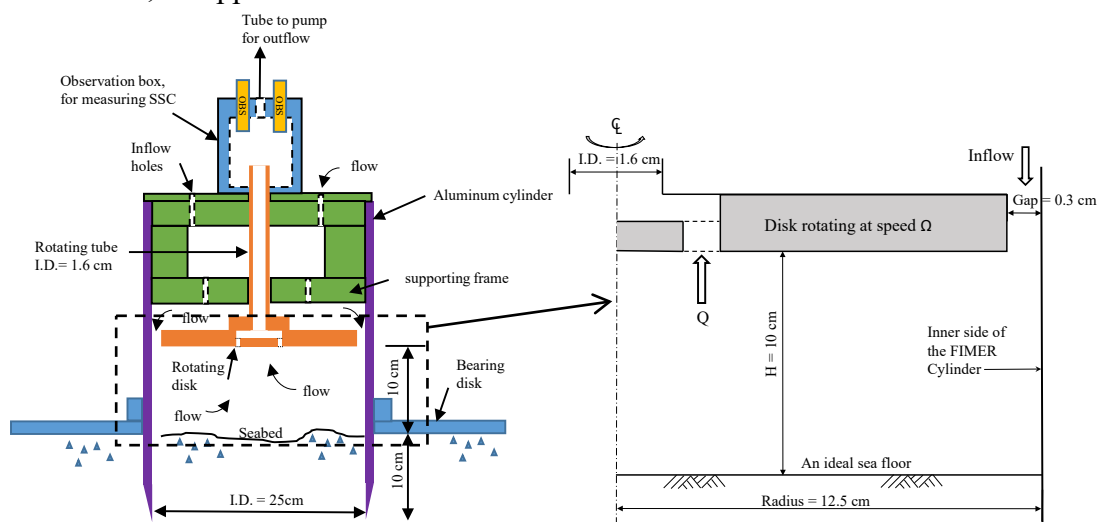


Fig. 1. The basic geometry of a fully automatically Field Instrument for Measuring bed Erosion Responses (FIMER). (Right figure is the FLUENT simulation domain for the suggested FIMER.)

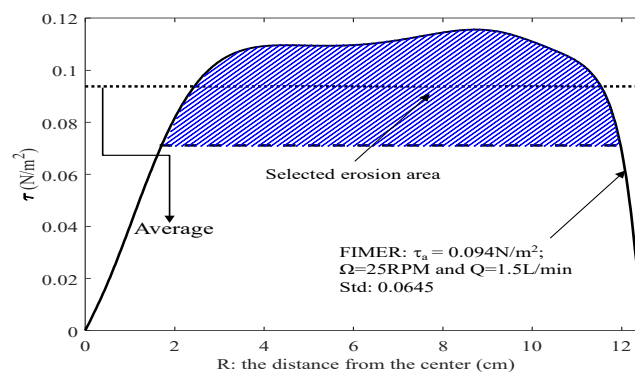


Fig. 2. The normalized bed shear stress distribution of three different benthic erosion chambers ($Q = 1.5 \text{ L/min}$, and $\Omega = 25 \text{ RPM}$; Std: standard deviation)



17th International Conference on
Cohesive Sediment Transport Processes
September 18-22, 2023
Inha University, Incheon, Republic of Korea



A novel, automatic rotating annular flume for cohesive sediment erosion experiments: Calibration and preliminary results

S.M. Figueroa¹ and M. Son¹

¹Department of Civil Engineering, Chungnam National University, Daejeon, Korea,
stevenmiguelfigueroa@gmail.com

1. Introduction

Flows of water in the environment (e.g. in a river or estuary) generally occur in complex conditions. This complexity can hinder a general understanding of flows and their related sedimentary processes, such as erosion and deposition. To gain insight in simplified, controlled conditions, hydraulic flumes are a popular type of laboratory research equipment. Linear flumes use pumps to recirculate water. As these pumps cause turbulence in the flow, they are not suitable for cohesive sediment studies because the high turbulence can disrupt fragile cohesive sediment flocs. To overcome this limitation, the rotating annular flume (RAF) was developed (Partheniades and Kennedy, 1966). The circular channel is effectively an “infinite channel” and thus avoids the need for pumps. To counteract the secondary circulation due to curvature, RAFs counter-rotate the bottom flume and the top lid. Furthermore, as the secondary circulation decreases as the flume radius increases, larger RAFs are considered better as they are less susceptible to secondary circulation. While only a handful of large RAFs exist (Cantero et al., 2004), flumes such as these are important as research based on them forms the basis of many commonly used theoretical and numerical sediment transport models. At present, several first-generation large RAFs are in disrepair or have been decommissioned. However, as new measurement techniques and cohesive sediment transport models become available, there remains a need to constrain cohesive sediment erosion and deposition processes. In addition, while the previous generation of RAFs were often manually controlled, new RAFs can have improved performance by automated operation.

2. Materials and methods

To further advance our understanding of cohesive sediment erosion and deposition processes, a large, automatic RAF (~4.0 m diameter, 0.5 m channel depth, 0.3 m channel width) has been constructed at the Hydraulic Laboratory at Chungnam National University (CNU), Korea (Figure 1A). The RAF has the ability to simulate both unidirectional (river) and bidirectional (tidal) flows with supporting instrumentation for measuring bed bulk density, bed level, bed shear stress, turbulence, suspended sediment concentration, and floc size. Here we will present calibration of the rotation rate with bed shear stress and preliminary results for unidirectional and bidirectional flow using natural cohesive mud (experiments shown in Figure 1B and 1C, respectively).

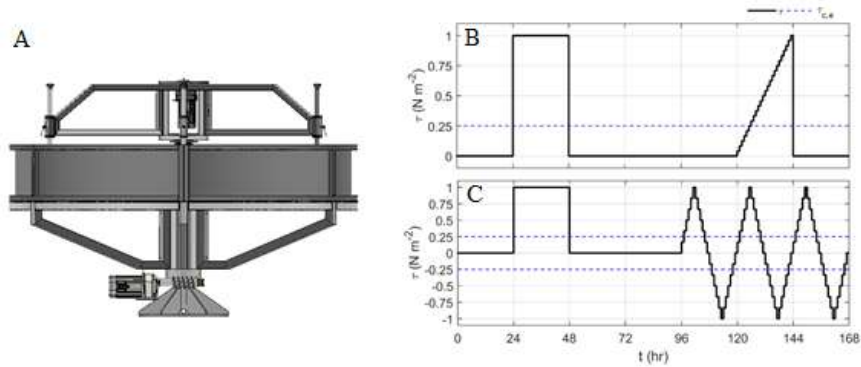


Figure 1. Rotating annular flume. (A) CNU RAF illustration, (B) river experiment, and (C) tide experiment.

3. Conclusions

Preliminary results indicate that the CNU RAF is a valuable tool for fundamental cohesive sediment transport research.

References

- Partheniades, E. and Kennedy, J.F. (1966). Depositional behavior of fine sediment in a turbulence fluid motion. *Coastal Engineering 1966*, 707-729. doi: <https://doi.org/10.1061/9780872620087.041>
- Cantero, M., Mangini, S., Pedocchi, F., Niño, Y. and García, M. (2004). Analysis of flow characteristics in an annular flume: Implications for erosion and deposition of cohesive sediments. *Critical Transitions in Water and Environmental Resource Management* 1-10. doi: [https://doi.org/10.1061/40737\(2004\)314](https://doi.org/10.1061/40737(2004)314)



17th International Conference on
Cohesive Sediment Transport Processes
September 18-22, 2023
Inha University, Incheon, Republic of Korea



In Situ Resuspension and Sedimentation Characteristics of Tropical Peat Sediments in Bengkalis Island

K. Yamamoto¹, S. Sutikno², N. Basir³, Y. Nakagawa⁴, K. Murakami⁵ and H. Shirozu⁶

¹ Graduate School of Sciences and Technology for Innovation, Yamaguchi University,
Yamaguchi, Japan, k_yama@yamaguchi-u.ac.jp

² Faculty of Engineering, University of Riau, Pekanbaru, Indonesia

³ Department of Civil Engineering, State Polytechnic of Bengkalis, Bengkalis, Indonesia

⁴ Port and Airport Research Institute, Kanagawa, Japan

⁵ Faculty of Engineering, Miyazaki University, Miyazaki, Japan

⁶ Department of School of Architecture and Urban Planning, Tokai University, Kanagawa,
Japan

1. Introduction

In the western part of Bengkalis Island, a peat spit from collapse and coastal erosion has formed in the northern part. A new sedimentary tidal flat of 1.46 km² has been formed behind it and a mangrove belt has been formed on the tidal flat. Yamamoto et al. (2017) estimated that the peat that decayed on the north coast of Bengkalis Island by 1988~2016 was about 3.8×10^6 tons. It was estimated that the tidal flat had 5.1×10^5 tons of peat-derived sediment that collapsed on another coast. However, it is necessary to clarify the resuspension and settling property of the peat particles and the actual movement and redeposition of suspended peat in seawater. In this study, in situ resuspension test and in situ settling velocity measurement were carried out. The effective density of peat particles was determined from sedimentation experiments.

2. Methods

The field resuspension experiment of the peat sediment was conducted on 13 January 2015 in a lagoon (1°34'54.42 N, 101°59'54.07 E) along the coast of the northwest of Bengkalis Island (Figure 1) using a resuspension device of bottom sediment. The resuspension apparatus itself is shown in Figure 2. The device was consisted of an acrylic square cylinder with an inner rectangle of 3 cm square placed on the sediment, and a peristaltic pump on board sucked up the water in the square cylinder with vinyl tubing from a side outlet, allowing water jet from the top acrylic tube (7 mm diameter) to be directed perpendicular to the bottom sediment from the top inlet tube. The relationship between flow rate and bottom shear stress was calibrated with the critical shear stress of sands. The jet flow rate was converted to the bottom shear stress using the relationship. Field experiments were carried out at two sites in the lagoon, where the bottom sediment. In the field experiments, the resuspension test apparatus was mounted on a steel pipe trestle (D:500 mm x W:500 mm). A commercially available 15 m waterproof digital camera was attached beside the square cylinder. It allows the resuspension column to be photographed from the side and judgement of the resuspension and sedimentation of peat particles. A 3 cm wide acrylic block was mounted directly next to the resuspension column and a waterproof LED light was mounted. Three millimetres slit with a black acrylic plate was provided in the resuspension column to converge the light flux. The resuspension test apparatus

was recorded using the macro movie function of a digital camera while it was being pulled up from the ship after landing on the seabed with a rope. The resolution during filming was full high definition (1080p). The field of view of the camera during the experiment was 2.54 x 1.58 cm.

3. Results

The results of the field resuspension experiments for peat and clay bottom sediment, determined from the filtration analysis of the sample water of suspended solids collected in the resuspension unit and the analysis of the intense thermal loss, are shown in Figure 3. Figure 3 shows that the resuspension limit bottom shear stresses existed for peat as well as clay, ranging from 0.1 Pa to 0.5 Pa. The clay had a limiting bottom shear stress of approximately 0.2 Pa, with higher resuspension fluxes at 3 m. From the above, peat also has a resuspension limit. The peat has a resuspension limit and can be treated in the same way as cohesive bottom sediment. From the settling velocity observation of the peat particles in water, these effective densities varied with their particle sizes. The effective densities decreased with their diameter of the peat particles. The degree of decomposition of the peat particles was evaluated with degree of humification. The degree of humification and effective density of same diameter were positively correlated. It is clarified that the changes of the peat particle densities have been depended on their degree of decomposition.

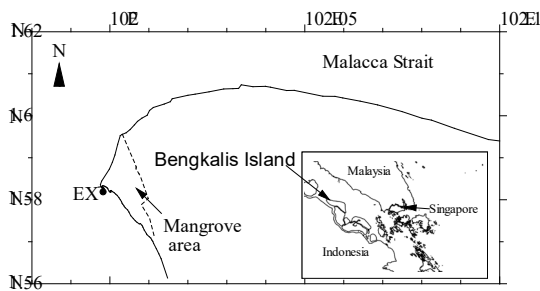


Figure 1. Study site of the resuspension test (EX) in Bengkalis Island, Indonesia
(a)

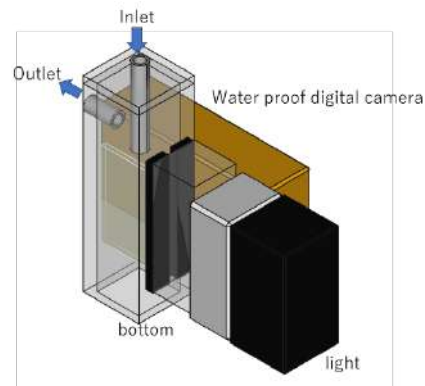


Figure 2. In situ bed resuspension device by turbulent jets
(b)

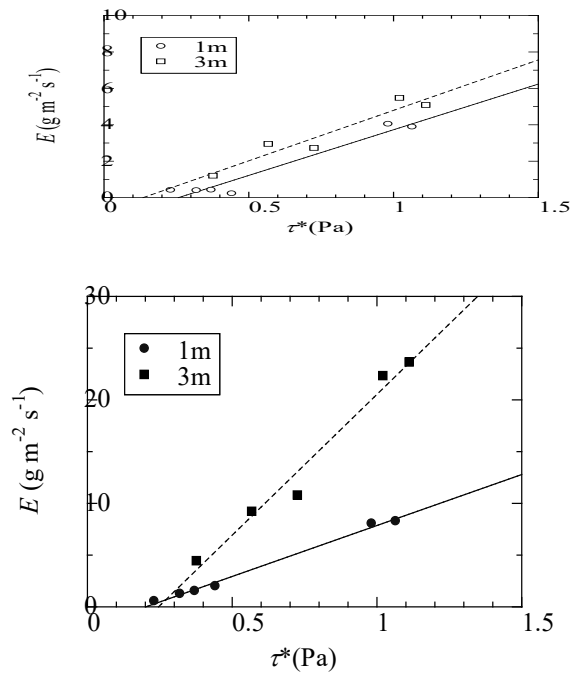


Figure 3. Resuspension flux of peat sediments (a) and clay (b) of the lagoon in Bengkalis Island, Indonesia

4. Conclusions

As a result of field resuspension experiments, it was found that the resuspension limit of bottom shear stress for peat sediment existed in the range of 0.1 Pa to 0.5 Pa. Clay had a resuspension limit for the bottom was approximately 0.2 Pa. Peat sediment also had a resuspension limit and can be treated in the same way as cohesive sediment. From the observation of the settling velocity of peat particles in water, their effective densities varied with their particle sizes. The effective densities decreased with the diameter of the peat particles. The degree of decomposition of the peat particles was evaluated with the degree of humification. The degree of humification and effective density of the same diameter were positively correlated. It has been clarified that the changes in the densities of peat particles have depended on their degree of decomposition.

Acknowledgments

This work was supported by JSPS KAKENHI Grant Numbers 17H01668, 26303015, JSPS bilateral research, “Establishment of the coastal peat sediment dynamics”

References

Yamamoto, K., Miyara, K., Kobayashi, T., Akamatsu, Y., Kanno, A., Basir, N. and Sutikno, S. (2017). Mangrove formation process behind the peat bar and the amount of the carbon storage in the tidal flat J. Japan Soc. Civ. Eng. Ser. B2 Coastal Eng, 73(2), 1573-1578.



17th International Conference on
Cohesive Sediment Transport Processes
September 18-22, 2023
Inha University, Incheon, Republic of Korea



Assessing the relationship between *in-situ* bed erodibility and suspended sediment concentration in intertidal flat

S.M. Choi¹, J.Y. Seo¹ and H.K. Ha^{1,*}

¹ Department of Ocean Sciences, Inha University, Incheon, Republic of Korea,
*hahk@inha.ac.kr

1. Introduction

Intertidal flats in semi-diurnal regimes are periodically submerged during high tides and exposed during low tides. Such repetitive conditions have profound impacts on the bed erodibility. The bed erodibility is usually determined by a competition between bed shear stress and internal resistance of bed at water-sediment interface. The bed erosion can be occurred when the bed shear stress induced by current and waves (t_{cw}) exceeds the erosion threshold (Sanford and Maa, 2001). In general, the self-weight consolidation forms the depth-varying erosion threshold and causes deeper sediment bed layers to be less erodible. Since the internal resistance of bed links to all physical, geochemical, and biological factors (Grabowski et al., 2011), the bed erosion can have different magnitudes even under the equivalent bed shear stress. During the submergence, the sediment bed expands by absorbing the water and newly receives suspended sediments from the tidal channel to undergo structural changes (Friedrichs, 2011). During the exposure, on the contrary, the sediment bed becomes dry due to evaporation and hardens by benthic microalgae. As such, the sediment bed under the repetitive submergence and exposure is constantly influenced by combined actions between disturbance and stabilization, making it more difficult to estimate its erodibility. To date, lots of research has attempted field and experimental measurements to reveal the relationship between bed erodibility and external forcings in intertidal flats. However, it was difficult to reflect the amount of sediments newly supplied from tidal channel or the variations in bed erodibility with tidal cycles. Therefore, the objectives of this study are (1) to quantify the relationship between bed erodibility and external forcing based on *in-situ* erosion experiments and mooring and (2) to reveal the proportion of suspended sediments by local resuspension (erosion) and horizontal advection.

2. Materials and methods

In Asan Bay, west coast of Korea, a mooring campaign had been conducted for two weeks (October 17–31, 2021). In the H-frame, a 6-MHz acoustic Doppler velocimeter (ADV, Nortek) was installed at 0.35 m above bed (mab). Two up-looking, 1000-kHz acoustic Doppler current profilers (RDI, Sentinel V20; Nortek, Signature) were installed in the trawl resistance bottom mount near the H-frame. They were used to estimate the t_{cw} and suspended sediment concentration (SSC). Over the mooring period, a total of 108 sediment cores had been collected by a gravity corer or diver during submergence, and by hand during exposure. A series of sediment erosion experiments (20 for submergence; 9 for exposure) had been conducted using Gust Erosion Microcosm System (GEMS). During the experiments, artificial shear stresses (0.01–0.6 Pa) were applied stepwise on the sediment surface. The changes in the erosion

parameters from the GEMS indicate the hydrodynamic conditions before the sediment sampling. For comprehensive interpretations of bed erodibility under varied tides and winds, representatives for both erosion parameters and τ_{cw} were selected. Two different methods were used to find the representatives based on the hysteresis of the cohesive sediment bed. The selected τ_{cw} was then used as an external force to explain the erosion parameters (Figure 1).

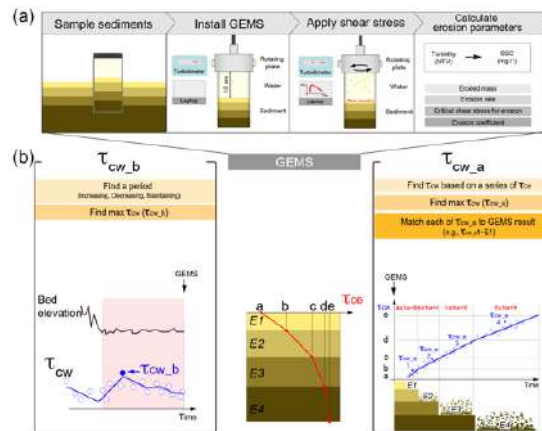


Figure 1. Conceptual diagram about (a) details of erosion experiment (GEMS) and (b) methods to explain erosion parameters with *in-situ* bed shear stress (τ_{cw})

3. Results and discussion

During the mooring campaign, 25 tidal cycles in semi-diurnal regimes occurred with about 6 hours of submergence and 5.7 hours of exposure. The erosion rate of sediment bed obtained at exposure was about $0.008 \text{ g m}^{-2} \text{ s}^{-1}$ at $t_b = 0.6 \text{ Pa}$, on average. This was 2.5 times lower compared to submerged sediments (erosion rate: $0.02 \text{ g m}^{-2} \text{ s}^{-1}$ at $t_b = 0.6 \text{ Pa}$), showing that the bed became harden and stabilized. No matter how stabilized the sediment bed was during exposure period, the bed erodibility during the submergence was mainly determined by t_{cw} and supply of suspended sediments from tidal channel. During submergence, the tidal currents had bi-directional flows to southeast (flood) and northwest (ebb). The magnitudes of depth-averaged current velocity were in the range of $0.02\text{--}0.24 \text{ m s}^{-1}$ and $0.01\text{--}0.39 \text{ m s}^{-1}$ during the flood and ebb, respectively. Most of SSCs at each tidal cycle usually increased up to approximately 50 mg l^{-1} at the early flood when current speed was high ($\sim 0.2 \text{ m s}^{-1}$), and then continuously decreased to 20 mg l^{-1} despite of increase in current velocity during the ebb. However, the τ_{cw} for the ebb could be increased up to 0.6 Pa due to strong winds ($> 6 \text{ m s}^{-1}$) and lowered water depth (wave height/water depth > 0.06), which caused drastic increases in SSC up to 50 mg l^{-1} . Such variations in SSC by τ_{cw} during the ebb were inversely related with the bed erodibility as measured by GEMS. It means that the larger τ_{cw} , the smaller the erodible sediments from the bed in the GEMS experiment, and vice versa. In fact, at $\tau_{cw} < 0.2 \text{ Pa}$ in intertidal flats, the τ_{cw} only made the sediment bed unstable without marked erosion, so the SSC in GEMS could be increased to 100 mg l^{-1} with high erosion rate coefficient ($0.25 \text{ g m}^{-2} \text{ s}^{-1} \text{ Pa}^{-1}$). When the τ_{cw} increased up to 0.6 Pa with a severe bed erosion, the erosion rate in GEMS was $0.01 \text{ g m}^{-2} \text{ s}^{-1}$, which was 3 times lower compared to that at $\tau_{cw} < 0.2 \text{ Pa}$. Applying the GEMS results to mooring data, at $\tau_{cw} < 0.2 \text{ Pa}$, the bed sediments were eroded by a floc erosion attributing 25–50% of total suspension. At $\tau_{cw} > 0.2 \text{ Pa}$, they were eroded by a surface erosion attributing 50–100% of the total.

4. Conclusions

- (1) The exposed sediment bed became stabilized with 2.5 times lower erosion rate compared to submerged sediment bed. The bed erodibility during submergence was mainly determined by t_{cw} , and barely related with that during exposure (~ 4.1 hours).
- (2) The variations in SSC by τ_{cw} during ebb were inversely related with the bed erodibility measured by GEMS. In calm conditions ($\tau_{cw} < 0.2$ Pa), the τ_{cw} only made the sediment bed unstable (high erosion rate coefficient: $0.25 \text{ g m}^{-2} \text{ s}^{-1} \text{ Pa}^{-1}$) without marked increase of SSC. Under the strong winds ($> 6 \text{ m s}^{-1}$), the increased τ_{cw} up to 0.6 Pa caused severe bed erosion, resulting in rapid increase of SSC and 3 times lower erosion rate ($0.01 \text{ g m}^{-2} \text{ s}^{-1}$) in GEMS compared to the erosion rate under the calm condition.
- (3) Applying the GEMS results to mooring data, the submerged bed was eroded through floc erosion ($\tau_{cw} < 0.2$ Pa) and surface erosion ($\tau_{cw} > 0.2$ Pa) with increasing τ_{cw} . During the surface erosion, the eroded sediments were constituted 50–100% of total suspended sediments resulting in the rapid increase of SSC.

References

- Friedrichs, C. T. (2011). Tidal flat morphodynamics: a synthesis. In: Wolanski, E., McLusky, D. (Eds.), *Treatise on Estuarine and Coastal Science*. Academic Press, Waltham, pp. 137–170. doi: 10.1016/B978-0-12-374711-2.00307-7
- Grabowski, R. C., Droppo, I. G., and Wharton, G. (2011). Erodibility of cohesive sediment: The importance of sediment properties. *Earth-Science Reviews*, 105(3-4), 101-120. doi: 10.1016/j.earscirev.2011.01.008
- Sanford, L. P., and Maa, J. P. Y. (2001). A unified erosion formulation for fine sediments. *Marine Geology*, 179(1-2), 9-23. doi: 10.1016/S0025-3227(01)00201-8

Session: Model II
14:00 – 15:40
Tuesday, September 19, 2023



17th International Conference on
Cohesive Sediment Transport Processes
September 18-22, 2023
Inha University, Incheon, Republic of Korea



Comprehensive analysis of siltation dynamics of approach channel: A case study of Deendayal Port, India

Balaji Ramakrishnan

Professor, Department of Civil Engineering, Indian Institute of Technology Bombay,
Mumbai, India, rbalaji@iitb.ac.in

1. Introduction

Morphodynamics, driven by the hydrodynamics, is a complex physical process, understanding of which is essential for engineers, especially for port and harbour, as siltation in navigational channel is undesirable for vessel movements. Dredging is an inevitable process, in order to keep the channels navigable, which cost significant expenditures to ports. Deendayal port takes significant efforts in keeping their approach channel navigable through continuous dredging, due to the consistent siltation process. It is reported that about 4.5 million-cubic-meter of quantity is dredged in a typical five-year plan period of Kandla port (Jayappa and Narayana, 2009), with an estimated amount of 500million rupees spent. This is large due to the presence of strong tidal currents and significant Suspended Sediment Concentration (SSC) (Nandhini et al., 2023; Satheesh and Balaji, 2016). This paper presents our research efforts to understand the siltation behaviour of navigational channels, through comprehensive analysis by using the powers of in-situ measurements, numerical modelling tools and remote-sensing techniques.

2. Methodology

The primary objective of the project was to analyze about the siltation behaviour of the approach channel and to suggest suitable engineering solutions to reduce siltation, which may help in reducing the expenditure towards dredging. Field measurements, carried out during pre- and post-monsoon seasons, include observations of tidal levels, currents (spatial and temporal) and suspended sediment concentration (SSC). A dedicated and exclusive numerical model is also developed, as part of this study, that cover the entire Kandla region to estimate the hydrodynamic conditions. An open-source, freely-available yet reliable software tool is employed for setting up the numerical model. Siltation behaviour of approach and navigational channels of Deendayal port in Kandla creek, Gujarat (Figure 1), is modelled using process based hydrodynamic and morphological modules of Delft3D numerical scheme. The spatial variations of SSC are also mapped using satellite imageries-based analysis. The results of the numerical model are appropriately calibrated and validated with the help of in-situ measurements. Relevant data collected by DPT, such as bathymetry and dredging details along the channel are also used for analysis the siltation behaviour. The tidal levels and currents of the numerical model are validated with in-situ measurements at different location. We have successfully adopted Eulerian and Lagrangian methods of observations of various environmental parameters through systematic field measurement campaigns. These in-situ data collected from these campaigns are used for calibration and validation of numerical model and satellite image processing algorithms. The various measurement types and successful use of

satellite imageries to obtain the SSC are discussed. Typical snap-shots the project tasks are shown in Figure 2 as graphical abstract. The modelling results revealed that siltation rates and morphological trends, which is useful for deriving the dredging management strategies. Site specific recommendation of sediment management system is given to the port authorities.



Figure 1. Location of the project.

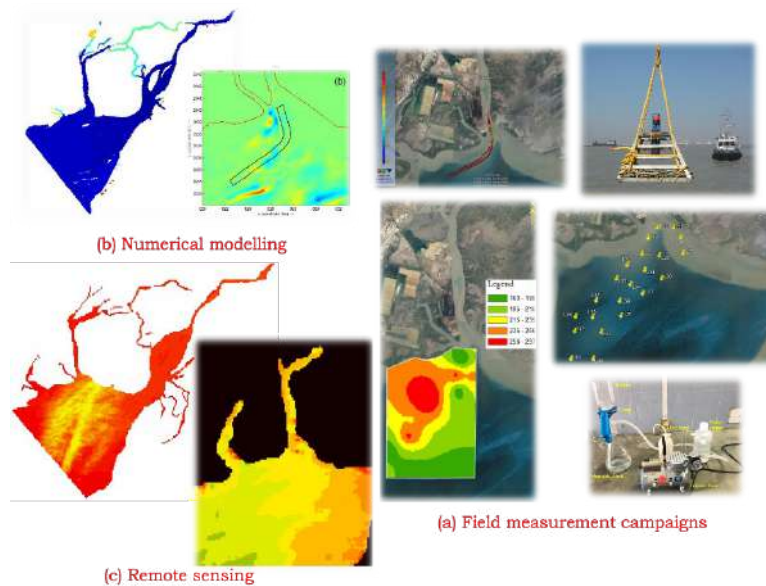


Figure 2. Graphical abstract of various project tasks.

3. Conclusions

The estimates of siltation from the developed numerical simulations of morphodynamics is in agreement with that of siltation quantities estimated by port authorities. After gaining confidence on the developed numerical model, options to reduce the siltation are attempted through the model studies that included (i) change in the alignment of the existing channel as well as by (ii) introducing porous barrier structures along the side of the channel to minimize siltation. Porous barriers of different alignment, length and orientation are analysed and a particular option observed to give maximum (by 46-56%) reduction in the siltation of navigational channel. The suggested option shall further be explored from the techno-commercial aspect, for possible implementation in Kandla and to reduce the expenditure towards maintenance dredging.

Acknowledgments

Ministry of Shipping, Government of India (Ref. No. DW/DTO-7/2015) and Deendayal Port Trust have jointly funded this research work. The author acknowledges port's in-kind support and logistics during the field measurement campaign, beyond the financial assistance to the research work. The author acknowledges support of all engineering staff, research scholars and students for their technical contributions during various task of this project.

References

- Jayappa, K. S., and A.C., Narayana. (2009), "Coastal Environments: Problems and Perspectives", New Delhi: I.K. International.
- Nandhini, D., Sriganesh, J., Murali, K and Sundar, V (2023) Field investigation of suspended sediment transport study in the Kandla creek, Gujarat, India, ISH Journal of Hydraulic Engineering, DOI: 10.1080/09715010.2023.2199701
- Satheeshkumar, J., Balaji R., (2016), Tidal power potential assessment along the Gulf of Kutch, Gujarat, India, Asian Wave and Tidal Energy Conference (AWTEC 2016), October 24 to 28, 2016, Singapore.



17th International Conference on
Cohesive Sediment Transport Processes
September 18-22, 2023
Inha University, Incheon, Republic of Korea



Intertidal Density-driven Sediment Flux into a Port in a Macro-tidal Environment

S.-B. Woo^{1*}, J.-S. Jeong², J. I. Song¹, H. S. Lee^{3,2}, Morhaf Aljber²

¹ Department of Ocean Science, Inha University, Incheon, Korea, sbwoo@inha.ac.kr

² Transdisciplinary Science and Engineering Program, Graduate School of Advanced Science and Engineering, Hiroshima University, Hiroshima, Japan

³ Center for the Planetary Health and Innovation Science (PHIS), The IDEC Institute, Hiroshima University, Hiroshima, Japan

1. Introduction

The high deposition rate of sediment in a port is a problem awaiting solution because it would put freight vessels at risk by shallowing a depth of a port. Once the depth becomes shallower than the navigational depth due to a deposition, dredging is required, incurring significant costs. Therefore, it is crucial to prevent or slow down sediment deposition in advance. To do so, it is essential to understand the mechanisms of suspended sediment (SS) transport and deposition. In this study, we propose a new perspective on the influence of baroclinic circulation on the transport of SS at a port scale.

2. Materials and Methods

2.1 Study area

The North Port is located in the central part of Gyeonggi Bay on the west coast of South Korea. Tides ranging over 9 meters and freshwater discharged from the Han River induce complex interactions between barotropic and baroclinic forces, especially during the summer, flood season. The North Port has been observed to experience an average annual deposition of approximately 80 cm over a span of four years based on seafloor topography data.

2.2 A numerical model: FVCOM-SWAN-CSTMS

Finite Volume Community Ocean Model (FVCOM) using the unstructured-grid system is an ocean circulation model adopted to describe complex coastlines and wet-and-dry processes on estuaries. A wind-wave model, Simulating WAve Nearshore (SWAN), and a sediment transport model, Community Sediment Transport Modelling System (CSTMS), were coupled with the FVCOM to analyze deposition/erosion of sediment and the causes focusing on a balance between baroclinic and barotropic forces inside the North Port.

The unstructured grid was designed to prioritize high resolution (maximum 50 m) for the North Port with 59,757 nodes and 113,918 cells, and 20 vertical layers based on a sigma coordinate system. We conducted simulations for winter (from 7 Feb to 19 Mar 2019) and summer (from 10 Jul to 30 Aug 2019), considering tides at the open boundary and river discharge from the Han River.

3. Results

3.1 Validation

The validation of surface and bottom SS concentration (SSC) using field measurements exhibited an R^2 value of 0.82, reproducing the trend of SSC depending on the tidal phase.

Detailed validations of the tide, current, salinity, and significant wave height can refer to Jeong et al. (2022).

3.2 Salinity-driven Circulation and Environment in the North Port

Low-salinity water from the Han River during the ebb tide discharged south in front of the North Port. During the subsequent flood tide, the low-salinity water flowed into the North Port, as shown by the salinity contour lines in Figure 1C. As the high tide approached, the seawater moved to the innermost part of the port. At that moment, the salinity outside the port reached its maximum due to the flood tide transporting high-salinity water from the outer sea to the upper channel.

The seawater with the highest salinity outside the port and the one with the lowest salinity inside the port maximized a salinity gradient-induced baroclinic force at the high tide (slack tide). This enhanced baroclinic force can cause outbalance and outperform the effects of the tidal current during the peak of high tide. As a result, near-bottom currents were observed to flow towards the inside of the port, creating anticlockwise circulations as depicted in Figure 1D. This contrasted with the typical direction of the tidal current during the ebb tide, which would normally be towards the outside of the port.

3.2 Suspended sediment transport in the port

The salinity gradient-induced near-bottom current transported the suspended sediment into the port near-bottom layer from the outer channel (Figure 1D). Because the SSC was usually higher outside the port than the concentration inside due to stronger currents (Figure 1A), the SS that flowed from outside was deposited in the port as the current diminished. Moreover, the SSC outside was higher during the ebb tide than during the flood tide (Figure 1B). As a result, the baroclinic current that developed mainly during the ebb tide could deliver sea water with high concentrations of SS into the port efficiently, causing a fast deposition rate of 35 cm/year from the model result.

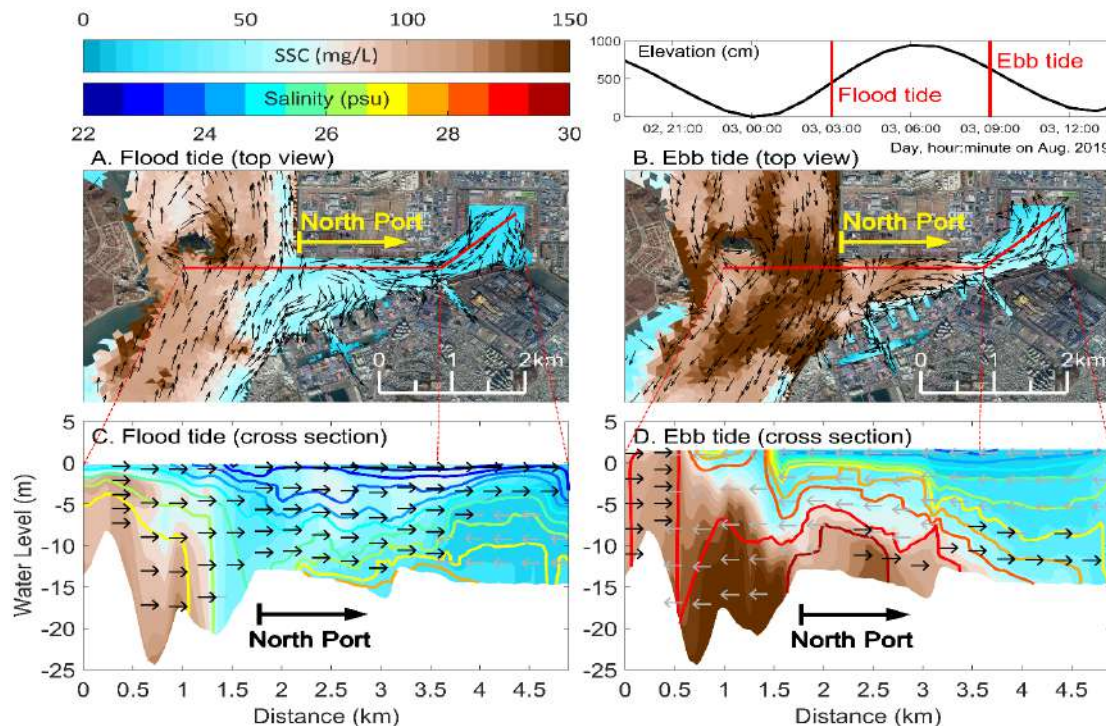


Figure 1. (A) - (B) Horizontal distributions of the suspended sediment concentration (SSC) and circulation averaged from the bottom to 35 percent of the total depth at the flood tide and ebb tide, respectively. (C) - (D) Along-port trans sections of the SSC (shades), salinity (contour lines), and circulation at the same time with (A) and (B), respectively. Vectors are unit vectors

indicating currents toward the inside (outside) in black (gray). These results are from the model during the rainy season and spring tide.

3.3 Suspended sediment influx amplification by tide

We selected four periods depending on the rainy/dry season and spring/neap tide and calculated the net flux of SS through a cross section of the port entrance at each period (Table 1). The largest amount of the inflow of SS was calculated during the RS (Rainy season and Spring tide) with 7.40×10^3 tons. Although fresh water was discharged similarly during RN (neap tide), the inflow diminished by 0.47×10^3 tons (6.5% of RS). This small inflow during neap tide was consistent during DN as well. Lastly, the baroclinic force in the port was affected mainly by the tidal range, as shown with the inflow of 5.29×10^3 tons during DS (71.5% of RS, 1050.8% of DN). The large tidal range was an essential prerequisite for a high inflow of SS, enhancing the baroclinic force in the port. The high river discharge intensified the inflow, but it was not essential for the high inflow of SS.

Table 1. Total net flux of SS during 4 tidal cycles at each period. A positive value of net flux indicates that SS flows into the North Port.

Period		RS		DS		RN		DN	
Season	Tide	Rainy season	Spring tide	Dry season	Spring tide	Rainy season	Neap tide	Dry season	Neap tide
River discharge	Tidal range	1700 m ³ /s	6.9 m	400 m ³ /s	5.8 m	1750 m ³ /s	3.0 m	600 m ³ /s	2.9 m
Net flux of SS		7.40×10^3 tons		5.29×10^3 tons		0.47×10^3 tons		0.50×10^3 tons	

4. Conclusions

The Incheon North Port is suffering from fast sediment deposition of approximately 80 cm/year, depicting an extremely higher rate than adjacent areas. We applied FVCOM coupled with SWAVE and CSTMS to investigate the sedimentation process in the port. The model results showed that low-salinity water discharged from the Han River entered the port and was trapped in the port. Between the trapped low-salinity water and high-salinity water outside, the baroclinic force was maximized, resulting in the baroclinic/salinity-driven current accompanying the influx of the near-bottom SS.

References

Jeong, J.-S. et al. (2022) 'Baroclinic Effect on Inner-Port Circulation in a Macro-Tidal Estuary: A Case Study of Incheon North Port, Korea', *Journal of Marine Science and Engineering*, 10(3). doi: 10.3390/jmse10030392.



17th International Conference on
Cohesive Sediment Transport Processes
September 18-22, 2023
Inha University, Incheon, Republic of Korea



The influence of lateral dynamics on the sediment dynamics in tidally dominated estuaries

M.P. Rozendaal^{1*}, Y.M. Dijkstra¹, H.M. Schuttelaars¹,

¹Delft Institute of Applied Mathematics, Delft University of Technology;
*corresponding author: M.P.Rozendaal@tudelft.nl

1. Introduction

The complex bathymetry and geometry of estuaries greatly affects the water motion and suspended sediment dynamics. The complex structure of the lateral bathymetry induces complex three-dimensional flows, that, in turn, drive complex three-dimensional sediment motion. Sediment tends to accumulate in the regions where the transport of sediment converges (Kumar, 2018). If the convergence is strong enough, a region may be formed where the levels of suspended sediment are highly elevated: an Estuarine Turbidity Maximum (ETM). Even though much attention has been given to the formation and dynamics of ETMs (see, e.g., Huijts, 2006), the influence of lateral bathymetry and dynamics on the formation of ETMs remains poorly understood. To improve our understanding, an idealized modeling approach is taken, where only the essential processes are taken into account. This allows us to gain fundamental insights into the physical processes governing sediment dynamics. Moreover, the idealized approach allows us to build a highly specialized model which is fast such that extensive parameter sensitivity studies can be performed.

2. Method

To study the lateral dynamics, iFlow3D is constructed, which is a three-dimensional idealised hydro and sediment dynamic model. This model can effectively handle highly realistic and complex geometries and bathymetries. Using Fourier analysis, the harmonic components of the water motion and suspended sediment concentration can be directly identified and computed, e.g., M₀, M₂, M₄ etc., without the need for time stepping methods and spin up time. Using these harmonic components, the net sediment transport can be computed. Using the concept of morphodynamic equilibrium, a dynamic equilibrium distribution of sediments can be determined and ETMs identified. The resulting model is fast enough such that parameter sensitivity studies can be performed and the parameter space explored.

3. Results

We consider the sensitivity of the sediment transport and the lateral sediment distribution to changes in the lateral bathymetric profile. We explore several bathymetric shapes from a rectangular profile to a Gaussian profile with pronounced channels and shallow areas, and we investigate the effects of width convergence. The general trends of the sediment distribution will be explained in terms of the underlying flow and transport processes.

References

K. M. Huijts, H. M. Schuttelaars, H. E. de Swart, and A. Valle-Levinson. Lateral entrapment of sediment in tidal estuaries: An idealized model study. *Journal of Geophysical Research: Oceans*, 111(12):1–14, 2006.doi:10.1029/2006JC003615.

M. Kumar. *Three-Dimensional Model For Estuarine Turbidity Maxima In Tidally Dominated Estuaries*. PhD thesis, Delft University of Technology, 2018.



17th International Conference on
Cohesive Sediment Transport Processes
September 18-22, 2023
Inha University, Incheon, Republic of Korea



Upstream Sediment Transport in the Elbe Estuary

H. Weilbeer¹, S. Fuerst¹

¹ Federal Waterways Engineering and Research Institute (BAW)
Wedeler Landstr. 157, 22559 Hamburg, Germany, holger.weilbeer@baw.de

1. Introduction

During the period 2013–2018, several striking hydrological and morphological changes took place in the tidal Elbe river in Germany, which contains an important coastal navigation route and flows into the North Sea. Significant increases of maintenance dredging quantities concerning fine grained sediments occurred in the Port of Hamburg (the third largest seaport in Europe), but also in fairway sections further downstream as well as in the ancillary areas and ports along the tidal Elbe. Comparably, sedimentation rates have also increased. In some sections, a strong fining of sediments in combination with a smoothing of the river bed could be observed. Simultaneously, changes in water levels and currents were noticeable (Weilbeer et al., 2021). The amplification of the tidal range was unusually large especially in the inner estuary, where measuring stations registered an increase in flow velocities and higher levels of turbidity (Figure 1).

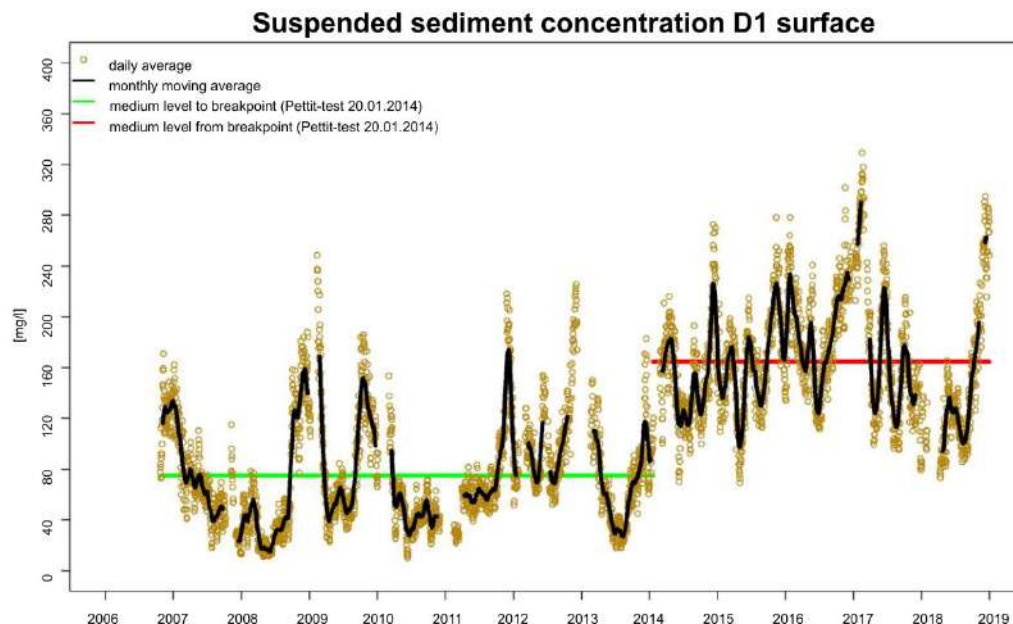


Figure 1. Increase of the turbidity – a shift to a higher level.

An increase of the turbidity could be observed at all measuring stations in the Elbe Estuary, but with a time shift over three months. The measuring stations further upstream registered these

shifts in the turbidity level later. A sequence of exceptional hydrological and meteorological events may be a possible reason for this upstream transport of fine sediments. It starts with a very high fresh water inflow in summer 2013 at the tidal barrier, which flushes out the fine sediments to the mouth. Since then no more flushing event happened. Then two storm events occur, on 28.10.2013 and on 5./6.12.2013, which remobilized a huge amount of sediments in the Outer Elbe. These sediments reached the fairway and are being transported upstream due to tidal pumping. The turbidity level remains high, because the sediment is trapped in the upper estuary and not completely removed by an adapted sediment management.

2. Modelling

The measured observations are now modelled by using the 3D-model of the Elbe Estuary. In order to understand the hydromorphological changes within the Elbe estuary hindcast simulations are applied. Several modelling approaches and parametrizations must be adapted (turbulence, settling velocity, deposition, consolidation, erosion fluxes) in order to simulate the observed upstream transport in the fairway. Real dredging data must be considered, too. The importance of specific modelling approaches is discussed. Later several studies are performed with the improved model for different time periods, comparing the results with site-specific validation data. As an example, the suspended load distribution in the mouth of the Elbe estuary at one point in 2016 with the current model setup is shown in Figure 2.

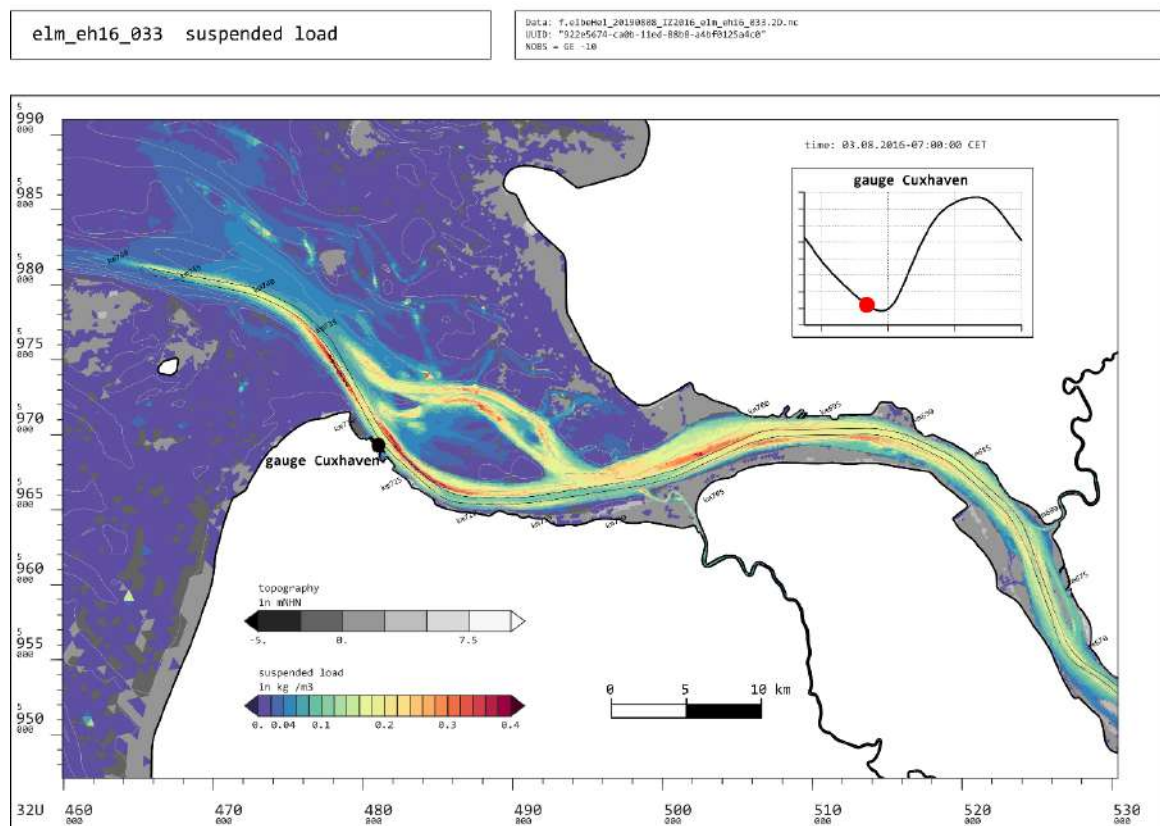


Figure 2: Suspended load distribution in the mouth of the Elbe estuary at one point (03.08.2016-07:00 CET) with the current model setup

3. Conclusions

Based on simulations with an improved 3D model of the Elbe Estuary it can be confirmed, that morphological changes, especially in the outer part of the estuary, are considered as responsible

for the described changes in the tidal Elbe system. These changes are superimposed by the consequences of an inflowing discharge of fresh water, which remained below-average since summer 2013, and are very likely to be amplified by a sediment management scheme not adapted to these recent developments. The gained knowledge will be used to forecast hydromorphological changes in the Elbe estuary with an operational numerical model and to give advice to the responsible administrations for a flexible and adapted sediment management.

Acknowledgments

The joint research project is funded by the German Coastal Engineering Research Council (KFKI). The funding is provided by the Federal Ministry of Education and Research (BMBF) and handled by Projektträger Jülich

References

Weilbeer, Holger; Winterscheid, Axel; Strotmann, Thomas; Entelmann, Ingo; Shaikh, Suleman; Vaessen, Bernd (2021): Analyse der hydrologischen und morphologischen Entwicklung in der Tideelbe für den Zeitraum von 2013 bis 2018. 73. DOI: 10.18171/1.089104.



17th International Conference on
Cohesive Sediment Transport Processes
September 18-22, 2023
Inha University, Incheon, Republic of Korea



Controls of the sediment composition in tidal systems

A. Colina Alonso^{1,2}, D.S. van Maren^{1,2,3} and Z.B. Wang^{1,2}

¹ Delft University of Technology, P.O. Box 5048, 2600GA Delft, the Netherlands.

A.ColinaAlonso@tudelft.nl

² Deltares, P.O. Box 177, 2600 MH Delft, the Netherlands

³ SKLEC, East China Normal University, Shanghai 200241, China

1. Introduction

Bed sediments in estuaries and tidal basins often consist of both sand and mud. Understanding where sand and mud prevail is crucial to understand and predict coastal evolution and biological activity. Yet this remains a challenge, since a distinct relation to accurately predict the bed composition is still lacking.

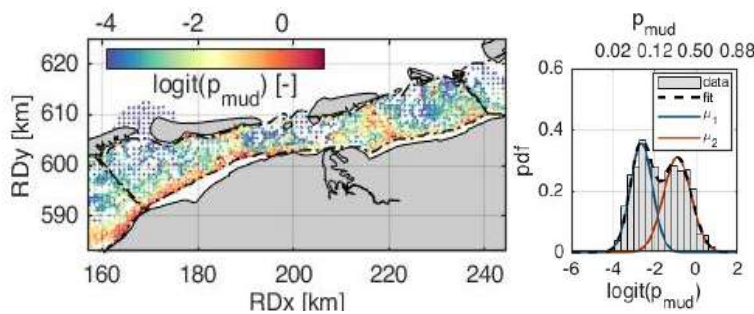


Figure 2: Mud content in the Wadden Sea sediment bed (logit-transformed) and its bimodal distribution.

Recent research (Colina Alonso, et al., 2022) has shown that the mud content in tidal basins tends to be bimodally distributed, revealing the existence of two stable equilibrium conditions (see also Figure 1). They found that the existence of multiple equilibrium conditions (as well as their values) is primarily controlled by the sediment deposition fluxes (rather than erosion), with bimodality originating from the dependence of suspended sand/mud concentrations on the local bed composition. Field data of the Wadden Sea (in The Netherlands and Germany) support these findings. Colina Alonso, et al (2022) argue that this dependence is most likely influenced by mud availability and the probability of sand to be transported towards muddy parts of the system. The aim of this research is to test this on a generalized case of a tidal basin and to further explore the factors controlling the composition of the sediment bed.

2. Methods

We make use of a morphodynamic model of a schematized tidal basin (Colina Alonso, et al., under review). Starting from a linearly sloping bed with a uniform sediment composition, we model 50 years of morphological evolution under tide- and wave-forcing for several scenarios with: 1) varying mud availability, 2) varying hydrodynamic forcing (wave heights, storm occurrence, and tidal prism) and 3) varying grain sizes of the sand fraction. Simulations are

performed with and without sand-mud interaction. Simulations with sand-mud interaction account for the combined erosive behaviour of sand-mud mixtures, including the dependence of the bed roughness on the sediment composition (van Ledden et al., 2003; Soulsby & Clarke, 2005; Colina Alonso et al.; under review). We subsequently analyse the simulated bed evolution, the spatial variation of the sediment composition in the upper bed and its bimodality.

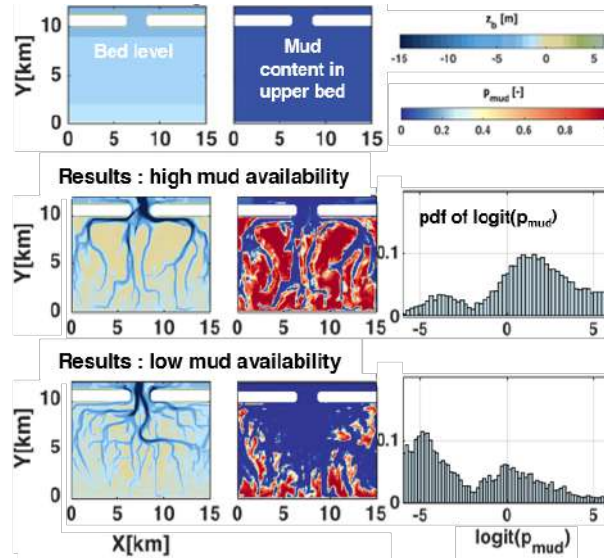


Figure 3: Initial model settings (upper panels) and results (lower panels) for two scenarios with varying mud availability.

3. Results

3.1 General morphodynamic evolution

Our models generate a complex pattern of tidal channels and flats in which, overall, the mud content increases in landward direction (Figure 2). Only simulations including sand-mud interaction are able to reproduce the bimodal character of the mud content in the sediment bed. It is important to correctly reproduce the bimodal distribution of the mud content since this indicates a correct representation of the bed sediment composition in the modelled system. Consequently, this distribution can be used as a model calibration metric.

The computed morphology - including the extent of the intertidal areas, channel patterns, but also the distribution of the mud content - is strongly steered by the explored input parameters. Below, we briefly discuss the effects on the sediment composition.

3.2 Mud availability

Our results show that the distribution of the mud content is most affected by the availability of mud. With decreasing availability, more intertidal areas move from a muddy (cohesive) state to a sandy (non-cohesive) state. Still, bimodality is observed for a wide range of conditions. However, when the mud availability is much larger (e.g., by increasing the offshore concentrations from 5 mg/l to > 100 mg/l), the bimodal character disappears, and only muddy intertidal flats evolve.

3.3 Hydrodynamic forcing

Increased wave forcing results in a smoother bathymetry and a more pronounced bimodality, which represents a sharper segregation between sandy ($p_{\text{mud}} \approx 2\%$) and muddy areas ($p_{\text{mud}} > 50\%$). Besides, the relative amount of sandy intertidal areas increases, most likely because of the larger transport capacity of sand. Increasing the tidal prism has the opposite effect, resulting

in sandy areas becoming muddy and the muddy areas becoming muddier, even though an increased tidal prism may also increase velocities and thus the sand-transport capacity. We believe this may be because an increased tidal prism also largely increases the net mud flux into the basin.

3.4 Sand grain size

Our model results show that intertidal flats become slightly sandier with a decreasing $D_{50,sand}$, because the increased mobility of sand enables transport to relatively calm conditions. This effect is however limited: simulations with $D_{50,sand} = 300 \mu m$ have approximately 10% less sandy shoal area compared to simulations with $D_{50,sand} = 150 \mu m$. A change in $D_{50,sand}$ does not necessarily lead to a shift in the modes of the bimodal distribution, which shows that the sand grain size influences the extent of sandy/muddy areas, but the muddy areas will not necessarily be more or less muddy.

4. Outlook

Our first results show that our schematised model can reproduce a realistic morphodynamic evolution of tidal basins, including the bimodal distribution of the mud content. This characteristic has been previously analysed for real-world systems and can now be used as a model calibration metric. So far, we have observed that the sediment composition is most strongly steered by the availability of mud within the system. We aim at further exploring the factors that control the sediment composition in sand-mud tidal basins by further quantifying their relative contributions and by further analysing the physical processes that play a role when changing these factors.

Acknowledgments

This project is funded by the Royal Netherlands Academy of Arts and Sciences (KNAW) within the framework of the Programme Strategic Scientific Alliances between China and The Netherlands, project PSA-SA-E-02.

References

- Colina Alonso, A., van Maren, D.S., Herman, P.M.J., van Weerdenburg, R.J.A., Huismans, Y., Holthuijsen, S.J., Govers, L.L., Bijleveld, A.I., Wang, Z. B. (2022). The existence and origin of multiple equilibria in sand-mud sediment beds. *Geophysical Research Letters*, 49 (22). doi: 10.1029/2022GL101141
- Colina Alonso, A., van Maren, D.S., Herman, P.M.J., van Weerdenburg, R.J.A., Huismans, Y., Wang, Z. B. (under review). Morphodynamic modelling of tidal basins: the role of sand-mud interaction.
- Soulsby, R. L., & Clarke, S. (2005). *Bed Shear-stresses Under Combined Waves and Currents on Smooth and Rough Beds Produced within Defra project*. HR Wallingford
- van Ledden, M. (2003). *Sand-mud segregation in estuaries and tidal basins (PhD thesis)*. Delft University of Technology.

Session: Seabed Processes
16:00 – 17:20
Tuesday, September 19, 2023



17th International Conference on
Cohesive Sediment Transport Processes
September 18-22, 2023
Inha University, Incheon, Republic of Korea



A Fuel Cell Type Sensor for Continuous Monitoring of Seabed Deposition and Erosion

K. Kim^{1,2}, Y. Nakagawa², T. Hibino¹, T. Nishimoto³ and K. Ajiki³

¹ Graduate School of Advanced Science & Engineering, Hiroshima University, Higashi-Hiroshima, Japan, seniorz@hiroshima-u.ac.jp

² Port and Airport Research Institute, Yokosuka, Japan

³ Chugoku Regional Development Bureau, Ministry of Land, Infrastructure, Transport and Tourism, Hiroshima, Japan

1. Introduction

Coastal areas are important habitats for various organisms and also serve as important resources for human activities such as fishing and tourism. However, these areas are vulnerable to environmental changes caused by climate change, which may result in more frequent and severe typhoons and concentrated rainfall. As a result, there is a growing need to understand how such changes are affecting the coastal environment, particularly the sedimentation processes on the seabed. To address this, the purpose of this study is to develop an electrochemical sensor that can continuously monitor the dynamics of seabed sediments. Monitoring the sedimentation processes in time series can provide new insights into the impacts of environmental changes on the seabed and coastal environments. The sensor developed in this study is unique in that it does not require a power supply, as it utilizes the power generation principle of fuel cells through an oxidation-reduction reaction. This makes it a stationary sensor that can be easily deployed in coastal areas for extended periods of time, providing continuous monitoring data.

2. Materials and methods

A sensor consists of circuit as shown in Figure 1(a) and measures the internal resistance of graphite cathode against current flowing due to potential difference between graphite and magnesium (Mg) electrodes (Aleman-Gama et al., 2021):

$$R_{\text{int}} = \left(\frac{\text{OCV}}{\text{CCV}} - 1 \right) R_{\text{ext}} \quad (1)$$

where R_{int} = internal resistance, OCV = open circuit voltage, CCV = closed circuit voltage, R_{ext} = external resistance. The external resistance was set to 6,790 Ω . Electric potential of each electrode was measured against an Ag/AgCl reference electrode. Because dissolved oxygen (DO) around the graphite electrode is consumed (*i.e.*, O_2 to H_2O reduction reaction; Song et al., 2019), R_{int} should be determined with DO concentration and diffusion rate. Using this principle, the sensor estimated the softness of deposited sediment or DO-rich water column. Sensor measuring R_{int} of seven layers at 5 cm intervals was designed in a 40 cm long cylindrical core. The core type sensor was installed by divers on the seabed in coastal area with a water depth of approximately 4.4 m (Figure 1(b) and 1(c)). The sensor penetrated approximately 30 cm into the seabed, leaving the top 10 cm exposed to water column. Continuous measurement was conducted for approximately 5 hours. Data loggers were wired and stored on the observation ship.

In order to evaluate results conducted in the field experiment, R_{int} of sediment with different moisture ratio was measured in the laboratory test. After adding seawater to the sediment, moisture ratio was adjusted by mixing thoroughly. Moisture ratio was determined from weight loss by drying at 100 °C for 4 hours. After then, the correlation between moisture ratio and R_{int} after 5 hours of measurement was investigated.

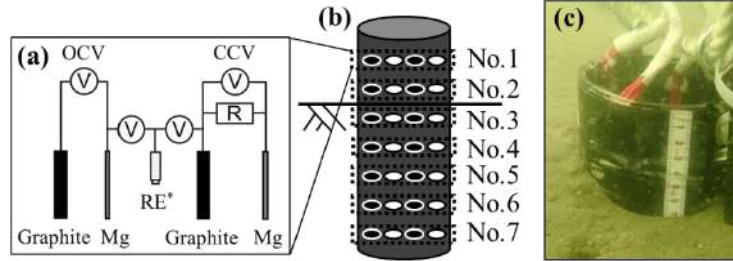


Figure 1. (a) Circuit for measuring internal resistance with potential difference. *RE: Ag/AgCl reference electrode. (b) Schematic diagram of sensor installed on *in situ* seabed. (c) photograph of the sensor.

3. Results and discussion

Figure 2(a) shows time-series R_{int} change at *in situ* seabed boundary. Sensors No.1 and No.2, which are in the water column showed relatively constant R_{int} during the measurement period. On the other hand, in No.3 to No.7, which are in the sediment layer, R_{int} was increased significantly probably due to DO depletion. *i.e.*, R_{int} readily distinguished between water column and sediment layer. In addition, R_{int} of No.2 was increased after 3 hours of installation. This should be due to new sediment deposition occurred by diver work of columnar core sediment sampling performed near the sensor, meaning that the sensor responds instantly to the sediment dynamics of erosion or deposition.

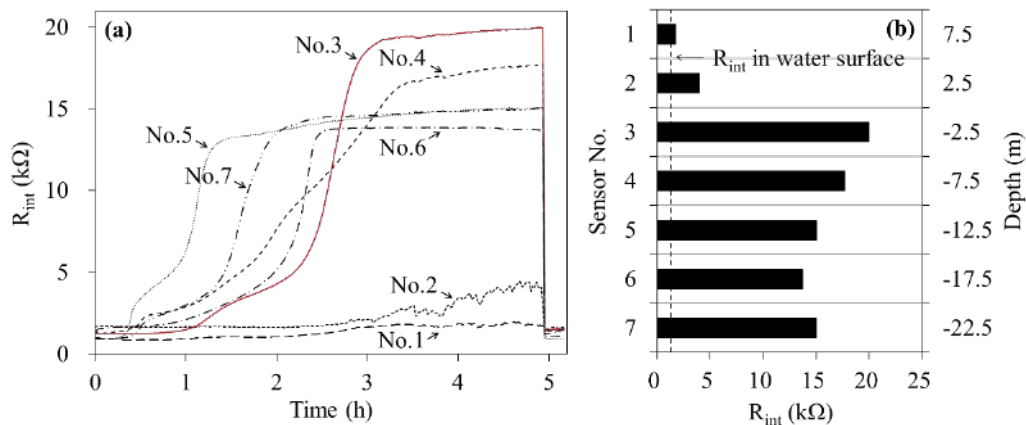


Figure 2. (a) Time-series R_{int} changes of *in situ* seabed boundary. The sensor was in the water surface for 20 minutes after 4.9th hour. (b) Vertical R_{int} distribution at the end of the experiment.

Figure 3(a) shows correlation between R_{int} and moisture ratio investigated from an indoor experiment. R_{int} was below 15 k Ω in all cases with a water content of 140% or less, but increased to 19 k Ω with a water content of 200%. The number of digits of R_{int} determined in laboratory test (15 to 20 k Ω) and *in situ* seabed (14 to 20 k Ω in Figure 2(b)) were identical, suggesting that vertical R_{int} distribution *in situ* may indicate moisture ratio of sediment. Figure 3(b) shows time-series potential change between graphite and Mg electrodes for each sediment sample in the laboratory test. In all cases, more than 95% of the total R_{int} was generated from graphite side, meaning that more than 95% of the R_{int} was polarization resistance of cathode due to DO depletion.

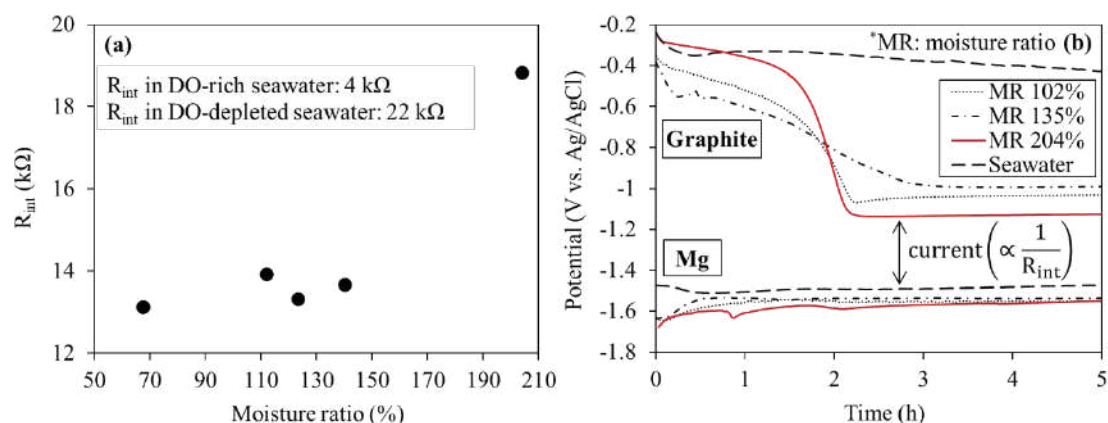


Figure 3. (a) Correlation between R_{int} and moisture ratio. (b) Potential change due to R_{int} between two electrodes.

4. Conclusions

A fuel cell type sensor was continuously captured vertical resistance distribution of *in situ* seabed boundary. This sensor is expected to be used for long-term observation on the seabed because it can spontaneously sustain chemical reactions (*i.e.*, DO reduction reaction) for sensing without an external power source. Laboratory tests confirmed that the resistance depends on the moisture ratio, which is one of indexes of bulk density of seabed, suggesting that measuring physical properties of seabed using electrochemical parameter. These findings suggest that real-time monitoring of changes in topography of seabed will be possible in the near future. To realize this, correlation between R_{int} and factors other than water content such as electrical conductivity and pH should be demonstrated to estimate bulk density quantitatively.

References

- Aleman-Gama, E., Cornejo-Martell, A. J., Ortega-Martínez, A., Kamaraj, S. K., Juárez, K., Silva-Martínez, S., and Alvarez-Gallegos, A. (2021) Oil-contaminated sediment amended with chitin enhances power production by minimizing the sediment microbial fuel cell internal resistance. *Journal of Electroanalytical Chemistry* 894, 115365. doi: 10.1016/j.jelechem.2021.115365
- Song, N., Yan, Z., Xu, H., Yao, Z., Wang, C., Chen, M., Zhao, Z., Peng, Z., Wang, C., and Jiang, H. -L. (2019) Development of a sediment microbial fuel cell-based biosensor for simultaneous online monitoring of dissolved oxygen concentrations along various depths in lake water. *Science of the Total Environment* 673, 272-280. doi: 10.1016/j.scitotenv.2019.04.032



17th International Conference on
Cohesive Sediment Transport Processes
September 18-22, 2023
Inha University, Incheon, Republic of Korea



Enhancing the quality and accuracy of mud settling and consolidation experiments

B. Brouwers¹, D. Meire and J. Vanlede¹

¹Flanders Hydraulics, Antwerp, Belgium. Joris.vanlede@mow.vlaanderen.be

1. Introduction

In the broader framework of its research on nautical bottom (in collaboration with the universities of Ghent and Leuven in Belgium), mud settling and consolidation experiments are regularly conducted at Flanders Hydraulics.

This presentation describes the revised measurement set-up. A protocol is suggested on how the mud should be conditioned in preparation of settling and consolidation experiments, in order to enhance the reproducibility. First results of modelling the observed consolidation behaviour (density, mud-water interface and effective stress) will be presented.

2. Revised consolidation columns

The large consolidation columns ($\text{Ø}170 \text{ mm}$) that were used in earlier research (e.g. for the port of Hamburg, Priola et al., 2020) are now outfitted with a gamma-ray densitometer, fitted on a moving frame (two degrees of freedom) to enable non-destructive measurements of the vertical density profile at a prescribed schedule.

The mud-water interface in the column is recorded automatically using cameras (IDS uEye, type UI-3200SE-C-HQ) with a resolution of 0.7 mm per pixel. Backlighting is used to improve the accuracy of the registration. The pore water pressure is measured by highly accurate water level measurements in the riser tubes, which are connected to the side of the large column every 20 cm. With a novel in-house developed measurement system, an accuracy of 10 μm , corresponding with a pressure of 0.1 Pa can be achieved.

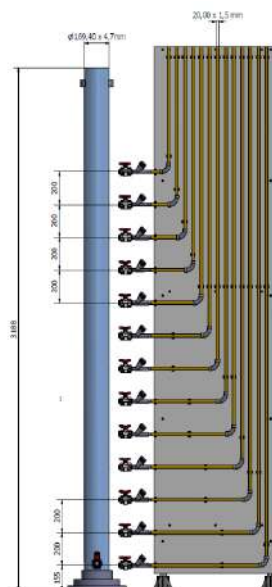


Figure 1: Revised consolidation column at Flanders Hydraulics.

3. Mud conditioning

The objective of conditioning is to homogenise the mud by agitation in preparation of settling and consolidation experiments. A sensitivity analysis (of duration and agitator type) shows the importance of homogenisation to achieve a good repeatability of the experiments (Brouwers et al., submitted).



Figure 2: Different mixing impellers used:

(A) Marine blade impeller; (B) Pitched blade impeller; (C) Paddle impeller.

A clear procedure for mud conditioning is presented, which enhances the reproducibility of mud behaviour and therefore allows for repeatable hydraulic experiments using mud.

4. Modelling

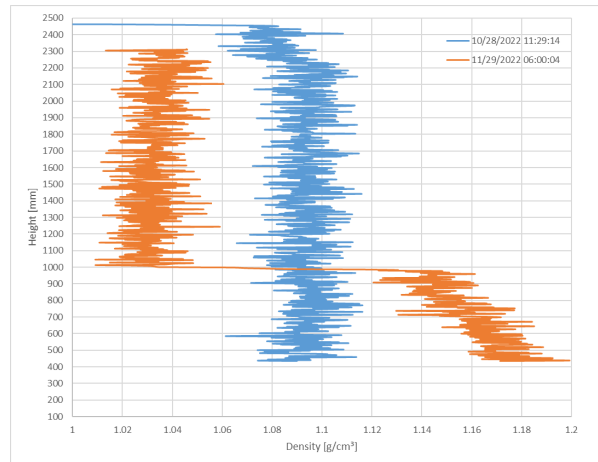


Figure 3: Observed density profile of a homogenised column with $\rho_{ini} \sim 1.09 \text{g/cm}^3$, at the beginning of the test and after one month

The observed consolidation behaviour (density, mud-water interface and effective stress) is modelled by numerical integration of the Gibson equation (eq. 1)

$$\frac{\partial \phi}{\partial t} = \frac{\rho_s - \rho_w}{\rho_w} \frac{\partial}{\partial z} (k \phi^2) + \frac{1}{\rho_w g} \frac{\partial}{\partial z} \left(k \phi \frac{\partial \sigma'}{\partial z} \right) \quad (1)$$

References

Brouwers, B., Meire, D., Toorman, E.A., van Beeck, J., Lataire, E. (submitted) Conditioning procedures to enhance the reproducibility of mud settling and consolidation experiments
 Pirola Igoa, E.; Ibanez, M.; Claeys, S.; Meire, D.; Mostaert, F. (2020). Experimental investigation on the consolidation behaviour of mud: Port of Hamburg. Version 3.0. FHR Reports, 18_009_1. Flanders Hydraulics Research: Antwerp



Estimation of sediment pickup rate in bare and vegetated channels

Yuan Xu^{1,2,3}, Qing He¹, Danxun Li², and Heidi Nepf³

¹State Key Laboratory of Estuarine and Coastal Research, East China Normal University, Shanghai, China, yuanxu@sklec.ecnu.edu.cn

²Department of Hydraulic Engineering, Tsinghua University, Beijing, China

³Department of Civil and Environmental Engineering, Massachusetts Institute of Technology, Cambridge, MA, USA

Abstract

Aquatic vegetation abounds in rivers, lakes, and coastal regions. It plays an important role in ecosystems, for examples, it enhances water quality, stabilizes riverbanks, and promotes soil carbon storage. During the past decades, however, the area of vegetated ecosystems has significantly decreased, leading to a growing interest in wetland restoration. To improve restoration effects, it is essential to understand how vegetation impacts flow and sediment motion. In this study, laboratory experiments were conducted to investigate the sediment pickup (or entrainment) over bare and vegetated beds with model vegetation (i.e., cylinder arrays) of different solid volume fractions, ϕ , and diameters, d (Figure 1). For the vegetated beds, measured pickup rate was closely correlated with turbulent kinetic energy, k_t , and τ -based model developed for bare channels significantly underestimated the pickup rate measured in vegetated channels (Figure 2a). Building on previous theoretical analyses and observations, this study proposed two k_t -based predictions for pickup rate that include the impact of both bed- and vegetation-generated turbulence (Figure 2b and 2c). The new models improve the prediction of pickup rate within vegetated regions.

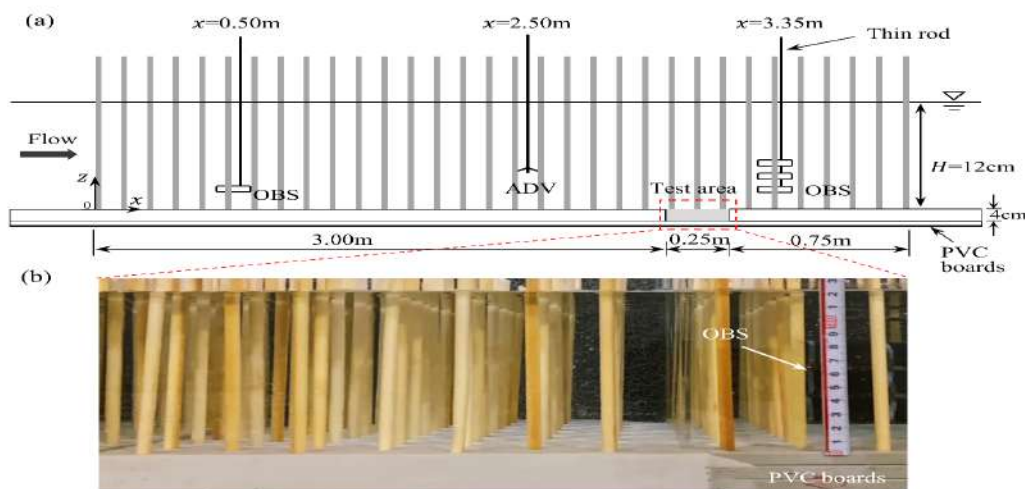


Figure 1. (a) Schematic of flume viewed from side. Not to scale. The gray area denotes test area. (b) Photo of the test area.

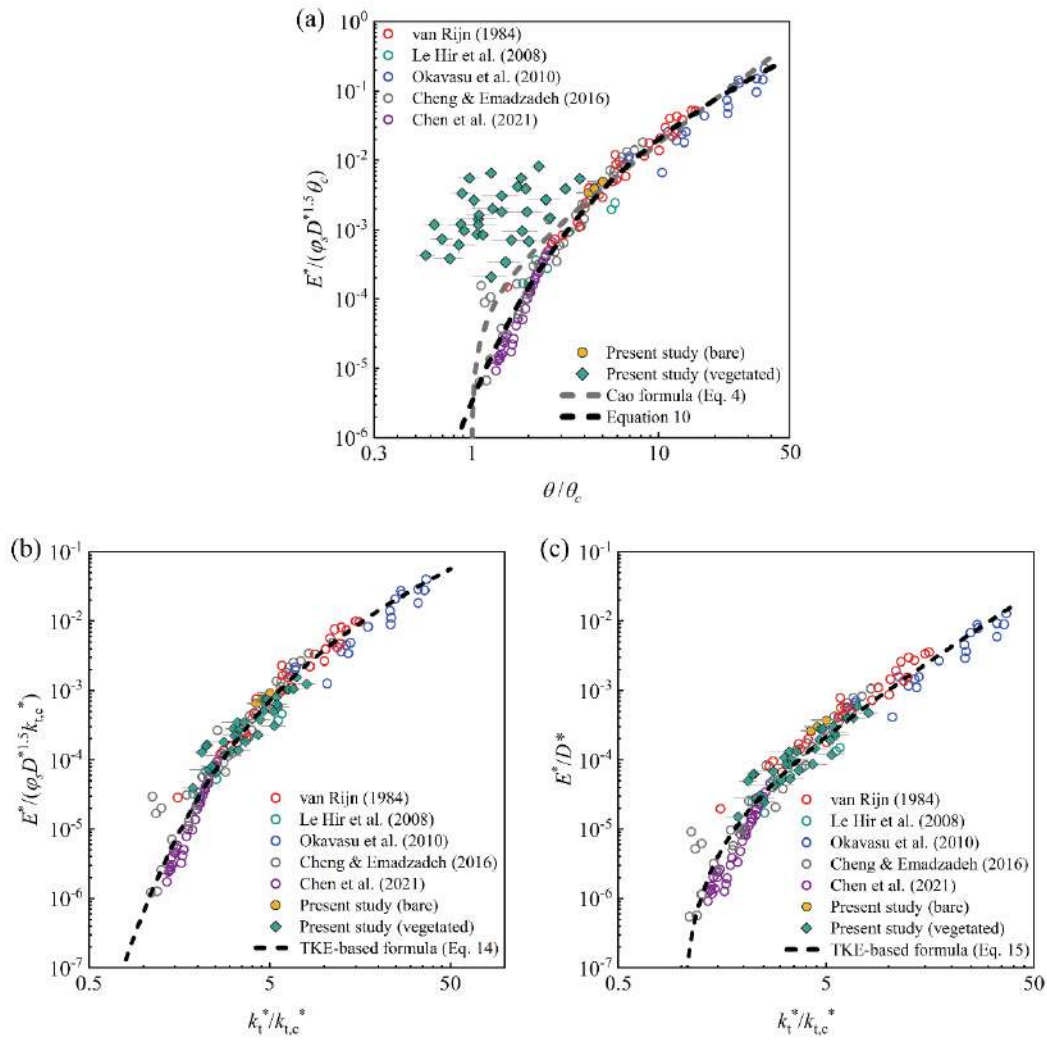


Figure 2. (a) Comparison of measured data with τ -based formula (grey dashed curve) and modified τ -based formula (black dashed curve). The circles and diamonds denote bare and vegetated cases, respectively. Solid symbols denote the data from this study. Open symbols represent the data from previous studies. (b) Comparison of measured data with k_t -based formula (bursting theory). (c) Comparison of measured data with k_t -based formula (empirical fit).



17th International Conference on
Cohesive Sediment Transport Processes
September 18-22, 2023
Inha University, Incheon, Republic of Korea



Nearbed concentration of cohesive sediments in the Río de la Plata estuary

F. Pedocchi¹ and R. L. Mosquera¹

¹ Instituto de Mecánica de los Fluidos e Ingeniería Ambiental, Facultad de Ingeniería,
Universidad de la República, Uruguay, kiko@fing.edu.uy

I. Introduction

The erosion of cohesive sediment beds, suspended sediment distribution, and the occurrence of self-stratification under waves is still an open area of research. Most of the advances has been on environments where the transport is dominated by currents, while studies focusing on cohesive sediment-wave interaction are still scarce. During our recent field measurements in the Río de la Plata, Uruguay, the shear stresses reached 20.5 Pa and nearbed concentrations 137 kg/m³. Using these data, we evaluated current formulations for estimating cohesive sediment nearbed concentration and erosion rate.

II. Theory

For non-cohesive sediments, the concentration in the bedload layer can be estimated as $c_b = \gamma_0 c_m (\tau_b / \tau_c - 1)$, for $\tau_b / \tau_c \lesssim 2$, with c_m the bed concentration, τ_b the bed shear stress and τ_c the critical shear stress, below which there is no transport. And this expression could be used for estimating the nearbed suspended sediment concentration. However, for $\tau_b / \tau_c \gtrsim 20$, it is expected that c_b tends towards c_m as noticed by Smith (1975). Extending these ideas to the concentration in the stirred layer (Mehta and McAnally 2008) over a cohesive sediment bed we obtain

$$c_b = c_m \frac{\left(\frac{\tau_b}{\tau_c} - 1\right)}{\left(\frac{\tau_b}{\tau_c} - 1 + \frac{1}{\gamma_0}\right)}. \quad (1)$$

For $\tau_b \gtrsim \tau_c$ we obtain Kandiah-Ariaturai-Partheniades expression

$$c_b = c_m \gamma_0 \left(\frac{\tau_b}{\tau_c} - 1\right) = \frac{E_{2\tau_c}}{w_e} \left(\frac{\tau_b}{\tau_c} - 1\right), \quad (2)$$

with $E_{2\tau_c}$ the erosion rate for $\tau_b = 2\tau_c$, and w_e an erosion velocity. At equilibrium, $w_e = w_s$ and $\gamma_0 = E_{2\tau_c} / c_m w_s \approx 0.002$; $E_{2\tau_c} \approx 1 \times 10^{-3}$ kg/m²s, $c_m \approx 500$ kg/m³, $w_s \approx 1 \times 10^{-3}$ m/s, $\tau_c \approx 0.1$ Pa (Traykovski et al. 2007, Maa and Mehta 1987). Note that for non-equilibrium conditions w_e may be a function of the hydrodynamics and sediment concentration.

III. Field deployment

During three months in 2018 a large instrumented tripod, which included among other instruments a Vector ADV, an multifrequency ABS, and an OBS, was deployed near the coast of Montevideo, Uruguay, close to an oceanic buoy which recorded waves and currents. The sediment deposits in the area are composed by silt and clay, with less than 1% in mass of fine sand, uniformly covering the bed and being several meters deep. During the deployment water temperature was between 10 and 18 °C, salinity between 0 and 28 psu, and water depth between

6.5 and 9 m; significant wave height reached 2.0 m and current velocity 1.1 m/s. With this setup we were able to estimate nearbed concentrations inverting ABS multifrequency profiles and shear stresses from the ADV measurements, using Styles and Glenn (2000) model. Figure 1 shows an example of the type of data we acquired during the deployment.

IV. Analysis

Figure 2 shows the equilibrium nearbed concentrations recorded during the deployment. Shear stresses for the combined current and wave data were computed using ADV data and the Styles and Glenn (2000) model. Data plotted on Figure 2 corresponds to equilibrium conditions, and for comparison purposes the erosion rates are computed from the concentration measurements assuming $w_s = 1 \times 10^{-3}$ m/s. Equations (1) and (2) are also plotted in Figure 2 using $\gamma_0 = 0.002$, $c_m = 480$ kg/m³, and $\tau_c = 0.1$ Pa (solid line), which corresponds to $E_{2\tau_c} = 0.96 \times 10^{-3}$ kg/m²s.

V. Discussion and conclusion

The agreement of Equation (1) with the data is outstanding considering that standard values used for γ_0 , c_m and w_s . It is also surprising how Equation (1) captures the curvature of the data. To our knowledge no previous evaluation of the Kandiah-Ariaturai-Partheniades expression for cohesive sediments under such large shear stress values had been reported in the literature. For example, erosion rates reported by Maa and Mehta (1987), and Vinzón (1998) went up to $E = 10 \times 10^{-3}$ kg/m²s and shear stresses went up to $\tau_b = 10\tau_c$, while in Figure 2 we include values up to $E = 150 \times 10^{-3}$ kg/m²s and $\tau_b = 200\tau_c$. One could argue that using $w_e = 1 \times 10^{-3}$ m/s in Figure 2 results in artificially large erosion rate values and that smaller values would be obtained if a smaller settling velocity and hindered settling were considered. However, the values of τ_b are also significantly larger than the values reported in the literature. Traykovski et al. (2007) mentions that Equation (1) overpredicted their measurements at the Po delta, which they attributed, correctly in the light of our results, to a limited sediment availability and not to a failure of Equation (1).

The large shear stresses and concentrations recorded during our measurements allowed us to show that the Kandiah-Ariaturai-Partheniades expression may be considered a limit case of the Smith (1975) expression for moderated shear stresses. Our results also show that the standard value of $\gamma_0 = 0.002$ seems appropriate for estimating the erosion of cohesive sediments. We plan to further explore the universal validity of these hypothesis by evaluating

$$\frac{\partial c_b}{\partial \tau_b} \frac{\tau_c}{c_m} = \gamma_0, \quad (3)$$

for cohesive sediments, given that according to Mehta and Parchure (2000) τ_c/c_m is approximately constant.

Finally, we would like to point out, that due to self-stratification, the suspended sediment concentration increases to very high values near the bed, allowing for a balance between erosion and deposition for much smaller erosion depths than would be expected if no self-stratification was developed. In other words, as in the case of armouring, self-stratification could be considered a mechanism by which the bed “defends” itself from further erosion.

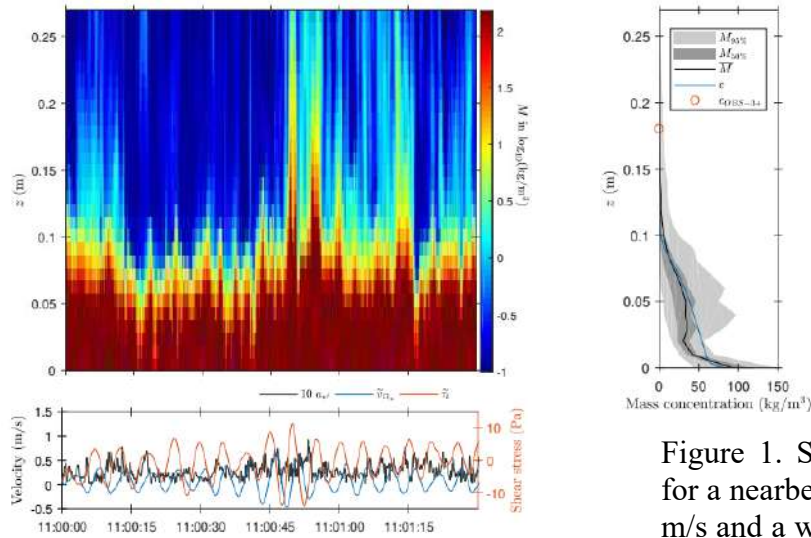


Figure 1. Sample concentration record for a nearbed current velocity $U_c=0.122$ m/s and a wave induced orbital velocity $U_w=0.34$ m/s.

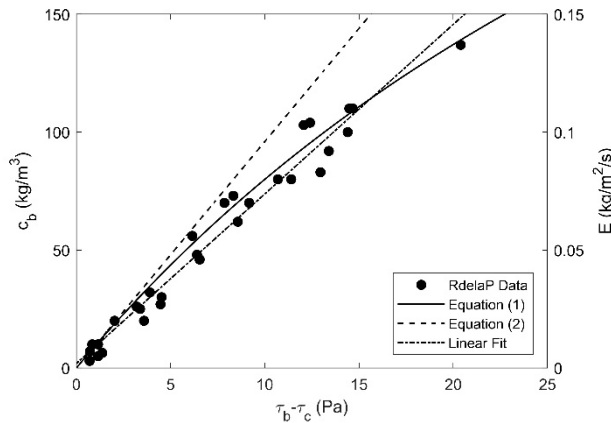


Figure 2. Recorded nearbed concentrations c_b and estimated erosion rates E , as function of the excess shear stress on the bed $\tau_b - \tau_c$. Equations (1) and (2) ($\gamma_0 = 0.002$, $c_m = 480$ kg/m³, and $\tau_c = 0.1$ Pa; and $w_s = 1 \times 10^{-3}$ m/s, which gives $E_{2\tau_c} = 0.96 \times 10^{-3}$ kg/m²s), and a linear fit to the data ($c_b = 7.19(\tau_b - \tau_c) + 1.21\tau_c$) are also included.

References

- Maa, P.Y. and Mehta, A. J. (1987). Mud erosion by waves: a laboratory study. *Continental Shelf Research*. [https://doi.org/10.1016/0278-4343\(87\)90030-6](https://doi.org/10.1016/0278-4343(87)90030-6).
- Mehta, A. J. and McAnally, W. H. (2008). Fine Grained Sediment Transport. In *Sedimentation Engineering: Processes, Measurements, Modeling, and Practice*. <https://doi.org/10.1061/9780784408148.ch04>.
- Mehta, A. J. and Parchure, T. M. (2000). Surface erosion of fine-grained sediment revisited. In *Proceedings in Marine Science*. [https://doi.org/10.1016/S1568-2692\(00\)80006-6](https://doi.org/10.1016/S1568-2692(00)80006-6).
- Smith, J. D. (1975). Modeling of sediment transport on continental shelves. <https://doi.org/10.2172/7156268>
- Styles, R. and Glenn, S. M. (2000). Modeling stratified wave and current bottom boundary layers on the continental shelf. <https://doi.org/10.1029/2000JC900115>.
- Traykovski, P., Wiberg, P.L., and Geyer, W.R. (2007). Observations and modeling of wave-supported sediment gravity flows on the Po prodelta and comparison to prior observations from the Eel shelf. *Continental Shelf Research*. <https://doi.org/10.1016/j.csr.2005.07.008>.
- Vinzón, S. B. (1998). A preliminary examination of amazon shelf sediment dynamics. PhD Thesis, University of Florida. <https://ufdc.ufl.edu/UF00091088/00001/>.

Session: Sediment Transport II
09:00 – 10:40
Wednesday, September 20, 2023



17th International Conference on
Cohesive Sediment Transport Processes
September 18-22, 2023
Inha University, Incheon, Republic of Korea



Storm-induced sediment transport and recovery in a tidal flat

Haisheng Yu¹, Zhong Peng¹, Weiming Xie^{1*}, Xianye Wang¹, Qing He¹

¹ State Key Laboratory of Estuarine and Coastal Research, East China Normal University, Shanghai 200241, China

Abstract

Storms have a significant impact on the sediment transport and morphodynamics in deltas and estuaries. The frequency of storms is expected to increase due to global climate change (Bacmeister et al., 2018). Previous studies have shown complex response and recovery of sediment transport and morphological changes under storm condition. For instance, both erosion and accretion can be induced by storms and the post-storm recovery time is unpredictable (Xie et al., 2021). Therefore, understanding the storm effects need more research. However, these studies are relatively limited because of the difficulties in obtaining in-situ data under extreme weather conditions.

The Yellow River Delta (YRD) is a microtidal delta with frequent extratropical cyclones. In this study, we investigated the effect of a storm in the YRD based on 11-day field measurements from September 28th to October 8th, 2021. The observation site was located approximately 100 m away from the salt marsh edge on the mudflat. We collected turbidity at 5 cm above the bed using RBR concerto3-C.T.D.Tu., and near-bed velocity using Nortek Vector ADV. Waves were measured through pressure sensors using RBR virtuoso3-D|wave16.

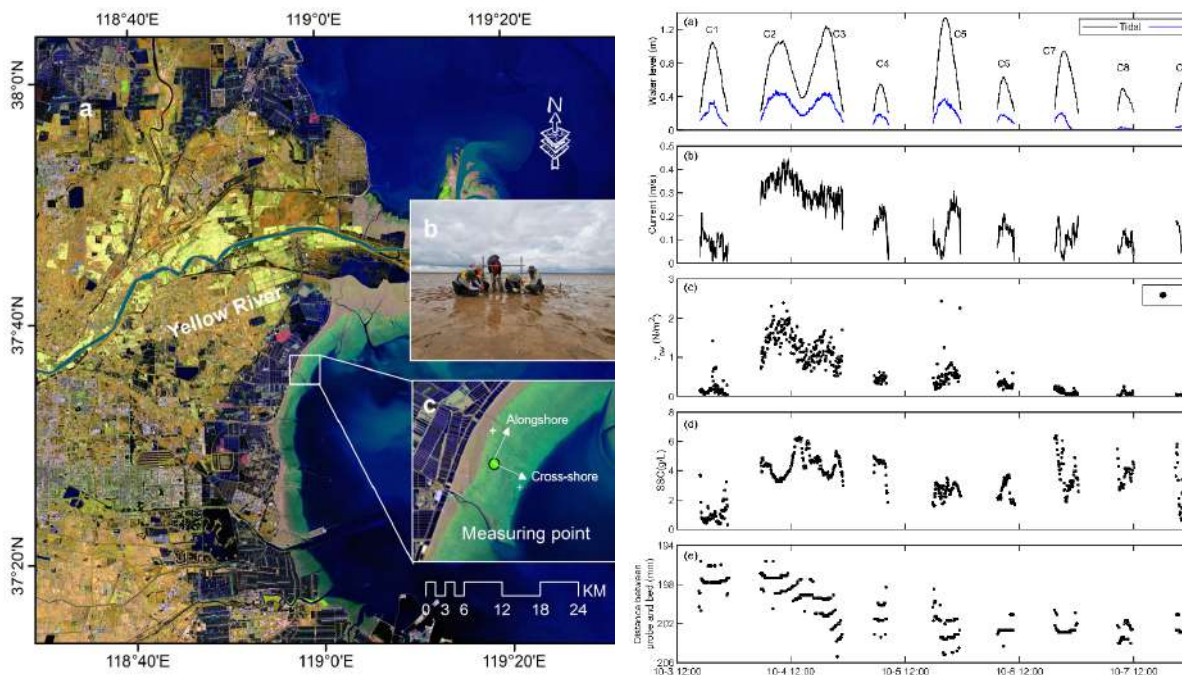


Figure 1. (a) Map of the YRD, (b) location of the study area, and (c) the in-situ tripod at the measuring point.

Figure 2. Time series of (a) tidal elevation and significant wave height, (b) velocity, (c) bed shear stress due to the combined current-wave action, (d) suspended sediment concentration (SSC), (e) changes of distance between ADV probe and bed surface.

The results indicate that significant changes in sediment dynamics and morphological changes due to the storm. During the storm (4th October, 2021), the inundation increased from 4th to twice a day and the bed shear stress increased from 0.23 N/m^2 to 1.25 N/m^2 , enhancing sediment resuspension. In addition, storms drive sediment southward to the outer delta, leading to a 10-mm erosion on average at the study site. In the post-storm period, the current decreased from 5th to 8th within 3 days. This results in slight accretion and the sediment median grain size decreased from $24.8 \mu\text{m}$ to $18.1 \mu\text{m}$. However, the system is unable to recover back to the pre-storm state due to the limited sediment transport into the system. Overall, the storm has strongly changed the sediment transport patterns and morphological changes, which should be carefully considered in the management and restoration of tidal flats in estuaries.

Acknowledgements

This work is financially supported by the National Natural Science Foundation of China (Nos. U2040216, U2243207, 42276217, 42206169). Financial supports from the National Key Research and Development Program of China (2022YFE0136700) and Shanghai Committee of Science and Technology (21230750600, 20DZ1204701) are also acknowledged.

References

- Bacmeister, J. T., Reed, K. A., Hannay, C., Lawrence, P., Bates, S., Truesdale, J. E., Rosenbloom, N., & Levy, M. (2018). Projected changes in tropical cyclone activity under future warming scenarios using a high-resolution climate model. *Climatic Change*, *146*(3), 547-560. <https://doi.org/10.1007/s10584-016-1750-x>
- Xie, W., Wang, X., Guo, L., He, Q., Dou, S., & Yu, X. (2021). Impacts of a storm on the erosion process of a tidal wetland in the Yellow River Delta. *CATENA*, *205*, 105461. <https://doi.org/10.1016/j.catena.2021.105461>



17th International Conference on
Cohesive Sediment Transport Processes
September 18-22, 2023
Inha University, Incheon, Republic of Korea



Seasonal influences on land-sea fine-grained particle dynamics

T.N Markussen¹, R. Verney¹

¹ DHYSED, Ifremer, Plouzané, France

1. Introduction

Estuaries play an important role in the land-sea exchange of suspended matter. Much focus has already been put into increasing our understanding of estuarine processes, with studies from micro- to macrotidal estuaries having been carried out in a multitude of locations. Most in-situ studies are based on data gathered at a timescale $<$ year. While this can give valuable and in-depth information about the dynamics of specific processes, the temporal resolution makes it difficult to understand the yearly dynamics and governing processes. Our study presents fine-grained suspended sediment dynamics gathered from eight years of field campaigns with unchanged data acquisition protocols, used instruments and locations, in the macrotidal Seine estuary and bay. Four locations in the land-sea continuum have been sampled and campaigns have been carried out in all four seasons in almost all years. The data presented here is based on measurements with CTD- and turbidity and fluorescence sensors, as well as current speeds from an ADCP and particle properties from a LISST. We focus on long-term dynamics ($>$ tidal cycle) rather than flocculation dynamics within a given tidal cycle. The long time series makes it possible to get a better idea of interannual dynamics as well as seasonal patterns, and the four locations illustrate how these dynamics and patterns play different roles along the land-sea continuum.

2. Results

On an overall spatial scale, we show how median particle size distributions increase from land (river) to sea (bay), while suspended matter concentrations decrease with close to two orders of magnitude (see Figure 1). On an overall temporal scale, we show how particle size distributions differ between seasons, but also how the scale of the differences to a large degree depends on the location. More specifically, largest median particle size distributions over the year coincide with lowest relative abundance of particles of sizes 10-50 microns at the estuary mouth, and of particles of sizes 100-200 microns at the bay locations. At the estuary mouth, these largest sizes are found in late spring whereas largest sizes are found in summer in the bay. We introduce a proxy for the ratio of organic and mineral content (OMC), being measured chlorophyll-a levels from a fluorometer divided by measured turbidity from an optical backscatter sensor, and show how the ratio is in good agreement with relative particulate organic matter content based on loss on ignition of filtered water samples.

2.1 The bay

At the bay locations, the upper range of particle sizes are generally found when organic/mineral ratios are high (Figure 1) and when current speeds are at their lowest. However, at the time of highest primary productivity, when chlorophyll-a contents are particularly high, median particle sizes are in some cases the smallest. We show how this is due to a larger presence of very fine-grained particles ($<$ 10 microns), indicating that the LISST captures the

phytoplankton spring blooms and the important concentration of diatom/phytoplankton cells. Thus, high OMC ratios with small median particle sizes are a sign of a phytoplankton bloom, whereas high ratios with large median particle sizes are a sign of a relatively big abundance of bio-rich flocs (see Figure 2). These bio-rich flocs do not settle as fast and are more resistant, therefore not breaking up as easily. Less break-up also explains why particles in the bay generally are larger than those in the estuary, and why the biggest abundance of the largest median diameters coincide with the smallest abundances of still relative large particles. In other words, the large bio-rich flocs are a result of a consecutive flocculation of already existing macroflocs, whereas in the estuary mouth the biggest flocs are the result of a consecutive flocculation of already existing strong microflocs. This highlights the importance of the intensity and timing of blooms on suspended matter dynamics.

2.2 The estuary

At the estuary mouth, particle characteristics and dynamics differ from further out in the bay. We note, that the results to a certain degree are limited due to issues with the LISST in the density-stratified waters. However, the longer-term dynamics and differences are still measurable. There are clear indications that stronger flocculation (and floc break-up) occurs in the estuary, compared to the bay. While organic matter dynamics seem to be the most important processes for particle transport and settling in the bay over the course of a year, the dominating processes change more over time at the estuary mouth. For instance, the shifting of the estuarine turbidity maximum (ETM) due to changes in river discharge strongly influences turbidity which at times is the most important factor. Generally, turbulence, turbidity and organic matter content all play different important roles at different times of the year, clearly impacting the flocculation and thus transport and settling potential. Still, biggest occurrences of the largest particles are found in spring, and the presence of organic matter is important. But lower SPM concentrations at this time means that the relative importance for the yearly transport and settling might be less important. At this point, we have not yet assessed the relative importance of the different seasons in terms of SPM transport potential, however this work will be carried out over the next months. In this way, the aim is to set up a conceptual model showing the relative importance of the different seasons, and the processes herein, on the transport and deposition of fine-grained particulate matter within and through the land-sea continuum.

2.3 Figures

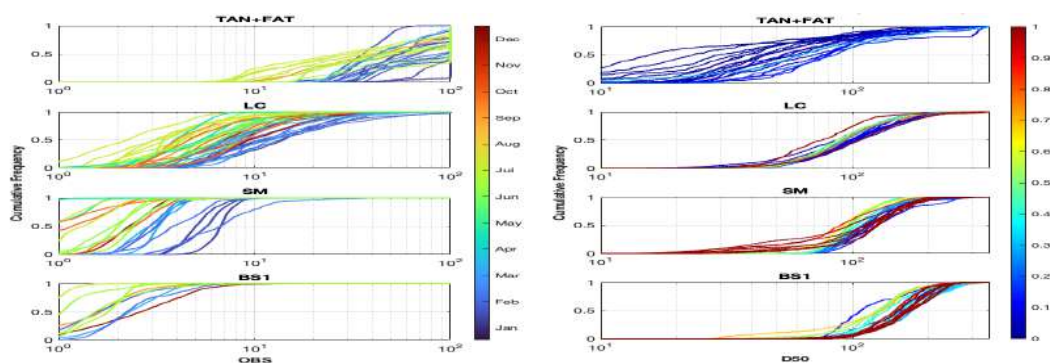


Figure 1. (left) Cumulative probability distributions of optical backscatter, OBS, coloured according to the time of year and location, and (right) cumulative probability distributions of median particle size, D50, coloured according to the OMC ratio and separated by location. FAT+TAN are located in the river, LC is at the estuary mouth and SM and BS1 are located at different places in the bay.

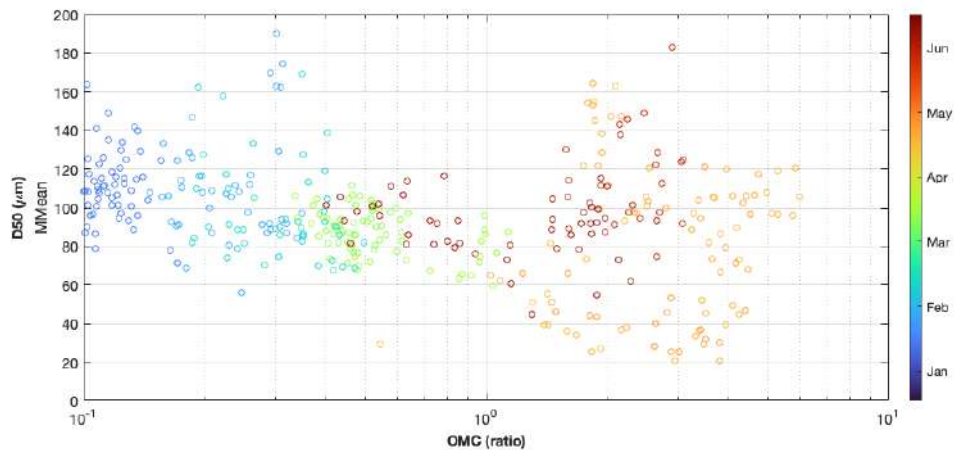


Figure 2. OMC plotted against D50 at the SM station in the bay, coloured according to the month of the year.

3. Conclusions

Based on data from eight years of field campaigns in the macrotidal Seine estuary, we focus on the seasonal dynamics of land-sea exchange of fine-grained suspended matter. We show clear increases in median particle sizes, probably due to enhanced floc strengths, and decreases in turbidity moving from land to sea. We highlight the relative importance of the spring bloom in the estuary and bay, but also of changes in ETM dynamics and hydrodynamics, particularly in the estuary. While the LISST clearly has limitations in the density-stratified waters and the sometimes highly changing turbidity regimes, the instrument is still able to show how different particle sizes, origins and characteristics change over the seasons. A conceptual model will be set up, presenting the relative importance of different seasons and different processes on the land-sea SPM dynamics.

Acknowledgments

Many thanks to all the crew of all the field campaigns and in particular to our two technicians Matthias Jacquet and David Le Berre without whom there would have been no data to analyze.



17th International Conference on
Cohesive Sediment Transport Processes
September 18-22, 2023
Inha University, Incheon, Republic of Korea



Morphodynamic time lag effects in response to reduced fluvial sediment supply from the watershed to the estuary

Chunyan Zhu¹, Leicheng Guo¹, Bas van Maren^{1,2,3}, Zheng Bing Wang^{1,2,3}, and Qing He*¹

¹ State Key Lab of Estuarine and Coastal Research, East China Normal University, China, qinghe@sklec.ecnu.edu.cn

² Faculty of Civil Engineering and Geosciences, Delft University of Technology, The Netherlands

³ Deltares, Delft, The Netherlands

1. Introduction

Worldwide estuaries have suffered a great loss in riverine sediment loads, which poses a threat to delta sinking, wetland loss, navigational and ecological problems (Besset et al., 2019; Syvitski et al., 2022). Therefore, understanding estuarine responses is essential to protect the deltas and estuaries.

The Yangtze Estuary is a large-scale estuary with pronounced sediment loss, mainly due to lots of upstream dam construction. The sediment load has decreased by 97% at Yichang station immediately downstream of the Three Gorges Dam (TGD). Farther downstream, the sediment load has decreased by 75% at tidal limit-Datong station, implying along-river sediment recovery. Within the estuary, the channels and shoals also exhibit complex responses, particularly in the mouth zone (Zhu et al., 2019). Although lots of studies have investigated the estuarine response to reduced sediment supply, the morphodynamic response time lag effects still need more research in terms of different morphological units.

2. Results

2.1 River-Lake response

We collected a series of field data to quantify the sediment gain and loss in the river-lake system in the middle-lower Yangtze River. We find that Dongting Lake and Poyang Lake shifted from net sedimentation to erosion in 2006 and 2000, and back to a sedimentation regime again after 2017 and 2018, respectively. Natural morphodynamic adaptation and sand mining play an important role in the regime changes in the Dongting Lake whereas sand mining dominates the abrupt changes in the Poyang Lake. The Dongting and Poyang Lake contributed maximum by 38% (2015) and 17% (2006) (respectively) to the sediment recovery in the erosion regime, whereas the riverbed erosion dominates the main sediment source. These changes in the relative contribution of sediment sources also indicates a response time of ~20 years in the lakes towards a new equilibrium state. It is noteworthy that the lakes' buffer effects may be overestimated as the supplied sediment from the lakes is rather small compared to the significant dam trapping in the upstream basin and sediment source from downstream degradation.

2.2 Estuarine response

Based on bathymetric maps from 1958 to 2019, we systematically evaluated the morphological development of the channels and shoals. We find that both the South Branch and North Channel

shifted from sedimentation to erosion in 1978, whereas the South Channel, North Passage, South Passage, and delta front shifted from sedimentation to erosion in around 2007. The channels are mainly deepened and narrowed during 1958-2019. The four tidal flats in the mouth zone, eastern Chongming shoal, eastern Hengsha flat, Jiudian shoal, and Nanhui flat shifted from sedimentation to erosion in 2016, 2010, 2007 and 2010, respectively (Figure 1). Moreover, the erosion occurred initially in the deep water and subsequently in the shallow parts. Overall, the channels and shoals within the estuary show a time lag that gradually moves downstream, upward, and northward. The Chongming shoal started eroding in recent years (2016) which suggests a time lag of approximately 30 years considering the sediment decline since the mid-1980s.

3. Conclusions

This study systematically interprets the morphological response to reduced sediment supply from the watershed to the estuary. In the river basin, we evaluated a 20-year buffering effects of river-lake systems, whereas within the estuary, we quantified the spatial changes in the morphological evolution of channels and shoals with a maximum 30-year time lag response. The results imply that management and restoration of rivers and estuaries should take into account the time lag effects on decadal time scales.

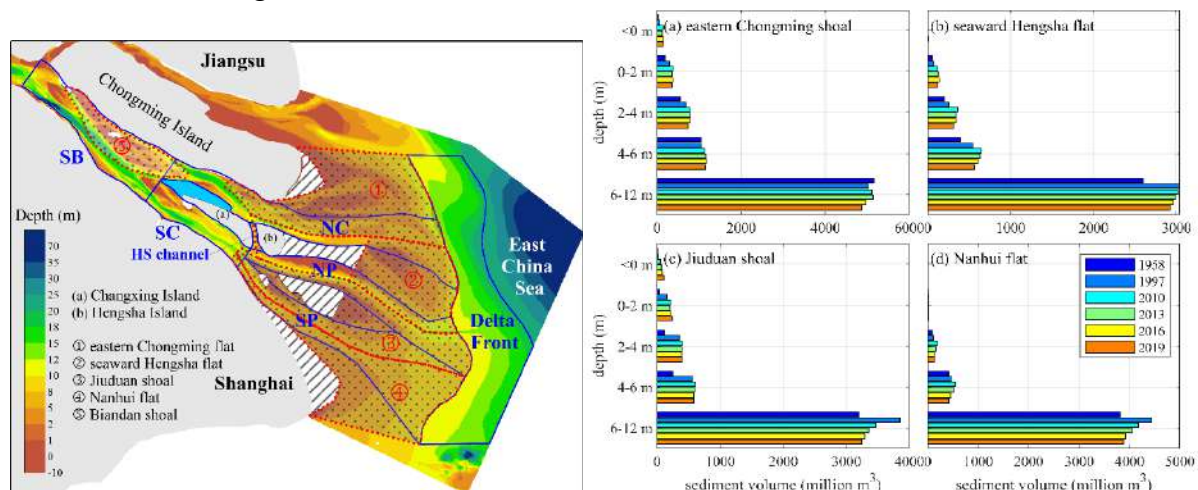


Figure 1. (left) Channels (blue lines) and shoals (red dotted lines) in the Yangtze Estuary. SB: South Branch, SC: South Channel, NC: North Channel, NP: North Passage, SP: South Passage, HS: Hengsha; (right) Sediment volume changes in the (a) eastern Chongming shoal, (b) seaward Hengsha flat, (c) Jiudian shoal, and (d) Nanhui flat during 1958-2019.

Acknowledgments

The authors would like to express appreciation for the support of the sponsors: Natural Science Foundation of China (NSFC) (Nos. 42206169, 51739005, U2040216), China Postdoctoral Science Foundation (No. 2022M721165) and Shanghai Pujiang Program (No. 22PJD020).

References

- Syvitski, J., Ángel, J. R., Saito, Y., Overeem, I., Vörösmarty, C. J., Wang, H., & Olago, D. (2022). Earth's sediment cycle during the Anthropocene. *Nature Reviews Earth & Environment*, 3(3), 179-196.
- Besset, M., Anthony, E. J., & Bouchette, F. (2019). Multi-decadal variations in delta shorelines and their relationship to river sediment supply: An assessment and review. *Earth-science reviews*, 193, 199-219.

Zhu, C., Guo, L., van Maren, D.S., Tian, B., Wang, X., He, Q. and Wang, Z.B., 2019. Decadal morphological evolution of the mouth zone of the Yangtze Estuary in response to human interventions. *Earth Surface Processes and Landforms*, 44(12), pp.2319-2332.



17th International Conference on
Cohesive Sediment Transport Processes
September 18-22, 2023
Inha University, Incheon, Republic of Korea



Sediment exchange in mudflat-creek-marsh continuum: The evolution mechanism of intertidal environments

Weiming Xie, Leicheng Guo, Yi Meng, Xianye Wang, Zhong Peng, Qing He

State Key Laboratory of Estuarine and Coastal Research, East China Normal University,
Shanghai, China, wmxie@sklec.ecnu.edu.cn

Abstract

Intertidal flats and saltmarshes are valuable ecosystems, and support land-ocean exchange of sediments and nutrients. They are also highly adaptive to tidal dynamics and vulnerable to sea-level rise and human activities. Tidal flats are usually composed of seaward bare mudflats, landward saltmarshes and tidal creeks. Sediment exchange among mudflats, tidal creeks, and salt marshes is important for tidal flat evolution, but the dynamics are insufficiently understood (Friedrichs, 2011; Mariotti and Fagherazzi, 2011; Xie et al., 2018). In this contribution, we conducted field measurements of hydrodynamics and sediment dynamics using bed-mounted tripod systems at three sites located at mudflat, tidal creek, and marsh edge in the Eastern Chongming tidal wetland of Yangtze Estuary (Fig 1). Field surveys persisted for a full spring-neap tidal cycle (>14 days) in both dry and wet seasons. Data showed that high suspended sediment concentration (SSC) associated with fluvial sediment source leads to net sediment deposition over the mudflats under asymmetric flow conditions, i.e., landward decreasing flow velocities. These newly deposited sediments are easy to be reworked and transported landward into tidal creeks. Overbank flow under high tides induces lateral sediment distribution from tidal creeks to surrounding saltmarshes, eventually maintaining saltmarsh accretion. Furthermore, we observe that larger sediment availability, saltmarsh growth and higher mean sea level conditions in the wet seasons (spring and summer) play vital roles in stimulating sediment deposition and trapping, resulting in overwhelming deposition of throughout mudflats and saltmarshes, whereas erosion may take place in the dry season owing to smaller sediment source and lower tidal height (Fig 2). Overall, this study highlights profound effect of sediment exchange in the mudflat-creek-marsh continuum in supporting tidal flat accretion and evolution, thus having implications for managing and conserving tidal flats under global climate changes.

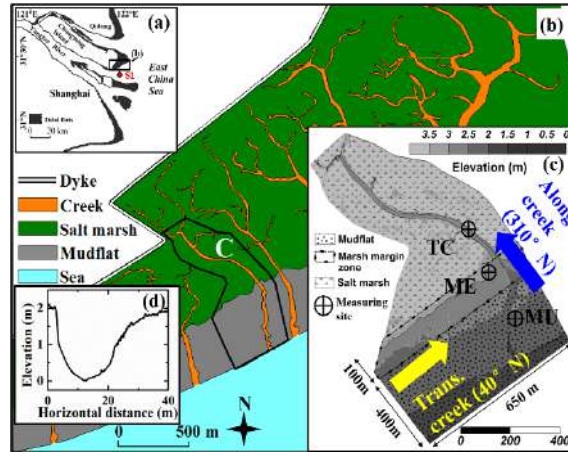


Figure 1. (a) Locations of Yangtze Estuary, (b) Eastern Chongming tidal flat, (c) study sites, and (d) tidal creek section.

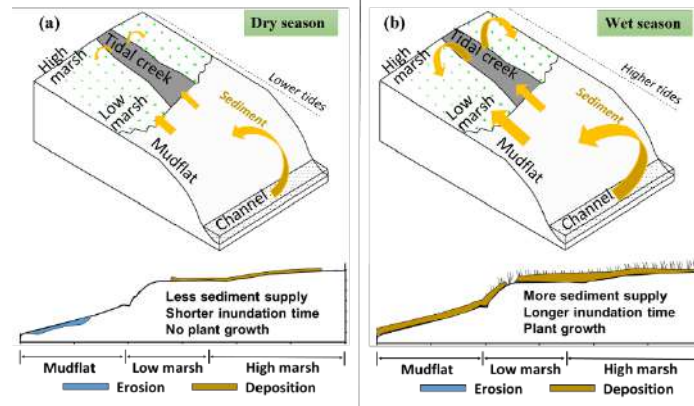


Figure 2. Conceptual models for sedimentary processes in a mudflat-creek-marsh system in (a) dry and (b) wet season.

References

- Friedrichs, C.T., 2011. Tidal Flat Morphodynamics: A Synthesis. *Treatise on Estuarine and Coastal Science*, edited by E. Wolanski and D. McLusky: 137-170.
- Mariotti, G., Fagherazzi, S., 2011. Asymmetric fluxes of water and sediments in a mesotidal mudflat channel. *Continental Shelf Research*, 31(1): 23-36.
- Xie, W., He, Q., Wang, X., Guo, L., Zhang, K., 2018. Role of mudflat-creek sediment exchanges in intertidal sedimentary processes. *Journal of Hydrology*, 567: 351-360.

Session: Fluid Mud
10:40 – 12:40
Wednesday, September 20, 2023



17th International Conference on
Cohesive Sediment Transport Processes
September 18-22, 2023
Inha University, Incheon, Republic of Korea



Shear Instabilities and Stratified Turbulence in an Estuarine Fluid Mud

Junbiao Tu,¹ Daidu Fan,¹ Alexis Kaminski,² William Smyth³

¹ State Key Laboratory of Marine Geology, Tongji University, Shanghai, China

² Department of Mechanical Engineering, University of California, Berkeley, California, USA

³ College of Oceanic and Atmospheric Sciences, Oregon State University, Corvallis, Oregon, USA

Introduction

The motion of estuarine fluid mud is modulated by the tidal cycle, with resuspension and entrainment during phases of high flow velocity and settling in slower flow. Current shear, induced by bottom friction, provides an energy source for shear instability, while stratification induced by concentrated sediment tends to stabilize the flow. Although this process has been reproduced in the laboratory, field observations of shear instability in FM remain scarce.

In this study we analyzed observations from the Changjiang estuary, examining hydrographic variations, echosounder images showing internal wave and instabilities, and velocity and density profiles synchronous with typical billow trains. The turbulence associated with the shear instabilities was also measured.

Observations

A dual frequency echosounder (24/200 kHz) was deployed to collect acoustic images. Vertical profiles of salinity, temperature, and turbidity were measured every 0.5 hr using a CTD with a built-in OBS 3+, sampling at 2 Hz. The OBS outputs were converted to suspended sediment concentration (SSC) using the filtered water samples. Concurrent near-bed observations were carried out using a bottom mounted tripod. An Aquadopp HR profiler was set to collect data with a sampling rate of 4 Hz.

Results

Around peak flood and peak ebb, large velocity differences were observed between 1 mab and 3.4 mab (Figure 2d). Remarkable SSC differences occur between 1 and 2 mab, indicating the presence of a sharp density interface at this region (Figure 2c). The interaction between current shear and mud-induced stratification might lead to the formation of internal waves and/or billows (Tu *et al.*, 2020). Such is the case in this study as well-defined billows were identified from the echosounder image at several periods covering both flood and ebb phase. These periods were also characterized by Ri below or fluctuating around 0.25 at regions below 1 mab, a condition favoring shear instability. Periods with extremely high Ri values suggest reduced flow or turbulence dampening by high SSC.

Discussions and Summary

The six examples shown in Figure 1 exhibit shear instabilities, (breaking) internal waves, and small-scale structure. The Ri values (estimated over 256s) in the regions with billows are well

below 0.25 at Hour 11.5 and Hour 25. For other periods, instability coincides with near-bed Ri below or fluctuating around 0.25. These periods were also characterized by large (interpolated) current shear in the mid-upper water column. The approximated Ri values are found to fluctuate around or slightly above 0.25 during these periods.

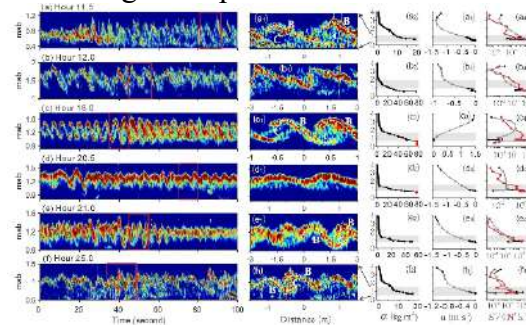


Fig. 1. Echosounder images and profiles of water-sediment mixture density, streamwise velocity, shear, and buoyancy frequency.

These results, including details of the interactions between velocity shear and mud-induced stratification, periodic occurrence and collapse of shear instability, and turbulent mixing, have broadened our understanding of fluid dynamics in a hyperturbid boundary layer. Our results may also suggest realistic modeling scenarios and allow for better predictions of sediment entrainment, mixing, and dispersion of FM in hyperturbid estuarine channels.

References

- Geyer, W. R., A. C. Lavery, M. E. Scully, and J. H. Trowbridge (2010), Mixing by shear instability at high Reynolds number, *Geophys. Res. Lett.*, 37(22).
- Tu, J., Fan, D., Lian, Q., Liu, Z., Liu, W., Kaminski, A., & Smyth, W. (2020). Acoustic Observations of Kelvin-Helmholtz Billows on an Estuarine Lutocline. *Journal of Geophysical Research: Oceans*, 125(4), e2019JC015383. <https://doi.org/10.1029/2019jc015383>
- Tu, J., Fan, D., Sun, F., Kaminski, A., & Smyth, W. (2022). Shear Instabilities and Stratified Turbulence in an Estuarine Fluid Mud. *Journal of Physical Oceanography*, 52(9), 2257-2271. <https://doi.org/10.1175/jpo-d-21-0230.1>



17th International Conference on
Cohesive Sediment Transport Processes
September 18-22, 2023
Inha University, Incheon, Republic of Korea



Practical prediction method of nautical depths in muddy areas

Kenji Sakata¹, Yasuyuki Nakagawa², Mitsuyasu Iwanami³

¹ National Institute for Land and Infrastructure Management, Yokosuka, Japan, sakata-k92y2@mlit.go.jp

² Port and Airport Research Institute, Yokosuka, Japan

³ Tokyo Institute of Technology, Tokyo, Japan

1. Introduction

In muddy areas with fluid mud layer, nautical depth concept could be applied to define the bed level considering the degree of obstacles or muddy sediments to ship navigation. We can measure bulk densities of fluid mud corresponding to nautical depths using any in-situ density sensor, though these measurements cause extra cost in practice.

The aim of this study is to establish a practical method to evaluate nautical depths efficiently with field data. We examined characteristics of observed acoustic data by echo sounding in response to the distribution of bulk densities of fluid mud through the field measurement in the Tokyo bay. In the present study, we propose the evaluation method of the vertical level with the bulk density of 1,200 kg/m³ using the field data of a multi beam sonar and lead line measurement.

2. Study site and field measurements

2.1 Study site

The study site is in the Tokyo East Passage, which is the navigation channel for the port of Tokyo, in Tokyo Bay (Fig. 1). Type of the bottom sediments are classified mainly as mud with fluid mud layer in the study site.

2.2 Field measurements and data analysis

Field survey was carried out in November in 2018 to obtain water depth and sediment data. For bathymetric surveys we used a multi beam sonar with a frequency of 400 kHz and single beam sonar with the lower frequency of 10 kHz. The data was compared with the lead line measurements. An in-situ densimeter, Mud Bug of Hydramotion Ltd., was also applied to get information on the vertical profiles of mud density near the seabed.

2.3 Measurement results

The vertical distances between the seabed surface observed by the multi beam sonar and the 1,200 kg/m³ density horizon are maximum 0.79 m (St.B) and minimum 0.16 m (St.D) (Fig. 2). We examined the relationships between the detected vertical profiles of the bulk densities and the detected bottom level by the echo sounding. The vertical distances between the bed levels detected by the multi beam sonar and the lead measurement ($h_{Lead} - h_{400}$) tend to decrease as the referenced sediment density increases. The referenced sediment density is defined as the bulk density at the depth of 0.1 m from the bed surface as $\Delta\rho_{0.1}$ (Fig. 3). This trend shows similar relationship between cone penetration and water content, where the penetration may decrease with the less water content in the falling cone test.

2.4 Practical prediction method for nautical depths

Considering the vertical distance between the seabed surface observed by multi beam sonar and the lead measurement, we obtained a relational equation (Eq. (1)) for seabed surface observed by multi beam sonar (h_{400}), the $1,200 \text{ kg/m}^3$ density horizon ($h_{\rho(1,200)}$), and lead measurement (h_{Lead}) (Fig. 4). The detail will be precisely demonstrated in the presentation.

3. Conclusions

Based on the field measurements, the vertical distances between the bottom levels detected by multi beam sonar and the lead measurements was quantitatively evaluated under the variable sediment density conditions. We proposed an efficient prediction method for nautical depths to detect of the layer of the bulk density the $1,200 \text{ kg/m}^3$ using multi beam sonar with a frequency of 400 kHz and lead measurements.

References

- Sakata, K., Iyama, S., Nakagawa, Y. and Iwanami, M. (2019). A study on relevance between seabed surface observed by acoustic sounding and wet density of fluid mud: Journal of Japan Society of Civil Engineers, Ser. B2, Coastal Engineering, vol.75, No. 2, pp. I_493-I_498. (In Japanese).
- Sakata, K., Nakagawa, Y., Iwanami, M. and Iyama, S. (2022). Efficient prediction method of nautical depths in muddy areas with fluid mud layer: Journal of Japan Society of Civil Engineers, Ser. B3, Ocean Engineering, vol.78, No. 1, pp. 1-10. (In Japanese).

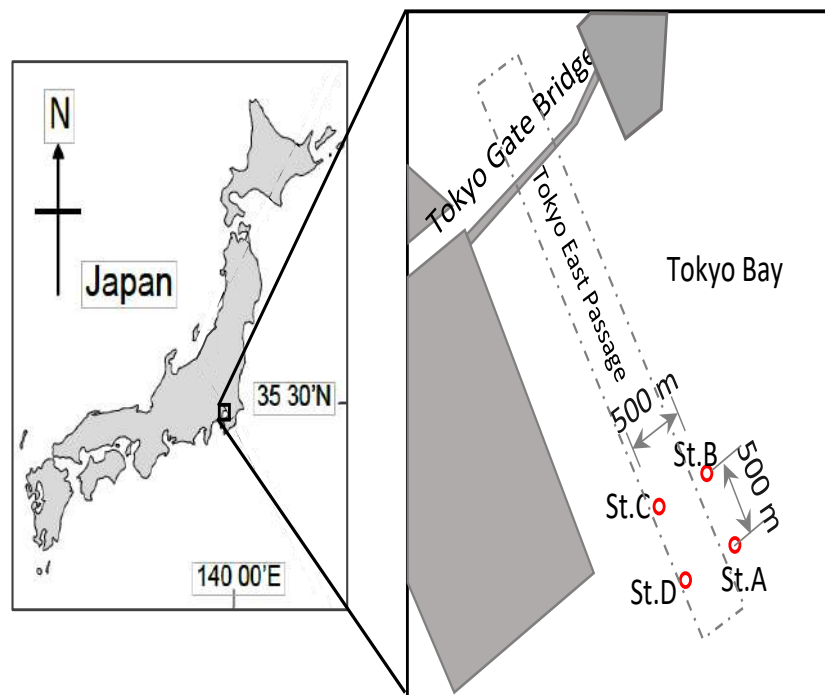


Figure 1. The location of study site

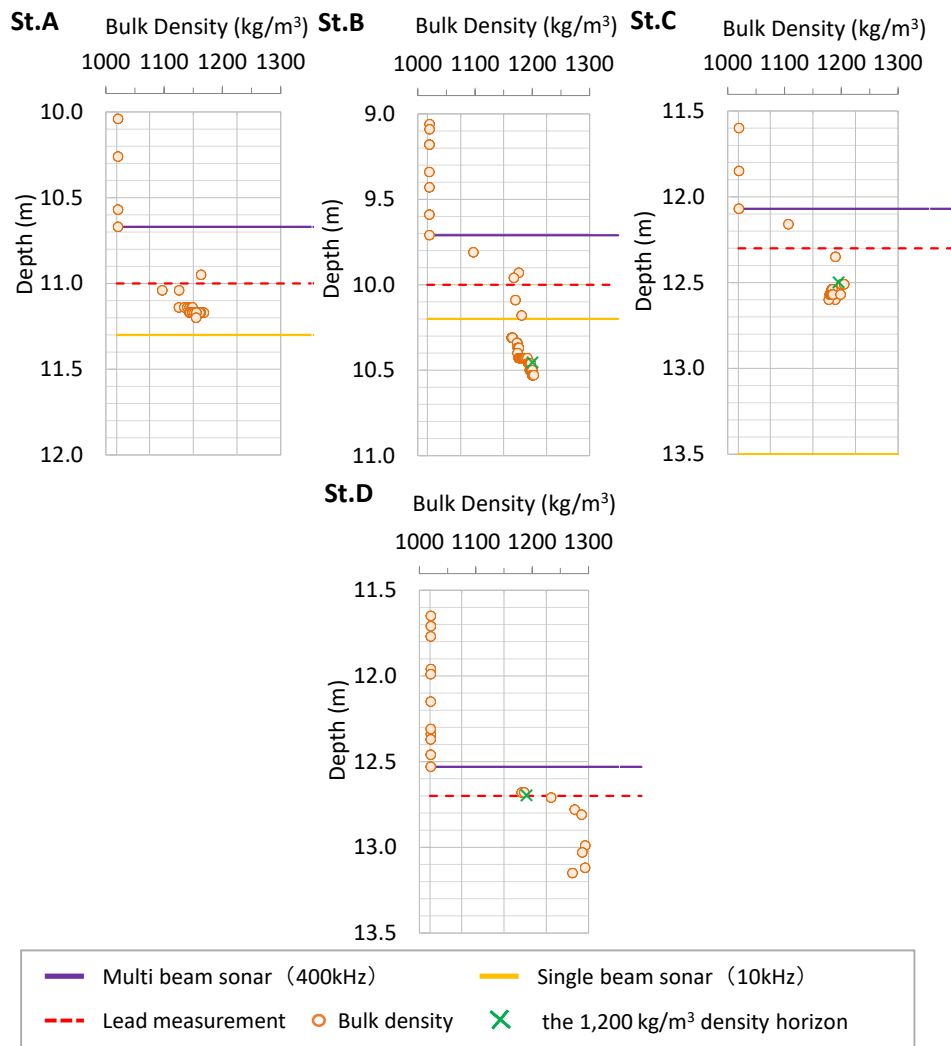


Figure 2. Observed seabed surfaces and vertical profiles of bulk density (Modified from Sakata et al. 2019)



17th International Conference on
Cohesive Sediment Transport Processes
September 18-22, 2023
Inha University, Incheon, Republic of Korea



Nautical depth and rheological analysis of fine sediments in Iranian Ports

F. Shokri Alikhanlou¹, M. Soltanpour¹, F. Samsami², and S.A. Haghshenas³

¹ Civil Engineering Department, K. N. Toosi University of Technology, Tehran 1996715433, Iran

soltanpour@kntu.ac.ir

² Civil Engineering Department, West Tehran Branch, Islamic Azad University, Tehran 1461988631, Iran

³ Institute of Geophysics, University of Tehran, Tehran 1435944411, Iran

1. Introduction

Cohesive sediments can be found in coasts around the world, including the south coast of the Caspian Sea and the north and northwest coasts of the Persian Gulf. The sediments that occur in these areas may form a soft to very soft mud layer, so called fluid mud, covering the surface of the bed. The fluid mud layer is composed of clays, silts, and other fine sediments combined with organic matter [1]. Although various rheological parameters of mud, such as yield stress, viscoelasticity, shear thinning, thixotropy, and structural recovery, are usually related to the density (e.g., [2]), the existence of organic matter can also change the rheological behavior. The accumulation of the fine sediments at harbors and access channels reduces the nautical depth and highly affects navigability.

The present research aims to analyze the rheological characteristics of natural mud samples at three major Iranian Ports, i.e., Imam Khomeini and Bushehr in the Persian Gulf and Anzali in the Caspian Sea. The laboratory analyses include sediment grain-size distribution, wet/dry densities, carbonate and organic matter content, and rheological tests under different water content ratios.

2. Study Area and Field Measurements

Bushehr Port is located at the north coast of the Persian Gulf, and Imam Khomeini Port is located at the end of the Musa Bay in the north-western part of the Persian Gulf. Anzali Port is at the sea boundary of the Anzali wetland, located at the south of the Caspian Sea. Figure 1 shows the locations of these three commercial ports of Iran, which are highly affected by fine sediments.

Disturbed and undisturbed sediment samples were taken from the ports. The particle-size distribution (i.e., sand, silt, and clay-size fractions), carbonate and organic matter content, and wet and particle densities of the collected samples in three different conditions (i.e., not-stirred, stirred, and diluted with demineralized-water) are listed in Table 1. The results of stirred tests can be interpreted for the application of the concept of active nautical depth, i.e., deliberate manipulating of the medium in order to both create and maintain its navigability [3].



Figure 1. Locations of Anzali Port in the Caspian Sea and Imam Khomeini and Bushehr ports in the Persian Gulf.

3. Results and Discussion

The rheological tests on the collected samples were conducted in three different conditions, i.e., not-stirred, stirred, and diluted with demineralized-water. Table 1 presents the physical and rheological properties of mud samples at Imam Khomeini and Bushehr ports, in which the Bingham model is used to determine the yield stress based on the rotational rheometry [1]. It is observed that the dry weight organic and carbonate contents of both samples lie close to 5% and 34%, respectively. These are mostly within the ranges familiar to the muds collected from European ports such as Emden (Germany), Harlingen, Delfzijl and Ijmuiden (Netherland), and Watchet (UK) [4].

Figure 2 shows two viscosity curves for the collected sediment samples from Imam Khomeini and Bushehr ports. In spite of the differences in the collected muds, it seems possible to implement the active nautical depth in these ports. However, a lower shear stress is needed at Imam Khomeini Port to reach the viscosity level of 2 Pa.s, which makes this port a more receivable candidate.

Table 1. The physical and rheological properties of mud samples.

Sample ID	Clay (%)	Silt (%)	Sand (%)	Carbonate Content (%)	Organic Content (%)	Wet Density (kg/m ³)	Particle Density (kg/m ³)	Yield Stress (Pa)
Imam Khomeini Port-Not stirred	25	73.2	1.8	33.5	5.8	1586	2630	516
Imam Khomeini Port-stirred						1586	2630	307
Imam Khomeini Port-diluted						1270	2630	3
Bushehr Port-Not stirred	38.5	41.3	2.8	34.4	4.5	1626	2654	207
Bushehr Port-stirred						1626	2654	107
Bushehr Port-diluted						1260	2654	6

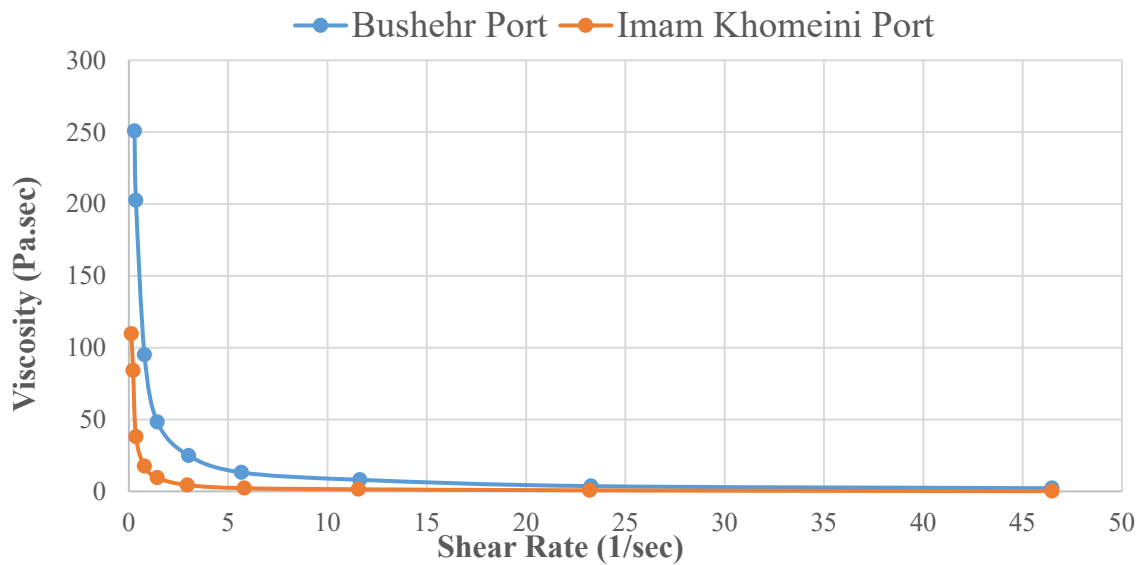


Figure 2. Viscosity curves for collected mud samples from Imam Khomeini and Bushehr Ports.

References

- Samsami F., Haghshenas S.A. , Soltanpour M. (2022). Physical and Rheological Characteristics of Sediment for Nautical Depth Assessment in Bushehr Port and Its Access Channel. *Water*, 14, 4116. <https://doi.org/10.3390/w14244116>
- Shakeel, A., Kirichek, A. & Chassagne, C. (2020). Rheological analysis of mud from Port of Hamburg, Germany. *J Soils Sediments*, 2553–2562. <https://doi.org/10.1007/s11368-019-02448-7>
- Wurpts R. (2005). 15 Years Experience with Fluid Mud: Definition of The Nautical Bottom with Rheological Parameters. *Terra Aqua*, 99 p.
- Kirby R., Soltanpour M., Greiser N., Van Der Made K. J., Barth R. (2016). Twin related aspects of engineered mud suspensions for the NW European and Iranian port industry, 12th International Conference on Coasts, Ports & Marine Structures, ICOPMAS, Tehran, Iran, CD, pp. 459-460.



17th International Conference on
Cohesive Sediment Transport Processes
September 18-22, 2023
Inha University, Incheon, Republic of Korea



Using Ultrasound Shear Waves to Measure Mud Rheological Properties A 10-year revisit

Maa, Jerome Peng-Yea¹, XioTeng Shan², Yuyang Shao², and Jae-II Kwon³

¹ Virginia Institute of Marine Science, maa@vims.edu

² Hohai University, Nanjing, China

³ Korea Institute of Ocean Science and Technology, Busan, Korea

1. Introduction

When sufficient sediments accumulate on the bed and become a fluid mud, it is obviously a non-Newton fluid. With time as it further consolidated, it becomes a solid material and may have some shear strength. During this process, it affects the dynamic of water flows above (e.g., wave attenuation, turbulence and shear stress distribution, etc.), and thus, also affects the sediment transport processes. A practical approach for measuring mud rheological properties (bulk density, ρ , shear modulus, G , and dynamic viscosity, μ), however, is not available yet. Although a preliminary acoustic approach was first introduced 10 years ago, not too much progress has been made because of the requirement on cross-disciplines and complex electrical devices. Because of the important, continuous effort devoted on this subject is worth. This study is to further explore the reasons for data scatter, as well as new and possible improvements.

2. Basic principal

Although with a critically low efficiency, acoustic shear waves can transmit through liquid. This limits the use of transmitting shear waves. On the other hand, however, it suggests the use of reflected shear waves. For pressure waves, transmitting into fluid is much easier. Both features should be used. Assuming the mud is a viscoelastic material and with the fact that both shear waves and pressure waves can be generated by using one single shear wave transducer, only one source shear wave transducer and one receiving pressure wave transducer are needed to measure ρ , G , and μ .

The wave reflection coefficient is defined as $R=(Z_1-Z_2)/(Z_1+Z_2)$, where Z is the acoustic wave impedance, and $Z=\rho C$, where C is wave speed. For practical application, the energy loss during wave transmission and interface coupling also needs to be know. Also it is impossible to carry out measurements right at the transducer-mud interface. Measurements have to be conducted at a near-by location. For this reason, a calibration process was developed to address this problem and it appears working fine. The remaining concerns are that data are quite scatter, and there still some unexplainable phenomenon.

3. Conclusions

With more experiments carried out later, the temperature information is included. It is evident that the change of temperature during an experiment will cause the change of viscosity and sound velocity. This may explain why the data are scattered. Although the change of sound speed in mud (due to temperature difference) has not been measured directly, it can expect that

the change of sound speed may also affect the selection of the correct data segment for doing Fast Fourier Transform (FFT). The FFT results may also change the interpretation on mud rheological property. With improvements on data measuring and processing, the development of this new acoustic approach becomes more robust.



17th International Conference on
Cohesive Sediment Transport Processes
September 18-22, 2023
Inha University, Incheon, Republic of Korea



Numerical Simulations of Towing Test Cases for Validation of a Three-Phase Flow Solver for Nautical Bottom Problems

D.S.Ch.Praveen¹, Marco S. Sotelo², Djahida Boucetta², Wim Van Hoydonck³, Marc Vantorre²,
Guillaume Delefortrie² and Erik A. Toorman¹

¹Hydraulics & Geotechnics Section, Department of Civil Engineering, KU Leuven, Leuven, Belgium, praveen.suryachalapraveen@kuleuven.be

²Maritime Technology Division, Ghent University, Belgium

³Flanders Hydraulics, Belgium

1. Introduction

The study of nautical bottom problems in muddy environments has become increasingly important due to the growing size of ships and traffic to ports in such areas. To ensure ship safety and optimize dredging operations, understanding the behaviour of ships sailing through mud is crucial. Previous research, such as Lovato (2023), simplified the problem by considering the fluid mud as a homogeneous fluid, either in a two-layer system with air and fluid mud or a three-layer system with air, water, and fluid mud as immiscible fluids. However, in reality, the nautical bottom problem is a three-phase problem with air, water and fluid mud; the air and water immiscible whereas the water and the fluid mud mixes leading to density gradients over the depth. Additionally, the fluid comprising water and mud needs to be treated as a mixture of water and cohesive sediments to account for the two-way and four-way coupling between the phases. In this context, a new three-phase CFD model has been developed by Praveen and Toorman (2023a). This model incorporates essential closures necessary to accurately capture the complex behaviour of fluid mud mixtures. The closures include mud rheology, obtained with a new rheometric configuration by Praveen and Toorman (2023b), a new dual-structure thixotropic model developed by Toorman & Praveen (2023), consolidation with pore-pressure data, and a wall-distance free low-Reynolds turbulence model.

The model needs validation comprising all the complex physical processes involved in the nautical bottom problem. To address this need for validation, towing experiments with a cylinder and a hydrofoil have been executed at Flanders Hydraulics in 2021 and 2022. These validation test cases, presented by Sotelo et al. (2023) for the cylinder and Sotelo et al. (2022) for the hydrofoil, provide comprehensive data for evaluating the performance of the three-phase model.

2. Methodology

2.1 Validation of the three-phase cohesive sediment transport model

The validation of the newly developed three-phase cohesive sediment transport model involves the towing of a cylinder and a hydrofoil in a long flume. In a first phase, the cylinder is towed through homogeneous fluid mud at various speeds ranging from 0.01m/s to 0.5m/s. In the second phase, the towing is performed in a three-phase system, including air, water, and fluid mud, at different speeds and under keel clearances (UKC). A similar methodology is employed

for the hydrofoil, but with a different range of speeds and UKC values. Detailed information regarding the experimental setup and results can be found in Sotelo et al. (2023) for the cylinder and Sotelo et al. (2022) for the hydrofoil.

For the validation test cases of the first phase, the fluid mud can be approximated as a homogeneous medium. An existing standard solver for two immiscible layers (often also called “two-phase”, but at macroscopic scale), such as the `interFoam` solver, available in the open-source CFD tool `OpenFOAM®`, can be used for comparison. However, the solver requires a non-Newtonian mud rheology closure to update the mixture viscosity and a thixotropy model to account for time dependent effects. Sotelo et al. (2023) applied this method to compare the drag values of the experiments with those obtained from the cylinder case with homogeneous fluid, considering only the equilibrium flow curve as rheological closure. The comparison suggests that the drag forces are comparable in magnitude, but as the speed increases, the underestimation in drag becomes more pronounced. The difference in drag at higher speed regimes could be due to uncertainty in towing experiments, rheology data, the assumption of the homogeneousness of fluid mud and the exclusion of pore-pressure variations and consolidation. Therefore, the newly developed three-phase solver will be used to investigate if there will be any improvements compared to simplified version of two-phase solver with homogeneous fluid mud.

In the second phase of the validation test cases, towing experiments are conducted in a three-phase scenario. To the best of the author’s knowledge, there is no existing model that can accurately capture the three-phase system. The closest solver available is the `multiphaseInterFoam`, which allows for modelling a system with three distinct immiscible layers. Sotelo et al. (2023) adopted this approach and found that the interface deformation of air-water and water-fluid mud are comparable to the experimental results, but the drag forces are again underestimated. This highlights the need to investigate the newly developed three-phase solver to improve the prediction of drag force and the flow field with the experimental data.

2.2 Sensitivity analysis

In addition to the validation process, the present study includes a sensitivity analysis of the thixotropy model and consolidation model with pore-pressure data in predicting the forces. The sensitivity analysis aims to understand the impact of the thixotropy model and the consolidation model on the force predictions, considering the influence of pore-pressure data. By varying the parameters of these models and comparing the results to experimental data, the study will identify the sensitivity of the models to different input parameters and provide insights into their relative contribution, their accuracy and reliability in capturing the complex behaviour of fluid mud mixtures.

A preliminary study conducted using the standard `interFoam` solver for homogeneous fluid mud indicates that the inclusion of the thixotropy model leads, as expected, to an increase in the drag force as the speed increases. However, a more detailed investigation is required using the final formulation of the dual-structure thixotropy model developed by Toorman and Praveen (2023).

3. Conclusions

By utilizing the three-phase solver, this study aims to enhance the modelling of the complex behaviour of fluid mud mixtures and accurately predict drag forces and flow characteristics in both the two-layer and three-layer scenarios. The results obtained from the simulations will be compared to the experimental data from the towing experiments, enabling a comprehensive validation of the model's performance and its potential for improved predictions in nautical bottom problems.

Through the sensitivity analysis, the study aims to determine the influence of the various closure parameters on the force predictions. This analysis will contribute to a deeper understanding of the physical processes involved in nautical bottom problems and provide valuable insights for improving the accuracy of the model or to simplify the cohesive sediment transport model.

Acknowledgments

This work is funded by the Research Foundation - Flanders through the FWO project G0D5319N,.

References

- Lovato, S. (2023). Sailing through fluid mud: Verification and validation of a CFD model for simulations of ships sailing in muddy areas (Doctoral dissertation, Delft University of Technology).
- Praveen, D.S.Ch., Toorman, E.A. (2023a). Development of a three-phase CFD model for cohesive sediment transport. Book Of Abstracts, INTERCOH 2023.
- Praveen, D.S.Ch., Toorman, E.A. (2023b). The determination of the true equilibrium flow curve for fluid mud in a wide gap Couette rheometer. (submitted to) *J. Non-Newtonian Fluid Mechanics*.
- Sotelo, M.S., Boucetta, D., Delefortrie, G., Vantorre, M., Toorman, E., Praveen D., and Van Hoydonck, W. (2022). Experimental study of a surface-piercing hydrofoil towed through muddy environments. In: Proc. 18èmes Journées de l' Hydrodynamique.
- Sotelo, M.S., Boucetta, D., Van Hoydonck, W., Praveen, D., Vantorre, M., Toorman, E., and Delefortrie, G. (2023). Hydrodynamic forces acting on a cylinder towed in muddy environments, (submitted and revised version under review) *Journal of Waterway, Port, Coastal, and Ocean Engineering*.
- Toorman, E.A., Praveen, D.S.Ch. (2023). A dual-structure thixotropy model for cohesive slurries, validated with wide-gap Couette viscometry for fluid mud. (in preparation for) *J. Rheology*.

Session: Sediment Transport III
09:00 – 10:40
Thursday, September 21, 2023



17th International Conference on
Cohesive Sediment Transport Processes
September 18-22, 2023
Inha University, Incheon, Republic of Korea



Dredging impacts on concentration and settling velocity of suspended particles in Gyeonggi Bay, Korea

H.J. Ha¹, S.M. Choi¹ and H.K. Ha^{1,*}

¹ Department of Ocean Sciences, Inha University, Incheon, Republic of Korea,
*hahk@inha.ac.kr

1. Introduction

Dredging in coastal areas is conducted to maintain navigation channel and harbor, and to mine sand and gravel. This influences the suspended sediment concentration (SSC) in the near and far field due to the dispersal and transport of overflow from dredge. The excessive increase of SSC caused by dredging plume is a key concern for marine ecosystem services. For instance, high SSC can reduce the primary production and the feeding efficiency of bivalves. The numerical models are commonly applied as part of the management of dredging operations to limit the impact on surrounding environments. They represent the sediment processes (suspension, advection, diffusion, settling, and deposition) through both empirical- and theoretical-based approaches. Variations in hydrodynamics and limited knowledge of the properties of suspended particles during dredging activities lead to large uncertainties in model estimates of sediment transport and fate. On-site observations on active dredging plume are required to better understand the dredging impacts on sediment concentration and settling velocity. In this study, therefore, a ship-borne survey with a package of acoustic and optic instruments was carried out at a sand mining site in Gyeonggi Bay, Korea.

2. Materials and methods

2.1 Study area

Gyeonggi Bay is a semi-enclosed shallow (< 50 m) area located in west coast of Korea. This region is characterized by a mega-tidal range (> 9 m) and a large sediment supply from the Han River. Transgressive sand ridges were widely distributed in the southern part of Gyeonggi Bay, and were preferential targets for sand mining (Lee et al., 2020). Over past three decades, the marine sands have been annually extracted with $2.5 \times 10^7 \text{ m}^3$ (Kim and Lim, 2009).

2.2 Field experiment

A ship-borne survey had been conducted along the major axis of surface plume on June 20, 2022. A 600-kHz acoustic Doppler current profiler (ADCP, RDI WorkHorse Sentinel) was mounted to the hull of the survey vessel. This provided the real-time profiles of acoustic backscatter to assist with location of the dredging plume and positioning of the LISST-Holo within plume. The acoustic backscatter was calibrated to SSC using the simplified sonar equation by Deines (1999). In-situ sizes and settling velocities (W_s in mm s^{-1}) of suspended particle were calculated through a digital holographic camera (LISST-Holo, Sequoia Scientific Inc.). A series of holographic images were analyzed using a software of Holo-Batch[®] for the reconstruction of particle images (Graham et al., 2012). The GRADISTAT program of Blott and Pye (2001) was used to calculate textural parameters of suspended sediments on the basis of the Folk and Ward (1957) percentile statistics.

3. Results

The distribution of SSC indicated that the dredging plume was heterogeneous in both space and time. Demarcation between the plume and surrounding seawater was seen clearly. The dredging plume reached down to 45 m with SSC ranging from 35–115 mg l⁻¹, and the water column out of the dredging plume was generally defined as low SSC in range of 6–10 mg l⁻¹. The SSC of the plume was highest near the dredger at a distance of 100 m and generally decreased with distance from dredger (Figure 1a). The suspended sediment was dispersed from the dredged area within 1 hour (Figure 1b). The overflow sample predominantly composed of mud showed unimodal distribution with a mode of 42.9 μm . The suspended sediments in the dredging plume were multimodal distribution with modes ranging from 104.8 to 256.1 μm . The median particle diameter (d_{50}) and W_s of suspended sediments in the dredging plume ranged from 129.4 to 147.0 μm and 0.48 to 0.59 mm s⁻¹, respectively. The d_{50} and W_s decreased to 37.8 μm and 0.07 mm s⁻¹ at 1 hour after the dredging ended. The results suggest that the dredging can lead to the rapid formation of large flocs with higher d_{50} and W_s .

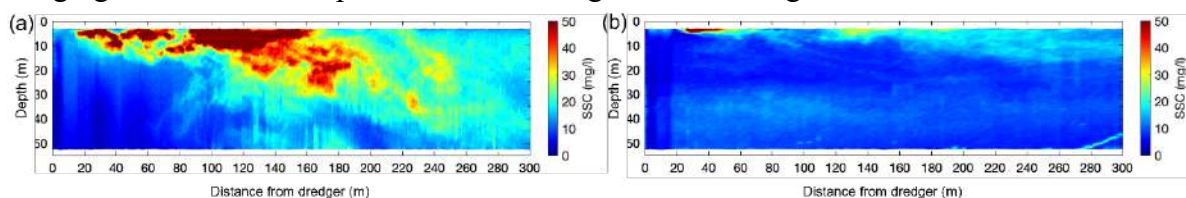


Figure 4. Distribution of suspended sediment concentration (SSC): (a) during and (b) after 1 hour the dredging.

4. Conclusions

Based on ship-borne survey, the SSC variation in dredging plume was studied and the data showed increments of particle sizes and W_s due to large flocs. During the dredging, SSC was about 10 times higher than the natural background concentration. After the dredging, SSC within the dredging area reduced to background levels in 1 hour. The W_s (d_{50}) of dredging plume ranged from 0.48 to 0.59 mm s⁻¹ (129.4 to 147.0 μm), which decreased to 0.07 mm s⁻¹ (37.8 μm) immediately after the dredging.

Acknowledgments

This research was supported by “Development of Advanced Science and Technology for Marine Environmental Impact Assessment” of Korea Institute of Marine Science & Technology Promotion (KIMST) funded by the Ministry of Oceans and Fisheries (KIMST-20210427).

References

- Blott, S.J., and Pye, K. (2001). GRADISTAT: a grain size distribution and statistics package for the analysis of unconsolidated sediments. *Earth Surf. Proc. Landforms* 26, 1237–1248. doi: 10.1002/esp.261
- Deines, K.L. (1999). Backscatter estimation using broadband acoustic doppler current profilers. In: *Proceedings of the IEEE sixth Working conference on Current Measurement*. San Diego, CA, pp. 249–253. doi: 10.1109/CCM.1999. 755249
- Folk, R.L., and Ward, W.C. (1957). Brazos river bar: a study in the significance of grain size parameters. *J. Sediment Res.* 27, 3–26. doi: 10.1306/74D70646-2B21-11D7-8648000102C1865D

Graham, G.W., Davies, E.J., Nimmo-Smith, W.A.M., Bowers, D.G., and Braithwaite, K.M. (2012). Interpreting LISST-100X measurements of particles with complex shape using digital in-line holography. *J. Geophys. Res.* 117, C05034. doi: 10.1029/2011JC007613

Kim, C.S., and Lim, H.S. (2009). Sediment dispersal and deposition due to sand mining in the coastal waters of Korea. *Cont. Shelf Res.* 29, 194–204. doi: 10.1016/j.csr.2008.01.017

Lee, H.J., Jeon, C.K., and Lim, H.S. (2020). Transgressive shelf sands around the Korean Peninsula: A brief review. *Ocean Sci. J.* 55, 465–475. doi: 10.1007/s12601-020-0035-5



17th International Conference on
Cohesive Sediment Transport Processes
September 18-22, 2023
Inha University, Incheon, Republic of Korea



How subsidence and cyclone driven sediment flux within Galveston Bay has caused elevated siltation within the Bayport Channel and Flare

Timothy M. Dellapenna^{1,2}, Nathalie Jung², Richard Schenk¹, Scott Sudduth¹, Peng Lin¹, and Jens Figlus³

¹Dept. of Marine and Coastal Environmental Sciences, Texas A&M University-Galveston Campus, Galveston, TX 77554

²Dept. of Oceanography, Texas A&M University, Galveston, TX 77554

³ Dept. of Ocean Engineering, Texas A&M University, Galveston, TX 77554

Abstract: The Bayport Flare/Channel, located with the San Jacinto Bay (SJB) portion of the northwestern corner of Galveston Bay, has experienced a 25% (6.25% annually) increase in siltation since Hurricane Harvey (2017). The floods associated with Harvey deposited 131.34×10^6 tons of sediment in Galveston and in the four years after Harvey, 27% of the deposit has eroded, increasing the bay's suspended sediment load by 9% annually. SJB has subsidence rates of 1.5-2.2 cm y^{-1} and has an average sedimentation rate of 2.6 cm y^{-1} , indicating that SJB is a net sediment sink. Sediment Trend Analysis (STA) was performed on a grid of sediment grab samples from the SJB area and reveals sediment transport convergence from all sides of SJB, with the dominant pathways from the most exposed portions of Galveston Bay to the south and southeast. This study concludes that the elevated siltation within the Bayport Flare/Channel is likely sourced from the eroded sediments sourced from the Hurricane Harvey flood deposit within Galveston.



17th International Conference on
Cohesive Sediment Transport Processes
September 18-22, 2023
Inha University, Incheon, Republic of Korea



Impacts of consecutive typhoons on the resuspension of sediment and microphytobenthos in the macro-tidal flat

S.W. Jeong¹, H.J. Ha¹ and H.K. Ha^{1,*}

¹ Department of Ocean Sciences, Inha University, Incheon, Republic of Korea,
*hahk@inha.ac.kr

1. Introduction

Tidal flat, a transitional area located between land and sea, plays an important role in both nature and human communities. Through the sediment accumulation on the tidal flat, pollutants and nutrients from the land are filtered and stored. Massive physical energies caused by extreme meteorologic events (e.g., typhoon) can be absorbed by tidal flat, protecting coastal area. Recently, the tidal flat is considered as a potential carbon-storable area through the sediment deposition and biological processes. In particular, microphytobenthos (MPB) controls nutrients within the sediment bed which is directly related to carbon trapping (Barranguet et al., 1997). MPB emits extracellular polymeric substances (EPS) to enhance its mobility, which can decrease sediment erodibility (Kim et al., 2021). Although there are more than 400 species of MPB in tidal flat of Korea, the knowledge gap still exists on the coupling/decoupling mechanisms between sediment and MPB.

The changes in sediment erodibility and primary productivity were well evaluated under various physical and biological conditions (e.g., seasons, tides, exposal of sediments, spatial comparison, and existence of vegetation) (Wiberg et al., 2013). However, there are few studies on extreme meteorological events such as typhoon. The hydrodynamic and benthic environment change drastically during typhoons, affecting MPB biomass and primary production. In Korea, several typhoons would episodically visit during the summer and fall, they are an extreme physical source to trigger MPB resuspension (Montani et al., 2003). Thus, main objectives are (1) to quantify the effect of typhoon on resuspension of the benthic sediment and MPB, and (2) to reveal coupling/decoupling mechanisms between benthic sediment and MPB.

2. Materials and methods

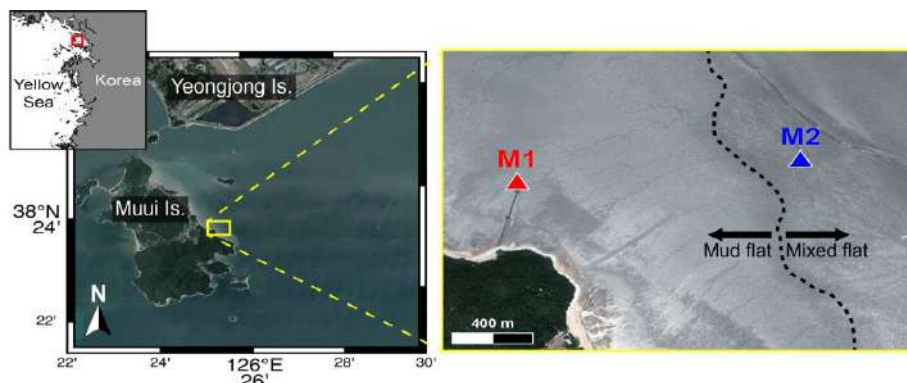


Figure 1. Aerial photograph of study area. Red and blue triangles indicate mooring sites (M1 and M2).

In the tidal flat of Muui Island, two mooring systems were deployed at mud flat (M1) and mixed flat (M2) from August 28 to September 24, 2020 (Figure 1). At both sites, the electromagnetic current meter (JFE Advantech, Infinity-EM) and chlorophyll-a/turbidity sensor (JFE Advantech, Compact-CLW) were installed. At M1, profiles of current velocity and suspended sediment concentration (0–0.7 m above bed (mab)) were measured using a 600-kHz acoustic Doppler current profiler (RDI, Workhorse Sentinel). At M2, water depth was measured by pressure sensor (RBR, solo D). Using Gust Erosion Microcosm System (GEMS), erosion experiments were conducted with sediment cores collected near the mooring sites.

3. Results and discussion

During the mooring period, two consecutive typhoons (#9 Maysak and #10 Haishen) with a maximum wind speed of 45 m s^{-1} passed through Korean Peninsula (category 5; intensity: “very strong”). The typhoon Maysak passed from 15:00 to 21:00, September 2, and the typhoon Haishen passed from 21:00, September 6 to 03:00, September 7. During post-typhoon period, suspended sediment concentration (SSC) drastically increased with bed shear stress of 0.05 Pa (Figures 2a and d). During pre-typhoon and typhoon-passage periods, both sites maintained low SSC (Figure 2d). It indicates that the extreme condition accompanying high bed shear stress flushed out suspended sediments. Under the calm conditions, SSC at both sites showed tidal variations, but surface sediment at M2 could be more easily resuspended than that at M1. Chlorophyll-*a* (Chl-*a*) showed similar range at both sites, and evident increment occurred after the two consecutive typhoons (Figure 2e). The Chl-*a* was maintained in a range of $0\text{--}14 \text{ mg l}^{-1}$ before 260 d (days in 2020). After 260 d, the Chl-*a* abruptly increased (up to 34 mg l^{-1}) and gradually decreased until the end of spring tide. Considering the Chl-*a* is a proxy for an amount of MPB, the increase of Chl-*a* during 260–268 d might be related with disturbance of benthic environments due to typhoons.

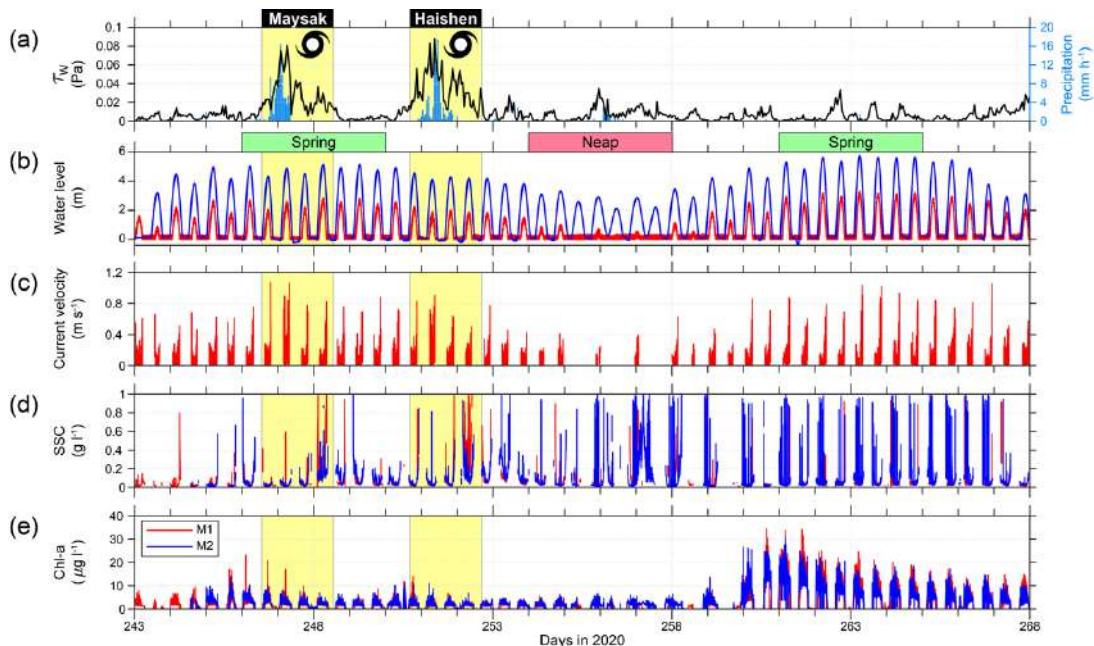


Figure 2. Time series of the mooring data: (a) wind induced bed shear stress (t_w , black line) and precipitation (light blue bar), (b) water level, (c) current velocity at 0.7 mab, (d) SSC at 0.3 mab, and (e) Chl-*a* at 0.3 mab. M1 and M2 are represented as red and blue lines, respectively. Yellow shaded zones denote the passage of two consecutive typhoons.

4. Conclusions

(1) Under two consecutive typhoons, typhoon-induced t_w and SSC showed objective aspect. SSC drastically increased up to 823 mg l^{-1} during post-typhoon period (247–249 d) with decrease of t_w . However, SSC was maintained low regardless of t_w increment from pre-typhoon to typhoon passage period (245–247 d).

(2) Chl-*a* (as a proxy of amount of the MPB) showed relatively low fluctuation (up to 14 mg l^{-1}) under typhoon during 1st spring tide indicating decouple between benthic sediments and MPB. After 260 d, Chl-*a* drastically increased (up to 34 mg l^{-1}) due to disturbance of benthic sediment environment.

References

- Barranguet, C., Herman, P.M.J., Sinke, J.J. (1997). Microphytobenthos and community composition studied by pigment biomarkers: importance and fate in the carbon cycle of tidal flat. *Journal of Sea Research*, 38(1–2): 59–70. doi: [10.1016/S1385-1101\(97\)00032-4](https://doi.org/10.1016/S1385-1101(97)00032-4)
- Kim, B., Lee, J., Noh, J., Bae, H., Lee, C., Ha, H.J., Hwang, K., Kim, D.U., Kwon, B.O., Ha, H.K., Pierre, G., Delattre, C., Michaud, P., Khim, J.S. (2021). Spatiotemporal variation of extracellular polymeric substances (EPS) associated with the microphytobenthos of tidal flats in the Yellow Sea. *Marine Pollution Bulletin*, 171: 112780. doi: [10.1016/j.marpolbul.2021.112780](https://doi.org/10.1016/j.marpolbul.2021.112780)
- Montani, S., Magni, P., Abe, N. (2003). Seasonal and interannual patterns of intertidal microphytobenthos in combination with laboratory and areal production estimates. *Marine Ecology Progress Series*, 249: 79–91. doi: [10.3354/meps249079](https://doi.org/10.3354/meps249079)
- Wiberg, P.L., Law, B.A., Wheatcroft, R.A., Milligan, T.G., Hill, P.S. (2013). Seasonal variations in erodibility and sediment transport potential in a mesotidal channel-flat complex, Willapa Bay, WA. *Continental Shelf Research*, 60: S185–S197. doi: [10.1016/j.csr.2012.07.021](https://doi.org/10.1016/j.csr.2012.07.021)



Different effects of cold front and tropical cyclone on short-term sediment dynamics in the delta front of the Changjiang Estuary

Xuefeng Wu ¹, Chunyan Zhu ¹, Jianliang Lin ^{1,2}, Jian Shen ³ and Qing He ¹

¹ State Key Laboratory of Estuarine and Coastal Research, East China Normal University, P.R. China, 52193904011@stu.ecnu.edu.cn

² School of Marine Engineering and Technology, Sun Yat-sen University, 519000, Zhuhai, China

³ Virginia Institute of Marine Science, College of William and Mary, USA

1. Introduction

Estuarine and coastal zones are highly sensitive to increasing flooding and erosion risks under storm conditions (Malvarez et al., 2021). This is more severe due to the increasing frequency and intensity of storms (Klotzbach et al., 2022).

Therefore, it is essential to understand storm-induced sediment dynamics in estuaries and deltas. Many studies have focused on the changes in hydrodynamics, sediment transport and morphological changes caused by cold front and tropical cyclones (Tesi et al., 2013). However, the difference of cold front and tropical cyclone in driving sediment transport and morphological changes is less understood and therefore needs more research.

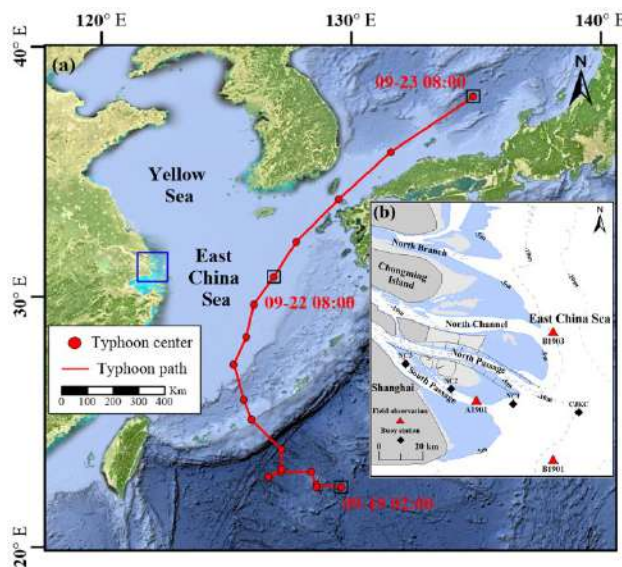


Fig 1. (a) The track of Typhoon Tapah in 2019; (b) study area of the Changjiang Estuary

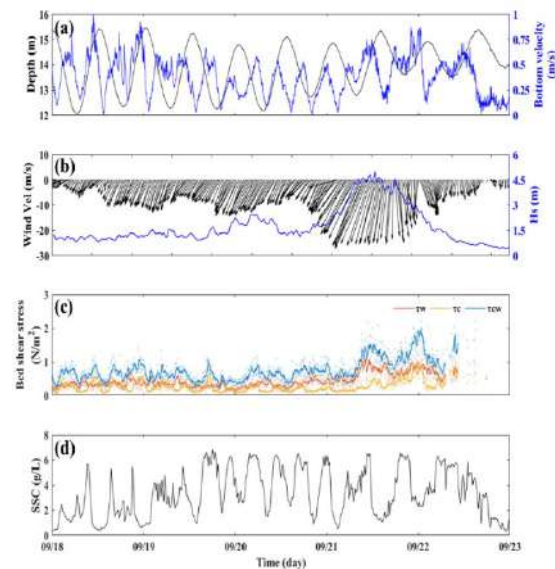


Fig 2. Time series of (a) depth (m) and near-bottom velocity (m/s), (b) the significant wave height (m) and average wind speed (m/s), (c) tide-induced, wave-induced and combined shear stress (Pa), (d) near-bottom SSC (g/L)

2. Study area

We conducted a field campaign covering both cold front and tropical cyclone during 14-25 September, 2019 in the Changjiang Estuary (Fig 1). From September 18 to 19, the northeasterly wind increased from force 6 to 8 due to the cold front. Meanwhile, the tropical cyclone Tapah was formed at 23:00 on September 18 in the Western Pacific and gradually moved northwest to the East China Sea, which intensifies into a severe typhoon at 8:00 on September 21. Three bottom tripod systems were deployed at A1901, B1903, B1901. The water depths at A1901, B1901 and B1903 are 9.2 m, 13.6 m and 14.7 m, respectively.

3. Results

We selected five tides representing calm condition, cold front period, intermediate period, typhoon formation period, typhoon period, and after typhoon period (Fig 2). The wind speed reached 13.1 m/s during the cold front, which is about 267% higher than that during calm conditions. During typhoon, the average wind speed was 19.5 m/s. The significant wave height and period were 1.9-5.0 m and 6.2-10.1 s, respectively during the typhoon.

The results suggest the average near-bottom suspended sediment concentration (SSC) in the delta front remained stable at 2.28 g/L during the cold front whereas it increased significantly and reached 4.54 g/L after the cold front. The increase in SSC is mainly caused by enhanced advective transport in the seaward direction and local sediment resuspension due to the cold front. During typhoon, the strong waves enhance local sediment resuspension and drive sediment southward, leads to SSC in 3.55 g/L higher than calm condition but slightly lower than cold front effect. The residual current and sediment transport during the cold front and typhoon are south-eastward and south-westward, suggesting that cold front strengthens longitudinal sediment transport in the channel whereas typhoon strengthens alongshore sediment transport towards Hangzhou Bay.

4. Conclusions

This study investigated storm-induced changes in sediment transport and the underling mechanisms caused by cold front as well as typhoon. The results indicate that the cold front causes seaward sediment transport to the delta front whereas the typhoon drives alongshore sediment transport the Hangzhou Bay. Consequently, the delta front shifted from sediment sink to source from cold front condition to typhoon period, resulting in the shift from erosion and deposition in a short-term. The findings gain insights into the changes in sediment dynamics under extreme weather conditions which is important for the management of estuaries and deltas.

Acknowledgments

This work is financially supported by the National Natural Science Foundation of China (Nos. U2040216 ,42206169) and Shanghai Committee of Science and Technology (21230750600, 20DZ1204701) are also acknowledged.

References

- Klotzbach, P.J., Wood, K.M., Schreck, C.J., Bowen, S.G., Patricola, C.M., Bell, M.M., 2022. Trends in global tropical cyclone activity: 1990–2021. *Geophysical Research Letters*, 49(6).
- Malvarez, G., Ferreira, O., Navas, F., Cooper, J.A.G., Gracia-Prieto, F.J., Talavera, L., 2021. Storm impacts on a coupled human-natural coastal system: Resilience of developed coasts. *Science of The Total Environment*, 768: 144987.
- Tesi, T., Misericocchi, S., Acri, F., Langone, L., Boldrin, A., Hatten, J.A., Albertazzi, S., 2013. Flood-driven transport of sediment, particulate organic matter, and nutrients from the Po River watershed to the Mediterranean Sea. *Journal of Hydrology*, 498: 144-152.

Session: Flocs II
10:40 – 12:40
Thursday, September 21, 2023



17th International Conference on
Cohesive Sediment Transport Processes
September 18-22, 2023
Inha University, Incheon, Republic of Korea



Estuarine light attenuation, scattering, and absorption as a function of suspended floc properties and other water column constituents

K.A. Fall¹, C.T. Friedrichs*², and G.M. Massey²

¹ Dept. of Civil & Environmental Engineering, University of Delaware, Newark, DE, USA

² Virginia Institute of Marine Science, Gloucester Point, VA, USA.

*Carl.Friedrichs@vims.edu, presenting & corresponding author

1. Extended Abstract

Observations of suspended floc characteristics, commonly measured water quality parameters (total suspended solids (TSS), total organic solids (OSS), chlorophyll *a* concentration (chl *a*), and absorbance of color dissolved organic matter (CDOM)) and optical properties (diffuse light attenuation (K_d) and scattering (b)) were collected on 20 cruises from 2014-2016 at various stations along the York River estuary along the York River estuary in Virginia, USA, and associated absorption (a) was estimated via model inversion. The response of scattering (b) and absorption (a) to estuarine flocs of varying size, density, and composition then was investigated. Systematic trends in the relative contributions of organic and inorganic solids (OSS and ISS) along with other water quality parameters to b , a , and K_d as an overall function of TSS concentration revealed that the contribution of non-algal suspended solids on K_d may be smaller than originally assumed, especially compared to other water quality constituents.

Simple expressions describing scattering and absorption due to non-algal particulate matter (b_{NAP} and a_{NAP}) averaged over photosynthetically active radiation (PAR) (400-700 nm) were determined, with efforts taken to account for the influence of algal particles (i.e., phytoplankton). Expressions from the literature relating phytoplankton scattering, absorption, biomass, and composition to observed chl *a* concentrations for estuarine conditions similar to the York were used to isolate contributions from phytoplankton cells and estimate OSS and ISS due to non-algal particulate matter (OSS_{NAP} , ISS_{NAP}).

Total scattering was measured directly in situ using a Laser In-Situ Scattering and Transmissometry instrument (LISST-100X). Scattering due to phytoplankton (b_{alg}) was subtracted, and a relationship in the form of a power law was derived to represent scattering by non-algal particulate matter (b_{NAP}). Combined with a literature-based relationship for b_{alg} , a simple model for total b was developed (Figure 1, left). A similar approach was taken for absorption. First, total absorption was estimated by applying the non-linear model of Kirk (1994) to in situ observations of K_d and b . Then, observation-based estimates of absorption by CDOM (a_{CDOM}), combined with literature-based relations for absorption due to water (a_w) and chl *a*, were subtracted from a to estimate absorption due to non-algal particulate matter (a_{NAP}). A simple best-fit empirical relationship, consistent with the assumption that organic solids absorb two-times that compared to inorganic solids was found. The expression for a_{NAP} was combined with the other constituents to produce a model for total a (Figure 1, right).

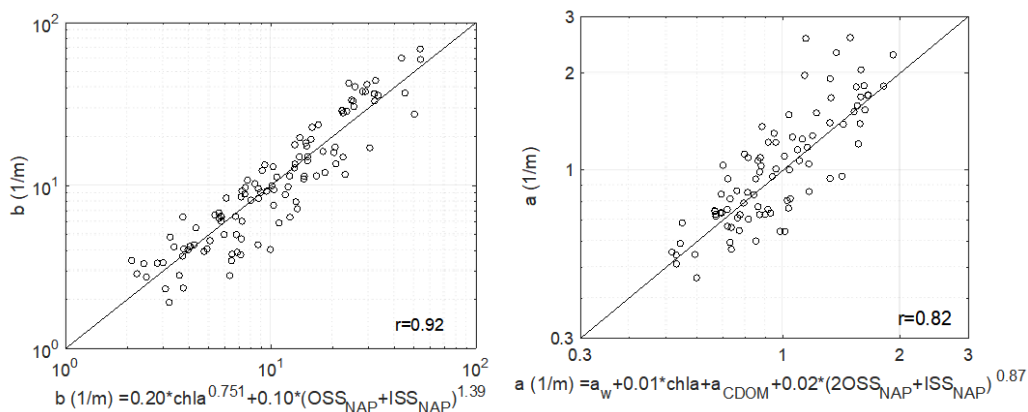


Figure 1. Comparison between observed and modeled scattering (left) and absorption (right) of light.

Total scattering was measured directly in situ using a Laser In-Situ Scattering and Transmissometry instrument (LISST-100X). Scattering due to phytoplankton (b_{alg}) was subtracted, and a relationship in the form of a power law was derived to represent scattering by non-algal particulate matter (b_{NAP}). Combined with a literature-based relationship for b_{alg} , a simple model for total b was developed (Figure 1, top). A similar approach was taken for absorption. First, total absorption was estimated by applying the non-linear model of Kirk (1994) to in situ observations of K_d and b . Then, observation-based estimates of absorption by CDOM (a_{CDOM}), combined with literature-based relations for absorption due to water (a_w) and chl a , were subtracted from a to estimate absorption due to non-algal particulate matter (a_{NAP}). A simple best-fit empirical relationship, consistent with the assumption that organic solids absorb two-times that compared to inorganic solids was found. The expression for a_{NAP} was combined with the other constituents to produce a model for total a (Figure 1, bottom).

A model based on Kirk (1994) for K_d over PAR was constructed from the above models for b and a as a function of commonly observed water quality parameters, such that measurements of a and b were no longer required as inputs. The model-data fit for K_d exhibited $r = 0.90$ with a mean error of 16.6%.

This study provided new insights into the influence on scattering and absorption of estuarine flocs that are composed of a mixture of inorganic solids, organic solids, and water. In the York, scattering and absorption were related to the nature of the flocs in the system. Floc scattering, which is proportional to floc cross-sectional area, increased faster than TSS because of strongly decreasing floc density. In contrast, absorption by flocs increased more slowly than TSS. This may be due to both that (i) organic solids, which form a greater fraction of floc content at low TSS, absorb about twice as much light per mass than inorganic solids, and (ii) the increased water relative to solids content of larger flocs may make them less opaque. The effects of varying organic and water content with changing TSS within the flocs notably alter the otherwise expected trends for optical response based on floc fractal theory.

2. References

Kirk, J.T.O., 1994. Light and Photosynthesis in Aquatic Ecosystems. Cambridge University Press.



17th International Conference on
Cohesive Sediment Transport Processes
September 18-22, 2023
Inha University, Incheon, Republic of Korea



Quantitative Evaluation of the Influence of Floc Composites on Floc Dynamics

O.D. Ajama¹, G. Lee¹, J. Chang¹, and W. Li^{1,2}, and J.I. Kwon³

¹ Department of Oceanography, Inha University, Incheon 22212, Korea

² CAS Key Laboratory of Marine Geology and Environment, Institute of Oceanology,
Chinese Academy of Sciences, Qingdao 266071, China

³ Coastal Disaster and Safety Research Department, Korea Institute of Ocean Science and
Technology, Busan 49111, Korea

1. Introduction

Flocs composites comprise organic and mineral particles, and interstitial fluids (water) which acts as a binding agent for constituent particles. The presence of interstitial fluids impact on the settling velocity, density, as well as the fractal dimension of flocs in suspension. However, there is limited knowledge on the quantity of interstitial fluids locked within flocs and how its relationship with floc composite particles influence floc dynamics in estuarine environments. Also, the recent introduction of particle imaging camera systems (PICS), combined with Laser In-Situ Scattering Transmissometry (LISST) and pump water sampling has made it possible to estimate the fractal dimension of flocs and their corresponding primary particle density (ρ_p) and size (d_p) (Fall et al., 2021). However, deployment for long observation periods may prove very challenging and unattainable. This necessitates the need to explore other methods of estimating the fractal properties of flocs.

In this study, we first apply PICS, LISST and pump water sampling data to decompose individual flocs into their composites, quantify their characteristics and examine how their interaction influence floc dynamics. Secondly, we derive new equations to compute the fractal dimension of sediments in suspension using LISST data and compare observed results with PICS-derived fractal dimension.

2. Model and Methodology

Quantifying Floc Composites

The density ρ_f of a floc in suspension of mass m_f and volume v_f acquired from PICS is given by the relation:

$$\rho_f = \frac{m_f}{v_f} \quad (1)$$

while its apparent density is given by the relation

$$\rho_a = \Delta\rho \cdot \frac{1}{\left(1 - \frac{\rho_w}{\rho_p}\right)} = \frac{m_p}{v_f} \quad (2)$$

where $\Delta\rho$ is the floc's excess density, ρ_w is the density of water, ρ_p is the primary particle density, and m_p is the mass of the primary particles that constitute the floc.

Eq. 2 can be re-arranged as

$$m_p = \rho_a \cdot v_f \quad (3)$$

Kranenburg (1994) showed that for a floc with uniform diameter d_f and primary particles diameter d_p , the excess density is given as:

$$\Delta\rho = \rho_f - \rho_w = (\rho_p - \rho_w) \left(\frac{d_p}{d_f}\right)^{3-F} \quad (4)$$

Eq. 4 can be expressed as:

$$\log(\Delta\rho) = \log[(\rho_p - \rho_w)d_p^{3-F}] - (3 - F)\log(d_f) \quad (5)$$

Plotting of eq. 5 gives the excess density distribution curve of the flocculation process over the range of floc/particles' diameter, and its slope can be used to determine the fractal dimension (F) of suspended particles. Fall et al., (2021) showed that eq. 5, combined with pump water sampling data can be used to compute ρ_p for floc suspensions that conform to the fractal model. However, for natural flocs that don't conform to the fractal model, the loss on ignition (LOI) method gives a good approximation of ρ_p . With ρ_p known, eqs. 1 and 2 can be used to obtain:

$$\frac{\rho_f}{\rho_a} = \frac{m_f}{m_p} \quad (6a); \quad \frac{\rho_f}{\rho_a} - 1 = \frac{m_w}{m_p} \quad (6b); \quad 1 - \frac{\rho_a}{\rho_f} = \frac{m_w}{m_f} \quad (6c); \quad \text{and}$$

$$1 \div \frac{\rho_f}{\rho_a} = \frac{m_p}{m_f} \quad (6d)$$

Multiplying eqs. 6b and 3 gives

$$m_w = \frac{m_w}{m_p} \cdot m_p \quad (7)$$

Eqs. 3 and 7 can be used to compute the mass of particle and interstitial fluid within flocs in suspension.

A New Method of Estimating Floc Fractal Dimension from LISST Volume Concentration

The volume concentration VC of a floc of a floc is given as

$$VC_f = f_s \cdot N_f \langle d_f^3 \rangle \quad (8)$$

where f_s is the shape factor, N_f is the number concentration of floc, and d_f is the floc size. The number concentration of flocs can further be expressed as:

$$N_f = \frac{N_p}{\langle N_p \rangle} \quad (9)$$

where the number concentration of primary particles that make up the floc is given as

$$N_p = \frac{m_p}{f_s \cdot \rho_p \langle d_p^3 \rangle} \quad (10)$$

and the number of primary particles that make up the floc $\langle N_p \rangle = \frac{d_f^F}{d_p^F}$

(11)

Inserting eqs. 11 and 10 into eq. 9, and eq. 9 into eq. 8 gives

$$VC_f = VC_p \cdot \langle d_p^{F-3} \rangle \cdot \langle d_f^{3-F} \rangle \quad (12)$$

where VC_p is the volume concentration of primary particles. Taking the log of both sides of eq. 12 gives

$$\log[VC_f] = \log [VC_p \cdot \langle d_p^{F-3} \rangle] - (F-3) \log[\langle d_f \rangle] \quad (13)$$

In this study, we collect floc data from a mudflat environment - the Aam tidal channel - in Songdo, South Korea, using the particle imaging camera system (PICS), Laser In-Situ Scattering and Transmissometry (LISST), Seabird SBE 19plus Profiler CTD and pump sampling instruments to understand the composition and fractal dimension of flocs in suspension. Casting was observed during spring and neap tides between 13th of May 2023 to 17th of June 2023, during which water samples were collected to determine reference values of the total suspended solids.

3. Results and Conclusions

The results from this study showed that floc interstitial fluid mass could be a few orders of magnitude higher than floc primary particles. Also, the mass ratios of particle to floc (m_p/m_f),

and water (interstitial fluid) to floc (m_w/m_f) are both about unity for incipient and fully developed stages of flocculation, respectively. The study further revealed that during flocculation, flocs gain more interstitial fluids than particles. The use of LISST to compute the fractal dimension of flocs showed very promising results with mean relative error (MRE) values less than 5% when compared to the PICS-derived fractal dimension. In conclusion, the study quantifies the interaction between floc composites and how they influence the fractal properties of flocs. It further provides a working method to study the fractal behaviour of flocs over tidal cycles.

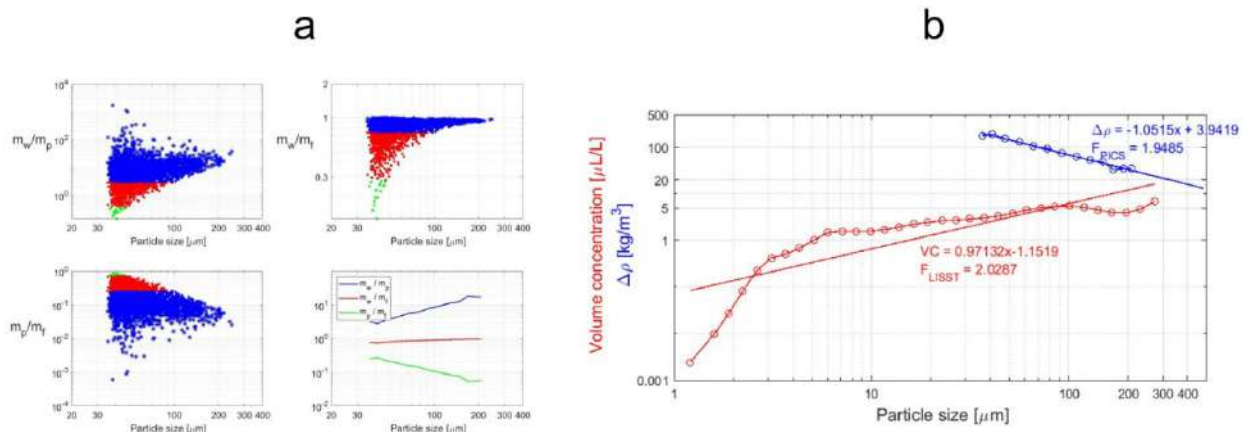


Figure 1: (a) A comparison of floc composites and their behaviour with flocculation. Green, red and blue circles represent incipient, developing and fully developed stages of flocculation. (b) Comparison between LISST (in red) and PICS-derived (in blue) fractal dimension.

References

- Kranenburg, C. (1994). Fractal structure of cohesive sediment aggregates. *Estuarine Coastal and Shelf Science*, 39, 451–460. <https://doi.org/10.1006/ecss.1994.1075>
- Fall, K. A., Friedrichs, C. T., Massey, G. M., Bowers, D. G., & Smith, S. J. (2021). The Importance of Organic Content to Fractal Floc Properties in Estuarine Surface Waters: Insights From Video, LISST, and Pump Sampling. *Journal of Geophysical Research: Oceans*, 126(1). <https://doi.org/10.1029/2020JC016787>



17th International Conference on
Cohesive Sediment Transport Processes
September 18-22, 2023
Inha University, Incheon, Republic of Korea



Field experiments on settling velocity and flocculation ability of muddy sediments in estuaries

S. Defontaine^{1,2}, I. Jalon-Rojas¹ and A. Sottolichio¹

¹ Univ. Bordeaux, CNRS, Bordeaux INP, EPOC, UMR 5805, F-33600 Pessac, France

² Ifremer – DYNECO/DHYSED, Centre de Bretagne, CS 10070, 29280 Plouzané, France,
sophie.defontaine@ifremer.fr

1. Motivation

The settling velocity is affected by the ability of cohesive sediments to flocculate and can vary over time and space in response to a range of environmental factors. Flocculation and floc break-up are impacted by different parameters along the tidal cycle. Suspended sediment concentration (SSC) and turbulence favour flocculation by increasing the probability of collision between particles (Eisma & Li, 1993). However, turbulent shear when sufficient may also be responsible for floc break up (Manning & Dyer, 1999; Pejrup and Mikkelsen, 2010). Low values of salinity can also influence the attractive forces between particles (Gibbs et al., 1989) and organic material may increase the stickiness of particles (Andersen & Pejrup, 2011). The aim of this study is to investigate the role played by these different factors on the settling velocity along the tidal cycle in two different regions (main estuary and tidal river) of a highly turbid and energetic macrotidal fluvio-estuarine system. Field work is challenging in very turbid and energetic estuaries, where knowledge is still scarce. Direct or quasi-direct multiple measurements of settling velocity are in development, especially by the use of simple quasi-in situ instruments.

2. Study site - Material and methods

The Gironde Estuary – Garonne Tidal river system is characterized by very high suspended sediment concentration reaching tens of grams per liter in surface waters. During the dry season, two estuarine turbidity maxima (ETM) can be observed: (i) a lower ETM in the salty central Gironde Estuary and (ii) an upper ETM shifted by tidal asymmetry in the Garonne Tidal River. Both ETMs have been sampled in this study through two field campaigns along a spring tidal cycle. A SCAF optical settling column was the main instrument deployed in both campaigns to estimate the settling velocity distribution of fine-grained sediment collected at the top and the bottom of the water column (Defontaine et al, 2023). Measurements of settling velocity, flocculation index, currents, SSC, salinity and organic content were carried out along the semi-diurnal tidal cycle in both locations. Organic content has been analyzed and sediments of both ETMs are characterised by a low POC/SPM ratio of ca. 1.5% and high C/N ratio of POM of 8.7 on average. This material can be considered composed of old refractory POC, which can be attributed to the very long residence time of the particles within the ETM (Etchebert et al., 2007; Savoye et al., 2012).

3. Results

In the lower ETM (Gironde Estuary) SSC were always below 3 g/L and settling velocities showed a flocculated mode, with relatively high variability, by one order of magnitude. Median settling velocities observed ranged from $2.04 \cdot 10^{-5}$ to $2.47 \cdot 10^{-4}$ m/s. Lower value is reached at the surface during slack time when the current velocity is closed to zero and the SSC decreased to its minimum. Higher values were reached at the bottom of the water column under high current intensity and maximum SSC. In contrast, in the Garonne Tidal River, the upper ETM was very turbid (SSC > 10 g/L), and suspended sediments were in the hindered settling regime during almost all the tidal cycle in the whole water column. Variability of the settling velocity was much lower and the whole results showed that the hindered settling regime is reached for a threshold SSC above 5 g/L.

The influence of salinity was distinct in both sites, with values around 9 and 2 in the Gironde Estuary and the Garonne tidal river, respectively. In the Gironde Estuary, a slight vertical stratification was observed after high tide, whereas the Garonne tidal river is characterized by well-mixed profiles of salinity. Our results do not put any correlation between salinity and settling velocity variability forward at any site. Even if salinity may play a role in the flocculation process, it seems that other processes had a more significant impact than salinity influence.

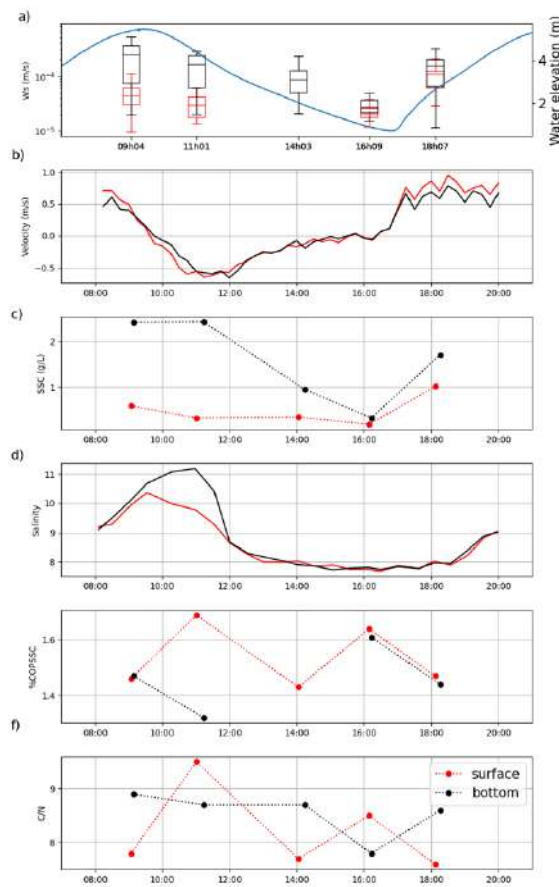


Figure 1. Time series over a semi-diurnal tidal cycle of a) settling velocity distribution (m/s) and water elevation (m), b) current velocity (m/s), c) SSC (g/L), d) salinity, e) %COPSSC and f) C/N along one tidal cycle at Fort Médoc (Gironde Estuary).

Acknowledgments

This study was supported by the EMPHASE project (ANR-FRQ). The authors are grateful to Camilla Lienart, Olivier Burvingt and Armelle Brouquier for their support during fieldwork and laboratory analysis.

References

- Eisma, D., Li, A., 1993. Changes in suspended-matter floc size during the tidal cycle in the Dollard Estuary. *Neth. J. Sea Res.* 31, 107–117.
- Manning, A.J., Dyer, K.R., 1999. A laboratory examination of floc characteristics with regard to turbulent shearing. *Mar. Geol.* 160, 147–170.
- Pejrup, M., Mikkelsen, O.A., 2010. Factors controlling the field settling velocity of cohesive sediment in estuaries. *Estuar. Coast. Shelf Sci.* 87, 177–185.
- Gibbs, R.J., Tshudy, D.M., Konwar, L., Martin, J.M., 1989. Coagulation and transport of sediments in the Gironde Estuary. *Sedimentology* 36, 987–999.
- Andersen, T.J., Pejrup, M., 2011. Biological influences on sediment behavior and transport. In: Wolanski, E., McLusky, D. (Eds.), *Treatise on Estuarine and Coastal Science*. Academic Press, Waltham, pp. 289–309.
- Defontaine, S., Jalon-Rojas, I., Sottolichio, A., Gratiot, N., & Legout, C., 2023. Settling dynamics of cohesive sediments in a highly turbid tidal river. *Marine Geology*, 106995.
- Etcheber, H., Taillez, A., Abril, G., Garnier, J., Servais, P., Moatar, F., Commarieu, M.-V., 2007. Particulate organic carbon in the estuarine turbidity maxima of the Gironde, Loire and Seine estuaries: origin and lability. *Hydrobiologia* 588, 245e259.
- Savoye, N., David, V., Morisseau, F., Etcheber, H., Abril, G., Billy, I., Charlier, K., Oggian, G., Derriennic, H., Sautour, B., 2012. Origin and composition of particulate organic matter in a macrotidal turbid estuary: the Gironde Estuary, France. *Estuar. Coast Shelf Sci.* 108, 16–28. <https://doi.org/10.1016/j.ecss.2011.12.005>.



17th International Conference on
Cohesive Sediment Transport Processes
September 18-22, 2023
Inha University, Incheon, Republic of Korea



Experimental study on the effects of sediment size gradation on the settling velocity of cohesive sediment

Yige Jing¹, Jinfeng Zhang^{1,2}, Qinghe Zhang¹, Jerome P.-Y. Maa³

¹ State Key Laboratory of Hydraulic Engineering Simulation and Safety Tianjin University, Tianjin, China

² Key Laboratory of Earthquake Engineering Simulation and Seismic Resilience of China Earthquake Administration, Tianjin University, Tianjin, China

³ Department of Physical Sciences, Virginia Institute of Marine Science, School of Marine Science, College of William and Mary, Gloucester Point, USA

Natural sediment exists in the form of a non-uniformly graded mixture of particles. Some (Fang et al, 2008) applied the average settling velocity of sediment to calculate sediment transport capacity, which can obtain a different form between nonuniform and uniform sediments. It's important to describe the settling of non-uniform sediment reasonably in order to study the sediment transport. At present, the formulas for the average settling velocity of non-uniform sediment are all based on the separate solution of each component (Pham Van Bang, 2013; Spearman, 2017; Sun, 2021), and there is a lack of unified expression considering the grain size distribution. Moreover, the accuracy of most sediment settling experiments is limited. To explore the above issues, a high-precision particle sedimentation observation system was established, and indoor sedimentation experiments based on this system were conducted for cohesive sediments.

A high-speed high-resolution camera and fiber-optic sensor were included, combined with PTV (Particle Tracking Velocimetry) algorithm in this settlement observation method. Two size distributions of cohesive sediments from estuarine coastal areas were used and nine initial mass concentrations were set. From the experiment, we obtained the measured gradation curves for the two samples at every concentrations as well as the average settling velocity.

This experiment method can observe the grain size distribution and settling characteristics of sediment from a micro perspective, and the following conclusions can be obtained from the experiment: (1) The flocculation and settling process of cohesive sediment particles can be observed for different concentrations and particle size distributions. The effect of sediment concentration and grain size distribution on settling velocity may not be independently. (2) The selectivity of sediment affects the overall average settling velocity. The stronger the selectivity, the stronger the inhibition of settling velocity. (3) This study proposes a settling velocity correction coefficient PD , and fits a static water settling velocity formula of cohesive sediments considering sediment concentration and grain size distribution according to experimental settling velocity.

References

Fang H., Chen M., Chen Q. One-dimensional numerical simulation of non-uniform sediment transport under unsteady flows. *International Journal of Sediment Research*, 2008, 23(4): 316-328. doi: /10.1016/S1001-6279(09)60003-2.

Spearman J., Manning A. J. On the hindered settling of sand-mud suspensions. *Ocean Dynamics*, 2017, 67(3-4): 465-483. doi: /10.1007/s10236-017-1034-7.

Sun Z.L., Zheng H., Xu D. Vertical concentration profile of nonuniform sediment. *International Journal of Sediment Research.*, 2021, 36(1):120-126. doi: /10.1016/j.ijsrc.2020.06.008.

Van L. A., Pham Van Bang D. Hindered settling of sand–mud flocs mixtures: From model formulation to numerical validation. *Advances in Water Resources*, 2013, 53(1): 1-11. doi: /10.1016/j.advwatres.2012.09.009.



17th International Conference on
Cohesive Sediment Transport Processes
September 18-22, 2023
Inha University, Incheon, Republic of Korea



Do cohesive sediment flocs contain sand particles and does it matter?

J.Spearman¹ and A.Manning^{1,2}

¹ Coasts and Oceans Group, HR Wallingford, j.spearman@hrwallingford.com

² School of Biological and Marine Sciences, Plymouth University

1. Introduction

The extent to which sand grains can be trapped within the fine sediment and organic matrix of a floc is still a contested scientific topic. Evidence for the interaction of sand and fine sediment was presented in measurements of floc settling velocities from different sand-mud proportions (Manning et al., 2011). These results were used to develop equations for settling velocity for different sand-mud percentages and concentrations and shear. Those equations were then used with numerical modelling to successfully reproduce time series of sand-mud concentration profiles from highly detailed field experiments (Spearman et al., 2011), providing further evidence of the interaction between sand and cohesive sediment flocs. Most recently those equations were also included in the *Regional Ocean Modeling System* implemented in the *Coupled Ocean–Atmosphere–Wave–Sediment Transport Modeling System* by Sherwood et al. (2018).

In the last decade the use of X-ray micro-tomography and electron microscopy on floc structure has demonstrated how organic material (extracellular polymeric substances, algae, bacteria, etc.) dominates the cohesion and structure of fine sediment flocs (e.g., Wheatland et al., 2020; Spencer et al., 2021, 2022). These techniques have also shown how clay and organic matrices can include sand particles in muddy sediments (Figure 1), though to date such techniques have not been applied to capture the structure of *flocs* including sand particles.

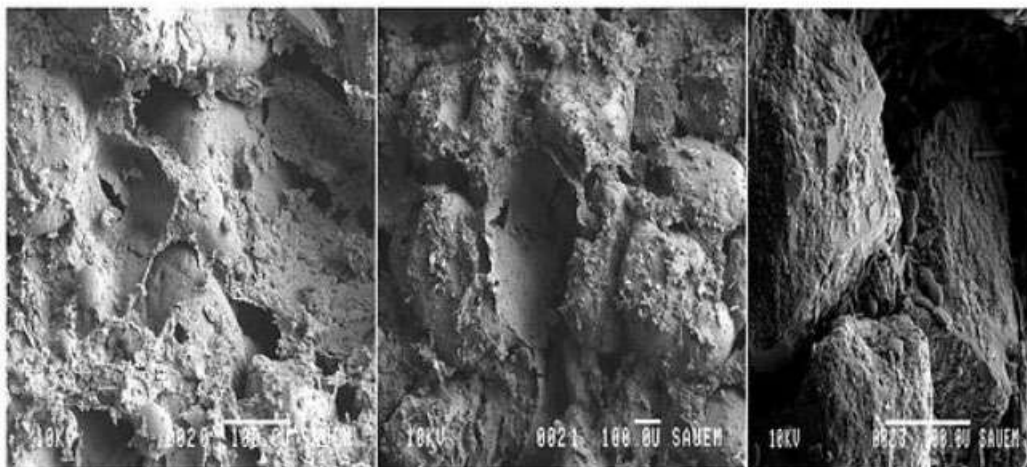


Figure 1: Electron microscope images of muddy sediments with varying biopolymer content: (left) a sand-clay matrix with biopolymer coating; (centre) sand grains blanketed by a biopolymer surface in the lee of a dune crest; (right) sand grains with diatoms and minimal biopolymer. Scale bar is 100 microns (from Hope et al., 2020).

One of the questions governing the interaction of sand particles with muddy flocs is whether, and how, this interaction changes the deposition flux of mud and sand. Most sediment transport modelling codes in use today assume segregation - i.e., there is little direct interaction between mud and sand in the water column, and the only interaction occurring at, and within, the sediment bed (e.g. as postulated by Van Ledden, 2003). The evidence from the earlier work by Manning et al. (2011) and Spearman et al. (2011) suggests this may not be true. However, the generally accepted assumption of independent settling of sand particles and mud flocs with the latter settling at a speed in the region of 1 mm/s, is normally a practical and successful approach to sediment modelling, and this could imply that any interaction between mud flocs and sand particles in the water column is not significant.

We examine this issue through the careful analysis of suspended settling data of sediment flocs resulting from the suspension of varying proportions of mud and sand, measured as part of the TKI - MUSA research project (<https://publicwiki.deltares.nl/display/TKIP/DEL112++MUSA>). The measurements of floc size and settling speed were undertaken using the high resolution LabsFLOC2 video system (e.g., Manning et al., 2006, 2017) using sediment samples collected both from the seabed and from the water column. These were used, together with the information about the mud and sand concentrations of the samples used, to infer how mud and sand particles are distributed within the floc population. A 1DV model was then used to examine whether the distribution of mud and sand within the floc population aligns with the observed field information. The results of the study were used to evaluate whether the interaction of sand and mud particles is important in a practical sense for sediment transport modelling.

References

- Hope, J.A., Malarkey, J., Baas, J.H., Peakall, J., Parsons, D.R., Manning, A.J., Bass, S.J., Lichtman, I.D., Thorne, P.D., Ye, L. and Paterson, D.M. (2020). Interactions between sediment microbial ecology and physical dynamics drive heterogeneity in contextually similar depositional systems. *Limnology and Oceanography*, <https://doi.org/10.1002/lno.11461>
- Manning, A. J. (2006). LabSFLOC – A laboratory system to determine the spectral characteristics of flocculating cohesive sediments. HR Wallingford Technical Report, TR 156.
- Manning, A.J., Whitehouse, R.J.S. and Uncles, R.J. (2017) Suspended particulate matter: the measurements of flocs. In: R.J. Uncles and S. Mitchell (Eds), *ECSA practical handbooks on survey and analysis methods: Estuarine and coastal hydrography and sedimentology*, Chapter 8, pp. 211-260, Pub. Cambridge University Press. <https://doi.org/10.1017/9781139644426>
- Manning, A.J., Baugh, J.V., Spearman, J.R., Pidduck, E.L. and Whitehouse, R.J. S. (2011). The settling dynamics of flocculating mud:sand mixtures: Part 1 - Empirical algorithm development. *Proceedings of the 10th International Conference on Cohesive Sediment Transport*, Rio de Janeiro, Brazil, May 2009, *Ocean Dynamics*, volume 61, number 2-3, 311-350, doi: 10.1007/s10236-011-0394-7
- Sherwood, C.R., Aretxabaleta, A.L., Harris, C.K., Rinehimer, J.P., Verney, R. and Ferré, B. (2018). Cohesive and mixed sediment in the Regional Ocean Modeling System (ROMS v3.6) implemented in the Coupled Ocean–Atmosphere–Wave–Sediment Transport Modeling System (COAWST r1234). *Geosci. Model Dev.*, 11, 1849–1871, <https://doi.org/10.5194/gmd-11-1849-2018>
- Spearman, J.R., Manning, A.J. and Whitehouse, R.J.S. (2011). The settling dynamics of flocculating mud:sand mixtures: Part 2 - Numerical modelling. *Proceedings of the 10th International Conference on Cohesive Sediment Transport*, Rio de Janeiro, Brazil, May 2009, *Ocean Dynamics*, volume 61, number 2-3, 351-370, doi: 10.1007/s10236-011-0385-8

Spencer, K.L., Wheatland, J.A.T., Bushby, A.J., Carr, S.J., Droppo, I.G. and Manning, A.J. (2021) A structure–function based approach to floc hierarchy and evidence for the non-fractal nature of natural sediment flocs. *Nature - Scientific Reports* 11, 14012. <https://doi.org/10.1038/s41598-021-93302-9>

Spencer, K.L., Wheatland, J.A.T., Carr, S.J., Manning, A.J., Bushby, A.J., Gua, C., Botto, L. and Lawrence, T. (2022). Quantification of 3-dimensional structure and properties of flocculated natural suspended sediment. *Water Research*, Volume 222, 118835, <https://doi.org/10.1016/j.watres.2022.118835>

Wheatland, J.A.T., Spencer, K.L., Droppo, I.G., Carr, S.J., Bushby, A.J. (2020). Development of novel 2D and 3D correlative microscopy to characterise the composition and multiscale structure of suspended sediment aggregates. *Continental Shelf Research*, Volume 200, 104112, <https://doi.org/10.1016/j.csr.2020.104112>

Van Ledden, M. (2003). Sand-mud segregation in estuaries and tidal basins. *Communications on Hydraulic and Geotechnical Engineering*, Report No. 03-2, ISSN 01169-6548.

Savenije, H. H. (2005). *Salinity and tides in alluvial estuaries* (New York: Elsevier). doi: 10.1016/B978-0-444-52107-1.X5000-X

Session: Model III
14:00 – 15:40
Thursday, September 21, 2023



17th International Conference on
Cohesive Sediment Transport Processes
September 18-22, 2023
Inha University, Incheon, Republic of Korea



Mud Mass Transport Around the Access Channel of Bushehr Port – the Persian Gulf

S. Movahedinejad¹, M. Soyuf Jahromi², S. M. Siadatmousavi³, A. Farhangmehr⁴ and S. A. Haghshenas^{5*}

¹ Department of Nonliving Resources of Atmosphere and Ocean, Faculty of Marine Science and Technology, University of Hormozgan, Bandar Abbas, Iran. sara.movahedi@ut.ac.ir

² Department of Nonliving Resources of Atmosphere and Ocean, Faculty of Marine Science and Technology, University of Hormozgan, Bandar Abbas, Iran.

soyufjahromi@yahoo.com.au

³ School of civil Engineering, Iran University of Science and Technology, Tehran, Iran.

siadatmousavi@iust.ac.ir

⁴ Institute of Geophysics, University of Tehran, Tehran, Iran. aref.farhangmehr@ut.ac.ir

⁵ Institute of Geophysics, University of Tehran, Tehran, Iran. sahaghshenas@ut.ac.ir

1. Introduction

The study of mud mass transport near access channels constructed in muddy environments is of high importance, as this issue is the major contributor to harbor siltation as well as sedimentation in access channels. Fine-grained cohesive sediments show complicated characteristics as compared to other sediment origins regarding their behavior. Hence, numerous researches are carried out to establish well validated physical and mathematical descriptions of the behavior and outcome of concentrated near-bed cohesive sediment suspensions and their interaction with the water column and the bed as well as the turbulence characteristics of sediment laden flow. Bushehr Port is located in south of Bushehr Bay in the north-western Persian Gulf (Figure 1), which is affected by a consequence of muddy deposits. The unique L-shaped access channel of the port with a length of 16 km is highly affected by significant sedimentation with an approximate rate of 900,000 m³/year, estimated for 2018. A recent study by Farhangmehr et al. (2021) has concentrated on the channel siltation mostly by suspended load; however, there are evidences of sudden sedimentation in certain parts of the channel during storm events, mostly through bed load fluid mud. This study focuses on realistic numerical simulations of the rate of suspended sediment and bed load in the Bushehr Port access channel such that the numerical model predicts the bed level change in this channel precisely.



Figure1. Bushehr Port and its access channel

2. Numerical Modelling

In this study the numerical finite volume model Delft3D (Deltares, 2014) is used for simulation of the waves and currents conditions over the study area. A one-dimensional model has been developed for modelling cohesive sediment transport in two phases of bed load and suspended load. The hydrodynamic model, which couples the wave and current modules of Delft3D software, provides 2DH wave-induced and tidal currents and the developed sediment model is run afterward. The sediment transport model was validated against the rates obtained from periodic hydrography surveys. Figure 2 depicts the simulated bed level change in a selected section of the channel after a three-day storm. It will be shown that the amount of simulated bed level change in the channel is in favourable agreement with observed values, obtained from periodic hydrography survey.

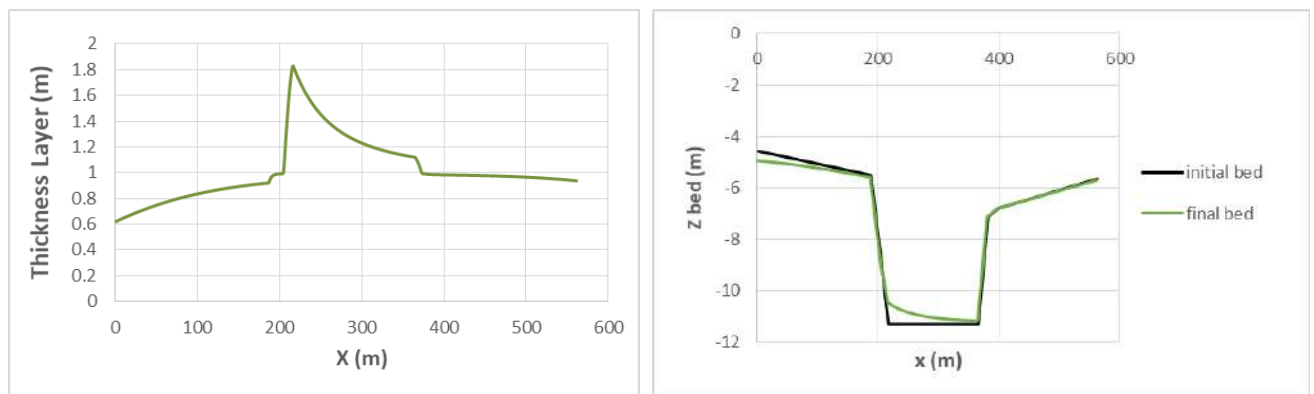


Figure2. A simulated thickness layer (left) and depth profile (right) across the access channel, showing reasonable sedimentation in the channel comparing with the observations.

3. Conclusion

The model is well capable of predicting sedimentation rates in the access channel. It is concluded that both suspended load and bed load contribute to the sedimentation process under different environmental conditions in this access channel.

References

Deltares (2014), Delft 3D-Flow User Manual, Delft Hydraulic, 684 p.

Farhangmehr, A., Haghshenas, S. A., Zarinfar, E., (2021): Investigating Sedimentation in Bushehr Port Access Channel, Adopting Periodic Sonar Surveys and Numerical Simulations, *International Conference on Cohesive Sediment Transport, INTERCOH 2021*, Delft, The Netherlands.



17th International Conference on
Cohesive Sediment Transport Processes
September 18-22, 2023
Inha University, Incheon, Republic of Korea



Assessing the environmental impacts of the bypass navigation channel in Mekong delta, Southern Vietnam

H.S. Nguyen¹, L.T.D. Tran¹, V.N. Dau¹, T.T. Huynh², and T.V. Bui¹

¹ Department of Earth Resources and Environment, Ho Chi Minh City University of Technology, Ho Chi Minh City 72409, Vietnam

² Department of Advanced Sciences and Technology Convergence, KNU, Sangju 37224, Korea

Abstract

The new entrance route to Hau river (Bassac river), known as “bypass navigation project”, is the most artificial navigation project in Tra Vinh province, southern Vietnam. The artificial project includes with 8 km of artificial canal routing the East Sea to Hau river through existing Quan Chanh Bo river to allow the 20,000 DWT cargoship to enter the Mekong delta mainland. The project was completed in 2017 and took their effects on the waterway traffic and logistic activities. However, the potential biological effects, bank erosion coupled with deposition risk have raised the questions to governments and scientist communities about its viability. This paper analyses the environmental impacts of the navigation channel in term of bank stability and sedimentation discharge. It was shown that, digging of new canal strongly affected the current velocity and hydrodynamic at the local region which may lead to increase the bank erosion. Meanwhile, the deposition rate in various scenarios (max, mean and min case) were estimated of 1,535,788.88 ; 1,204,065.68 and 872,342.48 m³/year. Based on this, an average of 691,483 m³ sediments should be annually dredged to ensure the safe movement of cargo ships through the channel.

Keywords: *Bypass project, artificial canal, ship-generated wave, bank erosion, sediment transport.*

Field measurement and monitoring

There were total 102 boreholes were taken for laboratory experiences to determine the grain size distribution and physical characteristic of the bank materials which effect the structure and eroding resistance of the riverbank.

The in-situ measurement of ship-generated wave was carried out to observe the amplitude of man-made generated wave. The number of ship-generated wave then was correlated with the shear stress that applies to the river bank.

Numerical modelling

This paper applied the MIKE (by DHI) numerical computing model to evaluate the potential impacts of the artificial projects on the hydrodynamic regime. Scenario models have been established to simulate the normal and completed projects condition varying the dry and rainy season.

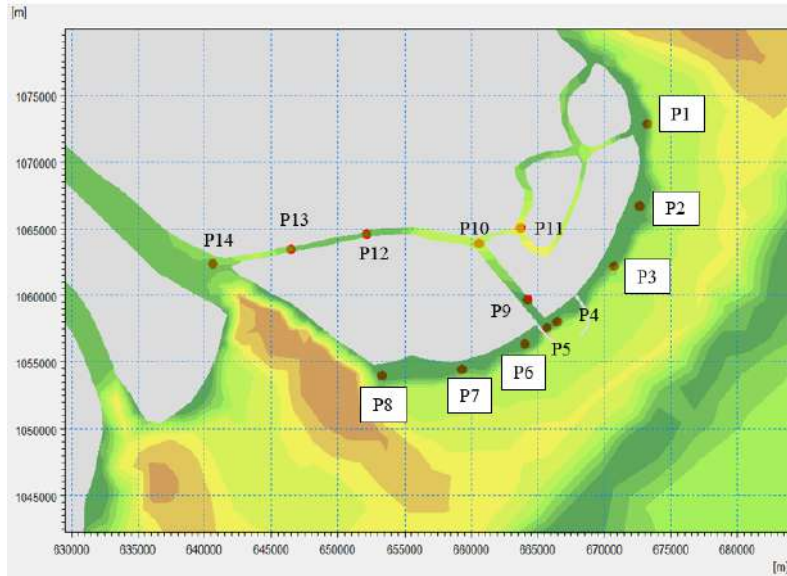


Figure 1. Finite mesh for the hydrodynamic model and monitoring points extracted from the simulation.

Results

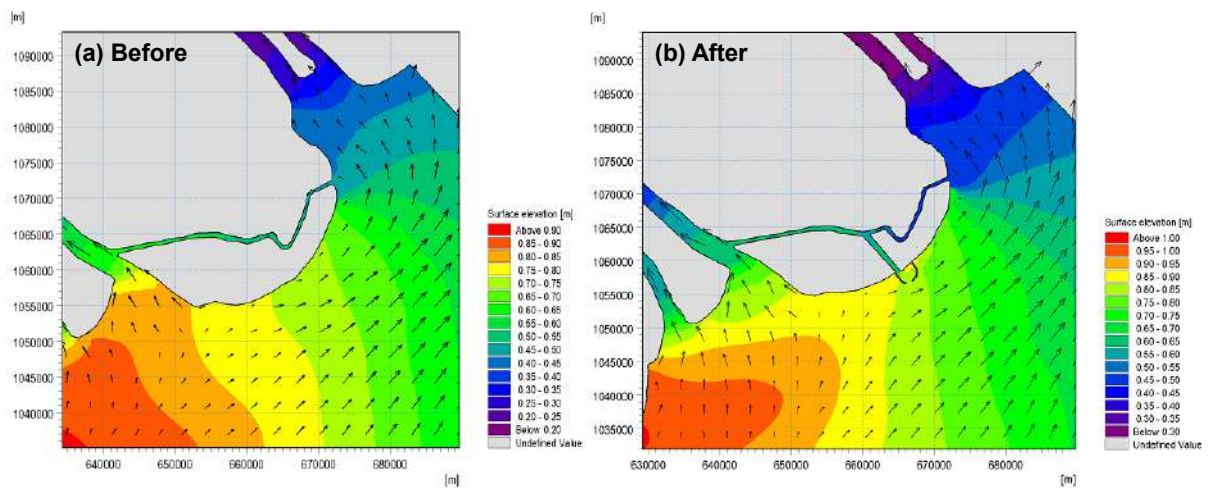


Figure 2. Change on current velocity due to artificial navigation channel

Table 1. Current velocity impacts by the artificial navigation channel

No.	Name	Position (m)		Rainy season (June)			Dry season (Nov)		
		X	Y	Before	After	+ / -	June	Nov	+ / -
P1	Truong Long Hoa	673204	1072833	0.35	0.26	-0.09	0.34	0.23	-0.11
P2	Ba Dong beach	672632	1066677	1.12	0.46	-0.66	0.94	0.43	-0.50
P3	Dan Thanh 1	670697	1062148	0.88	0.53	-0.35	0.74	0.41	-0.32
P4	DH1 Power plant	666432	1058015	0.39	0.77	+0.39	0.27	0.48	+0.21

No.	Name	Position (m)		Rainy season (June)			Dry season (Nov)		
		X	Y	Before	After	+ / -	June	Nov	+ / -
P5	Bypass Estuary	665685	1057575	0.45	0.92	+0.46	0.26	0.83	+0.57
P6	Dan Thanh 2	664014	1056344	0.55	0.74	+0.20	0.46	0.47	+0.01
P7	Dong Hai 1	659309	1054454	0.63	1.02	+0.39	0.47	0.66	+0.19
P8	Dong Hai 2	653329	1054014	0.64	1.07	+0.43	0.38	0.78	+0.39
P9	913 Ferry	664190	1059686	0.58	0.49	-0.09	0.42	0.52	+0.10
P10	QCB - Bypass canal	660584	1063907	0.63	0.64	+0.01	0.42	0.62	+0.20
P11	Long Toan	663706	1065006	0.69	0.67	-0.02	0.34	0.65	+0.21
P12	La Ban canal	652186	1064611	0.84	0.58	-0.26	0.64	0.60	-0.04
P13	Lang Sat Ferry	646470	1063467	1.29	0.65	-0.64	0.95	0.68	-0.27
P14	Dai An	640578	1062368	1.34	0.67	-0.67	0.97	0.47	-0.50

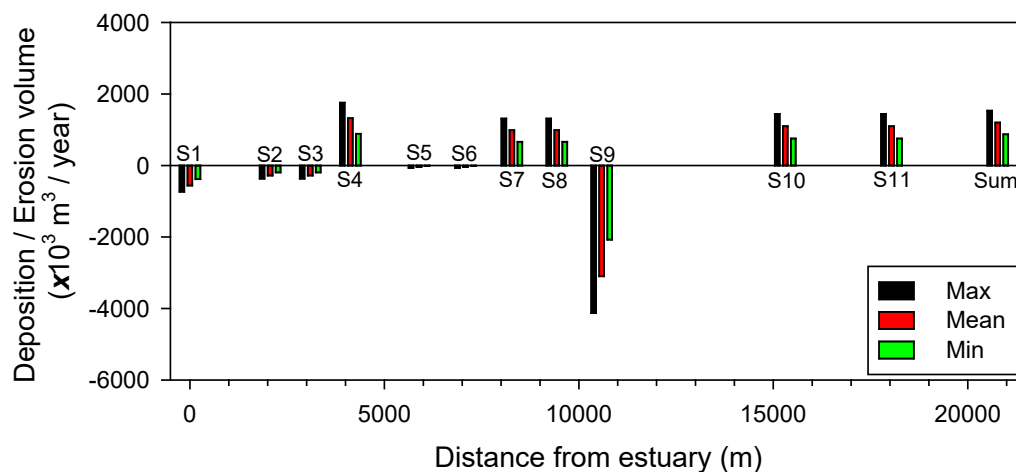


Figure 3. Calculated sediment deposition on the artificial navigation channel



17th International Conference on
Cohesive Sediment Transport Processes
September 18-22, 2023
Inha University, Incheon, Republic of Korea



Evolution of suspended sediment fluxes following seagrass loss in a mesotidal lagoon

Arnaud Le Pevedic^{1,2}, Florian Ganthy¹, Aldo Sottolichio²

¹ Ifremer, LITTORAL, Quai du Commandant Silhouette, F-33120 Arcachon, France,
alepeved@ifremer.fr

² Université de Bordeaux, UMR EPOC 5805, CNRS –Allée Geoffroy Saint-Hilaire, 33615
Pessac, France

1. Introduction

Seagrasses play a key role in mitigating erosion risks and ensuring navigation safety due to their capacity to control erosion and deposition fluxes. The contribution of seagrasses on sediment dynamics is twofold. First, they enhance the deposition processes, directly by collision of sediment particles against the foliage (Ganthy *et al.*, 2015) but also indirectly through the reduction of hydrodynamic conditions by damping wave energy and attenuating currents (Hendriks *et al.*, 2010). Moreover, seagrasses have a seabed stabilization function that hinders sediment resuspension (Gacia and Duarte, 2001) by mean of the root system which binds the substrate and the foliage which traps particles at the bottom of the canopy. Therefore, following the decline of seagrass meadows that occurred worldwide over the past decades (Waycott *et al.*, 2009), suspended sediment concentration is expected to have increased with detrimental consequences on economic activities. It is likely the case in Arcachon Bay, a mesotidal coastal lagoon located on the French Atlantic coast and sheltering Europe's largest *Zostera noltei* meadow, whose total coverage has dropped by 45% over the past three decades. Concurrently to this decline, the increasing need for dredging has been reported by the local authorities. Through the case of Arcachon Bay this work aims to provide an insight into the modification of fine sediment dynamics in response to seagrass loss in a mesotidal coastal lagoon.

2. Methods

Sediment dynamics was characterized by use of a bio-hydro-sedimentary model that accounts for the effects of vegetation on the structure of the flow, wave energy, as well as vertical sediment fluxes through two processes that are blocking and trapping. Blocking occurs when high leaf density canopies are bent under strong current velocities and the canopy forms a dense layer limiting particle deposition; while trapping refers to the collision of sediment particles against the foliage, resulting in the increase of their settling velocity. Additionally, this model considers the feedback between hydrodynamics and leaf reconfiguration and accounts for the modification of the flow and vegetation characteristics on the trapping and blocking processes. A scenario analysis is conducted using this modeling platform to study the response of sediment dynamics, namely horizontal and vertical fluxes of mud and fine sands, to the decline of seagrasses in Arcachon Bay. Such an analysis is performed by comparing the results of two simulations for which only the coverage map of *Zostera* meadows differs, corresponding to the pre- and post-decline coverage maps of the year 1989 and 2016, respectively.

3. Results and Discussion

The decline of *Zostera* meadows in Arcachon Bay (Figure 1a) modified the sediment fluxes as demonstrated by the increase of suspended sediment concentrations (SSC; Figure 1b), which nearly doubled at the whole lagoon scale and as far as the inlet. The largest increase rates of SSC are observed in the western part of the lagoon, with SSC 4 to 5 times higher in the post-decline scenario, in this area characterized by the largest seagrass loss. This evolution can be explained by the reduction of the capacity of seagrasses to retain sediment on the seabed and favor sediment deposition, along with the intensification of tidal currents and wave orbital velocities that followed the decline and further enhances the erosion processes.

The evolution of sediment dynamics induced a reconfiguration of the areas of net erosion and deposition, leading to variations of the seabed elevation. The tendency for mud and fine sands to be more easily resuspended and transported resulted in the redistribution of the sediment based on its grain size along with changes in the composition of the seabed surficial layer, notably muddification of the tidal flats and sandification of the western inner channels and their surroundings.

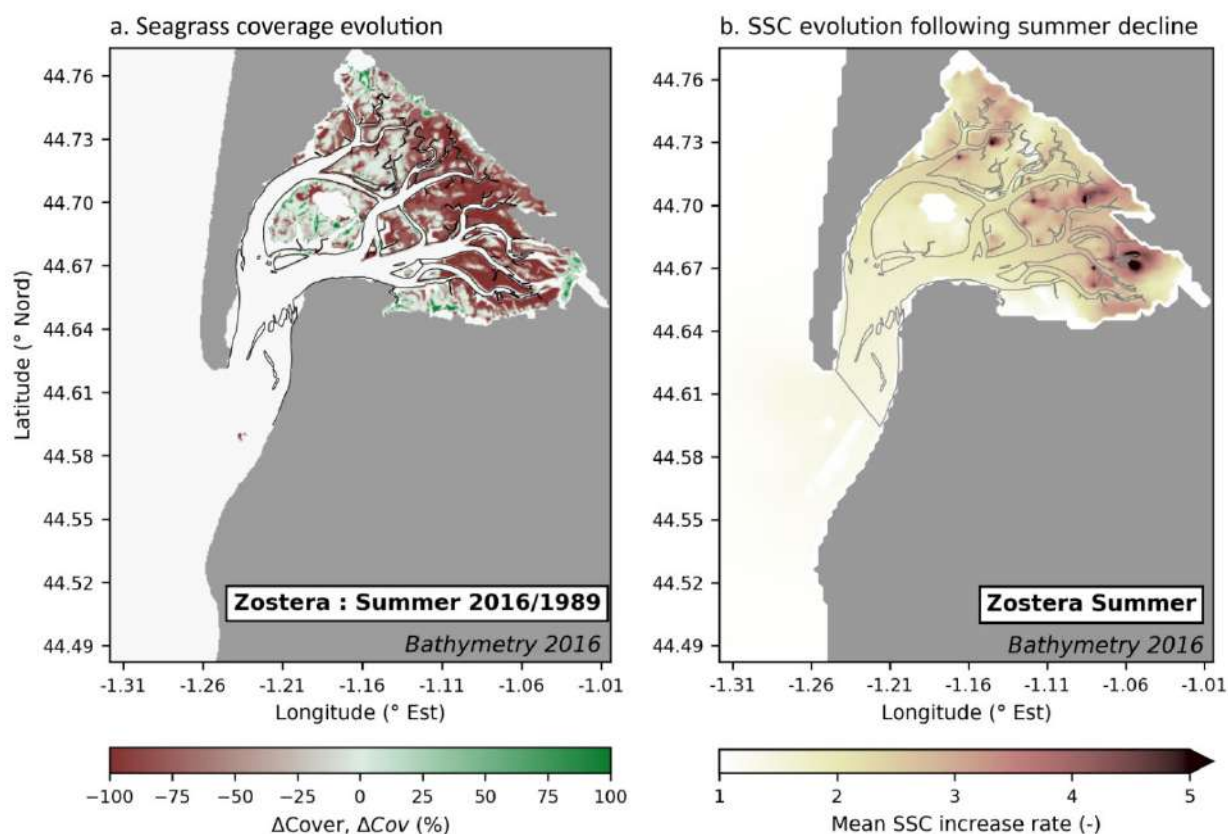


Figure 1. Evolution of *Zostera* meadow coverage (a) between the pre-decline (1989) and post-decline (2016) scenarios, brown areas represent regions in which seagrasses declined and green areas represent regions where seagrasses developed. Evolution rates of suspended sediment concentration (b) between 1989 and 2016, given as the ratio of post-decline concentration to pre-decline concentration.

4. Conclusion

This study shows that seagrasses control the sediment dynamics at the whole lagoon scale and their decline comes with great consequences since it induced an evolution of the bathymetry and reshaped the seabed sediment map. Modification of the erosion and deposition fluxes led

to a twofold increase of suspended sediment concentration and the infilling of the channels, which corroborates with the increase need for dredging reported over the last decade.

References

- Gacia, E., & Duarte, C. M. (2001). Sediment Retention by a Mediterranean *Posidonia Oceanica* Meadow: The Balance between Deposition and Resuspension. *Estuarine, Coastal and Shelf Science* 52(4):505-14. doi: [10.1006/ecss.2000.0753](https://doi.org/10.1006/ecss.2000.0753).
- Ganthy, F., Soissons, L., Sauriau, P.-G., Verney, R., & Sottolichio, A. (2015). Effects of Short Flexible Seagrass *Zostera Noltei* on Flow, Erosion and Deposition Processes Determined Using Flume Experiments. *Sedimentology* 62(4):997-1023. doi: [10.1111/sed.12170](https://doi.org/10.1111/sed.12170).
- Hendriks, I. E., Bouma, T. J., Morris, E. P., & Duarte, C. M. (2010). Effects of Seagrasses and Algae of the Caulerpa Family on Hydrodynamics and Particle-Trapping Rates. *Marine Biology* 157(3):473-81. doi: [10.1007/s00227-009-1333-8](https://doi.org/10.1007/s00227-009-1333-8).
- Waycott, M., Duarte, C.M., Carruthers, T. J. B., Orth, R.J., Dennison, W.C., Olyarnik, S., Calladine, A., Fourqurean, J.W., Heck, K.L., Hughes, A.R., Kendrick, G.A., Kenworthy, W.J., Short, F.T., & Williams, S.L. (2009). Accelerating Loss of Seagrasses across the Globe Threatens Coastal Ecosystems. *Proceedings of the National Academy of Sciences* 106(30):12377-81. doi: [10.1073/pnas.0905620106](https://doi.org/10.1073/pnas.0905620106).



17th International Conference on
Cohesive Sediment Transport Processes
September 18-22, 2023
Inha University, Incheon, Republic of Korea



Seasonal and interannual sediment dynamics in the Bay of Biscay: exploring 20y hindcast model results

Y. Fossi Fotsi¹, R. Verney¹, S. Le Gac¹, and A. Gangloff²

¹Ifremer – DYNECO/DHYSED, Centre de Bretagne, CS 10070, 29280 Plouzané, France

²Shom - Service hydrographique et océanographique de la marine, 29200 Brest, France

1. Introduction

Suspended sediment concentration (SSC) in water is an indicator of coastal dynamics and acts on water clarity, which is a determining factor for primary production. Sediment transport also implies changes in bed sediment properties, hence modifying physical habitats. Sediment fluxes at shelf scale are finally crucial when investigating small scale environments, such as bays and estuaries, hence providing reliable boundary conditions. The spatial and temporal variability of this parameter as a function of hydro-meteorological forcing and human activities has recently been highlighted by Mengual et al. (2017) on the scale of the Bay of Biscay shelf. The present study investigates the spatial and temporal variability of sediment transport at the shelf scale using a 20y 3D hydro-sedimentary model hindcast in the Bay of Biscay.

2. Materials and methods

2.1 Numerical modelling

The CROCO 3D hydrodynamic model (2.5km horizontal resolution, 40 generalized sigma-levels on the vertical) are coupled with the MUSTANG sediment transport model, and forced with tidal harmonics, hydro-meteorological forcings (ERA5, GLORYS CMEMS reanalysis) and waves (WW3 RESOURCECODE hindcast). The MUSTANG configuration uses three sediment classes: a gravel, a fine sand (200 μ m diameter) and a mud. Their initial distribution in the sediment compartment is derived from a compilation of surficial sediments maps (data.shom.fr), with a spinup of several months. The sand settling velocity is calculated from the grain diameter, while the mud settling velocity is computed from the formulation of Van Leussen (1994). The bottom shear stress combines the contribution of the current and the orbital wave velocities at the bottom (Soulsby et al., 1993), and integrates the spatially-variable roughness length estimated from the surficial sediment characteristics calculated by MUSTANG.

2.2 Satellite Ocean colour data

The surface suspended sediment concentration (SSC) products used in this study are derived from MODIS Aqua (2000-2020) at 1.2 km resolution, processed by Gohin (2011).

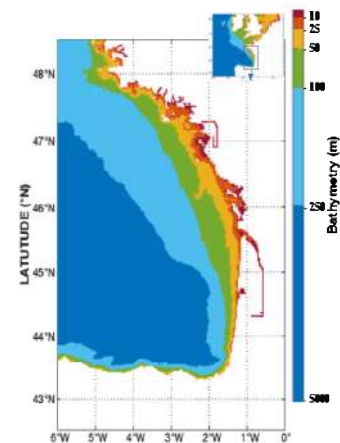


Fig. 1: CROCO-MUSTANG configuration and bathymetry in the Bay of Biscay

3. Results

In this study, we analyze the cross-shelf and along-shelf sediment transport dynamics from SSC and fluxes. Multiple scales are investigated: the mean/average behavior, the interannual and seasonal variability, and the impact of extreme/intense events and their contribution to the seasonal sediment transport patterns such as near bed and sub-surface SSC dynamics, horizontal fluxes and bed sediment evolution.

3.1 Calibration

Prior to the analysis, an evaluation of the model performance by comparing the modelled surface SSC with in-situ and satellite (MODIS) data was carried out between April 2007 and March 2008. The results showed that the model satisfactorily reproduces the major seasonal and event dynamics observed in situ and by satellite. As an example, Fig. 2, the median dynamics of the SSC on the bathymetric slice ($25 < h < 50$) highlights the good reproduction ($R=0.79$) of the spatial patterns and the order of magnitude of the surface SSC at the scale of the Bay of Biscay (1 to 2mg/l in summer and about 5mg/l in winter, up to 20mg/l during storm events). However, we can observe an overestimation of the simulated SSC concentration outside the energetic period.

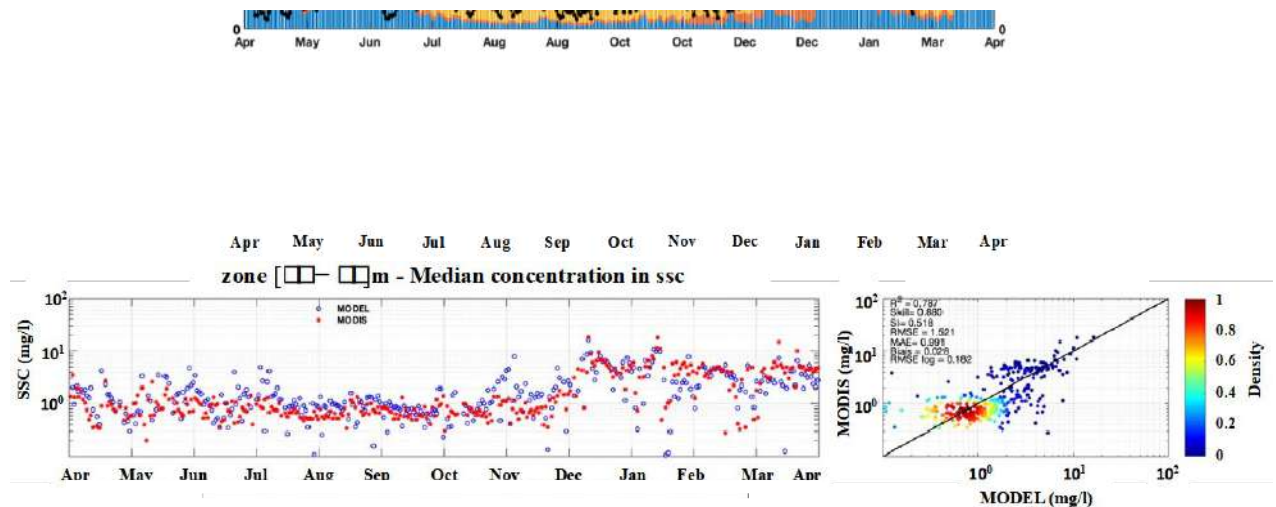


Fig.2: Daily time series of median surface SSC by bathymetric slice in the Bay of Biscay: MODIS and model comparison.

3.2 Seasonal SSC variability and fluxes dynamics in the Bay of Biscay

In the Bay of Biscay, the spatio-temporal variability of SSC gradients shows maximum concentrations near the coast and estuary mouths (Fig.3). The high SSC values in winter (Fig.3 d) contrast with the results in summer (Fig.3 b), illustrating that sediment transport is strongly influenced by river inputs and meteorological forcings.

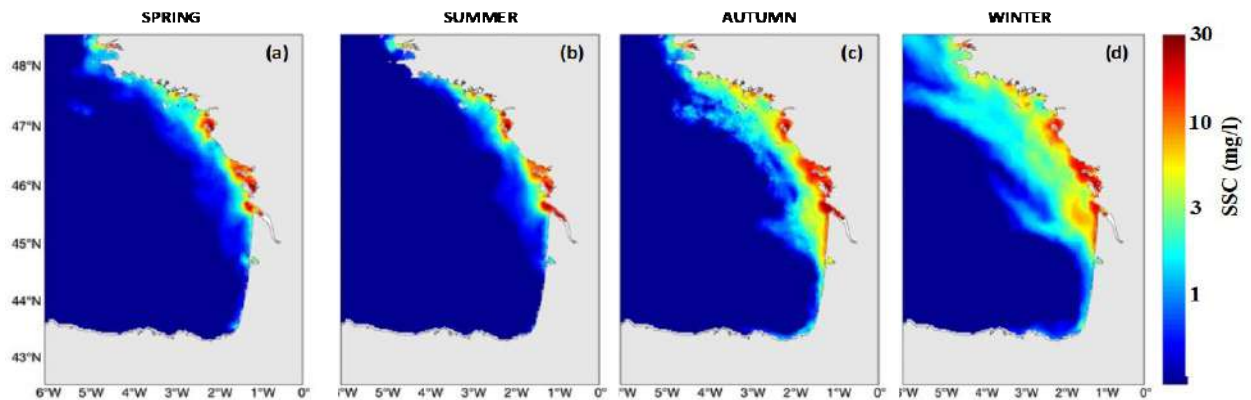


Fig.3: Seasonal maps of surface SSC concentrations simulated by CROCO-MUSTANG between April 2007 and March 2008.

About sediment fluxes, the main dynamics is dominated by storms and waves, with a transport towards the coast through the 50 m isobath (for instance off the Loire estuary mouth). The influence of river inputs is weaker, but measurable especially close to river mouths.

4. Conclusions

The present study is based on a hydro-sedimentary model in the Bay of Biscay to study sediment dynamics on seasonal to decadal time scales. The model simulates spatial structures and their variability patterns satisfactorily and results illustrate the role of hydrological and meteorological forcings on sediment dynamics at shelf scale. This modelling approach will be next coupled to low and high trophic models, and implemented to evaluate future trajectories of the shelf ecosystem forced by different RCP-SSP IPCC scenarios.

References

- Accensi Mickael (2022). RESOURCECODE. Ifremer, Scientific Information Systems for the sea. <https://doi.org/10.12770/d089a801-c853-49bd-9064-dde5808ff8d8>
- Gohin, F., 2011. Annual cycles of chlorophyll-a, non-algal suspended particulate matter, and turbidity observed from space and in-situ in coastal waters. *Ocean Science* 7, 705–732. <https://doi.org/10.5194/os-7-705-2011>
- Mengual, B., Hir, P.L., Cayocca, F., Garlan, T., 2017. Modelling Fine Sediment Dynamics: Towards a Common Erosion Law for Fine Sand, Mud and Mixtures. *Water* 9, 564. <https://doi.org/10.3390/w9080564>
- Soulsby, R.L., Hamm, L., Klopman, G., Myrhaug, D., Simons, R.R., Thomas, G.P., 1993. Wave-current interaction within and outside the bottom boundary layer. *Coastal Engineering, Special Issue Coastal Morphodynamics: Processes and Modelling* 21, 41–69. [https://doi.org/10.1016/0378-3839\(93\)90045-A](https://doi.org/10.1016/0378-3839(93)90045-A)
- Van Leussen, W., 1994. Estuarine Macroflocs and Their Role in Fine-Grained Sediment Transport. Ph. D. Thesis, University of Utrecht.



Suspended sediment dispersal offshore of the Ayeyarwady delta, Myanmar

C.K. Harris¹, M.J. Fair¹, E. Whitehead-Zimmers², and D. Yin¹

¹ Virginia Institute of Marine Science, William & Mary, Gloucester Point, VA USA,
ckharris@vims.edu

² Messiah University, Mechanicsburg, PA USA

1. Motivation and Research Question

The combined Ayeyarwady and Thanlwin Rivers deliver ~485 Mt of sediment/year to the northern Andaman Sea, the eastern portion of which includes a shallow muddy embayment called the Gulf of Martaban (Figure 1). This system has a monsoonal climate; precipitation is high during the summer when the winds tend to be energetic and from the southwest (SW), and dry during winter when winds tend to be moderate and from the northeast (NE). Within the macrotidal Gulf of Martaban, tidal amplitudes reach 3m during Neap tides, and 7m during Spring tides. Liu et al. (2021) argued that sediment would be trapped in the northern Andaman Sea during the SW monsoon when the surface currents along the delta flow eastward; and that sediment would be exported to the Bay of Bengal during the NE monsoon when surface currents flow westward (Figure 1). However, these characterizations were based on assessment of surface currents and turbidity, and little is known about near-bed currents and sediment fluxes. Recently analyzed geophysical observations and sediment cores provided evidence of a clinoform depocenter seaward of the Gulf of Martaban, and a second depocenter on the western side of the delta in the Bay of Bengal (Figure 1; Kuehl et al. 2019; Liu et al. 2021). Though limited, water column observations indicated the presence of near-bed fluid muds within the Gulf of Martaban (Kuehl et al. 2019; Harris et al. 2022). Based on these observations, we postulate that the Gulf of Martaban acts as a large “mixing bowl” for sediment, with delivery of sediment from the Gulf to the clinoform depocenter occurring during ebb Spring tides and extreme events. The question of whether Ayeyarwady and Thanlwin sediment contributes to the northwest depocenter remains unresolved.

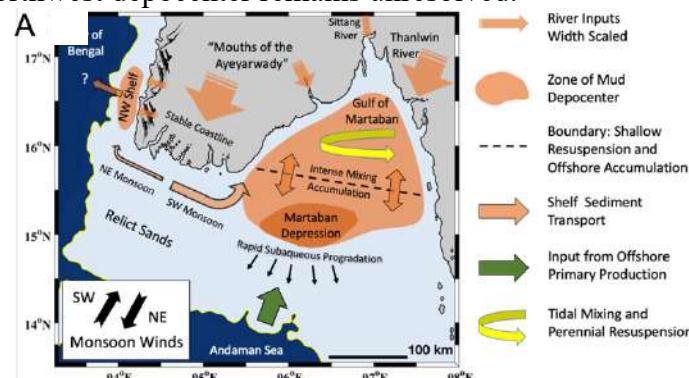


Figure 1. Conceptual model of study area. The Gulf of Martaban is hypothesized to trap sediment, and episodically supply it to the Martaban Depression clinoform. Conditions during the NE monsoon are hypothesized to deliver sediment to the NW shelf depocenter offshore of the west coast (Adapted from Kuehl et al. 2019; Flynn et al. 2022).

2. Methods

A coupled hydrodynamic, wave, and sediment transport model was used to explore suspended sediment dispersal offshore of the Ayeyarwady-Thanlwin Rivers. The model was implemented within the Regional Ocean Modeling System (ROMS), accounting for waves using SWAN (Shallow Waves Nearshore), and suspended sediment fluxes following Warner et al. (2008). Winds, tides, and open boundary conditions were specified from global model output. The model was run for two one-month cases: one representative of the winter NE monsoon, and one of the summer SW monsoon. Model estimates of suspended sediment dispersal were analyzed and compared to spatial patterns in field measurements and satellite images. The sediment flux results were compared to characterize the conditions most likely to transport suspended sediment to either depocenter. To evaluate the relative importance of tides, winds, waves, and open boundary currents on delivering sediment to the NW depocenter, additional “isolating” model runs were completed for the NE winter monsoon. In each isolating run, one of these physical forcing mechanisms were deactivated. We quantified the role of each forcing by comparing sediment fluxes for each of these isolating cases to that of the control case.

3. Results

Results from the control case that included all forcings (winds, waves, tides, and open boundary currents) were analyzed for the SW and NE monsoon model runs. Offshore of the Ayeyarwady delta, surface currents had a bidirectional pattern: flowing eastward during the SW monsoon and westward during the NE monsoon (Figure 2A, 2B). Bottom currents over the Ayeyarwady delta region had less seasonality. Seasonal signals were less significant within the Gulf of Martaban where both the surface and bottom currents were strongly tidally driven. Sediment resuspension was tidally-dominated within the Gulf of Martaban, with asymmetric tidal trapping maintaining the Gulf’s high turbidity. The Gulf acts as a “mixing-bowl”, having high sediment fluxes during flood and ebb tides, but relatively little net export. Sediment export from the Gulf was larger during the SW monsoon than the NE monsoon. The surface extent of the Gulf of Martaban turbid area showed strong variability over the spring / neap cycle (Figure 2C, 2D). During spring tides, the surface sediment expanded seaward, and high fluxes during these times delivered material to the vicinity of the clinoform deposit.

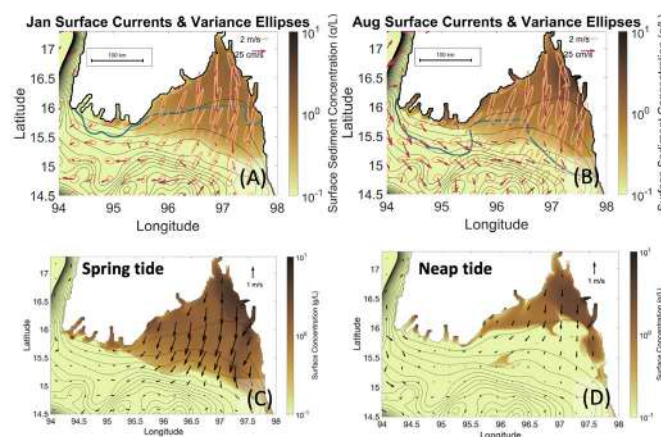


Figure 2. Modelled suspended concentrations and currents (arrows are speed, in (A) and (B) ellipses are variability). Top: averaged over Spring / Neap cycle for (A) NE and (B) SW monsoon. Bottom: peak (C) Spring and (D) Neap tides.

Next, suspended sediment fluxes for the control case were compared to those of the cases where tides, waves, winds, and open boundary currents were deactivated. Specifically, we analyzed the along-shelf sediment flux offshore of the Ayeyarwady delta where the northern Andaman Sea meets the Bay of Bengal. The numerical experiments that deactivated the various forcings showed that the tides were more important for sediment flux than either the waves or the winds. Though this model was for NE monsoon conditions, the net sediment flux was eastward, not westward as expected. For the control case sediment was imported into the northern Andaman Sea from the Bay of Bengal, rather than exported as expected for NE monsoon conditions. The net eastward currents over the mid- and inner-shelf were an extension of strong currents flowing southward along the western coast of the Ayeyarwady delta. When the open boundary currents were deactivated, however, the net sediment flux changed dramatically, changing direction to become westward as expected.

4. Conclusions

The coupled model of hydrodynamics and suspended sediment transport demonstrate that sediment flux is tidally driven within the Gulf of Martaban. Net sediment fluxes from the Gulf of Martaban southward toward the Martaban clinoform depression were larger during the summer (SW) monsoon than the winter (NE) monsoon. Fluxes showed high variability over the Spring / Neap cycle, with export toward the Martaban clinoform depression largest during Spring ebb tides. Sediment export toward the northwestern shelf depocenter was sensitive to conditions within the Bay of Bengal. When open boundary conditions from the Bay of Bengal were included, the model produced strong currents that imported sediment from the NW depocenter region into the northern Andaman Sea.

Acknowledgments

This was funded by the National Science Foundation, USA grants OCE-1737221. The authors appreciate conversations with S.A. Kuehl and E.R. Flynn (both at VIMS), and J.P. Liu (NC State), whose input helped improve the work.

References

- Flynn, Kuehl, Harris, and Fair, (2022). Sediment and terrestrial organic carbon budgets for the offshore Ayeyarwady Delta, Myanmar: Establishing a baseline for future change. *Marine Geology*, 106782. doi: 10.1016/j.margeo.2022.106782.
- Harris, C. K., Wacht, J. T., Fair, M. J., and Cote, J. M. (2022). ADCP observations of currents and suspended sediment in the macrotidal Gulf of Martaban, Myanmar. *Frontiers in Earth Science*. doi: 10.3389/feart.2022.820326.
- Kuehl, Williams, Liu, Harris, Aung, Tarpley, Goodwyn, and Aye, (2019). Sediment dispersal and accumulation off the Ayeyarwady delta – Tectonic and oceanographic controls. *Marine Geology* (417). 106000. doi: 10.1016/j.margeo.2019.106000.
- Liu, J. P., Kuehl, S. A., Pierce, A. C., Williams, J., Blair, N. E., Harris, C., K., Wa Aung, D., Aye, Y. Y. (2020). Fate of Ayeyarwady and Thanlwin Rivers sediments in the Andaman Sea and Bay of Bengal. *Marine Geology*, 106137. doi: 10.1016/j.margeo.2020.106137.
- Warner, J.C., C.R. Sherwood, R.P. Signell, C.K. Harris, and H. Arango. 2008. Development of a three-dimensional, regional, coupled wave-, current-, and sediment-transport model. *Computers and Geosciences*, 34: 1284 – 1306; doi: 10.1016/j.cageo.2008.02.012.

Session: Sediment Transport IV
16:00 – 17:00
Thursday, September 21, 2023



17th International Conference on
Cohesive Sediment Transport Processes
September 18-22, 2023
Inha University, Incheon, Republic of Korea



Application of sediment composition index to predict suspended particulate matter concentration in the North Sea

D. Tran¹, X. Desmit¹, R. Verney² and M. Fettweis¹

¹ Royal Belgian Institute of Natural Sciences, OD Nature, Brussels, Belgium,
dtran@naturalsciences.be

² IFREMER, Laboratoire DHYSED, Plouzané, France

1. Introduction

A proper understanding of sediment transport is extremely important in many areas of engineering and socio-economic development. On the time scale of months to years, the knowledge of where sediment accumulates could save billions of dollars on annual port dredging and beach nourishment. On length scales of deltas, estuaries and coastal zones, such knowledge plays a crucial role for decision makers to govern the development of a country or region. Nevertheless, in sand-mud environments, quantifying the variability of suspended particulate matter concentration (SPMC) and their constituents is essential but highly challenging. To better quantify the ratio of sand/mud in suspension, we previously defined a sediment composition index, such as

$$SCI = 10\log_{10}(OBS) - SNR \quad (1)$$

Where OBS is the signal measured by an optical backscatter sensor (in NTU) and SNR is the signal measured by an acoustic sensor (in dB) (Pearson et al 2021, Tran et al 2021). In this study, we propose a novel method of applying SCI to predict long-term, high-frequency SPMCs of the North Sea without the need of conducting sensor calibrations.

2. Approach

This study used data collected at station MOW1, situated about 3 km offshore of Zeebrugge, Belgium. Overall, data at MOW1 consists of hourly water samples, particle size distributions, turbidity, hydrodynamic conditions and chlorophyll concentration for the year 2013 during 125 tidal cycles, providing one of the most comprehensive field data sets in the North Sea. Figure 1 shows three steps in applying the SCI method to obtain SPMC from raw signals of OBS (Optical Backscatter Sensor) and ADV (Acoustic Doppler Velocimetry). First, the data was divided into 20 bins, i.e., 0-100, corresponding to the ratio of sand/mud in suspension and OBS and ADV signals (Fig.1 left). Second, the relationship between SCI and bins was plotted (Fig.1 right and Eq.1) to obtain mathematical functions for each mooring during 2013. More specifically, this step provides the relationships between 1) OBS and ADV and the ratio of sand/mud (Fig.1 left), 2) SPMC and raw ADV signal (not shown), and 3) SPMC and raw OBS signal (not shown). The function obtained from Mooring 59 (Jan 24th – Mar 7th, 2013) was chosen to apply for the entire year because it covered almost all ratios of sand/mud that occurred during the year. Last, raw data of OBS and ADV from different moorings were

applied to the functions derived in the previous step to compute the SPMC of the year 2013 and potentially of any other years at the same station.

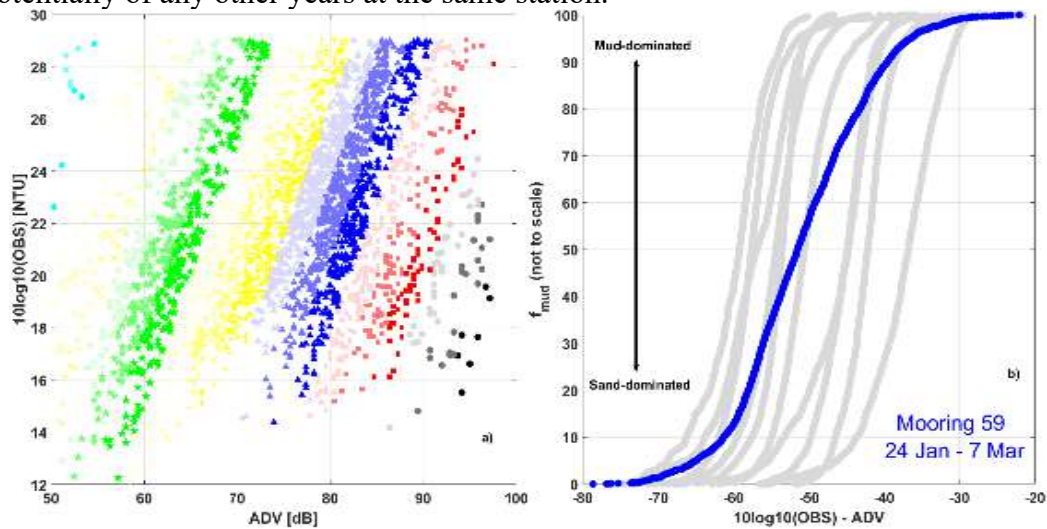


Figure 1. Left: field data illustrates a log-linear relationship between raw OBS and ADV signals of different bins. Right: data from each mooring was divided into 20 bins to derive a mathematical function, describing ratio of sand/mud in suspension as a function of raw OBS and ADV signals.

3. Results and conclusions

Overall, the application of the SCI method provided good predictions of SPMC from raw signals of OBS and ADV (Fig.2). It is worth mentioning that the range of concentration is from 0 – 3 g/L and there is no prior knowledge of particle size distributions and ratios of sand/mud of the suspension. There are two moorings at which the errors were greater than 100 mg/L, i.e., mooring 60 and 73. We noticed a relatively strong correlation between the activities of plankton, represented by the time series of Chlorophyll concentrations (Fig.2 right axis), and the performance of the SCI functions. For example, the Chlorophyll concentrations boosted up during mooring 60 to mooring 62 which might result in a significant error during mooring 60. Similarly, the rapid reduction in Chl concentration from mid-September might also cause the overestimation of concentration for mooring 73. Whereas, other moorings with or without plankton activities do not essentially influence the prediction of SCI functions as long as the Chl concentration is stable. One possible explanation is that under the blooming condition the relationship between OBS and ADV might not be log-linear anymore, or at least at a very different scale in comparison to no blooming. It is noted that in Figure 2, the time in Chl concentrations “timeseries”, i.e., orange stars markers, was relatively scaled to match with the time of each mooring.

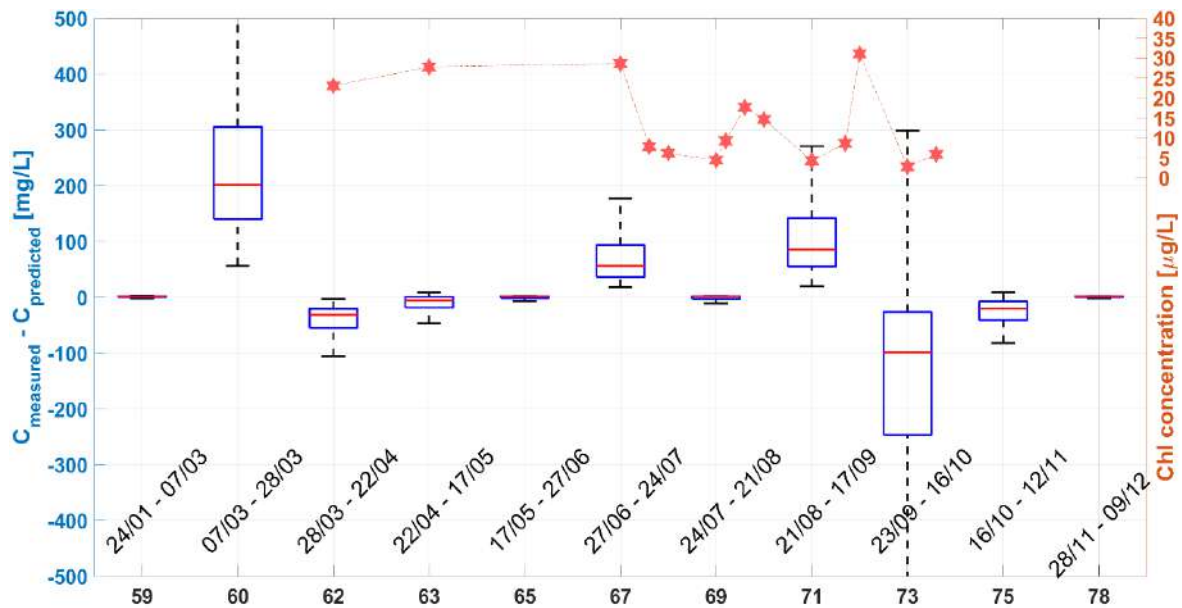


Figure 2. Concentration differences when applying SCI function from Mooring 59 for all the other moorings in the same year. Functions derived from other moorings can also be applied with similar procedure. However, functions obtained from mooring 59 provided the most accurate estimation.

In conclusion, results show that it is possible to develop SCI functions for, at least, a year from a small subset of field data. Such SCI functions then can be applied for the rest of the year in order to predict SPMC without any further requirements of particle size distribution and/or water sample calibrations. Nonetheless, during blooming period a correction coefficient is needed to account for the impact of plankton activities on the behaviours of the OBS and ADV sensors. In the future, we will apply this method for longer historical data and also conduct further investigation on the impact of plankton on the performance of optical and acoustic sensors.

Acknowledgments

This work is part of the research program “PiNS: Particle in the North Sea” funded by Belgian Science Policy and “EU_Sed” funded by Marie Skłodowska-Curie Postdoctoral Fellowship (No 101067047).

References

- Pearson, S., Verney, R., Prooijen, B., Tran, D., Hendriks, E., Jacquet, M., and Wang, Z., (2021). Characterizing the composition of sand and mud suspensions in coastal and estuarine environments using combined optical and acoustic measurements. *JGR: Ocean.* 126(7), e2021JC017354.
- Tran, D., Pearson, S.G., Jacquet, M., Verney, R. (2021) Investigating suspended particulate matters from multi-wavelength optical and multi-frequency acoustic measurements. *vEGU 2021.*



17th International Conference on
Cohesive Sediment Transport Processes
September 18-22, 2023
Inha University, Incheon, Republic of Korea



Estimating bed shear stress with inertial dissipation methods using suspended sediment concentration on the Songdo tidal flat

J. Chang¹, W. Li^{1,2}, G. Lee¹, and O.D. Ajama¹

¹ Department of Oceanography, Inha University, Incheon 22212, Korea

² CAS Key Laboratory of Marine Geology and Environment, Institute of Oceanology, Chinese Academy of Sciences, Qingdao 266071, China

1. Introduction

In steady uniform boundary layer, the dynamics of sediment resuspension and transport process is controlled by the near-bed turbulence (Nelson et al., 1995). And the turbulence is usually quantified by the bed shear stress τ_b , which scales with the shear velocity $u_* = (\tau_b/\rho)^{0.5}$, where ρ is the fluid density. Several different methods to infer bed shear stress have been developed during several decades (e.g., turbulent kinetic energy methods (TKEM), inertial dissipation methods (IDM)), based on the noninvasive, high-resolution flow observation of acoustic instruments (Kim et al., 2000). Lee et al. (2003) proposed an improved IDM and estimated bed shear stress using acoustic backscatter system (ABS) measurements of suspended sediment concentration. However, the constant setting of the sediment settling velocity introduced significant error to this method. With the development of optical instruments, digital floc cameras are capable of providing reliable measurements of sediment settling timescale (Mikkelsen et al., 2005; Smith and Friedrichs, 2015). Thus, in this study, we conducted comprehensive observations involving acoustic and optical instruments on the Songdo tidal flats for more than one month. By introducing the more accurate, time and/or elevation-varying settling velocity, we aim to improve the accuracy of estimating shear stress using suspended sediment concentration and to evaluate the performance of IDM under different hydrodynamic conditions.

2. Instruments Deployment and Methodology

2.1 Instruments Deployment

The observation was conducted at the Songdo tidal flat, Korea (Figure 1a). The instruments deployment was shown as Figure 1b-d. In addition to the mooring observation, we built the system support to do the casting observation involving Floc Camera, CTD and LISST during spring and neap tide respectively. The water samples were also collected during every cast to get the mass concentration of suspended sediment.

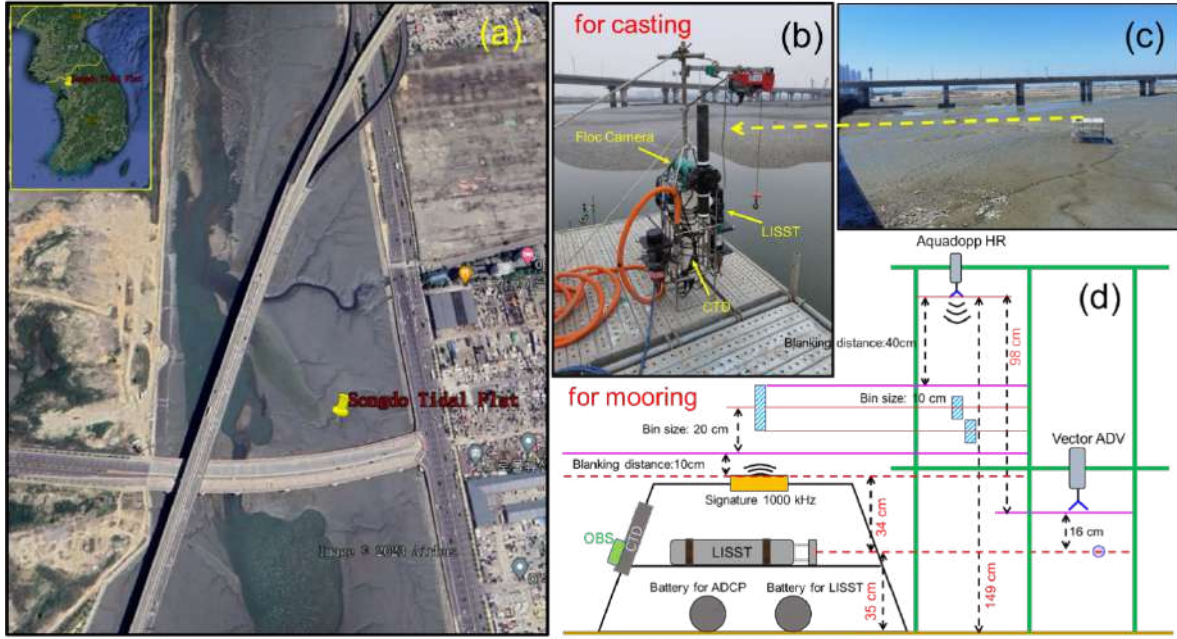


Figure 1. Location map of Songdo site and the instruments deployment.

2.2 Methodology

According to the IDM, three-dimensional TKE spectrum can be described in terms of its spectral density $\phi_{ii}(k)$ (with units of $L^3 T^{-2}$), rate of TKE dissipation ϵ ($L^2 T^{-3}$), and eddy wave number k (L^{-1}) or frequency f (T^{-1}), for which

$$\phi_{ii}(k) = \alpha_i \epsilon^{2/3} k^{-5/3} \quad (1)$$

or

$$\phi_{ii}(f) = \alpha_i (\epsilon U / 2\pi)^{2/3} f^{-5/3} \quad (2)$$

where α_i is one dimensional Kolmogorov constant (Tennekes and Lumley, 1972; Lee et al., 2003).

Suspended sediment concentration, serve as the passive tracers, exhibit a similar distribution of spectral density over an inertial subrange of wave numbers or equivalent frequencies in well-developed turbulent flows (Tennekes and Lumley, 1972). Then similar relationship can be derived:

$$\phi_s(k) = \alpha_s \epsilon_s \epsilon^{-1/3} k^{-5/3} \quad (3)$$

or

$$\phi_s(f) = \alpha_s \epsilon_s \epsilon^{-1/3} (U / 2\pi)^{2/3} f^{-5/3} \quad (4)$$

where $\phi_s(k)$ and $\phi_s(f)$ represent the spectral energy density of sediment concentration, ϵ_s is the rate of dissipation of

fluctuating sediment concentration, and α_s is an empirical constant pertaining to SSC. Within inertial subrange, the rates of TKE production equals to dissipation ϵ by viscosity:

$$\epsilon = u_{*c}^2 \partial u_c / \partial z = K (\partial u_c / \partial z)^2 \quad (5)$$

where K is time-averaged eddy diffusivity of magnitude. And u_{*c} is shear velocity due to currents and z is the height above the bed. Besides, K can be derived as:

$$K = \kappa u_{*c} z \quad (6)$$

where κ is von Karman's constant.

Assuming particle-suspending turbulence as a diffusional process characterized by a time-averaged eddy diffusivity of magnitude K . It equals to the sedimentation of particles with a setting velocity of w_s .

$$w_s C + K \partial C / \partial z = 0 \quad (7)$$

Then the dissipation rate ε_s of turbulence-driven fluctuations in scalar concentration C introduced in equations (3) and (4) is given by

$$\varepsilon_s = -\overline{w'c'} \frac{\partial C}{\partial z} \quad (8)$$

where w' and c' are the fluctuating part of setting velocity and sediment concentration. Additionally, the vertical, turbulent flux of sediment is:

$$\overline{w'c'} = -K \frac{\partial C}{\partial z} \quad (9)$$

Combining equations (7)-(9),

$$\varepsilon_s = (w_s C)^2 / \kappa u_{*c} z \quad (10)$$

Substitution of equations (5) and (10) into equations (3) and (4) yields:

$$u_{*c} = (w_s C) [\alpha_s \{\phi_s(k)\}^{-1} k^{-5/3} \kappa z^{-2/3}]^{1/2} \quad (11)$$

or

$$u_{*c} = (w_s C) [\alpha_s \{\phi_s(f)\}^{-1} f^{-5/3} (U/2\pi\kappa z)^{2/3}]^{1/2} \quad (12)$$

The w_s derived from Floc Camera. The C and U are from ADV or Aquadopp HR. Then shear velocity u_{*c} can be calculated based on the equations (11) and (12). More detailed introduction of IDM can be founded from Lee et al. (2003).

3. Results and Conclusions

The expected results will increase the accuracy of the bed shear stress derived from improved IDM using suspended sediment concentration. Moreover, the time series observations help us to evaluate the applicability of IDM at strong and weak currents. Time series of bed turbulence structure and its influencing factors can be also analysed.

References

- Kim, S. C., Friedrichs, C. T., Maa, J. Y., & Wright, L. D. (2000). Estimating bottom stress in tidal boundary layer from acoustic Doppler velocimeter data. *Journal of Hydraulic Engineering*, 126(6), 399-406. [https://doi.org/10.1061/\(ASCE\)0733-9429\(2000\)126:6\(399\)](https://doi.org/10.1061/(ASCE)0733-9429(2000)126:6(399))
- Lee, G. H., Dade, W. B., Friedrichs, C. T., & Vincent, C. E. (2003). Spectral estimates of bed shear stress using suspended - sediment concentrations in a wave - current boundary layer. *Journal of Geophysical Research: Oceans*, 108(C7). <https://doi.org/10.1029/2001JC001279>.
- Mikkelsen, O. A., Hill, P. S., Milligan, T. G., & Chant, R. J. (2005). In situ particle size distributions and volume concentrations from a LISST-100 laser particle sizer and a digital floc camera. *Continental Shelf Research*, 25(16), 1959-1978. <https://doi.org/10.1016/j.csr.2005.07.001>.
- Nelson, J. M., Shreve, R. L., McLean, S. R., & Drake, T. G. (1995). Role of near - bed turbulence structure in bed load transport and bed form mechanics. *Water resources research*, 31(8), 2071-2086. <https://doi.org/10.1029/95WR00976>.
- Smith, S. J., & Friedrichs, C. T. (2015). Image processing methods for in situ estimation of cohesive sediment floc size, settling velocity, and density. *Limnology and Oceanography: Methods*, 13(5), 250-264. <https://doi.org/10.1002/lom3.10022>.
- Tennekes, H., and Lumley, J. L. (1972) *A First Course in Turbulence*, 300 pp., MIT Press, Cambridge, Mass., 1972



17th International Conference on
Cohesive Sediment Transport Processes
September 18-22, 2023
Inha University, Incheon, Republic of Korea



Extracting suspended sediment concentration periodicity from diverse datasets

Y. Wang¹, H. Lin², Q. Yu² and S. Gao²

¹ School of Marine Science and Engineering, Nanjing Normal University, Nanjing, China,
ms.ywwang@gmail.com

² Ministry of Education Key Laboratory for Coast and Island Development, School of
Geography and Ocean Science, Nanjing University, Nanjing, China

Suspended sediment concentration (SSC) is a key parameter of physical and biogeochemical processes in nearshore waters, which is controlled by periodic forcing factors and exhibits periodic variations at multiple time scales. Identifying the key periods and extracting the corresponding amplitudes and phases can greatly help to characterize the representative features of SSC and further assist in physical interpretation. However, in actual observations, the SSC time series inevitably contains random or systematic data gaps, such as data gaps during high cloud cover periods in remote sensing time series and extensive data gaps during low tide periods in tidal flat measurements.

In this study, we obtained buoy hydrological data from the Xiaomiaohong tidal channel in Jiangsu, China, tripod observation data from the tidal flat along the channel edge, and SSC time series derived from hourly GOCI satellite images from 2011 to 2019 in the study area. We then used Lomb-Scargle periodogram and phase folding diagrams to extract the periodic information of the above data sets, and interpreted the differences in the multi-period SSC variations extracted from different data types in the same area. We further filtered the SSC data retrieved from the buoy echo intensity based on water level data, and designed random experiments as a control to simulate the data characteristics of systematic data gaps during low tide periods and investigate the impact of such gaps on periodicity extraction.

Remote sensing data successfully identified the periods of semidiurnal, diurnal, spring-neap, and seasonal variations, while high-resolution buoy data additionally identified the M₄ period. The phases of the SSC variations in the spring-neap tide extracted from remote sensing and buoy data were basically consistent, while the peak SSC appeared during peak flood and peak ebb, respectively. Sediment at the bottom of the tidal channel is suspended and diffused to the water column surface after being stirred up by waves during high tide, while the remote sensing retrieval area includes the tidal flats on both sides of the channel, where the sediment is transported into the water column during peak floods. The short duration of the semidiurnal tides enables this phase difference to be reflected. We also found that data missing during low tide period can cause the splitting of M₂ period into other harmonic periods, such as the μ_2 harmonic period of 12.87 hours, which is consistent with the results of tripod SSC data period identification.

This study uncovers variances in the efficacy of distinct datasets when extracting periodic features, thus aiding individuals in comprehending the range of application scenarios and constraints associated with such extractions.

References

- Lin, H., Q. Yu, Y. Wang, and S. Gao (2022), Identification, extraction and interpretation of multi-period variations of coastal suspended sediment concentration based on unevenly spaced observations, *Marine Geology*, 445, 106732, <https://doi.org/10.1016/j.margeo.2022.106732>.
- Lin, H., Q. Yu, Y. Wang, and S. Gao (2022), Assessment of the potential for quantifying multi-period suspended sediment concentration variations using satellites with different temporal resolution, *Science of The Total Environment*, 853, 158463, <https://doi.org/10.1016/j.scitotenv.2022.158463>.

Session: Sediment Transport V
09:00 – 10:40
Friday, September 22, 2023



17th International Conference on
Cohesive Sediment Transport Processes
September 18-22, 2023
Inha University, Incheon, Republic of Korea



Gravity-driven sediment transport processes on muddy coasts

Q. Yu¹, Y. Peng¹ and S. Gao¹

¹ Ministry of Education Key Laboratory for Coast and Island Development, School of Geography and Ocean Science, Nanjing University, Nanjing, China, qianyu.nju@gmail.com

Wave and/or current supported gravity-driven sediment flows (GDSFs) cause substantial sediment movement across the continental shelf, contributing to morphological evolution in many regions worldwide. However, they appear to occur episodically and ephemerally and, therefore, it remains a challenge to document them in detail with in situ measurements.

Here we present solid evidence of frequent generation of such flows over the shallow sea floor of a muddy open coast, Jiangsu Coast, China. They were triggered by wave resuspension and/or sediment settling from the overlying water column, maintained by wave- and/or current-induced bed stress, and terminated due to upward spreading of bottom sediment within the high concentration layer. Randomly selected GDSF events were analyzed to realize parameterization with a buoyancy-friction model; the resultant bed drag coefficient for two of the cases is higher than the value of 0.003, which is attributed to the additional drag at the interface between the overlying flow and the moving GDSFs. For GDSF events which developed at the low slack water, time lags of events at the break and toe sites of a cross-shore submarine slope were consistent with what could be expected in terms of gravity-driven velocities and distances, showing gravity-driven downslope movement of sediments across the gently sloping coast. Abnormal low drag bed coefficient and bulk Richardson number values for GDSF events at the toe site suggested that the momentum balance was not satisfied here and the local slope was not enough to provide the necessary gravity to drive the high concentration layers going on moving offshore.

Although short-lived, the observed GDSF events in the three different seasons indicate that they occur more frequently than previously thought. GDSF events result in considerable cross-shore sediment transport and sedimentation effects, highlighting the importance of GDSFs for the transport processes of sediments in muddy coastal areas, despite relatively brief duration and finite transport distance.

References

- Peng, Y., Yu, Q., Du, Z., Wang, L., Wang, Y., and Gao, S. (2022). The dynamics of wave and current supported gravity flows: Evaluation of drag coefficient and bulk Richardson number. *Mar. Geol.* 454, 106947.
- Peng, Y., Yu, Q., Du, Z., Wang, L., Wang, Y., and Gao, S. (2022). Gravity-driven sediment flows on the shallow sea floor of a muddy open coast. *Mar. Geol.* 445, 106759.



17th International Conference on
Cohesive Sediment Transport Processes
September 18-22, 2023
Inha University, Incheon, Republic of Korea



Foraminifera response to changes in mud sedimentation and marine environmental health, case of Bushehr port, Iran "

Shadan Nasser Doust¹, Mehrnoosh Abbasian¹, Majid Shah-hosseini², S. Abbas Haghshenas¹

¹Institute of Geophysics, University of Tehran, Tehran, Iran

²Department of Geography, Tarbiat Modares University, Tehran, Iran

Introduction

Foraminifera are ancient, single-celled marine organisms that have thrived in the oceans for more than 500 million years. They play a crucial role in marine food webs and serve as bioindicators of marine ecosystem health. Abundance and variety of Foraminifera as well as high sensitivity and fast response to environmental changes, makes them ideal for studying past and present environmental conditions. Foraminifera are highly sensitive to changes in water temperature, salinity, nutrient availability and pollutants. This makes them valuable tools for monitoring marine ecosystems and understanding the effects of natural and anthropogenic disturbances on these systems. Although not highly sensitive to small environmental changes, foraminifera are still useful bioindicators for tracking changes in marine ecosystems.

Marine In Danger (hereafter referred to MIND) is a decision-making approach that utilizes bioindicators, such as foraminifera, to assess the health of marine ecosystems. MIND enables users to analyze and interpret bioindicators in order to identify areas of concern and make informed decisions about marine management and conservation. It is an easy-to-use tool that can be used by anyone who is interested in assessing the health of marine ecosystems. In addition to assisting in developing conservation strategies and monitoring environmental impacts, MIND is particularly useful for decision-making processes related to managing marine ecosystems. The use of bioindicators such as foraminifera is essential for assessing marine ecosystem health and approaches like MIND are crucial for interpreting and applying this information to support informed decisions about the future of coastal ecosystems.

The study conducted at Bushehr Port located on the Northern coast of the Persian Gulf, aims to investigate the impact of mud deposition on foraminifera abundance and variety. Mud deposition in the port can have adverse effects on marine organisms due to reduced water clarity and oxygen levels in which Foraminifera are particularly sensitive. By analyzing the foraminiferal assemblages in sediment samples collected from three different sites within the port, the study aimed to determine changes in foraminiferal abundance and species composition.

Results and Discussions

The study's findings have implications for the management and conservation of marine ecosystems. Study findings guide effective marine ecosystem management and conservation by identifying conservation areas, suggesting plans, and improving practices to mitigate negative impacts. Foraminifera can act as early warning indicators of environmental changes and provide valuable information about the health of marine ecosystems. By understanding the impact of mud deposition on foraminiferal abundance, we can develop strategies to mitigate the effects of anthropogenic disturbances on marine ecosystems. This study highlights the importance of foraminifera and their role as bioindicators of marine ecosystem health.

The results indicate a negative correlation between mud content and foraminifera abundance. Furthermore, the diversity and species richness of foraminifera were found to be lower in areas with high mud content. Our findings suggest that the deposition of mud in the port area is a major factor impacting the health and diversity of the marine ecosystem. The study highlights the importance of monitoring and managing sedimentation in port areas to protect marine biodiversity and ecosystem health.

References

Aref Farhangmehr, S. Abbas Haghshenas, Ehsan Zrinfar, Investigating Sedimentation in Bushehr Port Access Channel, Adopting Periodic Sonar Surveys and Numerical Simulations, International Conference on Cohesive Sediment, 2021.

Farzin Samsami, S. Abbas Haghshenas, Mohsen Soltanpour, Physical and Rheological Characteristics of Sediment for Nautical Depth Assessment in Bushehr Port and Its Access Channel. *Water*, 2022, 14, 4116. <https://doi.org/10.3390/w14244116>

Mehrnoosh Abbasian, S. Abbas Haghshenas, Majid Shah-hosseini, Aref Farhangmehr, Hamid Rezaei, Azadeh Razavi Arab, Michael John Risk, Biodeposit dispersion around a deep cage finfish farm in the Northern Persian Gulf, *Regional Studies in Marine Science*, 2023, 102950, ISSN 2352-4855, <https://doi.org/10.1016/j.rsma.2023.102950>

S. Abbas Haghshenas, Farzin Samsami, & Azadeh Razavi Arab, & Mohsen Soltanpour, & Michael Risk, Sediment Constituent Analysis; Application of a new "Toolbox" for the study of Iranian coastlines. 10th International Conference on Coasts, Ports & Marine Structures (ICOPMAS), 2012.



17th International Conference on
Cohesive Sediment Transport Processes
September 18-22, 2023
Inha University, Incheon, Republic of Korea



Erosion, Transport, and Abrasion of Dense Mud Aggregates

S. Jarrell Smith¹, Kelsey A. Fall¹, David W. Perkey¹, Richard Styles¹, and Danielle R. Tarpley¹

¹ U.S. Army Engineer Research and Development Center, Vicksburg, Mississippi, USA
Jarrell.Smith@usace.army.mil

1. Introduction

Dense mud aggregates can be generated by soil or surface bed erosion, slope failure, biological processes, or dredging activities. These mud aggregates (also referred to as clasts, bed aggregates, fecal pellets, mud pebbles, among others) settle at much faster rates than their constituent particles, which can alter the transport mode, deposition, and ultimate fate of the sediment (Perkey et al. 2020). Because of these changes in transport mode and fate, the processes associated with transport of mud aggregates are of interest to palaeogeologists and management of port, channel, and reservoir sedimentation. The present study examines the production of bed aggregates through surface erosion of muddy beds, the transport modes of eroded aggregates, and the abrasion of these aggregates through the action of bedload transport. From these observations, a predictive model is developed and evaluated against laboratory and field data.

2. Materials and Methods

Sediments were sourced from 14 sites across diverse geological settings along the United States Great Lakes, Atlantic, and Gulf of Mexico coasts. Each sample was predominantly mud, but varied in size composition, clay mineralogy, organic content, and plasticity. Sediments were tested in minimally disturbed field state and in remolded condition with varying water content in the laboratory.

Field-collected and laboratory-prepared cores were eroded with the Sedflume erosion device (McNeil et al. 1996). Eroded aggregate size was optically measured immediately downstream of the eroded sediment surface and also by physical screening of the eroded sediment suspension. Aggregate abrasion was determined by two methods, measured size reduction of aggregates in a 12-m-long oscillatory flume and measured mass reduction in a table-top aggregate tumbler. In each case, aggregates were molded at a specific water content and cut to a specific size prior to introduction to the testing device. In the oscillatory flume, aggregate size was measured optically with an array of cameras; in the tumbler, change in aggregate size was determined by mass.

Based upon the observations of aggregate production and aggregate abrasion, an aggregate abrasion model was developed and evaluated for application in Eulerian sediment transport models. The model developed is an adapted form of the model presented by Parker (1991) for gravel abrasion in rivers. The model includes multiple mud aggregate size classes, and algorithms to estimate settling velocity, transport mode, bedload velocity, and mass transfers between size classes associated with abrasion. Initial testing of the model was conducted in a

simplified, time-resolved, 0D (spatial) application to evaluate solution schemes, accuracy, sensitivity, and computational expense.

3. Results and Conclusions

Surface erosion produced aggregates for nearly all samples and under a wide range of conditions. The abundance of mud aggregates varied from 10% to 70% of the total eroded mass. Both size and abundance of aggregates produced through surface erosion correlated with clay content and the Liquidity Index (LI), a derived quantity from Atterberg Limits testing. These results suggest that aggregate erosion may not be important at all sites and under all conditions, but aggregate erosion may be dominant for sediments with high clay content, especially if the water content is near or below the Liquid Limit.

Abrasion testing indicated that mm-scale mud aggregates initially transport as bedload. Additionally, Shields and Rouse parameters, commonly applied for non-cohesive sediment transport, appear to be appropriate descriptors for initial motion and suspension of mud aggregates. Aggregate size was observed to diminish with bedload transport distance, closely following the so-called Sternberg Equation developed for gravel abrasion in rivers.

$$D(x) = D_0 e^{-\alpha x} \quad (1)$$

where D is mud aggregate size, D_0 is the initial aggregate size, α is an empirical abrasion rate constant, and x is distance. While α varied considerably by site and aggregate density, LI explained most of the variability. Abrasion rates (α) determined from testing coupled with Equation 1 suggest that centimetre-scaled aggregates can transport kilometres to tens of kilometres before abrading to sizes that would transport in suspension.

Initial, 0-D testing of the numerical model framework indicates that the model with discrete size classes replicated analytical solutions and reproduced laboratory testing scenarios well within the confidence intervals of the observations. Computational time was found to depend on the number of aggregate size classes, the initial mass of aggregated material, and α . Computational expense for the aggregate abrasion model is estimated to be between 1% and 10%, excluding the additional computational expense of handling additional size classes by the transport model.

This study suggests that erosion and transport of dense mud aggregates could be important for certain applications, particularly for disturbances of densely consolidated sediments as produced by dredging, slope or bank failure, or extreme events.

References

- Perkey, David W, S Jarrell Smith, Kelsey A Fall, Grace M Massey, Carl T Friedrichs, and Emmalynn M Hicks. 2020. "Impacts of Muddy Bed Aggregates on Sediment Transport and Management in the Tidal James River, VA." *Journal of Waterway, Port, Coastal, and Ocean Engineering* 146 (5): 04020028. [https://doi.org/10.1061/\(ASCE\)WW.1943-5460.0000578](https://doi.org/10.1061/(ASCE)WW.1943-5460.0000578)
- McNeil, Joe, Catherine Taylor, and Wilbert Lick. 1996. "Measurements of erosion of undisturbed bottom sediments with depth." *Journal of Hydraulic Engineering* 122 (6): 316-324.
- Parker, Gary. 1991. "Selective sorting and abrasion of river gravel. I: Theory." *Journal of Hydraulic Engineering* 117 (2): 131-147.

Session: Mud Rheology/Consolidation
10:40 – 12:00
Friday, September 22, 2023



17th International Conference on
Cohesive Sediment Transport Processes
September 18-22, 2023
Inha University, Incheon, Republic of Korea



Application of Artificial Neural Network for Determining Rheological Properties of Mixed Sediment in the Persian Gulf

M. Hajibaba¹, F. Samsami² and S. A. Haghshenas³

¹ Civil Engineering Department, K. N. Toosi University of Technology, Tehran, Iran,
maryam_hajibaba@email.kntu.ac.ir

² Civil Engineering Department, West Tehran Branch, Islamic Azad University, Tehran, Iran,
samsami@wtiau.ac.ir

³ Institute of Geophysics, University of Tehran, Tehran, Iran, saahaghshenas@ut.ac.ir

1. Introduction

Rheological properties of cohesive and mixed sediment are of the utmost importance for assessment of sediment characteristics. The rheological features of sediment are affected by factors such as sediment composition, grain size, water content, carbonate and organic content and physico-chemical conditions. There are numerous machine learning algorithms for prediction tasks with different purposes. An artificial neural network (ANN) is one of the of the main tools used in machine learning models which has been broadly employed in different contexts including sediment properties prediction. In the present study, the rheological properties of mixed sediment are predicted by the Artificial Neural Network (ANN) method based on diverse datasets including Bushehr Port and its access channel, Imam Khomeini Port and some artificial sediment samples.

2. Methodology

The Bushehr Port, in the Soltani Estuary in the Bushehr Peninsula and Imam Khomeini Port at the end of Musa Estuary waterway are located on the coast of the Persian Gulf which considered as the most significant commercial ports in Iran. Collected samples from these ports are mostly mixed sediment consist of clay, silt, and very fine sand with organic matter which are characterized as cohesive and muddy sediment (Samsami et al., 2022; Oceans Research Co., 2020). In order to obtained sediment characteristics particle size distribution; organic and carbonate contents; rheometry; density, concentration and water content tests were performed for selected natural and artificial samples. Totally, 54 samples from collected surface and core samples from Bushehr and Imam Khomeini Ports and some artificial sediment samples were investigated and the obtained static and dynamic yield stresses from rotational and oscillatory rheological tests were used in this study.

Artificial Neural Network (ANN) as a subset of machine learning, is in control of collection of neurons in order to learn and train totally 70% of datasets and 30% for the verification. ANN is comprised of three layers, containing an input layer, one or more hidden layers, and an output layer (Figure 1).

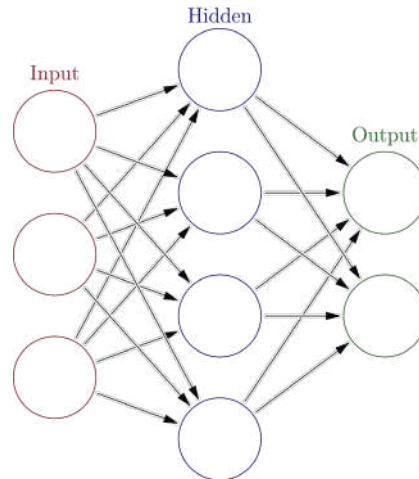


Figure 1. An artificial neural network layers (extracted from Wikipedia, 2023).

By considering the wide range of potential parameters affecting the yield stress of sediment, it is vitally important to define which datasets as the input of neural network. It was attempted to determine number of neurons and after some trial and errors, eight neurons were chosen to build a neural network in the present study. The neural network was trained by using the Luenberg-Marquardt training algorithm and at the end of training and creating the neural network, the performance of the network was evaluated by mean square error (MSE) and correlation coefficient (R) parameters. Figure 2 illustrates the performance of neural network for static and dynamic yield stresses, respectively.

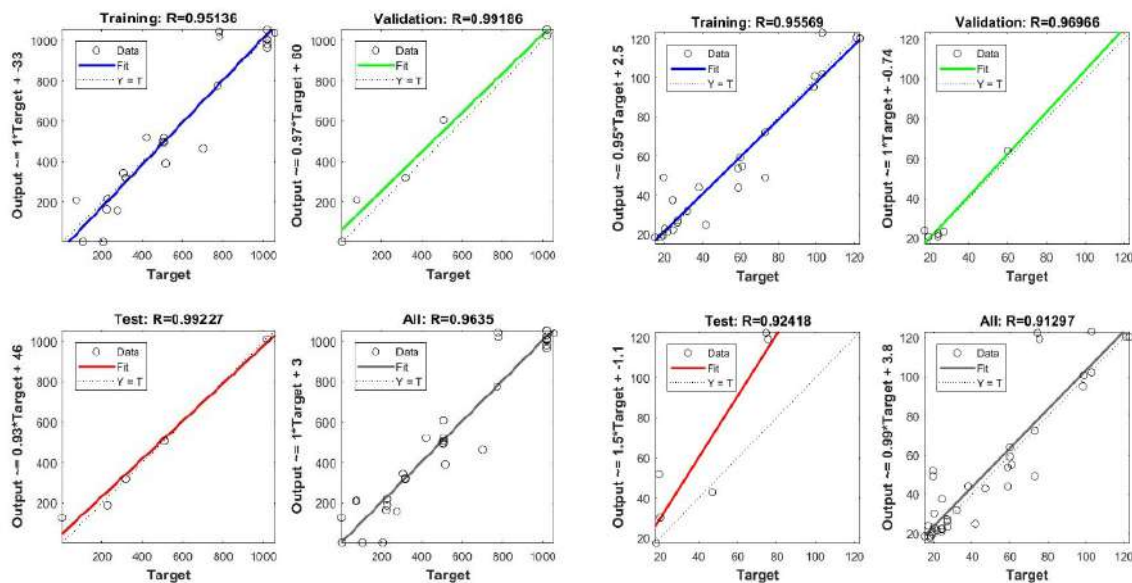


Figure 2. The performance of neural network for static (left) and dynamic (right) yield stresses.

3. Conclusions

The presented approach has provided a logical relationship between the measured parameters and the static and dynamic yield stresses. The obtained correlation coefficient values confirmed the promising ability of ANN for the performance prediction of yield stresses in this study. Moreover, due to the high ability in adaptive learning the proposed model could trained well from various potential parameters of yield stress.

References

- Oceans Research Co. (2020). Investigation of Sedimentation Pattern in the Bushehr Port after Its Development Project. Ports and Maritime Organization of Iran, Tehran, Iran.
- Samsami, F., Haghshenas, S.A., and Soltanpour, M. (2022). Physical and Rheological Characteristics of Sediment for Nautical Depth Assessment in Bushehr Port and Its Access Channel. *Water*, 14(24):4116. doi: 10.3390/w14244116
- Wikipedia contributors. (2023). Artificial neural network. In Wikipedia, The Free Encyclopedia. https://en.wikipedia.org/wiki/Artificial_neural_network



17th International Conference on
Cohesive Sediment Transport Processes
September 18-22, 2023
Inha University, Incheon, Republic of Korea



Simulation of fluid mud flow through FVCOM model with considering three-dimensional rheological properties

Gaochuang Shi, Qinghe Zhang, Jinfeng Zhang

State Key Laboratory of Hydraulic Engineering Simulation and Safety, Tianjin University,
Tianjin 30072, China

1. Introduction

Fluid mud often occurs in estuarine and coastal areas that are rich in fine sediment, posing a critical management problem (McAnally et al., 2007). To predict the fluid mud motion, many models have been proposed from the early depth-averaged models (Odd and Cooper, 1989) to the recent continuous simulating method (Le Hir et al., 2000; Chmiel et al., 2021). However, all previous numerical models adopted the apparent viscosity from the one-dimensional (1DV) rheological model, and missed the effect of velocity shear in horizontal directions, which may be significant in complicated coastal and estuarine situations.

In this presentation, in order to reflect fluid mud motion more accurately, we will develop a continuous modelling approach by introducing the apparent viscosity of the 3D Herschel-Bulkley model into FVCOM, and discuss the result differences due to apparent viscosities of 3D form and 1DV form.

2. Methods and Results

The apparent viscosity of the three-dimensional rheological model of Herschel-Bulkley body can be expressed as:

$$v_a = \left(K \sqrt{(2\mathbf{II}_E)^{n-1}} + \frac{\tau_0}{\sqrt{2\mathbf{II}_E}} \right) \quad (1)$$

where τ_0 , K , n are rheological parameters, \mathbf{II}_E is the second invariant of the rate of strain tensor. For laminar movement of the fluid mud, the vertical eddy viscosity coefficient K_m and horizontal eddy viscosity coefficient A_m in the FVCOM model are replaced by the apparent viscosity v_a .

The developed model is validated against the experiment of van Kessel and Kranenburg (1996) on the gravity current of fluid mud on a slope. Figure 1 shows satisfactory agreements between simulated and measured velocity and density profiles. Figure 2 displays the simulated fluid mud flow along the slope at the time of 40s. Figure 3 compares the results of fluid mud obtained by simulating an ideal scenario with both the 3D and 1DV models, displaying clear differences in their horizontal distribution.

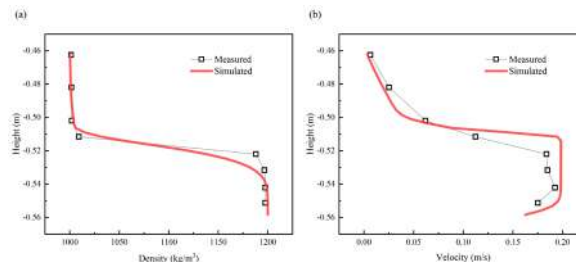


Figure 1. Comparison velocity and density profile with van Kessel and Kranenburg's experiment data, (a) density profile; (b) velocity profile; the red line is simulation results, squares: measured data.

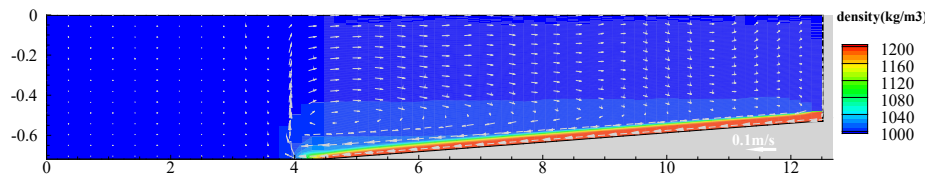


Figure 2. Snapshot of fluid mud movement

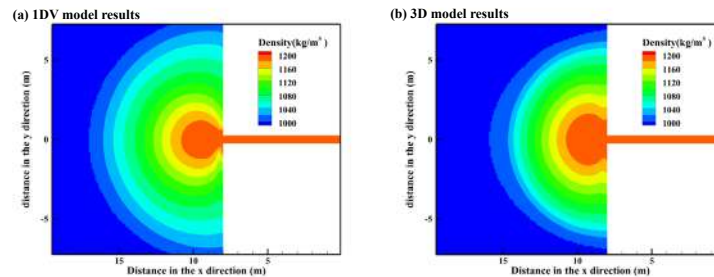


Figure 3. Comparison of Simulation Results between 1D and 3D Models

3. Conclusions

A 3D Herschel-Bulkley rheological model was introduced into the finite volume ocean model FVCOM through the apparent viscosity of the fluid mud. The developed model was verified by flume experiment about fluid mud. The simulation results show that the developed numerical model can simulate the fluid mud with obvious non-Newtonian properties, and reflect the continuous transition from Newtonian water body to non-Newtonian fluid mud body. Additionally, based on the comparison between results of the 3D and 1DV models, it was demonstrated that the 3D rheological model is more appropriate for complex hydrodynamic conditions in practical situations.

References

- Chmiel, O., Naulin, M., Malcherek, A., 2021. Combining Turbulence and Mud Rheology in a Conceptual 1DV Model – An advanced continuous modeling concept for fluid mud dynamics. *Die Küste*, 89 1–27. <https://doi.org/10.18171/1.089101>
- Kessel, T. van, Kranenburg, C., 1996. Gravity Current of Fluid Mud on Sloping Bed. *Journal of Hydraulic Engineering* 122, 710–717. [https://doi.org/10.1061/\(ASCE\)0733-9429\(1996\)122:12\(710\)](https://doi.org/10.1061/(ASCE)0733-9429(1996)122:12(710))
- Le Hir, P., Bassoullet, P., Jestin, H., 2000. Application of the continuous modeling concept to simulate high-concentration suspended sediment in a macrotidal estuary, in: *Proceedings in Marine Science*. Elsevier, pp. 229–247. [https://doi.org/10.1016/S1568-2692\(00\)80124-2](https://doi.org/10.1016/S1568-2692(00)80124-2)
- McAnally, W.H., Friedrichs, C., Hamilton, D., Hayter, E., Shrestha, P., Rodriguez, H., Sheremet, A., Teeter, A., ASCE Task Committee on Management of Fluid Mud, 2007. Management of Fluid Mud in Estuaries, Bays, and Lakes. I: Present State of Understanding on Character and Behavior. *J. Hydraul. Eng.* 133, 9–22. [https://doi.org/10.1061/\(ASCE\)0733-9429\(2007\)133:1\(9\)](https://doi.org/10.1061/(ASCE)0733-9429(2007)133:1(9))
- Odd, N.V.M., Cooper, A.J., 1989. A Two-Dimensional Model of the Movement of Fluid Mud in a High Energy Turbid Estuary. *Journal of Coastal Research* 185–193.



17th International Conference on
Cohesive Sediment Transport Processes
September 18-22, 2023
Inha University, Incheon, Republic of Korea



Turbulence measurements in a hyperturbid estuary

M. Becker¹, R. Kopte¹, M. Naulin², C. Maushake² and C. Winter¹

¹Institute of Geosciences, CAU Kiel, Otto-Hahn-Platz 1, 24118 Kiel, Germany,
marius.becker@ifg.uni-kiel.de

²BAW, Federal River Engineering and Research Institute, Hamburg, Germany

1. Introduction

The Ems estuary, located at the North Sea along the border between The Netherlands and Germany, has been studied intensively with respect to fluid mud and sediment transport (e.g., Van Maren et al., 2015; Winterwerp & Wang, 2013). A contiguous fluid mud layer covers the river bed over several tens of kilometers along the channel, far upstream of the salt intrusion (e.g. Talke et al., 2009). The water column exhibits a two-layer structure. High concentrations of flocculated cohesive sediments introduce a significant density anomaly. The stratification is controlled by a balance between hindered settling and entrainment (Winterwerp, 2002; Wolanski et al., 1988). Entrainment is observed mainly during the flood phase, while less or no entrainment occurs during ebb. Restratification after flood entrainment occurs early during the flood tide with a strong effect on the vertical velocity structure, a mechanism previously referred to as mud-induced periodic stratification (MIPS, Becker et al., 2018).

Earlier studies on fluid mud dynamics in natural environments lacked information on turbulence. Instead, based on time averaged velocity shear and stratification, the gradient Richardson number was often used in order to assess the influence of turbulent mixing on the velocity profile, the density structure, and the respective variations during the tidal cycle. This study presents new results on turbulence parameters, acquired during the MUDMEAS field survey in the Ems estuary.

2. The MUDMEAS survey

The MUDMEAS survey was conducted between 2021/09/20 and 2021/10/01. Ship-based data were collected at Weener, located relatively close to the weir, the upstream end of the tidally influenced part of the Ems tidal river. The ship was attached to dolphins aside the navigation channel. ADCP and SES data were acquired continuously. Current velocities in the fluid mud layer were measured by ECMs on a frame, placed on the muddy river bed aside the ship. Vertical OBS and CTD casts were collected during four tidal cycles, two tidal cycles in the first and in the second weak, during spring and neap tide conditions.

Turbulent shear was measured by two RSI *MicroPod* shear probes, which acquired horizontal and vertical shear, induced by the respective velocity fluctuations orthogonal to the orientation of each probe. The shear probes and the data logger were deployed in a streamlined housing, the *Podfish*. Due to the design, the shear probes were always oriented against the flow direction at the respective vertical position. This velocity was measured by an EM current meter on the *Podfish*. During each tidal cycle, the *Podfish* was moved step-wise in the vertical, collecting profiles across the water column. It was parked at a certain position for a few minutes before moving to the next vertical location. The snippets of shear data were analyzed for the

dissipation rate of turbulent kinetic energy (Lueck, 2013). In a first approach, this was done assuming shear spectra to follow the Nasmyth spectrum, ignoring potential effects of stratification on the shape of the spectra.

3. Results

Initial results regarding the velocity structure and stratification show neap-spring variations, with reduced tidal velocities and increased stratification during neap tide. Regarding along-channel variations of the fluid mud layer structure, the MUDMEAS location at Weener is compared to data collected further downstream at Jemgum. SSC and stratification were on average higher at Weener, both during neap and ebb tide, referring to comparable seasons and discharge conditions. Very little entrainment occurred during the ebb phase. High levels of turbulence were confined to the upper layer above the lutocline, as shown by the dissipation rate determined from segments of shear probe data. In contrast, entrainment was observed during the last part of the ebb tide at Jemgum, induced by the displacement of the main shear layer from a position above the lutocline down to the river bed, probably supported by comparatively higher ebb current velocities and less stratification.

A similarity between the two locations was the ebb-directed velocity in the fluid mud layer, which was observed after restratification during the last part of the flood. At Weener, these velocities reached 0.5 m s^{-1} during a period of essentially no turbulence below the lutocline. The ebb-directed fluid mud flow was observed during flood slack water until the beginning of the ebb tide (see Fig. 1, between 3 and 6 h). It was followed by a short term increase of velocity in the fluid mud layer, corresponding to a local maximum of the dissipation rate (at 6.5 h). This increased dissipation was separated vertically from high dissipation rates closer to the water surface by a local minimum at the height of the lutocline, indicating that there was less or no mixing between fluid mud and the upper part of the water column. Further analysis of turbulence, stratification and entrainment requires to revisit the procedure to estimate the dissipation rate.

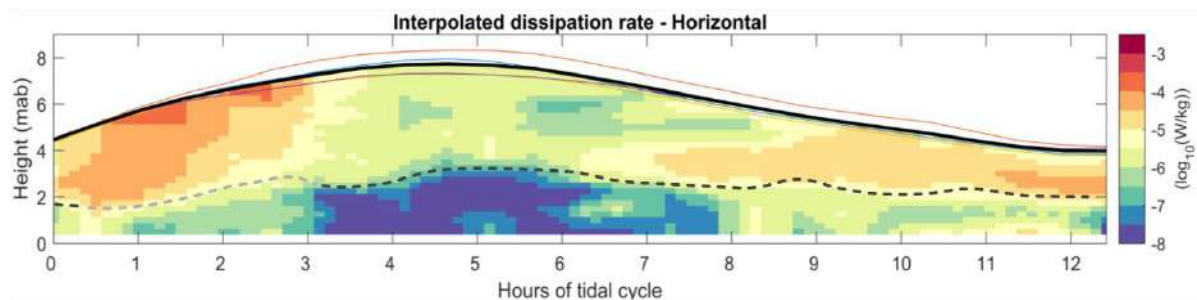


Fig. 1.: Dissipation rate derived from horizontal shear spectra, interpolated vertically and in time. Data collected during four tidal cycles is merged, ignoring differences between the tidal cycles, e.g. with respect to the vertical structure and temporal variations of density and mean velocity. The black line denotes the tidal cycle average of the water level elevation. Thin adjacent lines indicate the actual water level during each tidal cycle. The dashed line indicates the height of the lutocline.

Two issues were encountered during the preliminary analysis. The first is related to the way how the shear probes were used, relying on a certain mean velocity by which turbulent structures are advected past the shear sensors, assuming frozen turbulence. As this velocity decreases, the size of the largest detectable eddies decrease and the smallest detectable wave numbers increase. The inertial subrange may not be well resolved and a part of dissipation range is used to estimate the dissipation rate. Adversely, in case of low ambient velocity,

instrument noise affects shear in the dissipation range, which due to the nature of this noise may lead to an overestimation of the dissipation rate (Fer and Paskyabi, 2013).

The second issue is seen rigorously using the probably overestimated dissipation rates to determine the Ozmidov length scale, denoting the largest possible eddies in presence of stratification. First analysis shows that the inertial subrange is potentially influenced by internal waves during large parts of the tidal cycle, which was expected, owing to the high values of stratification. Given the high values of stratification, it is therefore suggested that the dynamics are controlled predominantly by layered stratified turbulence and that internal waves play an important role (see also Dyer et al., 2006).

Outlook

The aforementioned aspects will be addressed by further analysis of the acquired data set, in particular the stratification effects on turbulence measurements, which are not fully accounted for at this stage. The main focus will be on turbulence in the fluid mud layer and the respective influence of internal waves, which are already seen in a preliminary analysis of ADCP velocity data.

Acknowledgments

This research was funded by BAW, Federal River Engineering and Research Institute, Hamburg, Germany. The captain and the crew of the research vessel FK Littorina are thanked for their initiative and their support during the cruise. The measurements could not have been conducted without the help of Anna Wünsche, Filipe Galiforni Silva, Gabriel Herbst, and Hao Wu, who participated in the survey. Marius Becker is funded by KMS, Kiel Marine Science. Robert Kopte is funded by the Underway Research Data Project of the German Marine Research Alliance.

References

- Becker, M., C. Maushake, and C. Winter (2018), Observations of Mud-Induced Periodic Stratification in a Hyperturbid Estuary, *Geophysical Research Letters*.
- Dyer, K. R., M. C. Christie, and A. J. Manning (2004), The effects of suspended sediment on turbulence within an estuarine turbidity maximum, *Estuarine, Coastal and Shelf Science*, 59(2), 237-248.
- Fer, I., and B. Paskyabi (2013), Autonomous Ocean Turbulence Measurements Using Shear Probes on a Moored Instrument, *Journal of Atmospheric and Ocean Technology*, 31, 474-498.
- Lueck, R. (2013), RSI Technical Note 028, Calculating the Rate of Dissipation of Turbulent Kinetic Energy, Rockland Scientific.
- Van Maren, D. S., J. C. Winterwerp, and J. Vroom (2015), Fine sediment transport into the hyper-turbid lower Ems River: the role of channel deepening and sediment-induced drag reduction, *Ocean Dynamics*, 65(4), 589-605.
- Winterwerp, J. C. (2002), On the flocculation and settling velocity of estuarine mud, *Continental Shelf Research*, 22(9), 1339-1360.
- Winterwerp, J. C., and Z. B. Wang (2013), Man-induced regime shifts in small estuaries - I: theory, *Ocean Dynamics*, 63(11-12), 1279-1292.
- Wolanski, E., Chappell, J., Ridd, P., & Vertessy, R. (1988). Fluidization of mud in estuaries. *Journal of Geophysical Research*, 93, 2351–2361.



17th International Conference on
Cohesive Sediment Transport Processes
September 18-22, 2023
Inha University, Incheon, Republic of Korea



A new unified consolidation concept based on Terzaghi and Gibson theories

A. Malcherek¹, K. Kaveh¹

¹ Institute für Wasserwesen, Universität der Bundeswehr München, Germany,
andreas.malcherek@unibw.de, keivan.kaveh@unibw.de

1. Introduction

Mudflats which are commonly observed in estuarine environments are of great importance in coastal studies. One of the common processes in cohesive mudflats is self-weight consolidation which has received limited attention. Self-weight consolidation can be defined as a process in which a reduction in volume takes place by expulsion of pore water. According to [Dankers and Winterwerp, 2007], consolidation starts when the gelling volume concentration is reached. In this research, a new general concept was developed for one-dimensional self-weight consolidation with variable hydraulic conductivity to assess the role of consolidation process on estuarine morphodynamics. For this purpose, two main consolidation theories, including Terzaghi and Gibson theories were unified for relating the excess pore-water pressure to the solid volume concentration. The significant advantage of the proposed model is that it reduces the number of calibration parameters which are included in other models.

2. Consolidation methods

2.1 Terzaghi consolidation theory

Since Terzaghi published his consolidation theory in 1925, noteworthy process has been achieved in consolidation theory. The Terzaghi theory for the time-dependent loading is a one-dimensional theory and the procedure is applicable only to vertical flow of water through thick layers of fine-grained soil. The general time-dependent loading problem for a condition of one-dimensional consolidation where permeability is held constant reduces the differential equation as follows:

$$\frac{\partial p_e}{\partial t} = \frac{E}{\rho_w g} \frac{\partial}{\partial z} \left(k_f \frac{\partial p_e(z)}{\partial z} \right) + \frac{\partial \sigma_{zz}}{\partial t} \quad (1)$$

where p_e = excess pore-water pressure, z = vertical coordinate, t = time, $\partial \sigma_{zz} / \partial t$ = rate of loading, E = elasticity module, k_f = hydraulic conductivity, ρ_w = density of water and g = gravity [Terzaghi, 1925].

2.2. Gibson consolidation theory

The Gibson consolidation theory [Gibson et al., 1967] was initially proposed for pure mud relating the pore water release to the sediment void ratio. The equation can be rewritten with solids volume concentrations (φ_s) as time-dependent variable as:

$$\frac{\partial \varphi_s}{\partial t} + \frac{\partial}{\partial z} \left[\frac{k_f (1 - \varphi_s) \varphi_s}{\rho_w g} \left(g \varphi_s (\rho_w - \rho_s) - \frac{\partial \sigma'}{\partial z} \right) \right] = 0 \quad (2)$$

where φ_s = solid volume concentration, ρ_s = density of sediment and σ' = effective stress.

3. Proposed unified consolidation theory

By combination of Terzaghi and Gibson consolidation theories, this study investigates the one-dimensional consolidation problem of soil under variable hydraulic permeability and time varying loading. According to the proposed hybrid model, Terzaghi consolidation equation is used for calculation of the pore-water pressure and consequently the effective stress, while Gibson's equation is applied for calculation of solid volume concentration.

To achieve this, one important step is calculation of the rate of loading in Terzaghi equation. Considering the weight of each layer, the rate of loading can be written as:

$$\frac{\partial \sigma_{zz}}{\partial t} = \frac{\partial}{\partial t} \int_z^{z_s} \rho_b(z, t) g dz \quad (3)$$

where z_s = water surface elevation and ρ_b = bulk density. Substituting Equation 3 into Equation 1 gives:

$$\frac{\partial p_e}{\partial t} = \frac{E}{\rho_w g} \frac{\partial}{\partial z} \left(k_f \frac{\partial p_e(z)}{\partial z} \right) + \frac{\partial}{\partial t} \int_z^{z_s} \rho_b(z, t) g dz \quad (4)$$

and thus,

$$\sigma'(z, t) = \int_z^{z_s} \rho_b(z, t) g dz - \rho g (z_s - z) - p_e(z, t) \quad (5)$$

At each time step, the calculated effective stress (Equation 5) and the hydraulic conductivity from Kozeny-Carman relation (Equation 6) can be applied to close the Gibson's consolidation equation and to solve numerically the time-varying solid volume concentration.

$$k_f = c_1 \frac{g d_{10}^2 (1 - \varphi_s)^3}{\vartheta \varphi_s^2} \quad (6)$$

In Equation 6, c_1 = proportionality constant, ϑ = dynamic viscosity and d_{10} = diameters corresponding to 10% and 50% passing in grain size distribution

4. Results and discussion

In order to optimize the performance of the proposed numerical model, the experimental data taken from the Weser estuary in north-west Germany and processed in the laboratory were utilized. The obtained temporal density profiles were compared with those established on the laboratory-prepared samples according to defined time intervals. Fig. 1 shows a comparison between the experimental and simulated bulk density profiles in the vertical direction. According to the results and simulated evolution of volumetric sediment concentration, there is a good agreement between the obtained and experimental density profiles, especially during the consolidation phase ($t = 480$ and 960 min).

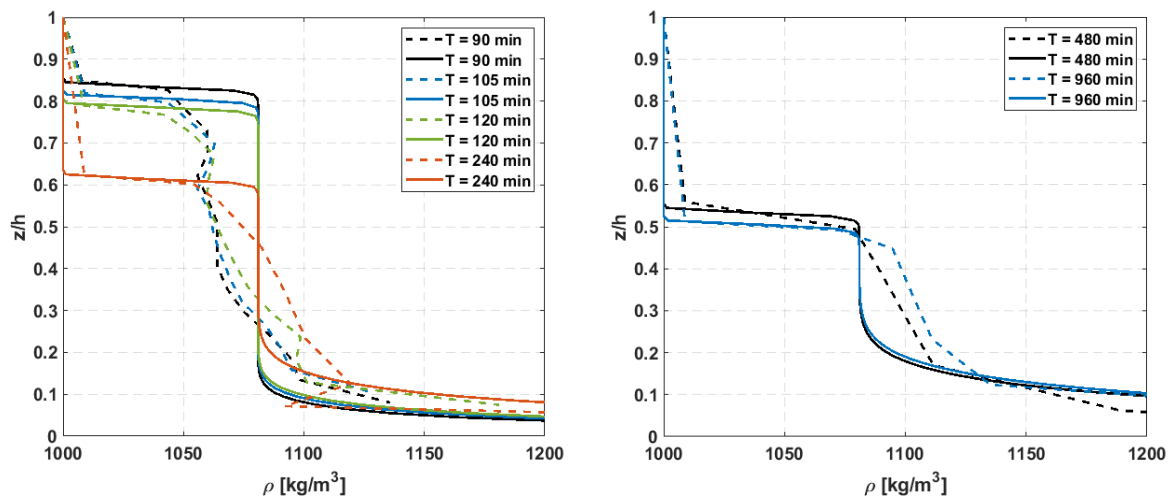


Figure 1. Comparison between the proposed model (solid lines) and experimental measurements (dashed-lines) during sedimentation and consolidation phases

5. Conclusions

A unified consolidation concept is developed by combining Terzaghi and Gibson's consolidation theories. Model validation against a benchmark settling experiment suggests that the implementation is sound. It is found that the proposed consolidation model is less dependent on proportionality factors, as only parameterization of calibration factor in the hydraulic permeability relation is required. Overall, the developed concept can be applied to bridge coastal morphodynamics with soil mechanics.

Acknowledgments

This project is carried out in cooperation with Institut für Wasserbau, Technical university of Hamburg (TUHH) and Bundesanstalt für Wasserbau (BAW). This research was funded by Bundesministerium für Bildung und Forschung (BMBF) and executed by Jülich Forschungszentrum.

References

- Carman, P. C. (1939). Permeability of saturated sands, soils and clays. *The Journal of Agricultural Science*, 29(2), 262-273.
- Dankers, P. J. T., & Winterwerp, J. C. (2007). Hindered settling of mud flocs: theory and validation. *Continental shelf research*, 27(14), 1893-1907.
- Gibson, R. E., England, G. L., & Hussey, M. J. L. (1967). The theory of one-dimensional consolidation of saturated clays: 1. Finite non-linear consolidation of thin homogeneous layers. *Geotechnique*, 17(3), 261-273.
- Kozeny, J. (1927). Über kapillare Leitung des Wassers im Boden-Aufstieg, Versickerung und Anwendung auf die Bewässerung, *Sitzungsberichte der Akademie der Wissenschaften Wien. Mathematisch Naturwissenschaftliche Abteilung*, 136, 271-306.
- Terzaghi, K. (1925). *Erdbaumechanik auf bodenphysikalischer Grundlage*. F. Deuticke.